

**Diagnosing Bone Fracture to Assess
Early Hominin Behaviour, Meat-Eating, and Socioecology
at FLK-Zinjanthropus, Olduvai Gorge, Tanzania**

by

James S. Oliver

A dissertation submitted in partial fulfillment of the
requirements of Liverpool John Moores University
for the degree of Doctor of Philosophy,
June 2015

© 2015

James Stephens Oliver

All Rights Reserved

- Table of Contents -

List of Tables	vii
List of Figures	x
Abstract	xiv
Acknowledgements	xv
Chapter 1: <i>Introduction: Problems and Promise in Defining Bone Fracture Agency and Assessing the Position of Early Homo in the Carnivore Guild</i>	1
1.1 Introduction	1
1.2 A Brief to Assessments of Carcass Acquisition by FLK-Zinj Hominins	4
1.3 A Brief on Zooarchaeological Assessments of Bone Fracture	9
1.4 Approach and Organization of This Study	11
Chapter 2: <i>Fracture Mechanics, Fractographic Features, and Fracture Patterns: Concepts and Examples for Understanding Bone Fracture</i>	14
2.1 Introduction	14
2.2 Bite Force vs. Impact Force	20
2.2.1 Bite Force Estimates	22
2.2.2 Hammerstone Impact Force Estimates	33
2.3 Bone as a Material	39
2.4 Fracture Mechanics	43
2.4.1 Stress & Strain	43
2.4.2 Mechanical Properties of Cortical Bone	45
2.4.3 Fracture Mechanics Axioms: Force, Nature of Indenter, and Type of Loading	49
2.5 Fractographic Features & Fracture Patterns: The Results of Loading Extremes	55
2.6 Synopsis	84
Chapter 3: <i>Research Framework: Hypotheses for Fracture Patterns and Features Among the Four Assemblages</i>	86
3.1 Introduction	86
3.2 Hypotheses to Test	87
Chapter 4: <i>Materials and Methods</i>	90
4.1 Introduction	90
4.2 Materials: Assemblage Descriptions	90
4.2.1 Hammerstone Fracture Experiments (EXP)	94
4.2.2 Amboseli Hyaena Den (AHD)	99

4.2.3 FLK-NN2	102
4.2.4 FLK LEVEL 22 aka FLK-Zinj	106
4.3 Methods: Fragmentation, Damage, and Fracture Feature Coding	109
4.3.1 Fragmentation	109
4.3.2 Types of Load Points (LDPTs) and Fracture Features	111
4.3.3 Fragments and Damages Diagnostic of Fracture Agent	116
Chapter 5: Results	120
5.1 Introduction	120
5.2 Fragmentation	121
5.2.1 Specimen Completeness: Length	121
5.2.2 Number of Fracture Lines per Specimen Length (#FLNs per SPECL)	125
5.3 Fractography: Load Point Frequencies, Types, and Fracture Features	128
5.3.1 Number of LDPTS	129
5.3.2 LDPT Types	143
5.3.3 LDPT Fracture Features	161
5.4 Carnivore and Hammerstone Damages: Fracture Agency and Overprinting	171
5.4.1 Carnivore Damage	172
5.4.2 Hammerstone Impact (Percussion) Damage	178
5.4.3 Co-Occurrence of Percussion Marks and Tooth Marks	180
5.4.4 Co-Occurrence of Percussion Marks or Tooth Marks at Loadpoints with Incipient Flakes, Radiating Cracks, Cones, or Later Stress Fracture Features	181
5.4.5 Estimating Hominin and Carnivore Fracture Frequencies in the FLK-Zinj Fossil Assemblage	184
5.5 Synopsis	185
Chapter 6: Discussion	193
6.1 Introduction	193
6.2 Fragmentation Patterns	195
6.3 Fractographic Patterns	199
6.3.1 Loadpoint Frequencies, Types, and Components	200
6.3.2 Fracture Features	204
6.4 Diagnostic Carnivore and Percussion Damage and Co-occurrence	207
6.4.1 Carnivore Damage	207
6.4.2 Percussion Damage	210
6.4.3 Co-Occurrence of Percussion Marks and Carnivore Damage	211

6.5 Co-Occurrence of PMs or TMs at LDPTs with IF, RC, CO, or LS Fracture Features and Estimates of Hominin Involvement in the FLK-Zinj Fossil Assemblage	211
6.6 Socioecological Implications of Hominin Activity at FLK-Zinj	215
Chapter 7: Summary and Conclusions	226
7.1 Introduction	226
7.2 Static vs. Impact Loading, Fracture Mechanics, and Fractographic Features	227
7.3 Fragmentation, Fracture Features, and Damages in the Study Assemblages	229
7.4 The Extent of early Homo Involvement with the FLK-Zinj Fossil Assemblage	235
7.5. Socioecological Implications of Food Transport by Oldowan Hominins	237
References Cited	239

List of Tables

Table 1.1. Frequency of cut marks (CM) percussion marks (PM) and tooth marks (TM) observed on ungulate long bones and metapodials in various Oldowan assemblages.	4
Table 2.1. Published bite force estimates in Newtons (N) for extant and extinct carnivores, marsupials, primates, and the alligator.	25
Table 2.2. Select experimental and Oldowan site hammerstone, manuport, and core weights.	35
Table 2.3. Estimated velocities (m/s) of karate and boxing punches, and hammerstone blows.	35
Table 2.4. Impact force in Newtons (N) for the mean (± 1 stdev.) of hammerstone weight, velocities, and pre-fracture travel distance.	36
Table 2.5. Force (N) required to break human tibiae and femora, and horse metacarpals.	38
Table 2.6. Mechanical properties of human and bovine femoral and tibiae (bovine compressive ultimate stress values) cortical bone.	46
Table 4.1. List of abbreviations used in this study.	92
Table 4.2. Denver Zoo carnivores used in feeding experiments.	95
Table 4.3. Summary of the fracture and feeding experiments conducted at the Denver Zoo.	97
Table 4.4. Experimental assemblage bone frequencies including NISP, MNE, and MNI frequencies for all bovid limb bones identified to element with a maximum dimension ≥ 20 mm.	98
Table 4.5. Number of identified specimens (NISP) and minimum number of individuals (MNI) (in parentheses) by element for the Amboseli Hyaena Den (AHD) assemblage.	100
Table 4.6. Amboseli Hyaena Den assemblage number of identified specimens (NISP), minimum number of elements (MNE), and minimum number of individuals (MNI) for all bovid, suid and equid limb bones identified to element with a maximum dimension ≥ 20 mm.	101
Table 4.7. Number of identified specimens (NISP) and minimum number of individuals (MNI) (in parentheses) by element and taxa for the FLK-NN2 assemblage.	104
Table 4.8. FLK-NN2 assemblage number of identified specimens (NISP), minimum number of elements (MNE), and minimum number of individuals (MNI) for all bovid, suid and equid limb bones identified to element with a maximum dimension ≥ 20 mm.	105

Table 4.9. Number of identified specimens (NISP), minimum number of elements (MNE), and minimum number of individuals (MNI) for all bovid, suid and equid limb bones identified to element with a maximum dimension ≥ 20 mm by element and taxa for the FLK-Zinj assemblage.	107
Table 4.10. FLK-Zinj assemblage number of identified specimens (NISP), minimum number of elements (MNE), and minimum number of individuals (MNI) for all bovid, suid and equid limb bones identified to element with a maximum dimension ≥ 20 mm.	108
Table 5.1. Mean specimen length (mm) of all long bone specimens ≥ 20 mm (excluding complete elements and ulnae) by size class.	122
Table 5.2. ANOVA p-values (except for (b) which are t-test values) for differences in the mean specimen length for all bovid specimens ≥ 20 mm (excluding complete elements and ulnae).	123
Table 5.3. Mean number of fracture lines per unit specimen length (mm) of long bone specimens ≥ 20 mm (excluding complete elements and ulnae) by size class and element portion.	126
Table 5.4. ANOVA (<i>c</i> , <i>and d</i>) and Student's t-test (<i>a</i> , because only two assemblages can be compared) p-values for differences in the mean number of fracture lines (#FLNs) per specimen length (SPECI) for all specimens ≥ 20 mm (not including complete elements, ulnae, and suidae).	127
Table 5.5: Load point (LDPT) frequencies observed on all long bones ≥ 20 mm in length for a) AHD, b) EXP, c) FLK-NN2, and d) FLK-Zinj.	131
Table 5.6. The total number of LDPTs excluding isolated LMRKs and the corresponding LDPTs per NISP frequencies for each assemblage.	136
Table 5.7. The total number of LDPTs excluding the ulnae and isolated LMRKs and the corresponding LDPTs per NISP frequencies for each assemblage.	137
Table 5.8. Probabilities (χ^2) for difference in assemblage loadpoint frequencies (excluding isolated loadmarks).	140
Table 5.9. Number of loadpoint (LDPT) types per number of identified specimens (NISP) and percentage of the total number of LDPTs for all specimens (excluding shaft fragments, the ulna and those with only an isolated LMRK)	144
Table 5.10. Chi-square probabilities (upper cell value), values (middle cell value), and degrees of freedom (lower cell value) for difference in loadpoint type frequencies between assemblages (excluding long bone shaft fragments and the ulna, and specimens with only an isolated loadmark).	148

Table 5.11. Number of identified specimens (NISP, excluding ulna and long bone shaft fragments), total number of loadpoints (excluding isolated loadmarks), number of specimens with one or more loadpoint, and the FLKS, FLKO, FRFE, and NTCH frequencies for all size class 1-4 specimens identified to element.	154
Table 5.12. Frequency of FLKS, FLKO, FRFE, and NTCH loading point components per specimen with one or more loading point.	155
Table 5.13. Chi-square (χ^2) probabilities (upper cell value) and values (lower cell value) for difference in loadpoint component frequencies (number of LDPTs with the component / number of LDPTs) between assemblages (excluding long bone shaft fragments and the ulna).	157
Table 5.14. Fracture feature frequencies for LDPTs for which fracture features were recorded for the (a) AHD, (b) EXP, (c) FLK-NN2, and (d) FLK-Zinj assemblages.	162
Table 5.15. Fisher's exact probabilities for difference in fracture feature frequencies (number of LDPTs with a feature / total number of LDPTs) in the AHD, EXP, FLK-NN2, and FLK-Zinj assemblages.	169
Table 5.16. Percentage of specimens (excluding the ulna and LBSF) that display carnivore damage in each assemblage. TM = tooth mark; LVRUP = carnivore leverup; CVRE LDPT = carnivore load point (tooth flake scar (TFLKS), tooth notch (TNTCH), and tooth loadmark (TMRK)).	173
Table 5.17. Percussion mark frequencies in the four assemblages for a) those associated with a LDPT, b) isolated percussion marks, and c) the totals.	179
Table 5.18. Frequencies of specimens that display both a percussion mark (PM) and carnivore (CVRE) damage, including a carnivore tooth mark on the fracture surface, medullary wall, or cancellous tissue (TM on FMC), a tooth mark on any part of the specimen, or evidence of a leverup (LVRUP), or a carnivore load point (CVRE LDPT).	180
Table 5.19. Frequencies of LDPTs with cones or partial cones (CO), lateral stress (LS), radiating cracks (RC), and incipient flakes (IF) that co-occur with a percussion mark (PM) or tooth mark (TM) (at the LDPT) observed on limb fragments (excluding the ulna and LBSFs) in the four assemblages.	183
Table 5.20. Summary of analyses	188

List of Figures

Fig. 2.1. Conceptual components of fractographic analysis.	17
Fig. 2.2. The means and ranges of estimated bite forces (N) for African taxa. Data and references given in Table 2.1.	32
Fig. 2.3. Estimated hammerstone-impact forces compared to forces produced by carnivore static loading.	37
Fig. 2.4. Structural components of bone from the macro to nano scale (modified after Weatherholt, Fuchs, and Warden (2012 Fig. 1) and Rho, Kuhn–Spearing, and Ziopos (1998, Fig. 1).	40
Fig. 2.5. The stress–strain curve.	44
Fig. 2.6. The three major types of stress, compression, tension, and shear.	44
Fig. 2.7. Plot of fracture toughness vs. Young’s modulus.	47
Fig. 2.8. Computer simulated and experimental plots of crack velocity vs. time and resulting crack undulations.	50
Fig. 2.9. Damage in glass plotted against applied stress.	50
Fig. 2.10. Crack patterns created in soda–lime glass showing an increase in damages and crack complexity with increasing force. (After Lawn and Wilshaw 1975, Fig. 21).	51
Fig. 2.11. Schematic diagram of tensile and compressive stress, and shock waves created by indenter contact with a material.	52
Fig. 2.12. Schematic diagram of a hertzian cone and its scar created by projectile impact (a) and a photograph showing a hertzian cone in which hackle marks and ripples are visible.	59
Fig. 2.13. Schematic diagram showing the locations of greatest tensile and compressive stress created during impact loading.	59
Fig. 2.14. Example from AHD of a typical flake scar and notch produced by carnivore gnawing.	60
Fig. 2.15. Example from AHD of an atypical flake scar and notch produced by carnivore gnawing.	60
Fig. 2.16. Examples of partial and complete cones produced on a cow bone by hammerstone impact.	61
Fig. 2.17. Example of a large and complete cone produced on a cow bone by hammerstone impact.	61

Fig. 2.18. Example of a large and nearly complete cone produced on a cow bone by hammerstone impact after being fed to hyaenas.	62
Fig. 2.19. Example of a very small cone (a dimple/dome) produced on a cow bone by hammerstone impact.	63
Fig. 2.20. Example of a small cone produced on a cow bone by hammerstone impact.	64
Fig. 2.21. Example of a moderate-size cone produced on a cow bone by hammerstone impact.	65
Fig. 2.22. Example of an impact shatter fragment produced experimentally on cow bone.	67
Fig. 2.23. Example of incipient flakes (aka ring cracks, aka concentric fracture lines) produced experimentally by hammerstone impact on cow bone.	68
Fig. 2.24. Example of a percussion mark (striae) produced experimentally by hammerstone impact on an cow bone.	69
Fig. 2.25. Example of complex flake scars created by experimental hammerstone breakage of cow bone.	69
Fig. 2.26. Example of complex flake scars created by experimental hammerstone breakage of cow bones.	72
Fig. 2.27. An example of damages created on a cow bone, first by experimental hammerstone fracture and then feeding of the broken bones to hyaenas.	72
Fig. 2.28. An example of hackle marks on a cortical flake created during by experimental hammerstone fracture.	73
Fig. 2.29. An example a lateral stress feature created by experimental hammerstone fracture.	73
Fig. 2.30. An example a lateral stress feature emanating from the partial cone loading point created by experimental hammerstone fracture.	74
Fig. 2.31. An example a lateral stress feature emanating from the loading point (angular indentation) created by experimental hammerstone fracture.	74
Fig. 2.32. Schematic diagram showing the chevrons and associated fringe fracture features whose convex side point back to the fracture point of origin and reveals the direction of fracture front movement.	78
Fig. 2.33. Example of how determination of fracture front movement directions are critical to the fractographic approach.	79

Fig. 2.34. Paired images (fracture, cancellous, and medullary wall surfaces above; cortical surface below) of a carnivore lever-up piece from AHD showing how the configuration of damages and fracture features aid in identifying loading points and fracture agent.	80
Fig. 2.35. An example a radiating cracks emanating from the loading point denoted by the (barely visible) percussion mark and complete cone created by experimental hammerstone fracture.	80
Fig. 2.36. Diagnostic tooth pits and scores created by Denver Zoo hyaenas.	84
Fig. 4.1. One of the Denver Zoo hyaenas gnawing a cow bone.	96
Fig. 4.2. Hyaena cub emerging from one of the Amboseli Hyaena Den entrances.	100
Fig. 4.3. Location of Olduvai Gorge, Tanzania.	103
Fig. 4.4. Olduvai Gorge, Tanzania.	103
Fig. 4.5. Olduvai Gorge Bed I stratigraphy at FLK-Zinj.	104
Fig. 5.1. Mean specimen length (mm) of all limb specimens ≥ 20 mm (excluding complete specimens and ulnae).	122
Figure 5.2. Plot of mean number of fracture lines per unit specimen length (mm) for limb specimens ≥ 20 mm by (a) 1-2 and 3-4 size classes and (b) size classes 1-4.	127
Fig. 5.3. Plot of total number of loadpoints (LDPTs) vs. number of identified specimens (NISP) for identified elements in the four assemblages.	137
Fig. 5.4. Point plot of frequency of loadpoints (LDPTs) per number of identified specimens (NISP) in Amboseli Hyaena Den (AHD), Experimental (EXP), FLK-NN2, and FLK-Zinj long bone assemblages (excluding specimens not identified to element - LBSFs, as well as the ulna, and isolated LMRKs) for (a) size class 1-2 and 3-4 specimens, and (b) size class 1-4 specimens >20 mm in maximum dimension.	138
Fig. 5.5. Point plot of mean number of loadpoints (LDPTs) per element, excluding isolated loadmarks (LMRKs) for size class (a) 1-2, (b) 3-4, and (c) 1-4 specimens.	142
Fig. 5.6. Point plot of the mean number of loadpoint (LDPTs) types per number of identified specimens (NISP) for (a) size class 1-2, (b) size class 3-4, and (c) size class 1-4 specimens (except long bone shaft fragments and the ulnae).	145
Fig. 5.7. Point plot of mean number of FLKSSs, FLKOs, FRFEs, and NTCHs for size class (a) 1-2, 3-4, and (b) 1-4 specimens identified to element with one or more LDPT.	156
Fig. 5.8. Principal component analysis of loadpoint (LDPT) component frequencies in each assemblage	160

Fig. 5.9. Correlation value (loadings) histogram for FLKS, FLKO, FRFE, and NTCH loadpoints in (a) principal component 1 and (b) principal component 2.	160
Fig. 5.10. Average number of fracture features (FRACFEAT) per loadpoint (LDPT) observed on size class 1-4 limb specimens excluding ulna and long bone shaft fragments.	165
Fig. 5.11. Point plot of the number of fracture features (IF = incipient flake; RC = radiating crack; BSc = bulbar scar; CO = cone; HK = hackle; LS = lateral stress; FR = fringe) per size class 1-4 LDPT (excluding LBSF and the ulna) in each assemblage.	165
Fig. 5.12. Principal component analysis of the mean number of the seven fracture feature types (IF = incipient flake; RC = radiating crack; BSc = bulbar scar; CO = cone (usually partial); HK = hackle; LS = lateral stress; FR = fringe) observed on LDPTs on size class 1-2 and 3-4 elements (excluding ULN and LBSF).	170
Fig. 5.13. Correlation value (loadings) histogram for seven fracture feature types (IF = incipient flake; RC = radiating crack; BSc = bulbar scar; CO = cone (usually partial); HK = hackle; LS = lateral stress; FR = fringe) observed on LDPTs on size class 1-2 and 3-4 elements in (a) principal component 1 and (b) principal component 2.	171
Fig. 5.14. Percentage of specimens (excluding the ulna and LBSF) that display carnivore damage in each assemblage. TM = tooth mark; LVRUP = carnivore leverup; CVRE LDPT = carnivore load point (tooth flake scar (TFLKS), tooth notch (TNTCH), and tooth load mark (TMRK)).	173
Fig. 5.15. Examples of hammerstone-fractured bone with tooth marks on the fracture surface and/or medullary wall (FMC).	176
Fig. 5.16. Ratio of the frequency specimens displaying a tooth mark (TM) to specimens that exhibit a carnivore break (CVRE BREAK) for each assemblage.	177
Fig. 5.17. Ratio of the frequency specimens displaying a tooth mark (TM) to specimens that exhibit a post-fracture TM on the fracture surface, medullary wall, and/or cancellous tissue for each assemblage.	177
Fig. 5.18. Histogram showing the frequencies of percussion marks (PMs) associated with a loadpoint (LDPT) and isolated PMs, and the frequency of the total number of identified specimens (NISP) that display a PM for the EXP and FLK-Zinj assemblages.	179
Fig. 5.19. Histogram of specimens that display both a percussion mark (PM) and carnivore damage, including a carnivore tooth mark on the fracture surface, medullary wall, or cancellous tissue (TM on FMC), a tooth mark on any part of the specimen, or evidence of a leverup (LVRUP), or a carnivore load point (LDPT).	181

Abstract

This study develops a fractographic method to diagnose hammerstone- and carnivore-induced fracture. This is important because interpretations of hominin entry into the carnivore guild and evolution of meat-eating are based on rare tool and tooth marks in Oldowan (2.5-1.8mya) fossil assemblages. Consequently, estimating hominin and carnivore involvement is difficult, and questions remain about Oldowan hominin's position in the carnivore guild and socioecology. One aspect of bone damage, fracture surfaces, is ubiquitous, but largely unstudied.

The fractographic (study of fracture surfaces) method is based on fracture principals, particularly how differences in static- and impact-loading affect material response and fracture features resulting from loading extremes. The method is applied to analysis of fracture features in a) the Amboseli Hyaena Den assemblage, b) an experimental hammerstone-broken assemblage, c) a Plio-Pleistocene assemblage previously interpreted as a carnivore accumulation, FLK-NN2 (Olduvai Gorge), and d) the zooarchaeological assemblage from FLK-Zinj, (Olduvai Gorge).

This is the first zooarchaeological/taphonomic study to demonstrate that a) static and impact fracture differ fundamentally in applied load size and material responses to loading extremes, b) impact-forces are significantly greater than the maximum carnivore bite-force, c) cones, incipient flakes, radiating cracks, and lateral stress features are characteristic of impact fracture, and e) Oldowan hominins at FLK-Zinj were responsible for breakage of 54% of the limb assemblage (a 37% – 40% increase over estimates based on percussion marks).

The socioecological implications of the habitual transport of food from death and/or kill sites to secondary locations are explored by examining reasons why social carnivores transport food. Aspects of modern carnivore behaviour suggest general mammalian constraints that may have predated food transport by early *Homo*. Early *Homo* food transport behaviour was structured by anti-predator defense strategies associated with a) foraging in an open habitat rich with competing predators, b) the lack of masticatory and digestive apparatus to quickly consume animal tissue, and c) the presence of altricial young in the hominin group.

Acknowledgements

I have passed through too many lives and worn too many hats to list everyone who has offered support, assistance, and encouragement. For those not mentioned here, you have my thanks.

Many people I do remember deserve special mention. First, I thank Henry Bunn for the opportunities and encouragement he provided so many years ago. He generously provided bone identification lists for both FLK-NN2 and FLK-Zinj. Without him this work never would have been started.

The Illinois State Museum, particularly Bruce McMillan, Bonnie Styles, Russ Graham (now at Penn State University) Jeff Saunders, and Erich Grimm, has provided years of collegial support. The institutional support and their friendship are greatly appreciated.

Early stages of my work were supported by a National Science Foundation Dissertation Improvement Grant and a grant from the Wenner-Gren Foundation. I thank the Tanzanian Dept. of Antiquities for permission to study the fossil material. I thank the National Museums of Kenya, Department of Paleontology for providing research space and assistance. I thank Laura Bishop, Pete Wheeler, and Andy Tattersall for their support and assistance in securing a studentship for me from Liverpool John Moores University.

I thank Laura Bishop for her advice and warm friendship. She put up with a lot; patiently putting things in perspective and repeatedly re-fitting my “blindness” I kept tossing aside. Her accurate assessment of me as a “magpie always chasing shiny objects” is only matched by her aim with orange peels. This work would not have been completed without her support and ever-present smile.

I thank my examiners Joel Irish and Tom Plummer. Our discussion was very useful, insightful, and a lot of fun. Thank you Tom for keeping me “in the battle”. Onward and forward....

The Springfield Milers BMW motorcycle club constantly reminded me of non-academic realities. You all are the best. Thanks guys.

I thank my 2 ex-wives Sheryl and Joann for their (sometimes grudging) support. Sheryl, the mother of my great kids, has been more than supportive these last several years. Her continuing love and friendship are deeply appreciated. Thanks to Deanna Glosser for letting me into her home and “furry family” – we should all be so lucky to have such generous friends. My children Bo and Hannah have put up with a lot, but have always been positive and loving, encouraging me to do what I do best. You both helped more than you know – thank you, but please learn from my mistakes.

My mother and father have had a bigger influence on this work than they realize. I am sorry my mother did not live to see me finish this bit of work. She was always there for me and always encouraged me to do what makes me happy. As a confirmed skeptic, my father taught me that prestigious titles and shiny reputations mean little – all select and arrange “facts” to create interpretations – learn by questioning accepted wisdom, regardless of the source.

This thesis is dedicated to the memory of Robson Bonnicksen. We disagreed often, did not always understand each other, but he was a mentor, colleague, and friend. He dreamed big dreams, achieved many, and, in the big-picture, was often right....

- CHAPTER 1 -

Introduction: Problems and Promise in Defining Bone Fracture Agency and Assessing the Position of Early Homo in the Carnivore Guild

1.1 Introduction

This thesis defines, develops and applies a new interdisciplinary method to identify hammerstone-broken bones to determine the extent to which early *Homo* engaged in meat eating. The framework of the method is built on fractography, the study of fracture surfaces, and fracture mechanics that differentiate fracture patterns and features created by static and impact loading. Defining the extent of early *Homo* reliance on animal tissue and its socioecological implications is important because the addition of meat to the diet is recognized as a critical process in the evolution of early *Homo* (e.g. Bunn 2001; Plummer 2004), which coincides with the age range (2.6 – 1.6mya) of the first stone technology, the Oldowan.

These behavioural developments also coincide with the appearance of at least three hominin genera, *Australopithecus*, *Paranthropus*, and *Homo*. Determining which genus or genera made the Oldowan tools and which added meat to their diet at what time(s) is problematic; however, most paleoanthropologists assume that members of our genus were the meat-eaters and maker of Oldowan tools because both behaviours were clearly major components of *H. erectus* behavioural repertoire (Plummer 2004). Cut marks on animal bones from 2.6mya Gona, Ethiopia assemblage with associated Oldowan artifacts (Semaw et al. 2003) and the 2.5mya assemblage from Bouri, Ethiopia (without associated Oldowan artifacts) (de Heinzelin et al. 1999), date the earliest beginnings of meat eating. Identification of a *Homo* jaw from 2.8mya deposits in the Afar, Ethiopia (Villmoare et al. 2015) would seem to confirm that members of our genera were the tool-makers. Recent, discovery of 3.3mya stone tools at Lomokwi 3, West Turkana (Harmand et al. 2015) mean that the start of this process might be even earlier. Not only is are these tools .5my older than the Ledi Geraru *Homo* jaw, the Lomekwian technology shares similarities with flakes

created by chimpanzees during nut-cracking. Which hominin made these tools is unclear, but *Kenyanthropus platyops* fossils are from nearby deposits of a similar age (Leakey et al. 2001). For now, however, the purpose of the Lomekwian industry and its link to meat processing remains unproven.

No consensus has formed about the 2.8mya jaw reported by Villmoare et al. 2015 and the oldest accepted early *Homo* remains are 0.3mya younger (Hadar, Ethiopia mandible A.L. 666; Kimbel et al. 1996) than the oldest Oldowan tools from Gona (Semaw et al. 1997, 2003). Consequently, it has been suggested that several genera were making Oldowan tools and likely added meat to their diet. Semaw et al. (2003), for example, have suggested that *A. garhi* was the maker of the Gona tools and cut marks on the basis of recovery of these hominin fossils from nearby and nearly contemporaneous deposits. Isotopic analysis (Cerling et al. 2011) indicates that *Paranthropus* (2.3 – 1.2mya) subsisted largely on C4 plants (grasses and sedges) or perhaps the meat of animals that consumed C4 plants (Sponheimer et al. 2006). Analysis of isotopes from South African hominins indicates little dietary difference between the australopiths and *Homo* (Lee-Thorpe 2000). And, functional analysis of *Paranthropus* hand and wrist suggest that tool-making was possible (Sussman 1991).

For present purposes, it is assumed that a member of our genus made the Oldowan artifacts and had added some meat to their diet around 2.6mya. Later Oldowan sites, 2.3 – 1.6mya, with evidence of carcass processing were likely created initially by *H. habilis* and *H. rudolfensis* with each creating archaeological sites when they were contemporaries on the landscape between 1.8 and 1.6mya (Plummer 2004). For the purposes of this study, it is assumed that the hominin species responsible for the Oldowan tools and bone accumulation at the 1.74 mya FLK-Zinjanthropus site analyzed here was *H. habilis* (*sensu stricto*). That said, other species and genera may have also been responsible and the Oldowan tool-maker and processor of animal carcasses will be referred to as early *Homo*.

Paleoanthropologists are necessarily interested in the mode, character, and extent of

meat-acquisition by early *Homo* because meat eating has been invoked to explain several biological evolutionary trends including changes in energetics, brain enlargement, gut reduction (Aiello and Wheeler 1995; Aiello and Wells 2002) maturation rates, and altriciality as well as a host of socioecological characteristics, e.g., range expansion (e.g., Aiello, 1997; Leonard and Robertson 1997; McHenry and Coffing 2000), cooperative behaviour, sexual division of labor and shifts in parental investment (e.g., Isaac 1978a, 1978b; Lovejoy 1981; McGrew 1992; Stanley 1992; Aiello and Wheeler 1995), landscape-use patterns (e.g., Aiello, 1997), food-sharing (Bunn and Kroll 1986; Isaac 1978a, 1978b; foraging strategies, group structure, and provisioning (e.g., Isaac 1978a, 1978b; Oliver 1994). Additionally, the degree to which early *Homo* relied on animal tissue is important in understanding their position in the carnivore guild and the corresponding adaptive behaviours related to this position (e.g., Brantingham 1998; Egeland 2007a, 2014).

Analysis and interpretations of the amount of meat in the diet of early *Homo* and, perhaps more significantly, the mode of acquisition vary. Most Plio-Pleistocene Oldowan assemblages exhibit evidence that both carnivores and early *Homo* were involved in assemblage creation. Consequently, rather detailed and intricate analyses using a variety of actualistic and experimental studies have been used in attempts to define the primary agent in the accumulation. The question can be simply stated – *Who ate what when?* Did hominins feed on complete carcasses via hunting or confrontational scrounging, or were they scavenging bits of meat and bone abandoned by carnivores?

Analyses of ancient bone assemblages have used the diagnostic *but rare tool marks* to define the extent of hominin activity in creating the assemblages (Table 1). In no Oldowan fossil assemblage does the frequency of percussion marks (PM) exceed 28% of the number of identified specimens (NISP). On average, only 11% of bones in Oldowan assemblages display percussion tool marks (cut and percussion marks). It is therefore difficult to accurately reconstruct early *Homo* subsistence behaviour and resolve the debate over early *Homo* meat acquisition strategies. One suite of damages are ubiquitous, but

Table 1.1. Frequency of cut marks (CM), percussion marks (PM), and tooth marks (TM) observed on ungulate long bones and metapodials in various Oldowan assemblages.

Site	% CM	% PM	% TM	Ref.
Kanjera	4.0	6.3	9.8	Ferraro et al. 2013
FLK-Zinj	11.6	–	–	Bunn and Kroll 1986
FLK-Zinj	19.9	–	25.8	Oliver 1994
FLK-Zinj	–	27.3	60.7	Blumenschine 1995
FLK-Zinj	18.7	–	60.7	Blumenschine as reported by Capaldo 1997
FLK-Zinj	–	15.1	17.7	Dominguez-Rodrigo and Barba 2007b
FLK-Zinj	19.8	–	–	Dominguez-Rodrigo and Barba 2007c
FxJj50	2.9	–	–	Bunn 1997
FxJj50	12.7	9.5	35.7	Dominguez-Rodrigo 2002
FwJj14A	15.0	3.0	1.2	Pobiner et al. 2008
FwJj14B	21.7	5.3	–	Pobiner et al. 2008
GaJi14	17.5	3.0	0.0	Pobiner et al. 2008

largely unstudied – *bone fracture surfaces*. This study examines fracture features and patterns as well as other damages (i.e., tool and tooth marks) and their configuration to provide more robust estimates of hominin and carnivore involvement in the creation of ancient bone assemblages, specifically the Plio-Pleistocene FLK-Zinj, Olduvai Gorge, Tanzania fossil assemblage. New estimates of early *Homo* involvement with this assemblage derived from this analysis serve as a base to explore the socioecological implications of an uncommon mammalian behaviour, food transport.

1.2 A Brief to Assessments of Carcass Acquisition by FLK-Zinj Hominins

Discussions of the character and mode of early *Homo* acquisition of animal tissue have a long and sometimes (unnecessarily) contentious history (Binford, 1981, 1986, 1988; Bunn and Kroll, 1986, 1988; Oliver, 1994; Selvaggio, 1994, 1998; Blumenschine, 1995; Capaldo, 1995, 1997; Monahan, 1996; Domínguez Rodrigo, 1997a, 1997b; Egeland et al., 2004; Pickering et al., 2005; Domínguez-Rodrigo and Barba, 2006, 2007; Blumenschine and Pobiner, 2007; Pobiner et al., 2008; Ferraro et al., 2013; Pante et al. 2012). All analysts (except Binford) agree that the FLK-Zinj assemblage exhibits evidence of carnivore

involvement in the form of tooth marks. The activities of early *Homo* are demonstrated by both cut and percussion marks, and hammerstone percussion notches (some of which display incipient flakes, see below). The meaning of the damage frequencies, and which actualistic and experimental analogues are most appropriate to inform interpretations, are the main subjects of debate.

Many have argued that hominins were meager scavengers of meat scraps and marrow remaining at abandoned carnivore-ravaged carcasses (Binford 1981, 1986, 1988; Shipman 1986; Blumenschine 1987, 1995; Blumenschine et al. 1992; Capaldo 1995, 1997; Selvaggio 1994, 1998; Pante et al. 2012; Pobiner 2015). These arguments are based largely on the similarly high tooth mark frequencies observed in actualistic assemblages and FLK-Zinj. On the basis of more recent estimates of the amount of tissue remaining on carcasses abandoned by felids and reanalysis of Blumenschine's original FLK-Zinj tooth mark frequencies, some have suggested more meat was potentially available, but the hominin foraging behaviour remains that of passive scavenging (Pante et al. 2012; Pobiner 2015).

Others have emphasized cut mark frequencies and their location on meaty elements (Dominguez-Rodrigo 1997a, 1997b, 1999a, 1999b, 2002; Dominguez-Rodrigo and Barba 2007c) as well as questioning Blumenschine's FLK-Zinj tooth mark frequencies (Dominguez-Rodrigo and Barba 2006, 2007b) in arguing that the FLK-Zinj early *Homo* had early access to meat-rich carcasses. The conclusion of these and other recent analyses is that the FLK-early *Homo* acquired meaty carcass parts via confrontational scavenging or perhaps hunting as originally envisaged by Bunn (e.g., Bunn 2001; Bunn and Ezzo 1993). Bunn's recent analysis of FLK-Zinj ungulate age-profile data also suggests early access and perhaps hunting (Bunn and Pickering 2010; Bunn and Gurtov 2014). Further, using Shannon's evenness index, which measures the evenness of skeletal element survivorship in relation to their frequency in a complete carcass, Faith et al. (2009) have argued that the high index for FLK-Zinj indicates early access to meaty carcasses.

Clearly this debate has revolved around some very real methodological and empirical issues, but the frequent sharp edge and volatility among debate participants is likely a reflection of the importance of ascertaining whether early *Homos* were passive scavengers, confrontational scavengers, or perhaps hunters. It is important to determine if one of these strategies characterizes 1.8mya hominin meat-acquisition behaviour because each suggests rather different amounts of meat in the diet. Furthermore, the addition of meat to early *Homo* diet has been tied to a number of other significant changes in hominin biological and cultural evolution.

Carnivore guilds may be defined on the basis of member body mass, diet, locomotion (Morlo et al. 2010), and trophic level (Brantingham 1998; Van Valkenburgh 1988, 1989, 1991). Carcass acquisition strategies largely define a carnivore's position in the carnivore guild and the level of inter-specific competition with other guild members. These strategies mirror those proposed for early *Homo* (Brantingham 1998). Top predators, also referred to as hypercarnivores, such as lions and leopards, acquire carcasses almost exclusively by hunting. Confrontational scavengers use their larger size and/or larger group size to supplant other carnivores from their kills. Within the African carnivore guild the spotted hyaena is the primary confrontational scavenger. If their numbers are sufficiently greater, other smaller carnivores, notably wild dogs and jackals, will supplant larger carnivores at a kill. As noted by Pereira et al. (2013), however, carnivore carcass acquisition strategies are often facultative. It seems likely that early *Homo* acquired carcasses in a variety of ways as well. Nevertheless, the three trophic levels of the carnivore guild are useful heuristic devices to discuss their behavioural implications for hominins.

Each of early *Homo* meat-acquisition strategies and their position in the carnivore guild has different implications for inter-specific competition with other predators and hominin behaviour (Brantingham 1998), particularly the level of co-operation and complexity of strategies needed for meat-acquisition. Non-confrontational or passive

scavengers are characterized as occupying a very low position in the carnivore guild. Animal tissue acquired by passive scavenging would be scraps of meat and bone marrow. Estimates of the actual amount of meat available from carnivore-ravaged carcasses vary depending on the carnivore principally responsible for the kill, among other factors. Felids, for example, have been shown to leave more meat on their abandoned carcasses (Pobiner 2015) than hyaenas (Blumenschine 1987, 1995). Other factors influencing the amount of meat available for secondary scavenging include whether the carnivore is solitary or part of a group, carnivore population densities and species diversity, and available “on the hoof” resources. Inter-specific competition is the over-riding factor. Solitary hyaenas, for example, find it impossible to displace lions from their kills, but packs are able to do so (Kruuk 1972). Population densities of some small to mid-size carnivores (e.g., wild dogs) are inversely related to densities of hyaenas and lions (Creel and Creel 1998). Similarly, lions facing frequent competition with hyaenas over kills in Ngorongoro and Serengeti, Tanzania, and Masai Mara, Kenya leave less meat for secondary scavengers than do lions in guilds where competition over kills is reduced (Pobiner 2015). Regardless of the amount of meat acquired, the ability of passive scavengers to compete directly with other carnivores would be low, as would the level of co-operative behaviour needed to secure an abandoned carcass. The level of danger from predators would be lower in passive scavenging than in either confrontational scavenging or hunting.

In contrast, confrontational scavenging involves active, direct competition for carcasses killed and/or defended by a carnivore. Thus, confrontational scavenging is a form of kleptoparasitism and would provide more meat and marrow to the thief than could be obtained via passive scavenging. Confrontational scavengers occupy a higher level in the carnivore guild than passive scavengers. Equally important is the complex suite of behaviours likely necessary to confront large and dangerous carnivores feeding on a carcass. Several variables would have to be consciously evaluated including differences in the carnivore and hominin group size, physical setting (e.g., how much of the surrounding

area could be scanned for competing predators), other carnivores waiting for a chance to feed, availability of natural projectiles, i.e., rocks, to drive off predators, distance to more protected area such as a woodland, etc. If hominins were to attempt takeover of a kill, some solutions to these evaluations would require a level of cooperative behaviours not required by passive scavenging. Further, the greater level of danger from predators no doubt influenced the composition of the foraging group. Because risks to overall group fitness would seem to be high, it seems unlikely that mothers with infants would be part of a foraging party where confrontational scavenging or direct competition with carnivores was likely to occur.

Meat acquisition via active and habitual hunting is a strategy of the top occupants of the carnivore guild. For hominins, this would obviously require an even greater degree of behavioural sophistication and cooperation. Hominins would have to know the locations where prey were known to pass, suitable nearby hiding places to await passing prey, and of course an effective technology capable of killing prey. If a kill were made, a further consideration would be how other hominin group members were informed of the carcass location to facilitate transport before other predators arrived. Hunting also implies a different foraging group structure, one likely much smaller (and male dominated?), perhaps made up of pairs, than with either passive or confrontational scavenging.

Finally, it must be emphasized that the amount of animal tissue at a kill is likely positively correlated with the level of competition and risk associated with acquiring that animal tissue. Consequently, the level of risk associated with each carnivore guild trophic strategy was likely a major factor in determining the level of food transport.

As mentioned above, the most direct evidence for early Homo involvement with the FLK-Zinj fossil assemblage is the relatively high frequencies of cut and percussion marks. And, the most direct evidence for carnivore involvement is the widely variable estimates of tooth mark frequencies.

1.3 A Brief on Zooarchaeological Assessments of Bone Fracture

The study of bone fracture has a long and sometimes contentious history in archaeology (e.g., Dart 1949a, 1949b; Binford 1981; Brain 1981; Bonnichsen 1979; Bonnichsen and Sorg 1989). It has been marred by differences in conceptual approaches, fracture nomenclature, levels of description and illustration, and a lack of agreement on which, if any, fracture patterns are diagnostic to carnivore, geological, or human agents. Both Bonnichsen (1979, Bonnichsen and Will 1980), who pioneered that study of bone fracture, and Johnson (1985) grounded their understanding of bone fracture in knowledge of bone as a material and fracture mechanics. While this grounding is a sound approach, its full utility has not been convincingly demonstrated. As well, the approach and many of the fracture features and concepts have been both ignored and misunderstood.

Nomenclature, particularly descriptions of fracture shape, e.g., the use of the term “spiral fracture”, has varied considerably (see Johnson 1985 for a discussion of the conflicting uses of various fracture shapes). Similarly, fracture terms borrowed from the material science literature have often not been adequately described or illustrated. Fracture mechanics concepts have not been stated as general principles related to substantive and observable differences in fracture features and patterns resulting from static and impact loading. Finally, and more critically, bone fracture studies have suffered from a lack of quantified data. Those arguing that certain fracture features and patterns (e.g., spiral fractures, incipient flakes, hackle marks, steeply-angled negative flake scars, etc.) are indicative of impact fracture with hammerstones have rarely provided quantified actualistic, experimental, or fossil data (e.g. Bonnichsen 1979; Johnson 1985). Their arguments are largely warranted by reference to the material science fracture literature. As a consequence of this lack of quantification, as well as a lack of sufficient descriptive detail and illustration, it has been easy for others to reject the utility of many fracture patterns and features proposed to be indicative of impact loading. Both Binford (1981) and Haynes (1981, 1982, 1983a) have documented carnivores may create what they term spiral

fractures, negative flake scars. Haynes further notes similar damages are created by trampling, and that carnivore flake scars may display hackle marks.

Attempts at presenting a synthetic approach to understanding bone fracture and defining fracture features believed to be diagnostic of agency have suffered from the particularly poor archaeological context of many fossil assemblages foisted as examples of prehistoric human involvement. For example, the first attempt to understand bone fracture using an understanding of fracture mechanics and lithic technology were applied to an argument that the redeposited Pleistocene bones on river banks from Old Crow Flats, Yukon, Canada with green fractures are evidence for a Pre-Clovis occupation of the New World (Bonnichsen 1979). A more poorly understood fossil assemblage could not have been chosen to evaluate this early attempt to understand bone fracture. The Ginsberg Experiment – an experimental butchery and marrow processing of an elephant carcass – but particularly its application in identifying supposed Pre-Clovis human involvement with other proposed Pre-Clovis sites, i.e., Dutton-Selby, Colorado, USA (Stanford et al. 1981) has been largely dismissed by the archaeological community. Consequently and unfortunately, many “threw the baby out with the bathwater”. A notable exception is Adrien Hännus’ work on the Lange-Ferguson Mammoth Site (1989, 1990) where impact fracture and flaking of mammoth bone is clear and accepted by even the most conservative of analysts (Grayson and Meltzer 2002). Another more controversial pre-Clovis mammoth assemblage displaying similar bone flaking and fracture features is at the Lovewell Reservoir Site (Holen 2007).

Although not explicitly grounded in knowledge of bone as a material or fracture mechanics, more recent experimental and actualistic studies have considerably refined and quantified descriptions of some fracture patterns and features created by carnivores and hammerstone impact. Capaldo and Blumenschine (1994) measured notches and associated negative flake scars created by experimental hammerstone-impact and carnivore gnawing. By measuring notch width, depth, and maximum flake scar width, they found that

carnivore teeth create smaller notches, which tend to be equidimensional (semi-circular), with smaller and narrower associated flake scars and a steeper fracture angle (approaching 90°). In contrast, hammerstone-impact notches were found to be broad with larger flake scars that exhibit a more acute fracture angle. Further, they note that what they call incipient flakes were observed exclusively on bones broken by hammerstone percussion. Subsequent studies have quantified fracture angle frequencies and seem to verify these earlier observations (Bonnichsen 1979; Johnson 1985; Blumenschine and Selvagio 1991) that impact fracture tends to produce more acute fracture angles compared to the near 90° angles created by carnivore gnawing. In an experimental study Alcántara et al. (2006), for example, found that carnivore created fractures were significantly more likely to display fracture angles approaching 90° while those created by percussion are more acute. Dominguez-Rodrigo and Barba (2007b), measured fracture angles in the FLK-Zinj assemblage and found most display acute angles suggesting many bones were broken by hammerstone impact. Not all studies have confirmed this pattern, however. A large proportion of impacted flake scars and notches, particularly those on the radius but not the humerus, in Pickering and Egeland's (2005) study display steeper angles. Measurement of fracture angles for this study was abandoned because of the difficulty in obtaining consistent measurements and because it was found that a large number of fracture surfaces display more than one fracture angle.

1.4 Approach and Organization of This Study

Not only have bone fracture studies suffered from a lack of quantification, there has been little attempt to understand bone fracture in terms of the fracture mechanics and the role played by bone's material properties. Advances in both the material sciences and zooarchaeological studies of fracture warrant attempting a synthesis and examination of specific fracture features that may differentiate carnivore- from hammerstone-broken bones. Understanding bone as a material, fracture mechanics and resultant fracture features aids in the identification of bone fracture agency.

The approach used here to understand bone fracture and discriminate between bones broken by carnivore chewing and those broken by hammerstone impact is based on principles and concepts derived from the fracture mechanics and fractographic (study of fracture surfaces) literature. Chapter 2 *Fracture Mechanics, Fractographic Features, and Fracture Patterns: Concepts and Examples for Understanding Bone Fracture* presents key aspects of fracture mechanics and the fractographic features resulting from loading extremes. This study emphasizes the profound differences between static and impact loading and how resultant modes of fracture development make it possible to fracture features and patterns characteristic of hammerstone-impact breakage.

Many zooarchaeological discussions of bone fracture note – often in passing – that static loading by carnivore teeth is different from the impact or dynamic loading created by hammerstone percussion sometimes adding that different fracture patterns are created (e.g., Capaldo and Blumenschine 1994; Pickering and Egeland 2005). This study is the first attempt to bound the problem by estimating the loads produced by carnivore chewing and hammerstone impact, and explains resultant fracture features in terms of loading extremes. Estimates of bite forces for a number of carnivores and impact forces are provided in Chapter 2 to substantiate the magnitude of difference between carnivore static and hammerstone impact loading. Chapter 2 also creates a framework to understand bone fracture in terms of established fracture mechanics principles, as well as the fracture consequences of loading extremes, static and impact loading; critically, this framework has been lacking in previous studies of bone fracture. Existing taphonomic and experimental studies of bone fracture are described and framed in terms of these fracture mechanics principles and understanding of how specific fracture features form.

Chapter 3 Research Framework: Hypotheses for Fracture Patterns and Features Among the Four Assemblages restates the fractographic and fracture mechanics principles as hypotheses to test in the analysis of four assemblages: 1) a modern actualistic assemblage accumulated by modern hyaenas, the Amboseli Hyaena Den (AHD); 2) an

experimental assemblage (EXP) of bones broken by the author with hammerstone and anvil some pieces of which were fed to hyaenas after breakage; 3) a Plio-Pleistocene fossil assemblage from Olduvai Gorge, Tanzania, FLK-NN2 that is thought to have been accumulated by hyaenas; 4) a Plio-Pleistocene zooarchaeological assemblage with both hominin and carnivore involvement, FLK-Zinjanthropus (aka FLK-level 22, from here on referred to as FLK-Zinj). This discussion demonstrates the utility these principles as heuristic devices to focus the analysis of bone fracture. *Chapter 4 Materials and Methods* describes four assemblages and methods for assessing the fractographic approach.

Chapter 5 Results assesses the expectations regarding bone fragmentation and fractographic features in the four assemblages. Also presented in this assessment are frequencies of diagnostic tooth and tool marks and their co-occurrence with a select set of fractographic features. In *Chapter 6 Discussion* the meaning of these fracture patterns and fracture feature frequencies are discussed in terms of the fractographic and fracture mechanics principles presented in Chapter 2. Here new estimates of early *Homo* involvement in the FLK-Zinj assemblage based on fractographic analyses are presented. Drawing on ecological constraints shared with carnivores occupying open environments, the early *Homo* socioecological implications of these new estimates are discussed.

- CHAPTER 2 -
***Fracture Mechanics, Fractographic Features, and Fracture Patterns:
Concepts and Examples for Understanding Bone Fracture***

2.1 Introduction

Early work on defining characteristics of hammerstone-fractured bone and attempts to differentiate it from bone fractured by other agents, particularly carnivores, focused on overall fracture shape. Spiral fractures on long bones were proposed to be indicative of percussion fracture (e.g., Dart 1957; Bonnichsen 1979), but paleontological and actualistic studies quickly showed that spiral fractures could be produced without hominin involvement and were only indicative of green fracture (e.g., Binford 1981; Haynes 1983; Johnson 1985; Meyers et al. 1980; Oliver 1989). More recent research on differentiating hammerstone- and carnivore-fractured bone has relied on relatively uncommon diagnostic trace features — the size of complete notches and associated flake scars, and tooth and percussion marks each produces (e.g., Binford 1981; Blumenschine and Selvaggio 1988; Capaldo and Blumenschine 1994; Haynes 1983).

This reliance limits the information that may be gleaned from a fragmented assemblage and, moreover, seriously constrains the accuracy in identifying the major fracture agent, because for any given assemblage relatively few percussion marks and notches are available for study. Experimental work, for example, has shown that the frequency of bone fragments displaying percussion marks is highly variable: Pickering and Egeland (2006) report 13.8% of the hammerstone broken NISP display percussion marks while Blumenschine and Selvaggio (1988) and Galan et al. (2009) observed percussion marks on 37.5% and 32.5% of the NISP in their experimental samples, respectively. This roughly parallels the range of percussion-marked specimens in Plio-Pleistocene zooarchaeological assemblages (Table 1.1). With the exception of noting the importance of radiating fractures (Johnson 1985) and the analysis of fracture angles (Pickering et al. 2005; Dominguez-Rodrigo and Barba 2007b), and notches (Capaldo and Blumenschine

1994; Galan et al. 2009), information held in various fracture features on the more numerous fracture surfaces has been largely ignored. Every long bone fragment has at least two fracture surfaces. Each fracture surface may display fracture features (e.g., radiating cracks, cones, hackle marks, fracture front movement directional indicators, lateral stress, etc. – see below) and the cortical medullary/cancellous surfaces may display damages (e.g., percussion marks, tooth marks, miscellaneous abrasions, etc.) that may inform us about the fracture agent.

Accordingly, an understanding of fracture mechanics and an assessment of a configuration of fractographic features and marks on fracture surfaces offers a more robust and holistic method for the identification of fracture agent. It is argued here that differentiating carnivore and hammerstone fractured bone not only requires an assessment of trace features (e.g., tooth and cut marks, notches, and flake scars), but an understanding of bone's structural organization and characteristics, fracture mechanics, the way in which each agent induces fracture and the fracture surface features each may produce. In developing a conceptual basis for understanding differences between hammerstone- and carnivore-induced fracture particular emphasis is placed on a) the rate of force application, b) the amount of force applied, c) the surface area over which force is applied, and d) the shape of the indenter that contacts bone and applies the force. These vast differences in the mode and character of force application by hammerstone impact and carnivore chewing may then inform us about differences that may be expected in the fracture patterns and fracture surface features each may produce.

The outline of bone fracture concepts relevant to discerning fracture agent developed here relies on two related fields of the material sciences, fracture mechanics and fractography. Fracture mechanics is the study of how solids fail by the formation and propagation of cracks that disrupt the otherwise solid body thereby causing structural failure. It is concerned with loads applied to materials, the stresses (tensile, compressive, and shear) different loadings create, the strains of the material as an initial manner to

relieve the applied stress, the formation of cracks around material flaws, and how stress is released in the form of cracks. Fractography, a term first used by Zapffe and Clogg (1944), is an interdisciplinary field closely tied to fracture mechanics that *examines fracture surface topography* of solids to understand how materials develop irrecoverable damage, fracture, and how fracture fronts are propagated under various types of loading conditions. *Its basic premise is that fracture surface features reflect both the fracture properties of the material as well as the conditions — in particular load amounts, rate of loading, and indenter size and shape — that initiated fracture* (Hull 1999; Quinn 2007). Fractographic analysis can help identify fracture origin, direction of fracture front movement, how the material was loaded, material defects, and environmental and material conditions at the time of fracture.

In industry and medicine both fields are critical to understanding the tolerance limits of materials and situations in which those limits are approached as well as reconstructing the failure of equipment, implants, and bone (e.g., Eskul 1993; Fréchette 1990; Kim et al. 2008; Medvedovski 2010; Stevenson et al. 2001; Zioupos et al. 2006). Engineers use fractography and fracture mechanics to define the cause of fractures in equipment in normal use as well as those resulting from accidents and catastrophic events such as airplane explosions (e.g., Krishnan et al. 1993; Roylance 2001) and develop new products less prone to failure. In medicine and dentistry, for example, an understanding of the strength and fracture properties of pins, implants, and crowns and the bones or teeth they are used to repair is necessary. A similar understanding of the bone fracture properties and tolerance limits is often required in the safety design of a multitude of products, particularly those in the container, transportation, and military industries. Moreover, knowledge of bone fracture properties and fractographic features has also proven useful in accident reconstruction and industrial forensics where the fracture agent, cause, and contextual conditions are unknown. Fractography draws on knowledge of a material's physical properties, fracture mechanics, event context, fracture surface features, and

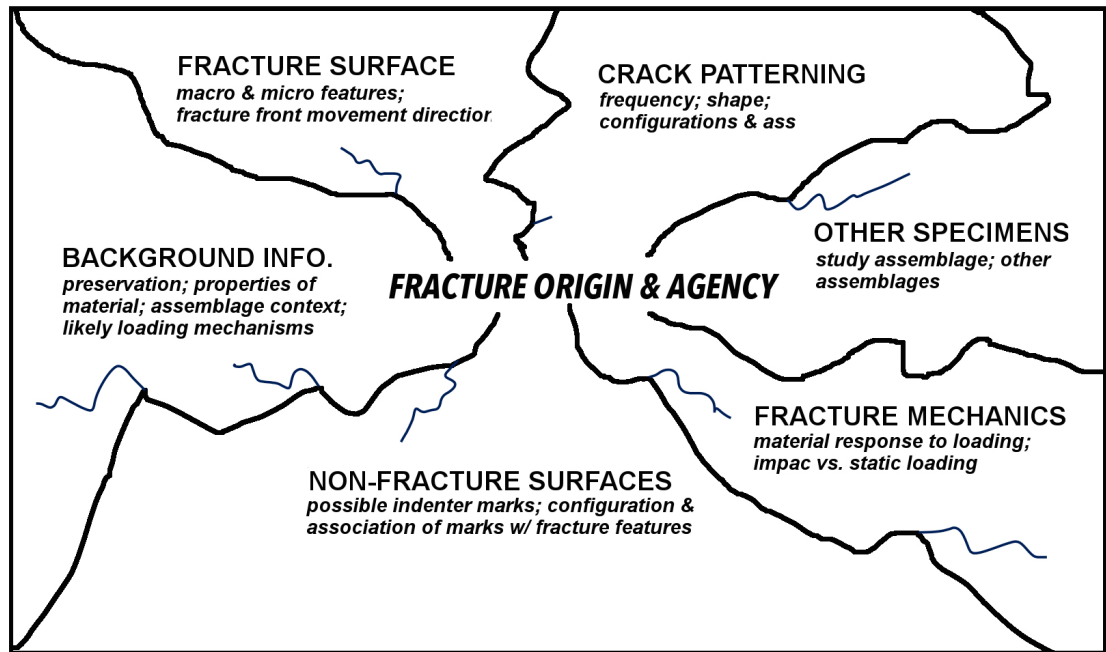


Fig. 2.1. Conceptual components of fractographic analysis (modified after Quinn 2007, Fig. 1.4).

comparative material. It is a holistic approach to understanding and interpreting the causes, origin, and agency of material failure (Fig. 2.1).

Notably, fractographers rarely attempt to quantify the frequency of features described here; the presence, absence, and expression of some features are taken as indicative of certain loading conditions. Fractographic analysis relies largely on visual, *subjective assessments* of fracture’s topographic features that seek to understand the context of the fracture event. As noted by Quinn (2007) fractographic analysis is to large degree a matter of pattern recognition. As noted by Quinn (2007: 2-3, 5) fractography

“...is often learned gradually and autodidactically by experience over many years [which may be] regard[ed] as a subjective practice...The reality is that...[it] is in fact objective and quantitative to an experienced fractographer....An important element of fractographic analysis is **pattern recognition**. Certain types of fracture leave telltale fracture patterns on the fracture surfaces, or in the breakage patterns or shapes of the fragments...markings may be more subtle and can be overlooked but *fractography is a cumulative learning experience*... step-by-step accumulation of experience is necessary. One may consult textbooks, reference articles, and even this Guide to help acquire knowledge, but there is no substitute for hands-on direct eyeball and microscopy experience.” (italics added)

As shown below, while some features are nearly diagnostic of carnivore static loading or

impact loading by hammerstones, it would be a mistake to treat the fractographic approach as a simple, “cookbook” method to the identification of bone fracture agent. It can do so, but its strength as outlined here lies with the tools it provides for understanding how the fracture surfaces, features, loading point characteristics, fragment size and shape, and surficial damages are inter-related. It is on this level of (experience-derived) pattern-recognition that most insights into bone fracture and assemblage creation are found.

Significantly, the fracture mechanics and fractographic literature indicates that regardless of the material involved (ceramics, glass, metal, or bone) impact- and static-loading because of their vastly different loading characteristics often yield different fracture patterns and fracture surface features (e.g., Quinn 2007). Broadly speaking, the basis for proposing that fractography and an understanding of fracture mechanics aids in identifying fracture features that are useful in diagnosing carnivore- from hammerstone-induced fractures, lies with differences in a) the amount of force or stress each agent can apply, b) the size of the indenter, c) the rate of load or stress application, and d) how the stress is dissipated. Stated another way, the visual analysis of bone fracture patterns and fractographic features, one structured by an understanding of fracture mechanics, the material, and context of the fracture event, permits assessment of the relative amount of force applied to bone and its manner of application. If the fracture features indicate high levels of force were applied, then impact fracture may be inferred.

That said, *few features discussed below are unequivocally diagnostic of hammerstone or carnivore fractured bone.* Impact- and static-loading do share some similar properties and can create some similar appearing fracture features. In cases where similar features are produced, it is the strength of their expression and their co-occurrence with certain other fracture features that allow *probabilistic statements* about the relative amount and manner of stress application, and thus by extension, fracture agent. It must be emphasized that to achieve more accurate estimates of hominin and carnivore involvement in a fragmented assemblage, the damages, however diagnostic they seem to be, cannot be

treated in isolation. Rather, it is more fruitful, although admittedly more difficult, to assess a suite of fracture features, their relationships to each other and other damages within an overall understanding of fracture mechanics, mechanisms behind feature creation, and bone as a material. Building this holistic framework of bone fracture is the focus of this chapter.

This chapter is divided into five main sections. The first section, *2.2 Bite Force and Impact Force Estimates*, establishes the considerable differences between the static loading inflicted by carnivore chewing and the impact loading created by hammerstone battering. It is often casually noted that static and impact loading are different (e.g., Bonnicksen 1979; Johnson 1985; Dominguez–Rodrigo and Barba 2007b): Static and impact loading are simply stated to be different with no definition or discussion of exactly what the differences mean. Here, the amount of loading created by static carnivore chewing and hammerstone impact are provided and discussed. This discussion of carnivore static and hammerstone impact loading establishes the necessary context for appreciating subsequent discussions.

The hierarchical structure of bone and its influence on fracture propagation and orientation are briefly summarized in the second section *2.3 Bone as a Material*. In the section, *2.4 Fracture Mechanics*, some fundamental principles of fracture mechanics of brittle materials are outlined. Particular detail is given to the differences between static and dynamic fracture in the amount and rate of loading, manner of energy dissipation in a propagating crack, and the role of indenters. The fractographic features, fracture patterns, and aspects of fragment size and shape resulting from static– and dynamic–loading are discussed in section *2.5 Fractographic Features*. Included in this section are, examples (images) of these fracture features and fracture patterns as they appear in fractured bone. Finally, the last section, *2.6 Summary and Expectations*, these discussions are summarized, in terms of differences in the frequencies fractographic features and fracture patterns expected to be observed in the four study assemblages.

2.2 Bite Force vs. Impact Force

It has been recognized for some time that carnivores load bone in a static manner whereas hammerstones do so dynamically (e.g., Bonnicksen 1979). Archaeological studies of bone fracture have not, however, been explicit why this difference is important. That is, with few exceptions and with limited detail (e.g., Bonnicksen 1979; Morlan 1980; Johnson 1985), zooarchaeological studies of bone fracture have given just cursory, or more often implied, acknowledgement of this difference. Just how different these loading modes are has not been stated. The relationships between the amounts of energy imparted, its mode of application, the manner in which strain is released, and the fracture features produced by each agent have not been explored. Here estimates of levels of force carnivore teeth and hammerstones apply are presented and discussed. Force is measured in Newtons (N). A Newton is the standard international unit of force where 1N is the amount of force required to accelerate a mass of one kilogram at a rate of one meter per second squared, ($1\text{N} = 1 \text{ kg}\cdot\text{m}/\text{s}^2$)

Although detailed in section 2.4 *Fracture Mechanics* below, it is useful here to briefly outline the major characteristics of static and impact loading to appreciate why their resultant applied forces are so different. Static and impact loading are two very different ways to create stress and impart energy to a material. Static loading is characterized by a) its gradual increase in load until b) a relatively constant rate of force application is attained, and c) the relatively long periods of time the load and material are in contact. The formula for calculating static loading force (F) is

$$F=m*a$$

where m is the mass of the object and a is its acceleration. Static loads are often applied in a cyclically and the material experiences elastic or quasi-plastic deformation (Lawn 1998).

In contrast, impact loading includes kinetic energy (the energy an object has because it is in motion) and therefore the load is applied instantaneously with a very short period of

contact. The contact period is usually estimated by the amount of material compression before failure. Thus, the formula for calculating impact-loading force

$$F=(1/2mv^2)/d$$

where m = mass of the moving object, v = the object's velocity, and d = the distance of its travel into the material before fracture.

As discussed in the above fracture mechanics and fractographic discussions, understanding many concepts and particularly the presence/absence and expression of many fracture features are dependent on the amount of energy (the capacity to do work) imparted to the material to propagate fracture (the work done). Although force (any influence that tends to change the motion of an object) is not energy, *it is a manifestation of energy*. This distinction between force and energy is important, but for purposes here (because among other reasons we know that carnivore and hammerstone forces can accomplish the work of fracture) it is possible to use force as a proxy for the relative amounts of energy carnivore static– and hammerstone impact loading impart to bone. Of course, a number of variables may influence both the amount of force each may apply (animal strength, age, dental health, teeth used to exert force, tooth and hammerstone geometry and size, level of hunger, etc.) to bone as well as the amount of force required to break a particular bone (age, density, geometry, etc.). Although these variables may be important in determining the force or energy used to break a particular bone by a particular carnivore or a particular hammerstone, they need not be considered to define the potential forces each agent may apply.

What should be kept in mind is that that similar bite force (BF) estimates for two or more different taxa, e.g., large felids and hyaenas, does not necessarily indicate similar abilities to fracture bone. Tooth geometry is obviously one important variable; felids have relatively slender, blade–like carnassials, whereas those of hyaenas are more robust and conical. Jaw gape (the distance between canine tips in an open jaw) is another particularly important variable because it defines the size of the object that can be easily chewed. Thus,

one of the reasons why extant felids are not known for habitual bone-crunching behaviour is that their gape is smaller than that of hyaenas. For example, the gape of *C. crocuta*, has been measured as 151mm while that of *P. leo* is 91mm (Christiansen and Adolfssen 2005).

Here the amount of force in Newtons (N) generated by extant and extinct carnivores, a reptile, and a few primates in static-loading are listed and compared to those generated by hammerstone impact. It is shown that carnivores apply relatively low forces while hammerstones can apply a much greater force, often by orders of magnitude. These data serve to bound the problem of characterizing fractures generated by relatively small and relatively large amounts of energy as defined in the fracture literature (see below).

2.2.1 Bite Force Estimates

Bite force (BF), measured in Newtons (N), in vertebrates has been estimated in a variety of ways. Direct measurements are made using force transducers (“bite bar”) or hydraulic occlusal gauges to measure the BF of living and awake animals (Abu Alhija et al. 2010; Binder and Van Valkenburgh 2000; Binder pers. comm. 2004; Lindner et al. 1995). Most bite forces for extant (Christiansen and Wroe 2007; Thomason 1991; Wroe et al. 2005) and extinct (Wroe et al. 2005) taxa have been estimated by reconstructing musculature in 2D measuring physiological cross sectional area to provide an estimate of muscle force, and then calculating BF from jaw geometry using lever mechanics, i.e., the “dry skull” method). Estimates may also be calculated by constructing 3D models and performing finite element analysis (Wroe et al. 2010).

Published bite force estimates (at the carnassials) for vertebrates are summarized in Table 2.1. Although the estimation techniques vary, and the ranges are wide for any given taxon, where different studies have examined the same taxon, the BF estimates are broadly similar. For example, the dry skull method has yielded similar BF estimates for *V. vulpes* (304.0N, 298.4N, and 239.0N), *A. jubatus* (736.0N, 635.1N, 475.1N, and 509.1N), and *P. onca* (1755.0N, 1253.6N, 1348.0N, and 1361.2N), among others. Variability is notable, however. *P. leo* estimates range from a low mean of 1833.1N (Christiansen 2007) to a

single high estimate of 3405.4 (Christiansen and Adolfssen 2007). Even where different techniques are used, the estimates are similar. Using a hydraulic force meter Lindner et al. (2005) report a mean BF of 474.5N (± 323.8) for *C. familiaris* breeds weighing >34kg while using the dry skull method Christiansen & Wroe 2007 report a single estimate of 549.8N. Two of three *C. crocuta* single BF estimates using the dry skull method given by Wroe et al. (2005; 1569.0N) and Christiansen and Adolfssen (2007; 1421.6N) are close to (and are within one standard deviation of) the mean of 1706.8N (± 873.0) observed by Binder (pers. com. 2004; see Binder and Van Valkenburgh 2000) for fully adult animals (greater than 60 months in age, the age they achieve their maximum bite force potential) using a bite bar. Christiansen and Wroe's (2007) lower dry-skull estimate of 985.5N, however, is close to Binder's mean BF estimate of 1224.1N (± 817.7) when 20–60 month old animals are included. Further, the maximum BF of about 4510.5N observed by Binder and Van Valkenburgh (2000, Fig. 3) may well be an outlier. The overwhelming majority (35 of 40) of adult spotted hyaena bite-forces are well below 2000N.

Of the extant African carnivores for which bite forces have been estimated, six produce bite forces of over 1000N (Fig. 2.2). The mean of all estimates for *P. leo* is 2586.8N (range = 1833.1 – 3405.4N), the largest of the extant African carnivores. The mean of all *C. crocuta* estimates is 1189N, an estimate remarkably close to that of an adult BF of 1180N derived from Binder and Van Valkenburgh's (2000) regression equation. In addition to *C. crocuta* and *P. leo*, maximum bite forces of over 1000N have been estimated for *H. brunnea* (1223N), *P. pardus* (1377N), *H. hyaena* (1097N) and *C. familiaris* (1394N).

The bite forces of only a few extinct African Plio–Pleistocene carnivores have been estimated using the dry skull method. All are felids and only the *Machairodus* sp. BF estimate exceeds 1000N (1741.9N = mean of *M. aphanistus* and *M. giganteus*; Christiansen 2007). *Homotherium* sp., *Megantereon* sp. and *Metailurus* sp. BF estimates are 780.1, 488.3, and 529.1N, respectively. To these may be added *crude* estimates for

Dinofelis sp., *Pachycrocuta brevirostrus*, and *Crocuta* sp. (*dietrichi* & *ultra*) by using the body sizes of similar extant carnivores. Most *Dinofelis* sp., material, for example, is larger than *P. pardus* but smaller than *P. leo* (Werdelin and Lewis 2001). Using the mean *P. pardus* BF and an estimated weight of 149kg for *Dinofelis* sp., the size of a small lion or tiger (Legendre and Roth (1988) or about 1.7 times the weight of a large *P. pardus*, a mean *Dinofelis* sp. BF of 1712.5N is seems reasonable. Bite forces of 3585.6N for *P. brevirostrus*, 2121.5N for *Crocuta* sp. (*dietrichi* & *ultra*), 757.0N for *Chasmaporthetes nitidula*, and 1662N for *Canis lycoanoides* are based on their estimated weights of 150kg (Dennell et al. 2008), 80kg, ~35kg (Turner 1990), and 80kg (Hemmer 2000), respectively.

Although estimates do not exist for African crocodiles, the American alligator (*Alligator mississippiensis*) has a bite–force of about 9500 N, the greatest bite–force of any living animal yet measured (Erickson et al. 2003). It is likely the Nile crocodile (*Crocodylus niloticus*) is capable of applying very similar if not a greater force. It is also interesting to note human BF estimates. Modern urban human bite forces measured with bite bars have yielded estimates of 430.2N (Pruim et al. 1980), 564.4N (van Eijden 1991), 464.7N (Radsheer et al. 1999), and 573.4N (Abu Alhaija et al. 2010); all overlap by one standard deviation. Bite force estimates for hunter–gatherers seem to be considerably greater. Finite element analysis of a female Kung! San skull yielded an estimate of 1317N (Wroe et al. 2010) and the mean BF of a large sample of the Inuit Eskimo is reported to be 1235N (Waugh 1937). It is unclear, however, if these are bilateral or unilateral estimates. If they were in fact based on unilateral measurements halving the published values would bring them into line with the unilateral bite–bar estimates. The *P. boisei* BF estimate of 2161N as well as that of 831N for *A. africanus* seem reasonable given their differences in body size and dentition.

Table 2.1. Published bite force estimates in Newtons (N) for extant and extinct (†) carnivores, marsupials, primates, and the alligator. African taxa are shown in bold. Bite forces for extinct African carnivores given in italics are very rough estimates based on similarity of their estimated weights with extant carnivores of a similar species and the bite force of the similar extant taxa. See the footnotes and text for explanations of specific estimates.

Taxa	Common Name	min	max	mean		ref.
					±1sd	
MAMMALIA: Primates						
	<i>Homo sapiens</i>	286.0	654.0	430.2±146.1		1
	"	424.0	749.0	564.4±89.9		2
	"	186.0	888.0	464.7		3
	"		1317.0			4
	"	290.0	965.0	573.4±140.2		5
	"			1235.0		6
	<i>Pan troglodytes</i>		1511.0			4
	<i>Gorilla gorilla</i>		1723.0			4
	<i>Pongo pygmaeus</i>		1031.0			4
	<i>Hylobates lar</i>		136.0			4
	<i>Australopithicus africanus</i> †		831.0			4
	<i>Paranthropus boisei</i> †		2161.0			4
MAMMALIA: Carnivora						
Canidae						
	<i>Alopex lagopus</i>		322.0			7
	"		203.7			8
	"		138.0			9
	<i>Atelocynus microtis</i>		295.5			9
	<i>Canis adustus</i>		233.2			9
	<i>Canis aureus</i>		217.9			9
	<i>Canis dirus</i> †		1577.0			7
	<i>Canis familiaris</i>	85.0	1394.0	474.5±323.8		10
	"		549.8			9
	<i>Canis latrans</i>		554.0			7
	"		289.6			9
	<i>Canis lupus dingo</i>		555.0			7
	<i>Canis lupus hallstromi</i>		487.0			7
	<i>Canis lupus lupus</i>		1033.0			7
	"		1262.3			8
	"		773.9			9
	<i>Canis (Xenocyon) lycoanoides</i> †		1262.0			13
	<i>Canis mesomelas</i>		187.5			9
	<i>Cerdocyon thous</i>		182.7			8
	"		178.2			9
	<i>Chrysocyon brachyurus</i>		725.3			8
	"		510.8			9
	<i>Cuon alpinus</i>		541.0			7
	"		379.0			8
	"		397.9			9
	<i>Fennecus zerda</i>		55.8			8
	"		64.8			9
	<i>Lycalopex vetulus</i>		130.5			8
	"		133.5			9
	<i>Lycaon pictus</i>		694.0			7
	"		854.0			8
	"		556.8			9
	<i>Nyctereutes procynoides</i>		108.9			8
	"		145.9			9
	<i>Otocyon megalotis</i>		86.6			8
	"		111.3			9
	<i>Pseudalopex culpaeus</i>		258.5			9

Table 2.1. continued.

Taxa	Common Name	min	max	mean ±1sd	ref.
<i>Pseudalopex griseus</i>	S. Am. Gray Fox		223.4		9
<i>Pseudalopex gymnocerus</i>	Pampas Fox		205.4		8
"	"		177.5		9
<i>Speothos venaticus</i>	Bush Dog		272.0		8
"	"		233.5		9
<i>Urocyon cinereoargenteus</i>	Grey Fox		198.0		7
"	"		134.1		9
<i>Vulpes bengalensis</i>	Bengal Fox		127.6		9
<i>Vulpes chama</i>	Cape Fox		134.0		9
<i>Vulpes ferrilata</i>	Tibetan Sand Fox		214.5		9
<i>Vulpes pallida</i>	The Pale Fox		94.9		9
<i>Vulpes rueppelli</i>	Rüppell's Fox		99.6		9
<i>Vulpes velox</i>	Swift Fox		141.5		9
<i>Vulpes vulpes</i>	Red Fox		304.0		7
"	"		298.4		8
"	"		239.0		9
Felidae					
<i>Acinonyx jubatus</i>	Cheetah		736.0		7
"	"		635.1		8
"	"		475.1		11
"	"		509.1		9
<i>Caracal caracal</i>	Caracal		203.8		8
"	"		251.4		9
<i>Catopuma temminckii</i>	Asian Golden Cat		309.0		9
<i>Felis catus</i>	Domestic Cat		118.1		9
<i>Felis chaus</i>	Jungle Cat		294.6		8
"	"		181.7		9
<i>Felis margarita</i>	Sand Cat		155.4		9
<i>Felis nigripes</i>	Black-footed Cat		92.9		9
<i>Felis silvestris</i>	Wildcat		105.0		7
"	"		152.6		9
<i>Herpailurus yaguarondi</i>	Jaguarundi		227.0		7
"	"		104.6		8
"	"		129.7		9
<i>Leopardus geoffroyi</i>	Geoffroy's Cat		180.8		8
"	"		169.4		9
<i>Leopardus pardalis</i>	Ocelot		256.9		8
"	"			301.2	11
"	"		306.0		9
<i>Leopardus tigrinus</i>	Oncilla		110.4		8
"	"		97.2		9
<i>Leopardus wiedii</i>	Tree Ocelot		112.6		8
"	"		101.4		9
<i>Leptailurus serval</i>	African Serval		223.2		8
"	"			271.3	11
"	"		263.3		9
<i>Lynx canadensis</i>	Canada Lynx		225.3		9
<i>Lynx lynx</i>	Eurasia Lynx		454.9		8
"	"			329.7	11
"	"		310.2		9
<i>Lynx rufus</i>	Bobcat		162.0		7
"	"		289.1		9
<i>Neofelis nebulosa</i>	Clouded Leopard		1051.0		7
"	"		587.8		8
"	"			547.4	11
"	"		544.3		9
<i>Oncifelis colocolo</i>	Pampas Cat		196.9		9
<i>Oncifelis guigna</i>	Kodkod		114.6		9
<i>Otocolobus manul</i>	Pallas's Cat		155.4		9

Table 2.1. continued.

Taxa	Common Name	min	max	mean ±1sd	ref.
<i>Panthera leo</i>	African Lion		3085.0		7
"	"		3405.4		8
"	"		1833.1		11
"	"		2023.7		9
<i>Panthera onca</i>	Jaguar		1755.0		7
"	"		1253.6		8
"	"		1361.2	1348.0	11
"	"		837.0		9
<i>Panthera pardus</i>	Leopard		837.0		7
"	"		1376.8		8
"	"			851.1	11
"	"		964.4		9
<i>Panthera tigris</i>	Tiger		2789.0		7
"	"		3007.2		8
"	"			1839.0	11
"	"		2164.7		9
<i>Panthera uncia</i>	Snow Leopard		884.8		8
"	"			556.8	11
"	"		603.5		9
<i>Pardofelis marmorata</i>	Marbled Cat		151.4		8
"	"		185.3		9
<i>Prionailurus bengalensis</i>	Leopard Cat		93.7		8
"	"		94.4		9
<i>Prionailurus planiceps</i>	Flat-headed Cat		172.4		8
"	"		145.1		9
<i>Prionailurus rubiginosus</i>	Rusty-spotted Cat		108.6		9
<i>Prionailurus viverrinus</i>	Fishing Cat		255.6		9
<i>Profelis aurata</i>	African Golden Cat		281.5		8
"	"		336.6		9
<i>Puma concolor</i>	Mountain Lion		864.0		7
"	"		905.6		8
"	"			775.4	11
"	"		773.2		9
<i>Smilodon fatalis</i> †	dirk-tooth cat		1933.0		7
"	"		1528.6		11
<i>Dinofelis sp.</i> †	false saber-tooth cat		1712.5		17
<i>Smilodon populator</i> †	dirk-tooth cat		1649.7		11
<i>Homotherium crenatidens</i> †	saber-tooth cat		798.7		11
<i>Homotherium latidens</i> †	saber-tooth cat		754.8		11
<i>Homotherium serum</i> †	saber-tooth cat		786.8		11
<i>Machairodus aphanistus</i> †	saber-tooth cat		1714.4		11
<i>Machairodus giganteus</i> †	saber-tooth cat		1769.3		11
<i>Megantereon cultridens</i> †	dirk-tooth cat		494.9		11
<i>Megantereon sp.</i> †	dirk-tooth cat		481.7		11
<i>Metailurus major</i> †	false saber-tooth cat		682.7		11
<i>Metailurus parvulus</i> †	false saber-tooth cat		375.4		11
Herpestidae					
<i>Bdeogale crassicauda</i>	Bushy-tailed Mongoose		90.2		9
<i>Crossarchus platycephalus</i>	Flat-headed Kusimanse		63.0		9
<i>Cynictis penicillata</i>	Yellow Mongoose		56.6		9
<i>Galidia elegans</i>	Ring-tailed Mongoose		58.4		9
<i>Herpestes auropunctatus</i>	Small Indian Mongoose		46.8		9
<i>Herpestes edwarsi</i>	Indian gray mongoose		75.2		9
<i>Herpestes fuscus</i>	Indian Brown Mongoose		80.9		9
<i>Herpestes ichneumon</i>	Egyptian Mongoose		148.5		9
<i>Herpestes pulverulentus</i>	Cape Grey Mongoose		54.3		9
<i>Ichneumia albicauda</i>	White-tailed Mongoose		104.7		9
<i>Mungos mungo</i>	Banded Mongoose		53.7		9
<i>Rhynchogale melleri</i>	Meller's Mongoose		86.0		9

Table 2.1. continued.

Taxa	Common Name	min	max	mean ±1sd	ref.
	<i>Salanoia concolor</i>			52.4	9
Hyaenidae					
	<i>Pachycrocuta brevirostris</i> †			3585.6	14
	<i>Crocuta</i> spp. (<i>dietrichi</i> & <i>ultra</i>)			2121.5	15
	<i>Crocuta crocuta</i>	291.4	4510.5	1706.8±873.0	12
	"			1569.0	7
	"			1421.6	8
	"			985.5	9
	<i>Hyaena brunnea</i>			1222.8	8
	"			1029.6	9
	<i>Hyaena hyaena</i>			1097.0	7
	"			1041.5	8
	"			889.2	9
	<i>Chasmaporthetes nitidula</i>			757.0	16
Mustelidae					
	<i>Aonyx capensis</i>			348.0	9
	<i>Aonyx cinerea</i>			113.3	9
	<i>Conepatus humboldti</i>			76.1	9
	<i>Conepatus semistriatus</i>			80.2	9
	<i>Eira barbera</i>			243.4	9
	<i>Enhydra lutris</i>			394.2	9
	<i>Galictis cuja</i>			85.8	9
	<i>Gulo gulo</i>			408.3	8
	"			348.5	9
	<i>Ictonyx striatus</i>			72.2	9
	<i>Lutra canadensis</i>			219.7	9
	<i>Lutra felina</i>			152.0	9
	<i>Lutra longicaudis</i>			189.8	9
	<i>Lutra lutra</i>			216.0	9
	<i>Lutra maculicollis</i>			141.8	9
	<i>Lutra perspicillata</i>			306.8	9
	<i>Lutra sumatrana</i>			151.6	9
	<i>Martes americana</i>			70.0	9
	<i>Martes flavigula</i>			121.5	9
	<i>Martes foina</i>			98.9	9
	<i>Martes martes</i>			116.6	9
	<i>Martes pennanti</i>			184.3	9
	<i>Meles meles</i>			349.0	7
	"			255.2	8
	"			282.2	9
	<i>Mellivora capensis</i>			317.7	9
	<i>Melogale everetti</i>			71.4	9
	<i>Mephitis macrura</i>			61.9	9
	<i>Mephitis mephitis</i>			99.9	9
	<i>Mustela africana</i>			21.1	9
	<i>Mustela altaica</i>			32.2	9
	<i>Mustela erminea</i>			30.4	9
	<i>Mustela frenata</i>			22.8	9
	<i>Mustela lutreola</i>			46.0	9
	<i>Mustela nivalis</i>			18.4	9
	<i>Mustela putorius</i>			88.0	9
	<i>Mustela vison</i>			58.5	9
	<i>Mydaus javanensis</i>			58.2	9
	<i>Poecilictis libyca</i>			28.4	9
	<i>Pteronura brasiliensis</i>			614.3	9
	<i>Taxidea taxus</i>			322.8	8
	"			316.6	9

Table 2.1. continued.

Taxa	Common Name	min	max	mean ±1sd	ref.
Procyonidae					
	<i>Ailurus fulgens</i>			335.9	8
	"			244.9	9
	<i>Bassaricyon alleni</i>			87.5	9
	<i>Bassaricyon gabbii</i>			91.7	9
	<i>Bassariscus astutus</i>			87.1	9
	<i>Bassariscus sumichrastris</i>			116.3	9
	<i>Nasua nasua</i>			87.1	8
	"			133.4	9
	<i>Nasuella olivacea</i>			64.1	9
	<i>Potos flavus</i>			128.3	9
	<i>Procyon cancrivorus</i>			267.5	8
	"			237.7	9
	<i>Procyon lotor</i>			176.4	8
	"			176.7	9
Ursidae					
	<i>Ailuropoda melanoleuca</i>			1815.9	9
	<i>Tremarctos ornatus</i>			1536.8	8
	"			946.6	9
	<i>Ursus americanus</i>			758.0	7
	"			1174.1	8
	"			1003.6	9
	<i>Ursus arctos</i>			1180.0	7
	"			1417.6	8
	"			1894.9	9
	<i>Ursus malayanus</i>			1441.7	8
	"			1189.6	9
	<i>Ursus maritimus</i>			2403.9	8
	"			2349.6	9
	<i>Ursus thibetanus</i>			706.0	7
	"			819.8	8
	"			1135.7	9
	<i>Ursus ursinus</i>			708.9	8
	"			712.0	9
Viverridae					
	<i>Arctictis binturong</i>			356.7	8
	"			351.2	9
	<i>Arctogalidia trivirgata</i>			139.8	9
	<i>Civettictis civetta</i>			148.4	8
	"			231.3	9
	<i>Cryptoprocta ferox</i>			239.7	9
	<i>Cynogale bennettii</i>			192.8	9
	<i>Eupleres goudotti</i>			50.0	9
	<i>Fossa fossa</i>			110.8	9
	<i>Genetta genetta</i>			88.4	8
	"			132.3	9
	<i>Gennetta tigrinus</i>			265.0	7
	<i>Macrogalidia musschenbroeki</i>			270.5	9
	<i>Nandinia binotata</i>			54.1	8
	"			116.4	9
	<i>Paguma larvata</i>			177.6	9
	<i>Paradoxurus hermaphroditus</i>			123.2	9
	<i>Prionodon linsang</i>			57.9	9
	<i>Viverra megaspila</i>			226.9	9
	<i>Viverra zibetha</i>			163.3	9
	<i>Viverra zibetha</i>			192.3	9
	<i>Viverricula indica</i>			75.5	8
	"			101.1	9

Table 2.1. continued.

Taxa	Common Name	mean			ref.	
		min	max	±1sd		
MAMMALIA: Marsupilia						
Dasyuridae						
	<i>Dasyurus maculatus</i>		308.0		7	
	<i>Dasyurus viverrinus</i>		123.0		7	
	<i>Sarcophilus harrisii</i>		553.0		7	
Thylacinidae						
	<i>Nimbacinus dicksoni</i> †	Thylacine Marsupial	465.0		7	
	<i>Thylacinus cynocephalus</i>	Tasmanian Tiger	1176.0		7	
Thylacoleonidae						
	<i>Priscileo roskellyae</i> †	diprotodont marsupial	227.0		7	
	<i>Wakaleo vanderleurei</i> †	"Marsupial Lion"	875.0		7	
	<i>Thylacoleo carnifex</i> †	"Pouch Lion"	2102.0		7	
	<i>Thylacosmilus atrox</i> †	"Pouch Sabre"	658.0		7	
REPTILIA: Crocodylia						
Alligatoridae						
	<i>Alligator mississippiensis</i>	American Alligator	217.0	13172.0	6803.0	13

1: Pruim et al. 1980. Measurements of modern urban individuals taken with a force transducer (bite bar) at P1, M1, and M2. Values given here reflect the sum of the M1 and M2 measurements divided by 2 because the published data sum of left and right side bite-force measurements.

2: van Eijden 1991, Table 1. Measurements of modern urban individuals taken at 17 different bite positions with a force transducer at the I1, PM2, and M2 . Values shown here are the mean of the PM2 and M2 values.

3: Radseer et al. 1999, Table 5A. Measurements of modern urban individuals taken with a force transducer at the P2 and M1. Values given here are the average of means for males and females, and the associated minimum and maximum values.

4: Wroe et al. 2010, Fig. 3a .Bite-force modelled using finite element analysis. Maximum bite force measured at the M2. The human is a Kung! San female.

5: Abu Alhaija et al. 2010, Table . Bite force measurements taken with hydraulic force meter at the M1. Estimates represent the two largest bite forces in trials of six per individual.

6: Waugh 1937 (cited by Wroe et al. 2010). Value given is mean of a large sample of Inuit Eskimo.

7: Wroe et al. 2005. Bite-force at the carnassial estimated using "dry skull" method.

8: Christiansen and Adolfssen 2005. Carnassial bite force estimated using "dry skull" method.

9: Christiansen and Wroe 2007, Table 1. Bite-force estimated using "dry skull" method. Bite force values given here are for the carnassials; canine bite force values are not included.

10: Lindner et al. 1995, Table 1. Bite-force measurements taken with a hydraulic force meter. Only the bite-force measurements (n= 29) for five dogs weighing over 34kg are given above.

11: Christiansen 2007. Bite forces at the carnassials for extant felids are the means of several skulls (cheetah, 9; ocelot,13; serval, 10; European Lynx, 12; Puma, 10; Clouded Leopard, 12; Jaguar, 9; Leopard, 8; Tiger, 14; Snow Leopard, 9). Values for extinct taxa are based on single skulls.

Table 2.1. continued.

12: Binder pers. com. 2004; Binder & Van Valkenburgh 2000. Bite force data provided by Binder pers. com. (2004) and methods discussed by Binder and Van Valkenburgh (2000). Bite force measured with transducers (bite bar). The maximum of incisor and carnassial bite forces recorded; nearly all are likely carnassial bite force values. Values shown here are based on fully adult animals > 60 months in age (n = 20; range = 291.4 - 4510.5N). The sample size, mean, standard deviation, and range values for other age groups are a) <12 months (weaned) 19, 391.0, 627.9, 28.8 - 2918.0, b) 12 - 20 months (permanent dentition in place and skull growth stops) 64, 371.0, 105.2, 94.0 - 547.1, and c) 20 - 60 months (bite force increases dramatically) 20, 741.5, 346.5, 328.6 - 1356.7.

13: Hemmer (2000) states size is comparable to large modern European wolf, *C. lupus* (80kg; Heptner & Naumov 1998).

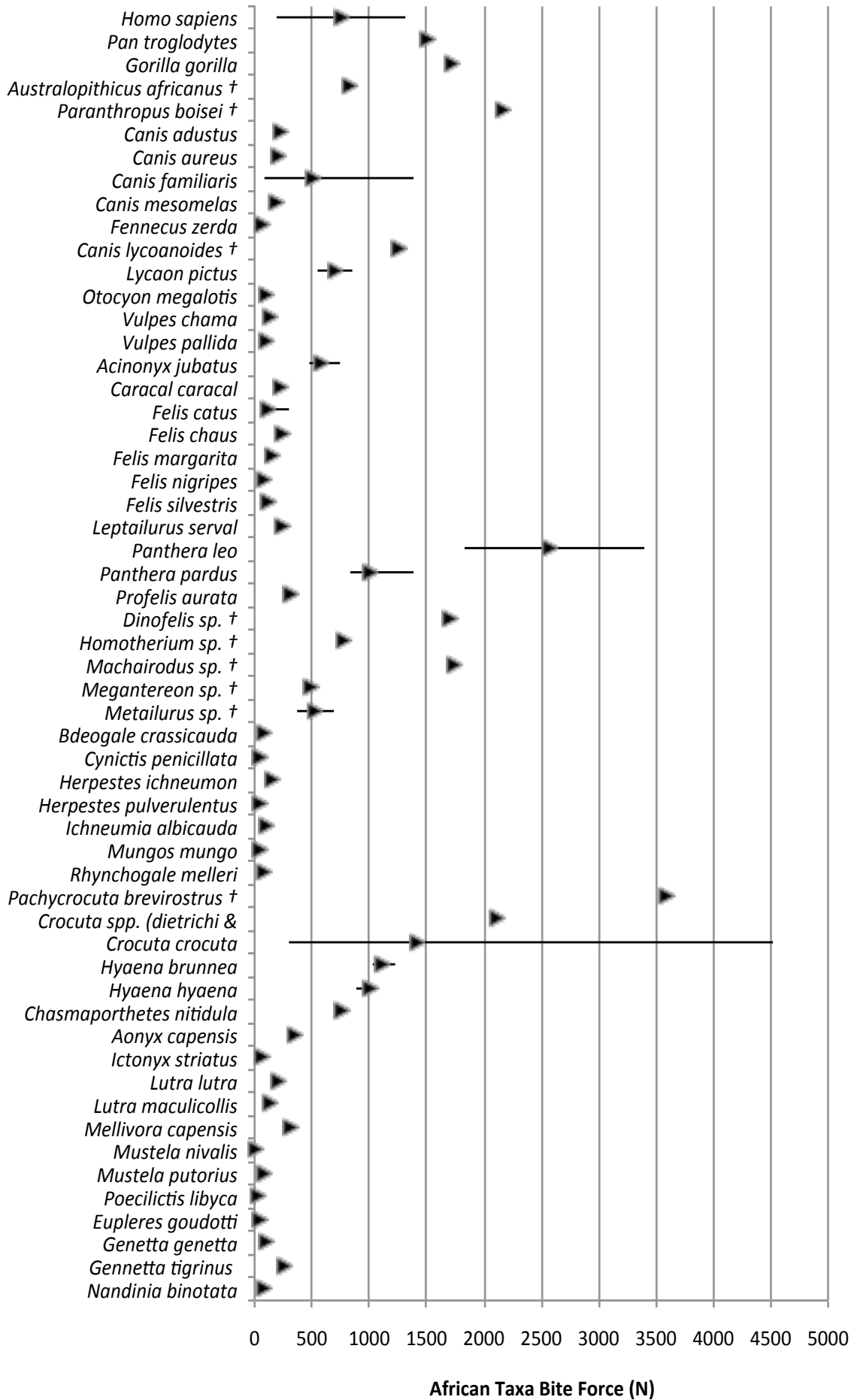
14: Dennell et al. (2008) gives the weight of *P. brevirostrus* as 150kg, but Palmqvist et al. (2011) using regression analysis of various extant hyaenid measurements estimate the weight to be 110kg. Although not directly equivalent to bite force, Palmqvist et al. (2011) estimate the bite strength of *P. brevirostrus* to be similar to that of *P. tigris* (mean = 2654N). This estimate is, however, similar to the common bite force measured by Binder (pers. comm.). The bite force for *P. brevirostrus* estimated here is calculated as the mean maximum *C. crocuta* bite force (2121.5N) times the weight difference ($110/65 = 1.69$).

15: Turner (1990) notes that the size of *C. dietrichi* and *C. ultra* are within the range of variation for modern *C. crocuta*. Thus, estimate of *Crocuta* sp. bite force given here is the mean of maximum *C. crocuta* bite forces values.

16: Turner (1990) notes that *Chasmaporthetes* dentition is smaller than most hyaenas, that the pre-molars lack the large cones present in other hyaenas, and overall look like cheetah teeth. The weight of (~41kg) and bite force are estimated to be 75% that of a large *H. hyaena*.

17: Anyonge (1993) gives an estimated weight of 80 - 100kg, but Legendre & Roth (1988) give an estimated weight of 149kg for *D. abeli*, which is 1.7 times the weight of *P. pardus*. The bite force of *Dinofelis* is estimated to be 1.7 times that of the mean for *P. pardus*.

Fig. 2.2. The means (triangles) and range (line) of estimated bite forced (N) for African taxa. Data and references given in Table 2.1.



2.2.2 Hammerstone Impact Force Estimates

Although the force of hammerstone and anvil breakage of bone has not been measured, it may be estimated with the impact force formula given above, $F=(1/2mv^2)/d$ (where m = mass of the hammerstone, v = hammerstone velocity, and d = the distance of hammerstone travel (into the bone in meters) before fracture). The resulting force in Newtons (N) is an average of the forces applied. The actual forces are often much greater in rigid or brittle materials because the change in kinetic energy and material failure is nearly instantaneous. That is, the velocity of the impactor stops almost immediately upon striking the object. The distance the impactor travels into the object is an accepted proxy for the time it takes for velocity to reach zero. For hammerstone impacts all of these variable values are known, or can be accurately estimated.

Weights of hammerstones (m) used in experimental bone breakage and flint knapping are given in Table 2.2. Excluding Bonnicksen's (1979) use of a very heavy 5.7kg hammerstone, the mean hammerstone weight used in this set of experimental studies is 0.9kg. Oldowan lithics from FLK–Zinj variously classified as hammerstones, non-modified stones (aka manuports), cores, and cores with fracture angles (de la Torre and Mora 2005; Mora and de la Torre 2005) that potentially could have been used to break bone have a mean weight of 0.33kg. By comparison, the potential bone smashing tools in the ST complex at Peninj (de la Torre et al. 2003) have a mean weight of 0.46kg. Overall the FLK–Zinj and Peninj hammerstones have a mean weight of .39kg (\pm .09kg). Thus, a reasonable weight of Oldowan hammerstones seems to be 0.3 – 0.5kg.

Hammerstone velocity (v) may be estimated with measured velocities of hammerstones used in lithic manufacture (Dapena et al. 2006), and those of karate and boxing punches (Atha et al. 1985; Nakayama 1966; Smith and Hamill 1986; Vos and Binkhorst 1966; Walilko et al. 2005; Walker 1975) whose velocities likely bound the upper limits of hammerstone velocity. Based on these data hammerstone velocities are

estimated to have a range of 4.7 – 13.5m/sec. The mean of 9.5 ± 1.7 m/sec is taken to be the likely range of hammerstone velocities (Table 2.3).

Like the impact of a hard object on other brittle materials, the distance (or time) of hammerstone travel into bone before fracture (d) is no doubt small. Rather than assume instantaneous failure at impact, however, a distance of between 0.5 and 1.5mm is estimated based on the measured depth of percussion marks created in this study. Many were less than 0.5mm and none were greater than 1.0mm in depth. Low d estimates seem most reasonable given the small depth of percussion marks observed in bone breakage experiments presented here. Stopping distances of 2.0mm are likely extreme over-estimates, but are included here to conservatively bound expected impact forces. The mean impact force of various hammerstone weights and velocities where d is 0.05 – 1.5mm are presented in Table 2.4. Additionally, the experience of this author as well as Plummer (pers. com. 2010) is that even when an impact breaks bone, the hammerstone will rebound off of the bone, a response that indicates a nearly instantaneous change in hammerstone velocity. These estimates indicate that under most conditions hammerstones easily deliver forces of several thousand Newtons. The mean of all calculated impact forces for these 0.3 – 0.5kg hammerstones at velocities of 7.5 – 11.0m/sec easily exceeds the maximum force observed for a mammalian carnivore, 4510N for *C. crocuta* (Binder and Van Valkenburgh 2000) by orders of magnitude (Fig. 2.3).

Only when d is defined as very large (3.0 – 2.0mm) do small hammerstones (0.3 – 0.4kg) with low velocities (7.5 – 8.5m/sec) overlap the maximum-recorded mammalian bite force (asterisks in Figure 2.3). On average, hammerstone impact forces (black circles in Fig. 2.3) are estimated to be between 4.8 (6890N) and 17.4 (24704N) times those typically produced by adult spotted hyaenas (1420N). The bite force estimates for large extinct felids and hyaenas are also considerably smaller than the mean hammerstone impact forces. Although crude, even the giant short-faced hyaena (*P. brevirostrus*) bite force estimate of 3586N given here is only slightly larger than the impact force created by

Table 2.2. Select experimental and Oldowan site hammerstone, manuport, and core weights.

Assemblage	Wght (kg)	Reference
Experimental		
hammerstone	5.70	Bonnichsen 1979
hammerstone	0.75	Bunn 1989
hammerstone	0.95	Rolian et al. 2011
hammerstone	0.85	this study
hammerstone	1.00	Plummer pers. com.
hammerstone	0.63	Dapena et al. 2006
<i>mean experimental "hammerstone"</i>	0.84	
FLK-Zinj		
non-modified stones (manuports)	0.29	de la Torre and Mora 2005
cores	0.26	de la Torre and Mora 2005
hammerstones w/ fracture angle	0.40	Mora and de la Torre 2005
hammerstones	0.38	Mora and de la Torre 2005
Peninj ST Complex		
manuport	0.53	de la Torre et al. 2003
cores	0.42	de la Torre et al. 2005
hammerstones	0.44	de la Torre et al. 2004
<i>mean Oldowan "hammerstone"</i>	0.39	
<i>st.dev.</i>	0.09	
<i>range</i>	.26 - .53	

Table 2.3. Estimated velocities (m/s) of karate and boxing punches, and hammerstone blows.

Punch/Hammerstone/Hammer: Reference	Mean	StDev	Range
<i>Karate/Boxing Punch</i>			
Atha et al. 1985	8.90	-	-
Cesari & Bertocco 2008	6.54	2.12	3.87 - 9.74
Nakayama 1966	8.65	-	4.7 - 12.6
Neto et al. 2007	5.99	1.39	4.9 - 7.6
Pieter and Pieter 1995	9.67	3.36	6.0 - 16.26
Smith and Hamill 1986	11.50	0.66	10.48 - 12.34
Voigt 1989	9.50	-	8.2 - 10.7
Vos and Binkhorst 1966	12.51	1.48	10.8 - 14.2
Walilko et al. 2005	9.14	2.06	6.1 - 11.7
Walker 1975	~7.0	-	-
<i>mean punch</i>	9.16	2.07	3.87 - 16.26
<i>Hammerstone</i>			
Dapena et al. 2006	9.45	0.90	8.8 - 10.1
<i>mean hammerstone</i>			
Overall			
<i>mean</i>	9.18	1.85	3.87 - 16.26

Table 2.4. Impact force in Newtons (N) for the mean (± 1 stdev.) of hammerstone weight (see Table 2.2), velocities (see Table 2.3), and post-impact travel distances here estimated to be at a maximum of 3.0 - 0.5mm. An impact travel distance of 1.5 - 0.5mm is judged to be the best estimate for travel distance into bone based on the depths of impact marks in the EXP assemblage that never exceed 1.0mm.

Hstn wght @ velocity	Mean Impac Force (N)		
	@ 3.0 - 2.0mm	@ 1.5 - 0.5mm	@ 3.0 - 0.5mm
0.3kg @ 7.5m/s	3468.8	10312.5	6890.6
0.3kg @ 8m/s	3946.7	11733.3	7840.0
0.35kg @ 7.5m/s	4046.9	12031.3	8039.1
0.3kg @ 8.5m/s	4455.4	13245.8	8850.6
0.35kg @ 8m/s	4604.4	13688.9	9146.7
0.4kg @ 7.5m/s	4625.0	13750.0	9187.5
0.3kg @ 9m/s	4995.0	14850.0	9922.5
0.35kg @ 8.5m/s	5198.0	15453.5	10325.7
0.45kg @ 7.5m/s	5203.1	15468.8	10335.9
0.4kg @ 8m/s	5262.2	15644.4	10453.3
0.3kg @ 9.5m/s	5565.4	16545.8	11055.6
0.5kg @ 7.5m/s	5781.3	17187.5	11484.4
0.35kg @ 9m/s	5827.5	17325.0	11576.3
0.45kg @ 8m/s	5920.0	17600.0	11760.0
0.4kg @ 8.5m/s	5940.6	17661.1	11800.8
0.3kg @ 10m/s	6166.7	18333.3	12250.0
0.35kg @ 9.5m/s	6493.0	19303.5	12898.2
0.5kg @ 8m/s	6577.8	19555.6	13066.7
0.4kg @ 9m/s	6660.0	19800.0	13230.0
0.45kg @ 8.5m/s	6683.1	19868.8	13275.9
0.3kg @ 10.5m/s	6798.8	20212.5	13505.6
0.35kg @ 10m/s	7194.4	21388.9	14291.7
0.4kg @ 9.5m/s	7420.6	22061.1	14740.8
0.5kg @ 8.5m/s	7425.7	22076.4	14751.0
0.3kg @ 11m/s	7461.7	22183.3	14822.5
0.45kg @ 9m/s	7492.5	22275.0	14883.8
0.35kg @ 10.5m/s	7931.9	23581.3	15756.6
0.4kg @ 10m/s	8222.2	24444.4	16333.3
0.5kg @ 9m/s	8325.0	24750.0	16537.5
0.45kg @ 9.5m/s	8348.1	24818.8	16583.4
0.35kg @ 11m/s	8705.3	25880.6	17292.9
0.4kg @ 10.5m/s	9065.0	26950.0	18007.5
0.45kg @ 10m/s	9250.0	27500.0	18375.0
0.5kg @ 9.5m/s	9275.7	27576.4	18426.0
0.4kg @ 11m/s	9948.9	29577.8	19763.3
0.45kg @ 10.5m/s	10198.1	30318.8	20258.4
0.5kg @ 10m/s	10277.8	30555.6	20416.7
0.45kg @ 11m/s	11192.5	33275.0	22233.8
0.5kg @ 10.5m/s	11331.3	33687.5	22509.4
0.5kg @ 11m/s	12436.1	36972.2	24704.2

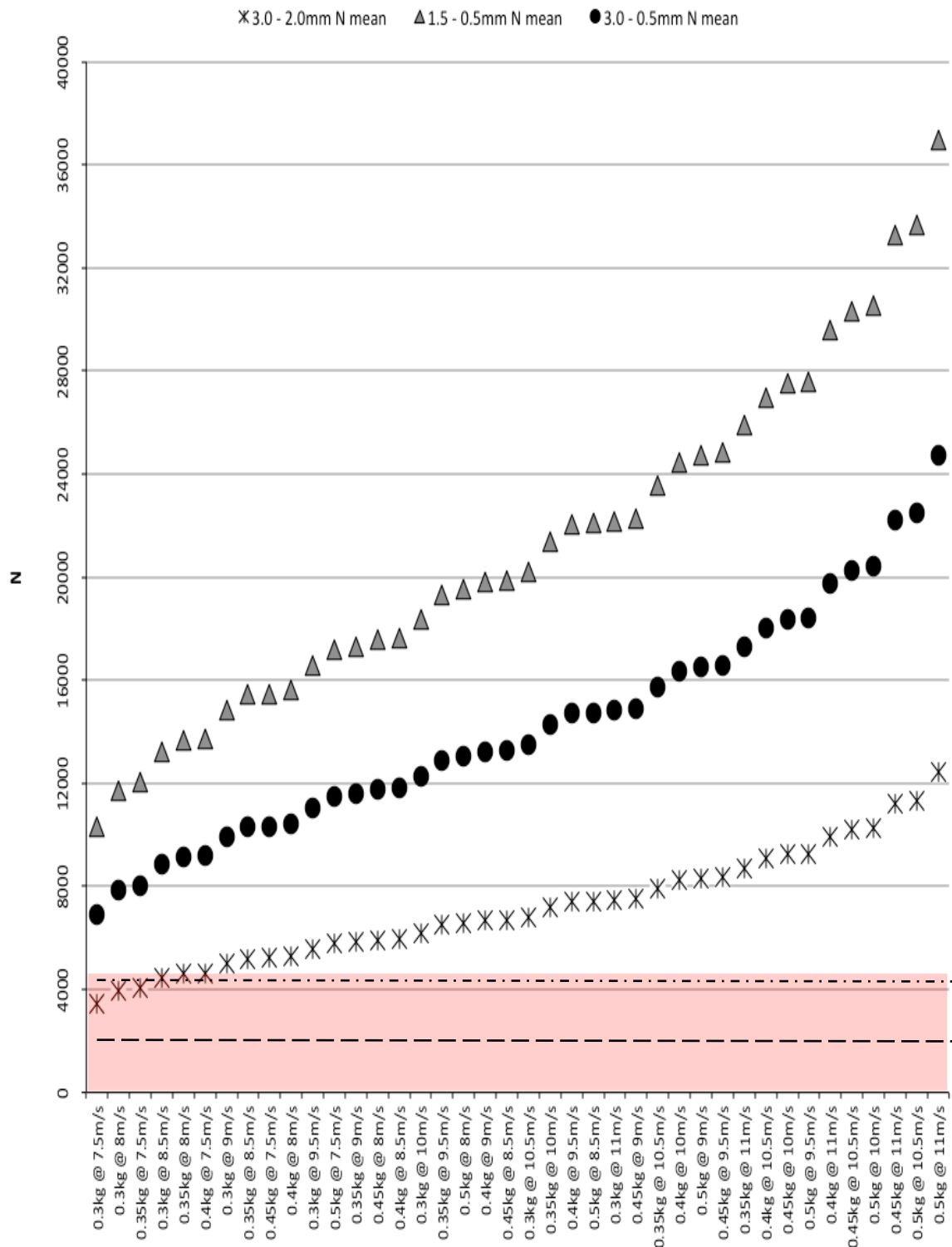


Table 2.5. Force (N) required to break human tibiae and femora, and horse metacarpals.

Ref.	Element	Notes	Static/ Impact	n	Mean	StDev	Range
Rable et al. 1996	human tibia	defleshed; 3-point impact test; impact velocity 3m/s	Impact	32	5757.2	2156.0	2475 - 12206
Martens et al. 1986	human femur	defleshed; 4-point impact test; midshaft loading; impact load time <200ms; midshaft failure	Impact	28	6410.0	1453.0	nd
Martens et al. 1986	human femur	defleshed; 4-point impact test; midshaft loading; impact load time <200ms; distal end failure	Impact	5	4879.0	643.0	nd
Kress & Porta 2001	human tibia	cadaver; impact sled/cart (50kg); anterior impact; impact velocity 7.5m/s; impactor size .04m; other experiments not included due to size of impactor (.1m) and cushioning of impactor plate	Impact	1	6240.0	na	na
Strømsøe et al. 1995	human femur	defleshed; 3-point bending test: load rate of 1mm/min ⁻¹	Static	14	4481.4	1998.5	1400 - 8000
Courtney et al. 1995	human femur	mean age = 74yrs; defleshed; impact to femur head (lesser troch. on "anvil" to simulate a fall)	Impact	8	3440.0	1330.0	nd
Courtney et al. 1995	human femur	mean age = 74yrs; defleshed; impact to femur head (lesser troch. on "anvil" to simulate a fall)	Impact	9	7200.0	1090.0	nd
		mean human			5486.8	1290.8	nd
Lawrence et al. 1994	horse mc	defleshed; 3-point bending test;	Static	46	14226.5	7340.6	245 - 27704

small hammerstones (0.3 – 0.4kg) at moving at low velocities (7.5 – 8.5m/sec), and having *exceedingly* large travel distances (2.0 – 3.0mm). As indicated above, it seems unlikely that hammerstones with such low velocities and weights will take longer to stop their travel.

It is also worth noting that although they do not *exactly* replicate either hammerstone– or carnivore–induced bone fracture, those static and impact fracture experiments that are available further bound the problem by providing estimates of the forces needed to break human and horse bone (Table 2.5). Unlike hammerstone impact and carnivore bites some of the experimental bones were defleshed and all lacked a supporting object (anvil or opposing carnassial) opposite the loading point. Thus, because supports concentrate force, these force to fracture estimates are likely somewhat higher than those where underlying supports are present. Nevertheless, these force to fracture estimates show that the largest observed carnivore bite forces are lower than most of those observed necessary to break human and horse bones. Estimated hammerstone impact forces (Table 2.4, Fig. 2.3), however, are well within this reported range. Further, these data suggest that carnivore–induced fractures at the midshafts (where cortical bone is thickest) of intact limb bones (where the structural integrity has not been compromised by chewing on epiphyseal ends) are rare occurrences for size class 3–4 mammals.

2.3 Bone as a Material

A material's physical properties at all scales (macroscopic, microscopic, and molecular) influences how fractures form. The hierarchical structure of long bone gives it an architecture enabling it to sustain daily compressive, tensile, and shear stresses. Excellent discussions of bone growth, bone structural properties and bone as a material found in Currey (2002), Ham (1969), Andrew and Hickman (1974), and Sambrook (2001) are followed here. The structural hierarchy of bone, its macroscopic and microscopic architecture, and material anisotropy that give it its stiffness and elasticity to withstand normal use, are illustrated in Figure 2.4.

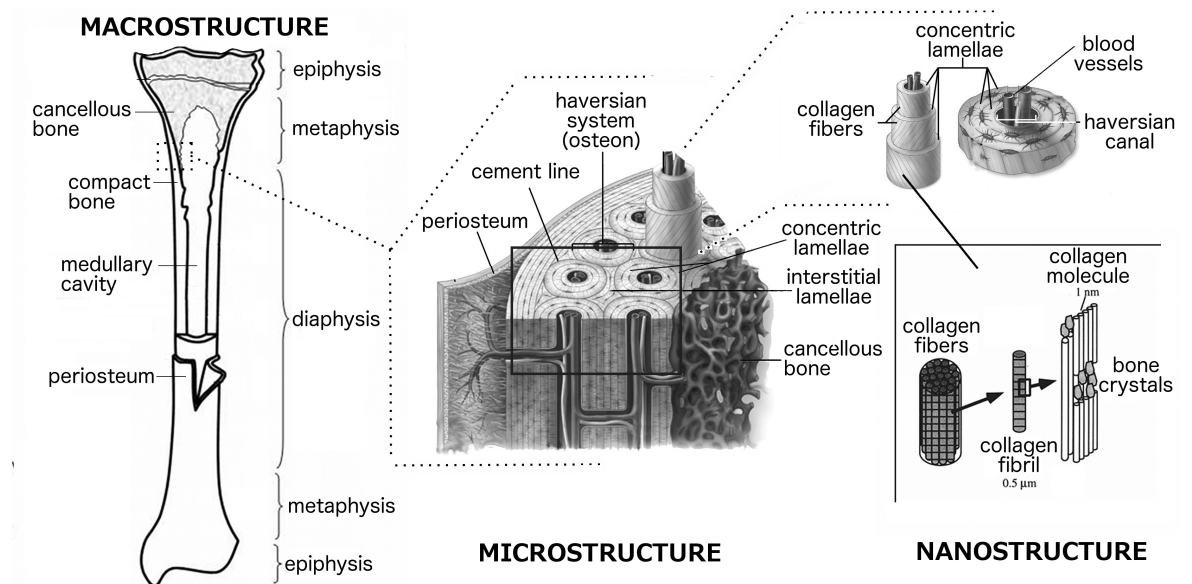


Fig. 2.4. Structural components of bone from the macro to nano scale (modified after Weatherholt, Fuchs, and Warden (2012 Fig. 1) and Rho, Kuhn–Spearing, and Ziopos (1998, Fig. 1).

Bone is a connective tissue that supports and binds together parts of the body. It is comprised of an organic component, mainly collagen, an inorganic component, mainly hydroxyapatite, and water (~10%, ~65%, and ~25% wet weight, respectively). Lipids and blood fill voids in fresh bone. Bone is formed by osteoblast cells that deposit collagen fibrils that form the structural template for and cause deposition of hydroxyapatite crystals which form on and between fibrils thereby cementing them into collagen bundles about 3–5 μm thick (Andrew and Hickman 1974). The collagen bundles are laid down roughly parallel to the bone’s long axis to form laminae surrounding a capillary, but they spiral within individual lamina, and the specific direction varies from one lamina to the next. Cement layers separates bone laid down around different capillaries. Osteoblasts encased in newly deposited bone become osteocytes that are connected to each other via canaliculi. If not remodeled (by osteoclasts that resorb bone and osteoblasts that lay down new bone) the bone is called primary. In most mammals primary bone is found near the outer edge of the bone shaft. Here, circumferential lamellae encapsulate the long bone shaft. Less well-organized circumferential bone usually also line the medullary wall. Osteoclasts are bone-destroying cells that, in combination with osteoblasts, can create secondary osteones, or

Haversian bone within previously deposited interstitial matrix. Osteons have a diameter of 200 – 300 μ m and are oriented longitudinal to the bones' long axis. Most mammal bone contains varying concentrations of secondary osteons. Covering the circumferential lamellae is the periosteum, which acts as an attachment substrate for tendons and carries blood vessels and capillaries to maintain the circumferential bone.

At the macroscopic scale long bones consist of a tubular shaft, the diaphysis, comprised of compact bone, epiphyseal ends made up of cancellous bone, and transitional area, the metaphysis in which compact bone grades into cancellous bone. Cancellous bone is a lattice of trabecullae, which are arranged coincident with lines of normal force; colloquially, but significantly, it acts as a shock absorber. Compact bone, comprised of circumferential lamellae, haversian, and primary bone, forms the shaft of mammalian long bones that surround the medullary cavity filled with marrow. Compact bone's primary mechanical role is to provide rigidity and strength to support the body and prevent fracture. Compact bone is much more dense than cancellous bone. At the metaphysis compact bone begins to thin and cancellous bone is found in increasing proportions approaching the epiphyses. At the articular ends only a thin layer of compact bone overlies this cancellous core whose architectural lattice is designed to absorb compressive loads and shocks. The presence of cancellous bone at the epiphyseal ends, gives long bones further compressive strength, but less tensile strength.

It is this hierarchical structure of bone, both in terms of composition (collagen bundles and hydroxyapatite crystals) as well as its microscopic (circumferential, haversian, and primary bone) and macroscopic (marrow filled cylinder of compact bone with cancellous epiphyseal ends) structure that gives bone its ability to survive load application, its toughness, and plays an important role in understanding gross aspects of bone fracture under loading extremes.

The microscopic arrangement of collagen bundles and hydroxyapatite gives bone considerable ability to bend, absorb stress, and prevents fracture under normal compressive

loads, i.e., those applied parallel to the long axis. Long bones can withstand greater compressive than tensile or shear loading. As a material then, bone is mechanically anisotropic; its mechanical strength and toughness vary in different directions. Collagen has a low modulus of elasticity (a material's tendency to be deformed elastically, i.e., non-permanently, under application of a force), while apatite crystals have a high modulus of elasticity. As the elastic modulus increases the material's resistance to fracture decreases. Collagen is elastic and can absorb more tension forces than apatite crystals that are brittle but give bone compressive strength. Further, bone microstructure can influence fracture propagation and the orientation of fracture lines. Nalla et al. (2003) and Koester et al. (2008) note for example that bone micro-structure, particularly the longitudinal orientation of collagen bundles and the relatively strong mineral cement lines surrounding longitudinally oriented osteons, means that all things being equal bone will preferentially split longitudinally. Li et al. (2012) also note that cement lines between osteons and the interstitial lamellae tend to be a locus of fracture propagation. Thus, it takes more energy to overcome bones' strength in the transverse plane. Note for example that dessication cracks follow these natural lines of weakness in bone (Tappen 1969) and, similarly, the sub-parallel orientation of collagen bundles in the humerus tends to create curvilinear fractures (Davis 1985).

Bone macrostructure, cancellous ends separated by a dense shaft of compact bone, also play a role in bone fracture. Notably, cancellous bone absorbs considerable energy in propagating fractures. Thus, unless applied loads are particularly high, fractures initiated on the shaft typically will not cross through the cancellous ends. A bone's cortical thickness and shaft geometry are two other macroscopic features that play a significant role in bone fracture propagation. Less thick walled bones fracture more easily than those with thick walls so the bones of smaller animals are more easily broken than those of larger animals (Davis 1985). Because the ratio of cortical bone to shaft diameter is often greater at muscle attachments and crests, they can influence fracture presence/absence and

orientation. At lower levels of stress fractures will tend to propagate (continue) outside these areas of greater cortical thickness or are deflected by their density rather than cutting through them.

2.4 Fracture Mechanics

In order to appreciate the fractographic consequences of different loading modes, indenter size and shape, and the relative amounts of energy imparted, it is necessary to have some appreciation of bone's mechanical properties and its fracture mechanics. The study bone fracture mechanics are, broadly speaking, engineering studies focused on assessing the fracture of small bone samples to develop mathematical models necessary for industrial and biomedical applications (Currey 2002). With few exceptions (e.g., injuries sustained in vehicle crashes and equine veterinary research) the fracture mechanics of whole bone have not been studied in detail. Nevertheless, summaries bone fracture studies (e.g. Currey 2002) as well as the study of fracture of glass, plastics, and composites (e.g., Hull 1999) outline *broad principles of fracture mechanics necessary to interpret resultant macroscopic fracture features*. Further, as noted by Bonnichsen (1979; Bonnichsen and Will 1980), fracture mechanics principles and concepts relevant to the understanding of bone fracture may be drawn from studies of lithic fracture (e.g., Cotterell and Kamminga 1987, 1990; Odell 2004; Tsirk 1996, 2010) familiar to students of stone tool technology.

Some basic aspects of fracture mechanics, i.e. the relationship between stress and strain, are first briefly discussed. The material properties of bone are then presented, followed by a discussion of some major principles of fracture mechanics that highlights how extremes in loading force, indenter size and shape, and loading mode influence fracture behaviour.

2.4.1 Stress & Strain

Solid materials fracture when an applied load or stress creates greater strain than the material can absorb via elastic deformation. Strain is a measure of deformation of an object under stress – the change in the length of the object produced by force divided by its

original length ($strain = d/L$). Stress is the force or load applied to a material per unit area (F/A ; usually expressed as N/m^2). The stress–strain curve shown in Fig. 2.5 illustrates these relationships. The maximum strain any unit of compact bone can show before failure is about 3% (Currey 2002). Failure (fracture) occurs via either brittle cracking or plastic flow.

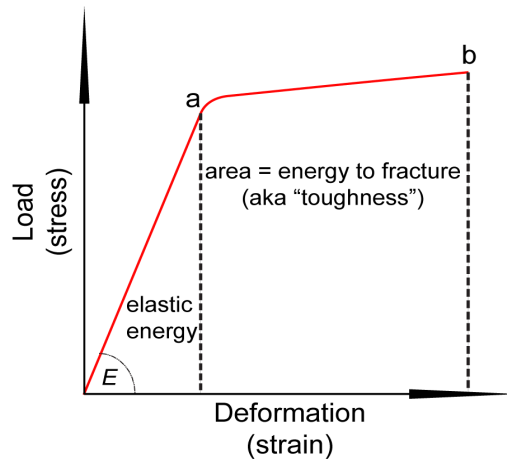


Fig. 2.5. The stress–strain curve. Materials will elastically deform under low stress levels. That is, a material can absorb the energy of a load via recoverable changes in size/shape. E denotes the measurement of this ability to absorb stress elastically, Young’s modulus of elasticity. At a certain point (a), the yield point, however, the material begins the transition from elastic to plastic deformation. Above this point permanent, plastic changes in size and shape occur. Continued application of increasing stress causes deformation throughout the material until failure, the fracture stress (b), occurs. The area under the yield and fracture points is a measure of the energy absorbed via fracture, its resistance to crack propagation, and is referred to as fracture toughness.

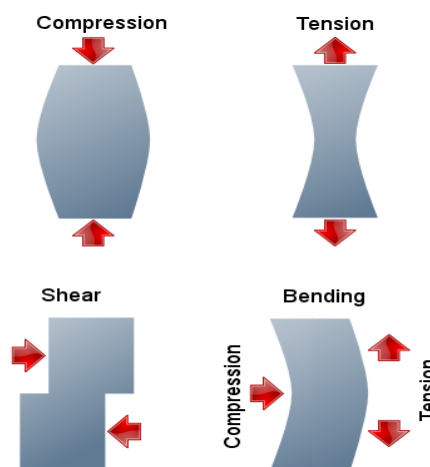


Fig. 2.6. The three major types of stress – compression, tension, and shear. All may occur in combination. For example, bending an unsupported material by applying a compression load on one side produces tension on the other side of the material.

When stress applied to a material causes it to crack or tear, the fracture mechanism is brittle cracking. As a result cracks propagate easily and quickly. Materials that deform (show strain) prior to rupture fail by plastic flow. The mode of failure is largely dependent on the material itself. Ductile materials have the capacity to absorb high levels of energy but will show obvious changes in shape. When cracks do form, crack propagation is slow and stable because of ductile materials ability to absorb energy. Thus, considerably more energy is usually required to fracture a ductile material than a brittle material. Isotropic materials such as glass and chert break by brittle cracking and require less energy to induce failure. Although bone is anisotropic and will behave in a viscoelastic manner under the application of low levels of stress, i.e., it will bend and partially fail via plastic flow, it behaves as an isotropic brittle solid under transverse loading (Hoo 2011; Katz et al. 1984), particularly when dynamic loads are applied (Currey 2002).

The three types of stress are tensile, compressive, and shear (Fig. 2.6). Even in bones initially subjected to considerable compression or shear, fractures are largely created by tension. Where part of a material undergoing compressive stress, as when indenters like carnivore teeth or hammerstones apply force, tensile stresses are created in immediately adjacent areas. Both static- and impact-loading with indenters begin as compressive stress, but fractures are usually initiated just outside of the indenter contact area (outside the zone of compression immediately below the indenter) by tensile stress. However, pointed statically applied indenters act as wedges, first working into the material by crushing which creates a deformed zone of debris which forces crack growth by the creation of lateral tensile stresses when the load is removed (Cotterell and Kamminga 1987).

2.4.2 Mechanical Properties of Cortical Bone

Most studies have examined small blocks ($<2\text{cm}^2$) of cortical bone in order to model specific mechanical properties of whole mammalian elements including toughness (usually expressed as pressure in Mega Pascals, MPa) and strength. Generalizing from these studies to whole bone is difficult because mechanical properties may vary by taxa,

Table 2.6. Mechanical properties of human and bovine femoral and tibiae (bovine compressive ultimate stress values) cortical bone. Note that a) most values vary by less than 20%, b) in most cases Young's modulus and stress values are greater for the larger bovine bone with thicker cortical walls, c) the human bone displays a slightly better ability to deform, and in particular d) although the bovine toughness values are greater, they are quite similar to the human values. Generally, these data indicate that although the specific values vary between species, human and bovine bone, and likely most mammalian bone have similar mechanical properties. Values in parentheses are those given by Currey (2002). Table modified after Hoo (2011, Table 2.5) and references therein and Currey (2002:Table3.2).

Property	Human	Bovine	% difference
Elastic (Young's) Modulus, GPa			
<i>Longitudinal</i>	17.6	20.4	13.7
<i>Transverse</i>	9.6	11.7	17.9
<i>Bending</i>	14.8	19.9	25.6
Shear modulus, GPa	3.51	4.14	15.2
Poisson's ratio	0.39	0.36	8.3
Tensile yield stress, MPa			
<i>Longitudinal</i>	115	141	18.4
<i>Transverse</i>	-	-	
Compressive yield stress, MPa			
<i>Longitudinal</i>	182	196	7.1
<i>Transverse</i>	121	150	19.3
Shear yield stress, MPa	54	57	5.3
Tensile ultimate stress, MPa			
<i>Longitudinal</i>	133 (133)	156 (150)	14.7
<i>Transverse</i>	51 (53)	50 (54)	2.0
Compressive ultimate stress, MPa			
<i>Longitudinal</i>	195 (205)	237 (272)	17.7
<i>Transverse</i>	133 (131)	178 (171)	25.3
Shear ultimate stress, MPa	69 (67)	73 (70)	5.5
Bending ultimate stress, MPa	208.6	223.8	6.8
Tensile ultimate strain			
<i>Longitudinal</i>	0.0293	0.0072	306.9
<i>Transverse</i>	0.0324	0.0067	383.6
Compressive ultimate strain			
<i>Longitudinal</i>	0.022	0.033	33.3
<i>Transverse</i>	0.0462	0.042	10.0
Shear ultimate strain	0.33	0.39	15.4
Bending ultimate strain	-	0.0178	
Fracture toughness, MPa \sqrt{m}			
<i>Longitudinal</i>	3.5	3.6	2.8
<i>Transverse</i>	5.3	5.7	7.0

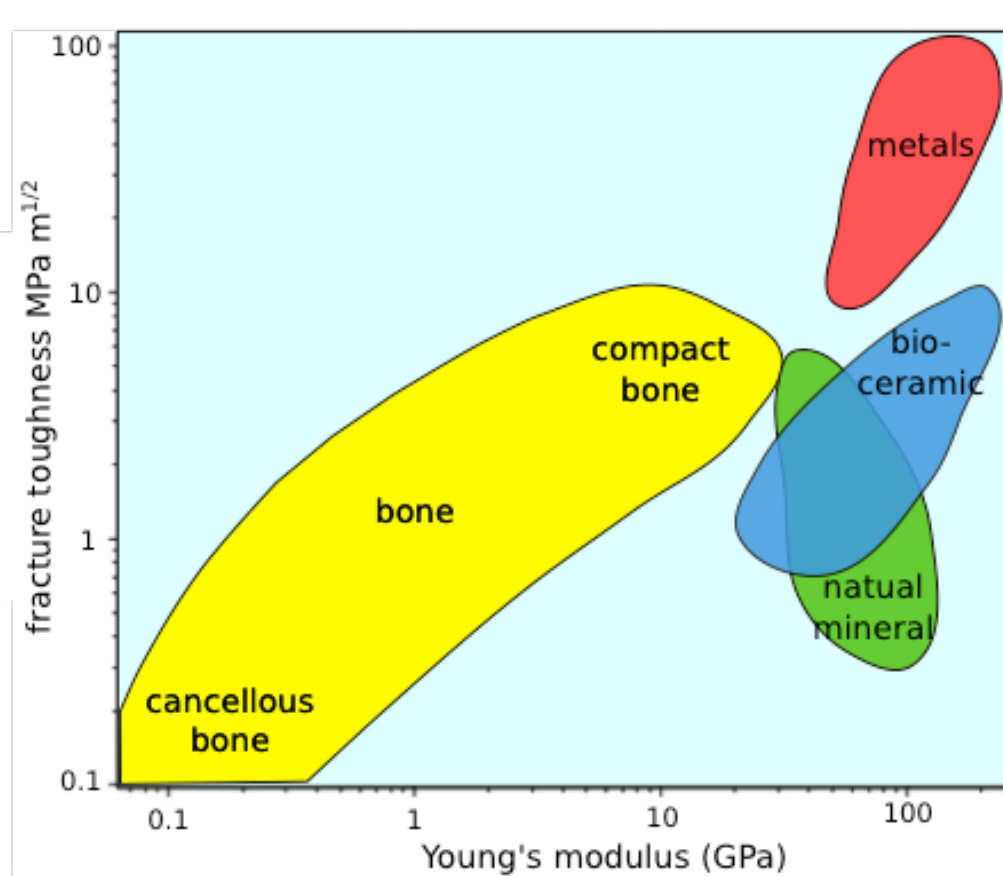


Fig. 2.7. Schematic plot of fracture toughness vs. Young's modulus illustrating the wide range of characteristics for a variety of natural and man-made materials. Note also that although their components are identical, the different architecture of human cortical bone (black arrows) and cancellous bone (grey arrows) results in very different fracture toughness and elasticity properties. Graph modified after Wegst et al. (2010).

element, age, cortical thickness, and geometry among other factors (Currey 1984; Hoo 2011; Wang et al. 1998). For purposes here, however, specific estimates of bone's mechanical properties are less important here than knowing whether or not they are comparable across mammalian taxa. Because later aspects of this study will examine a variety of taxa, it is important to document the overall similarity of the material properties of mammalian compact bone, particularly fracture toughness, because these properties play a major role in determining the resultant fracture (Cotterell and Kamminga 1987; Odell 2002).

There are very few studies of the mechanical properties of non-human bone, cow bones being the most studied (Table 2.6). While specific values vary between species, all material properties of human and cow bone are quite similar, particularly when compared

to those of other materials (Fig. 2.7). Differences in the values shown in Table 2.6 seem to be correlated with body size. For example, regardless of the direction of the applied load, the elastic modulus (the ratio of the amount of applied stress to the resulting elastic deformation, i.e., “ E ” in Fig. 2.5) is greater for the larger cow than human bone. This positive correlation with body size is also seen in the shear modulus (the ratio of the amount of applied shear stress to the resulting shear deformation), the tensile, compressive, and shear stress yields (the level of a stress at which the material begins to plastically deform, i.e. point “a” in Fig. 2.5), and the tensile, compressive, shear, and bending ultimate stress yields (the maximum amount of a stress the material can endure, i.e., point “b” in Fig. 2.5). Although variable, measures of strain show that, overall, the smaller human bone is will deform more than the larger cow bones. Given their shared hierarchical architecture, all mammalian bone should have similar mechanical properties with variation in values being related to body and bone size.

As with other material properties of human and cow bone (Table 2.6), fracture toughness (the ability of a material to resist or impede crack propagation, usually measured by the Stress Intensity Factor K_c , and expressed as $\text{MPa}\sqrt{\text{m}}$) values reported for other taxa are also a) broadly similar, b) may vary by body size, and c) display planar variation (i.e., all of the taxa studied have greater ability to resist fracture on the transverse plane than parallel to the bones long axis). This planar difference in bone fracture toughness as well as its ability to withstand greater compressive than either tensile or shear stresses may influence both fracture patterns and fractographic features resulting from different levels of applied force. For example, the greater compressive toughness transverse to bone’s long axis means that less force is required to create fractures oriented roughly parallel to the bones long axis than those on a transverse or oblique plane. Additionally, in part due to the largely longitudinal orientation of bone’s structural units (i.e., osteons, lamellae, cement lines, and collagen bundles) noted above, and as discussed in the fractography section

below, fracture surfaces parallel to the long axis appear smoother than those oriented transversely.

2.4.3 Fracture Mechanics Axioms: Force, Nature of Indenter, & Type of Loading

Several variables – the amount of force applied (and the consequent energy imparted to the material), indenter size and shape, and the mode of loading (static or impact) play major roles crack development, overall fracture patterning, and the expression of resultant fractographic features (Quinn 2007; Hull 1999). This section contrasts how a) high vs. low levels of applied force (stress), b) use of large vs. small indenters, and c) static vs. impact loading, influence the fracture mechanics and aspects for fracture patterning, particularly the extent of fragmentation.

Amount Force Applied & Energy Imparted: Force is any factor that can cause a material or object to undergo a change in speed, direction, or shape. The unit for force is the Newton (N). As more force is applied, more stress (the force over an area; N/m²) is created in the material. When a change occurs in the material to which force is applied, energy has been imparted and work is done.

In the fracture of solid materials, the work is the creation of fracture surfaces. Thus, the greater force applied, the greater the energy imparted, and the greater the damage created. Consequently, the applications of either low or high amounts of force have definable consequences for fracture patterning.

First, the greater the energy imparted, the greater speed a crack may achieve. With enough energy, once initiated cracks should theoretically be able to travel at the speed of sound, but in practice their speed is considerably less, on the order of 0.5 – 0.7 the speed of sound. This is because at high velocities the crack tip becomes unstable with branches and undulations developing that slow crack speed (Marder 1996; Marder and Fineberg 1996; Sharon, Gross, and Fineberg 1995; Yoffee 1951). The influence that energy imparted has on crack speed and its associated influence on crack complexity and feature expression is shown in Figure 2.8. Second, as shown in Figures 2.9 and 2.10, the greater

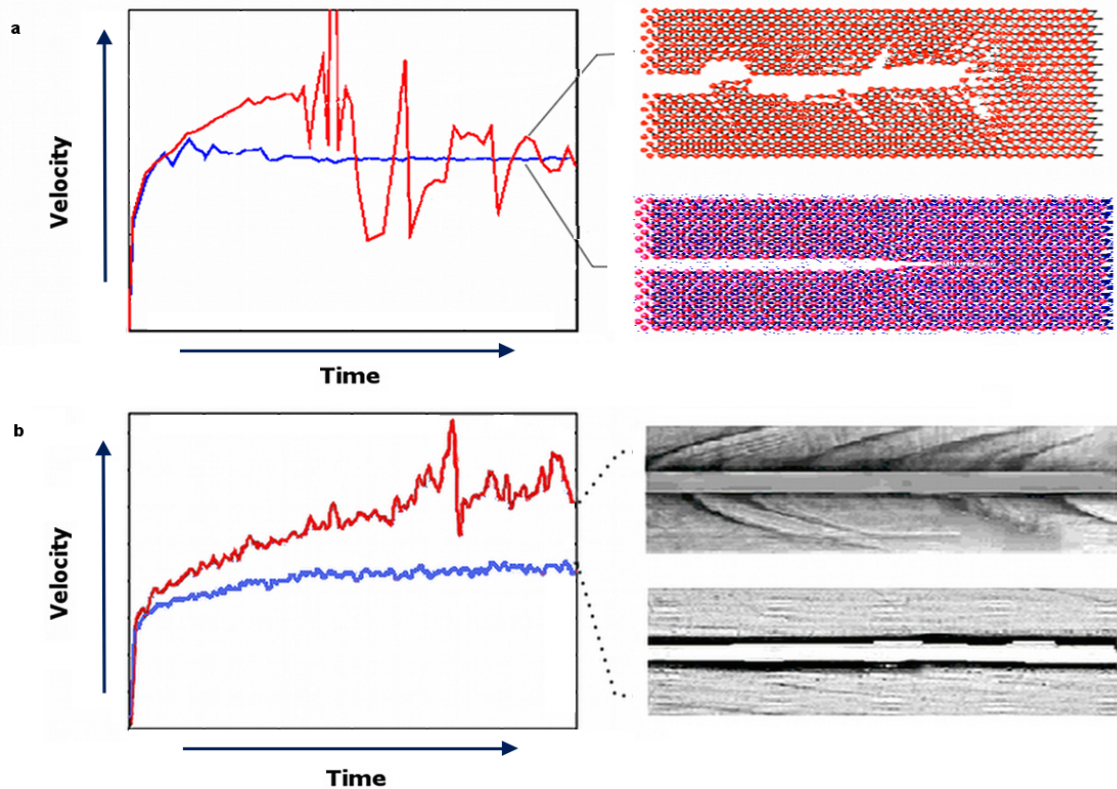


Fig. 2.8. Schematic diagram of computer simulated (a) and experimental (b) plots of crack velocity vs. time (left) and resulting crack undulations (right). Depending of the force applied, crack velocity varies and causes different levels of crack undulations. With a lower force the crack velocity is rather uniform (blue lines) and results in a smoother fracture surface (a: lower right; b: lower right). When more force is applied, the crack velocity increases until the crack becomes unstable and undulates wildly (red lines) resulting in a rougher fracture surface with more branching (a: upper right; b: upper right). Graph modified after Marder and Fineberg (1996) and Marder (1996). See also Marder and Gross (1995).

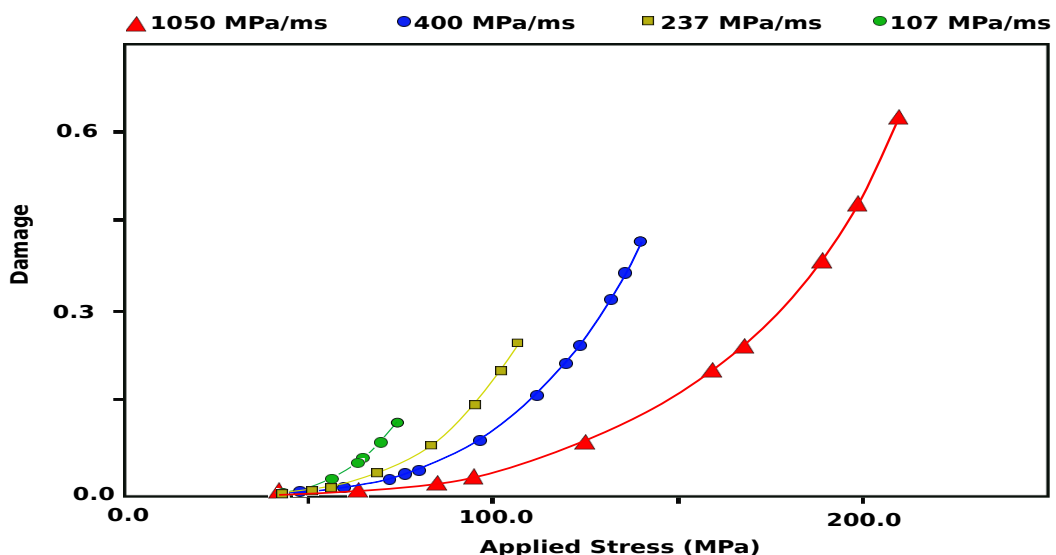


Fig. 2.9. Damage (measured as the ratio of the volume of indenter contact below which no damage occurs and the volume of the indenter contact where accumulated stresses cause crack propagation) plotted against applied stress. Note that as both the applied stress and the rate of loading increase, Damage to the material increases. (Data from Bouzid et al. 2001, Fig. 8).

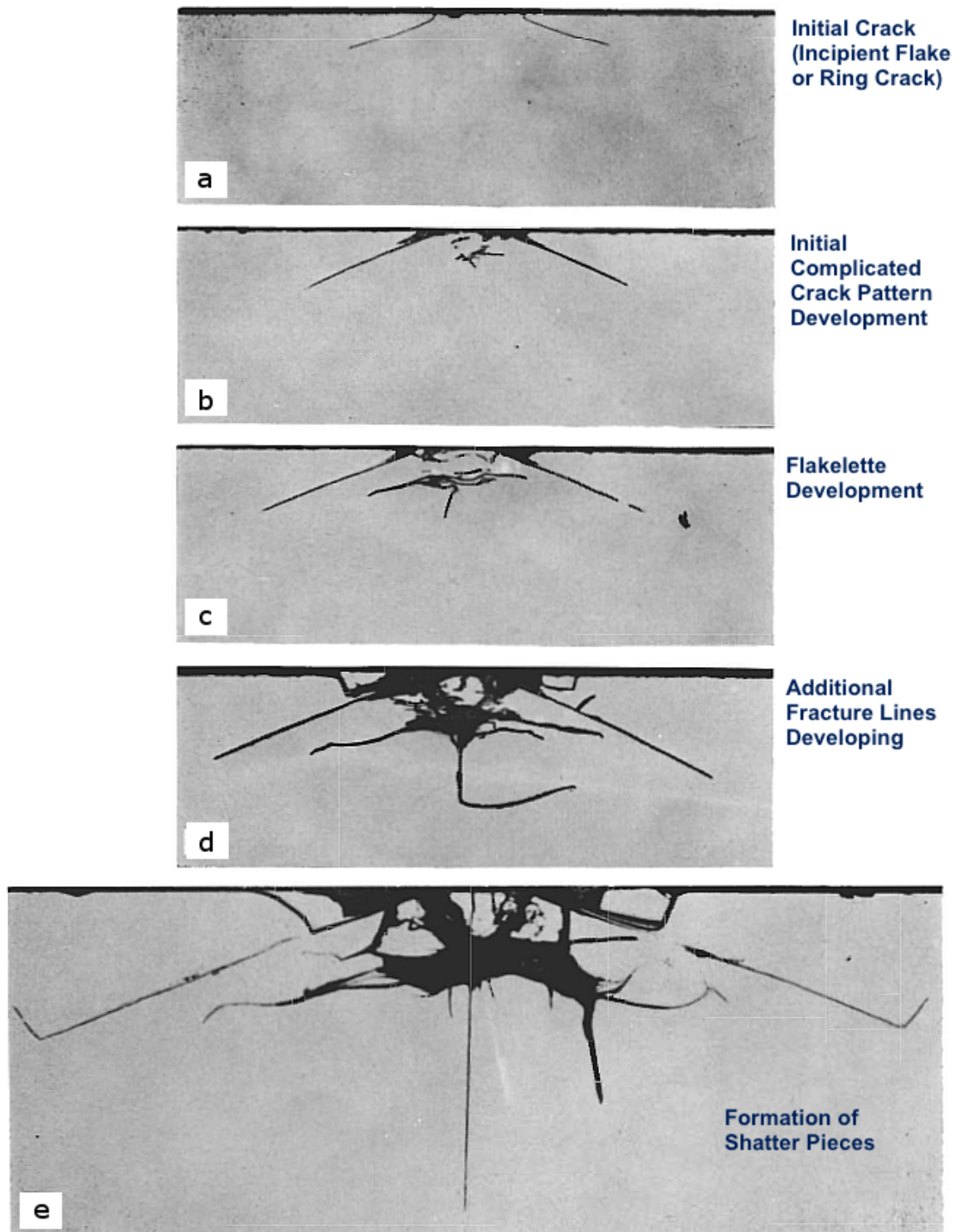


Fig. 2.10. Section-and-etch profiles of crack patterns created in soda-lime glass by an indenter (tungsten carbide, $r = 0.5\text{mm}$) at (a) 100 N, (b) 140 N, (c) 180 N, (d) 266 N, and (e) 500 N showing an increase in damages and crack complexity with increasing force. Modified after Lawn and Wilshaw 1975, Figure 21.

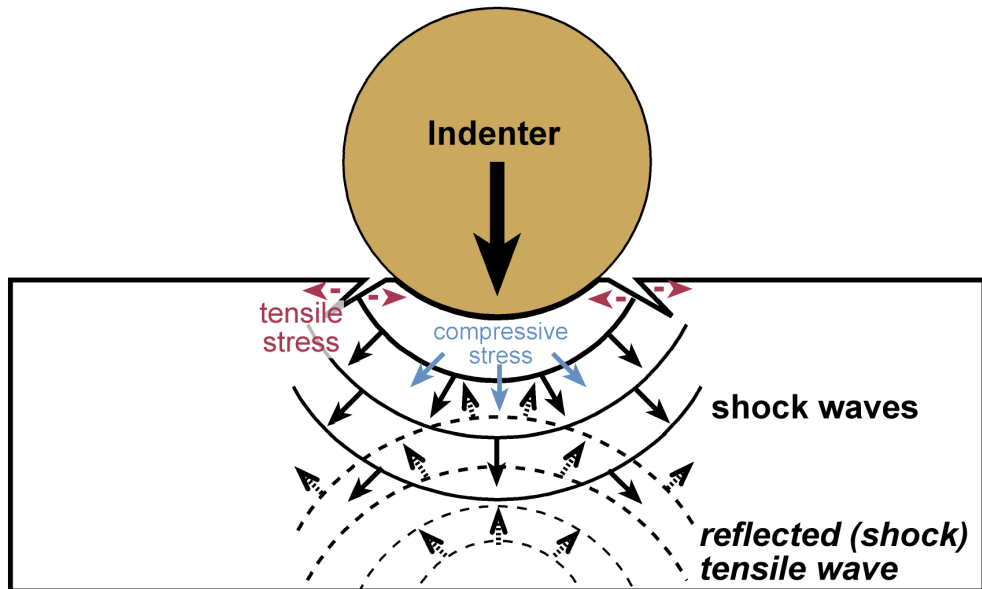


Fig. 2.11. Schematic diagram of tensile and compressive stress created by indenter contact with a material. The impact shown here creates shock waves that travel faster than cracks created by either initial stress or their resulting relief waves. Shock waves reflected from free surfaces then intersect with propagating cracks, remaining initial stresses, and relief waves causing further fragmentation.

the applied stress the greater the resultant damage. The greater the applied force, the greater the fracture surface area, and consequently fragments, that are created (e.g., Bouzid et al. 2001; Becker 2002; Griffith 1921; Varner 2002; Woodward et al. 19991). Thus, when both the loading rate and amount are high – as with hammerstone impact – crack speed as well as crack creation and overall damage will be greater than when lower amounts of force are applied slowly – as with carnivore chewing. This positive relationship between the rate of loading and the resultant damage is particularly clear in images of fractures in glass created under different loads (Fig 2.10).

Third, the rapid, violent application of high levels of force, such as occurs with impact loading, creates shock waves (Fig. 2.11) that travel faster than developing crack (e.g., Bourne et al. 1994). The interaction of shock waves with each other, free surfaces, and cracks causes greater comminution and greater expression of fractographic features (see below). This increase in damage caused by the interaction of shock waves with developing fractures is in addition to that generated by rapidly moving cracks.

A fourth definable consequence for fracture patterning is that because fragmentation influences the length of individual fractures, the average dimensions of the sum of individual fractures are inversely related to the amount of energy imparted. Quinn (2007:4–10) summarizes the relationship between imparted energy, crack branching, length, and fragmentation:

“The distance a propagating crack travels before branching is directly related to the stresses and stored energy in the component. The greater the stored energy, the shorter the distance to branching... Low stress, low energy fractures create minimal branching and hence few fragments. High energy fractures cause extensive fragmentation.”

Similarly, Bouzid et al. (2001: 842–843) states

“[with low stress] then relatively few flaws are activated. The distances between fragments are long and consequently the corresponding fragments are large. In contrast, if the stresses achieved are higher, many more flaws are activated. Consequently, fracture–propagation distances are shorter with smaller time to failure and fragment sizes.”

Medical studies (among others) of bone breakage have confirmed this link between the severity damage and imparted energy (e.g., Beardsley et al. 2002, 2004).

Finally, the amount of energy imparted to a material influences the presence/absence, type, and degree of expression of fracture features created (e.g., Ball and McKenzie 1994; Becker 2002; Quinn 2007). The higher the force applied and energy imparted to a material, the more fractographic features that form, the greater their visual clarity of expression, and the more features present that indicate the direction of fracture propagation and the fracture origin or loading point. Fractographic features and their expression under different loading conditions are outlined in a below section. Much of the above can be tied to Griffith’s theory of fracture (1921) that stated energy has to be supplied to create new surfaces and that the more potential energy of the exterior load, the more fracture surfaces that are created.

The Role of Indenters: Indenter size and shape influence fracture behaviour patterning, and feature expression in a number of ways. Because pointed indenters concentrate the load, they tend to require less energy to create fracture than blunt indenters

that apply the load over a much larger area. However, small indenters tend to produce less stress in a highly localized area and therefore create less damage than larger indenters. In contrast, because of their broader contact area, larger indenters spread out the load creating multiple cracks. The reason for this difference is that the greater the area over which stresses are spread, the more frequently they intersect “flaws” (pre-existing cracks, voids, etc. that act as stress concentrators and from which all cracks are initiated) in the material that allows the formation of more cracks. (e.g., Bouzid et al. 2001). Consequently, damages and fractographic features are more limited and localized with small conical indenters than those created by larger more flat indenters where force is applied over a larger area. It is recognized, for example, that the size and expression indenter damage increases with impact velocity and the size of the indenter (e.g., Ramrakhiani et al. 1980).

Static vs. Impact Loading: Differences in fracture behaviour (resulting from differences in applied force, energy imparted to a material, and in indenter size and shape) are also a consequence of the mode of loading – static vs. impact. Static and impact loading are two very different ways to create stress and impart energy to a material. Static loading is characterized by a) its gradual increase in load until b) a relatively constant rate of force application is attained, and c) the relatively long periods of time the load and material are in contact. The formula for calculating static loading force (F) is

$$F=m*a$$

where m is the mass of the object and a is its acceleration. Static loads are often applied in a cyclically and the material often experiences some elastic or quasi-plastic deformation (Lawn 1998).

In contrast, impact loading includes kinetic energy (the energy an object has because it is in motion) and therefore the load is applied instantaneously with a very short period of contact. The contact period is usually estimated by the amount of material compression before failure. Thus, the formula for calculating impact-loading force

$$F=(1/2mv^2)/d$$

where m = mass of the moving object, v = the object's velocity, and d = the distance of its travel into the material before fracture.

Thus, at least two aspects of static vs. impact fracture mechanics are different. First, as noted above, extremely rapid load application causes the material to behave as a brittle solid with instantaneous failure whereas static loading may begin with elastic deformation prior to fracture. Thus, the fundamental difference between static and impact loading is the rate of loading. Second, whereas static loading only creates s (secondary or shear) waves, the instantaneous loading created by impact generates both s and p (primary or compression) waves. Unlike s waves, compression waves move faster than the propagating crack. Complex interactions are created as they are reflected from adjacent and newly created free surfaces (fracture surfaces) as well as the slower moving s waves. Stress waves (both p and s) and their interactions causes failure to occur in different locations simultaneously and are the dominant mechanism of impact fracture (e.g., Bourne et al. 1994; Bouzid et al. 2001; Woodward et al. 1991). Thus, one reason – perhaps the primary one – why impact loading tends to create more damage (i.e., more fragments and fracture surfaces) is the production and complex interactions of shock and secondary waves with each other and free surfaces.

2.5 Fractographic Features & Fracture Patterns: The Results of Loading Extremes

The above brief overview provides the necessary context for discussing specific fracture patterns and fracture features created by static– and impact–loading. Most of the features discussed below (i.e., cones, lateral stress, chevrons, and bulbar scars), occur on the fracture surface. A few (ring and radiating cracks and indenter marks) are found on the cortical surface of the material. While impact– and static–loading may create some broadly similar features, many, particularly when they co–occur, are indicative of high–speed loading and the application of considerable force. Few fracture features are directly indicative of static loading, but their degree of expression or clarity is usually less pronounced (Quinn 2007). Similarly, as suggested by the above discussion of fracture

mechanics, the complexity of loading points (fracture origin) is greater in impact than in indentation or static origins (Varner 2002: 664). Flakelettes, secondary flakes scars and multiple hinge terminations often occur just below the loading point of percussion-induced flakes (Tsirk 2010).

Due to the variety of features produced by impact fracture, and the comparative lack of or poor expression of features created by static loading, this discussion is structured around fractographic features and fragmentation patterns that commonly result from impact fracture. First discussed are larger scale features, fragmentation patterns, notches, hertzian cones, associated flake scars, ring cracks (aka concentric fracture lines, aka incipient flakes). This is followed by a discussion of finer scale fracture surface features including hackle marks, lateral stress, and features indicative of the direction of fracture front movement. Indenter marks, i.e., tooth and percussion marks, are then described. Where static- and impact-loading may create cursorily similar features, contrasts in the expression and character of each are noted. Examples of fracture features are illustrated with examples from the fractographic, fracture mechanics, and lithics technology literature. As well, examples of these features on bones fractured by carnivore chewing and hammerstone impact are provided. Attention to features described here constitutes the framework for holistic fractographic analysis, an appreciation of the expression of these fracture features and their co-occurrence, and, moreover, an understanding of how these features are created (utilizing information of bone as a material, fracture mechanics, and the radically different loading levels produced by carnivore chewing and hammerstone impact).

Fragmentation: Zooarchaeologists have tried to assess fragmentation in a variety of ways, e.g. element survivorship, NISP:MNE ratio (e.g., Lyman 1994), fragment shape (e.g., Villa and Mahieu 1991), and element completeness (e.g., Bunn 1982, 1989). In most cases the assumption or hypothesis (explicit or implicit) is that hominin processing of bone for marrow should result in greater fragmentation than other processing agents, notably

carnivores. Although some studies give reason to believe this is true, only a few studies, notably Bunn (1982, 1989) and Pickering and Egeland (2006), present supporting comparative data.

Bunn's (1982, 1989) analysis of element completeness in the Khwee San hunter-gatherer, Sokimau hyaena den, and FLK-Zinj assemblages, for example, estimated element completeness as the percentage of a complete limb shaft circumference and length (shaft or limb end circumference: <50%, >50%, complete; shaft length: <50%, >50%; limb end length: <50%, >50%, complete element) represented by a specimen. Element completeness was shown to be greater in the assemblage created by hyaenas, than in the Khwee San and FLK-Zinj assemblages. Schick et al. (2007) have shown recently, however, that fragmentation indices from the Umari hyaena den assemblage are comparable to those of numerous East African Plio-Pleistocene archaeological assemblages, including FLK-Zinj. They note, however, that most of this fragmentation is accounted for by smaller animals, not the thicker cortical-walled bones of animals larger than hyaenas. Other ethnoarchaeological studies do show a relationship between fragmentation and the relative amount of marrow present in an element. In his study of assemblages accumulated by Aché hunters of Paraguay, Jones (1983) found that the shafts of monkey bones with little marrow space (1–3ml) were complete (94% complete shafts), whereas 89% of deer bones with greater marrow space were incomplete. White (1992) found a similar pattern in the Mancos human assemblage where bones with larger marrow cavities were broken more frequently than bones with smaller marrow space. Gauld and Oliver (in prep) observed a similar pattern in the late Neolithic human cannibalism assemblage from Domuztepe, Turkey.

The NISP:MNE ratio, when complete bones are excluded (Lyman 1994), is a straightforward method to compare the degree of fragmentation in assemblages. The greater the number of specimens that do not contribute to the MNE value, the greater the fragmentation (see also Villa and Mahieu 1991; Lyman 1994).

As noted above, material scientists recognize that the greater force applied to a material, the greater the resultant damage, e.g., number of fracture surfaces, fragments, and expression of fractographic features (Griffith 1924; Piekarski 1970; Beardsley et al. 2004; Quinn 2007). Thus, it seems useful to analyze fragments size and the number of fracture surfaces in an assemblage as a means to assess fragmentation. Assemblages broken largely by hammerstone impact should display a larger number of smaller fragments and specimens should have more fracture lines than in assemblages created by carnivores.

Hertzian Cone: Hertz (1881) first described the cone crack and diagnostic cone, the Hertzian cone, produced when a brittle body is loaded by a spherical indenter. It is widely accepted that conchoidal fracture and the formation of hertzian cones, partial cones, and flake scars with a percussion scar are characteristic of impact fracture (Cotterell and Kaminga 1987). This fracture is created by a cone of compressive force that propagates through a solid material quickly creates an area of great tensile stress just outside the contact radius that begins extending downward and outward through the material causing the cone-shaped fracture, the hertzian cone (Fig. 2.12). Notably, immediately after impact this area of greatest tensile stress just below the surface extends beyond the limits of the indenter as well as the main fracture (Fig. 2.13; Lawn and Marshall 1979; Lawn 1998). Ring cracks (see below) and truncated or partial cones (see below) are commonly formed in this area outside of the main hertzian crack during high-energy loading. Where impact-loading occurs near a material's free edge (where energy can be dissipated preventing complete cone formation) a partial cone forms. Here, hertzian fracture is referred to by the terms cones and cone fragments. They are not referred to as a bulb of percussion and flakes as is common in lithic analysis because, as noted by Cotterell and Kaminga (1987), what sometimes appear to be percussion bulbs as well as flakes can be created by pressure flaking and other static forces. Force gradually applied by small pointed indenters (e.g. carnivore teeth) in static-loading may create what appear to be bulbs and bulbar scars, but the fracture mechanics and applied forces are quite different, resulting in less frequent and

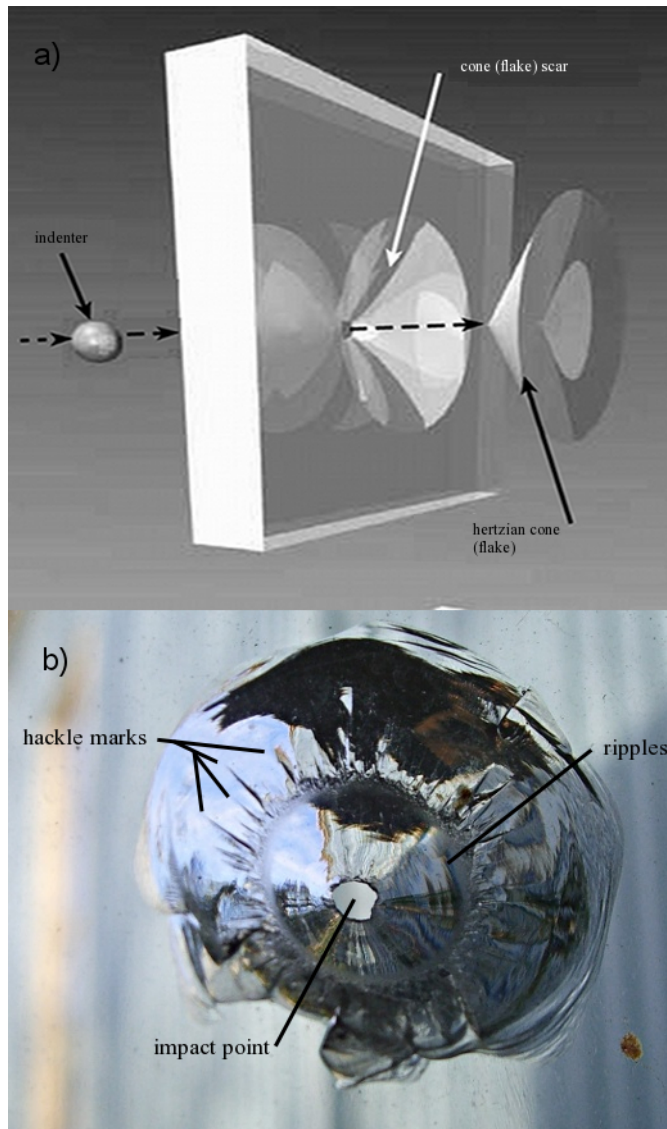


Fig. 2.12. Schematic diagram of a hertzian cone and its scar created by projectile impact (a) and a photograph showing a hertzian cone in which hackle marks and ripples are visible.

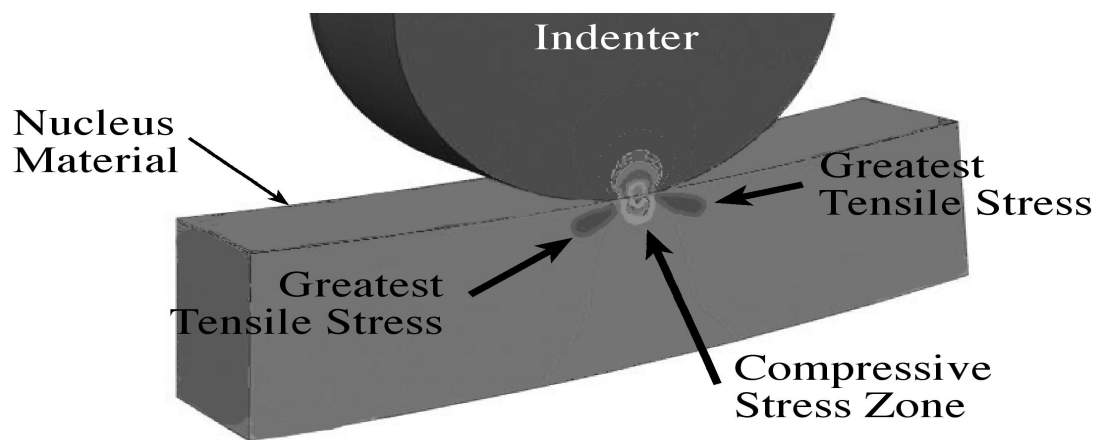


Fig. 2.13. Schematic diagram showing the locations of greatest tensile and compressive stress created during impact loading.



Fig. 2.14. Example from AHD of a typical flake scar and notch produced by carnivore gnawing. Note that the flake scar is narrow, single, and simple, lacking multiple scars and hinge terminations. Note also the rather steep fracture angle (near 90°), and the equidimensional, semi-circular notch. The very shallow bulb is contained within the flake scar itself. Hackle marks that point up towards the center of the notch are also visible.



Fig. 2.15. Example from AHD of an atypical flake scar and notch produced by carnivore gnawing. Note that in contrast to the tooth flake scar shown in Fig. 2.14, the upper flake scar shown here is rather broad with a less steep fracture angle. The lower flake scar with its rather steep fracture angle (near 90°), and the equidimensional, semi-circular notch is more typical of flake scars produced by carnivores. Note also that a bulb is clearly visible on the upper flake scar, but that it appears as a separate feature that does not define the entire scar. Arcuate feathering marks are present on the left side of the upper flake scar.



Fig. 2.16. Examples of partial (middle three) and complete cones (left and right) produced on a cow bone by hammerstone impact. The apex of this cone is clearly visible on the top partial and the left and right complete cones. Note that the cone/partial cone are equivalent to the entire flake and are not simply a bulb on a larger flake.

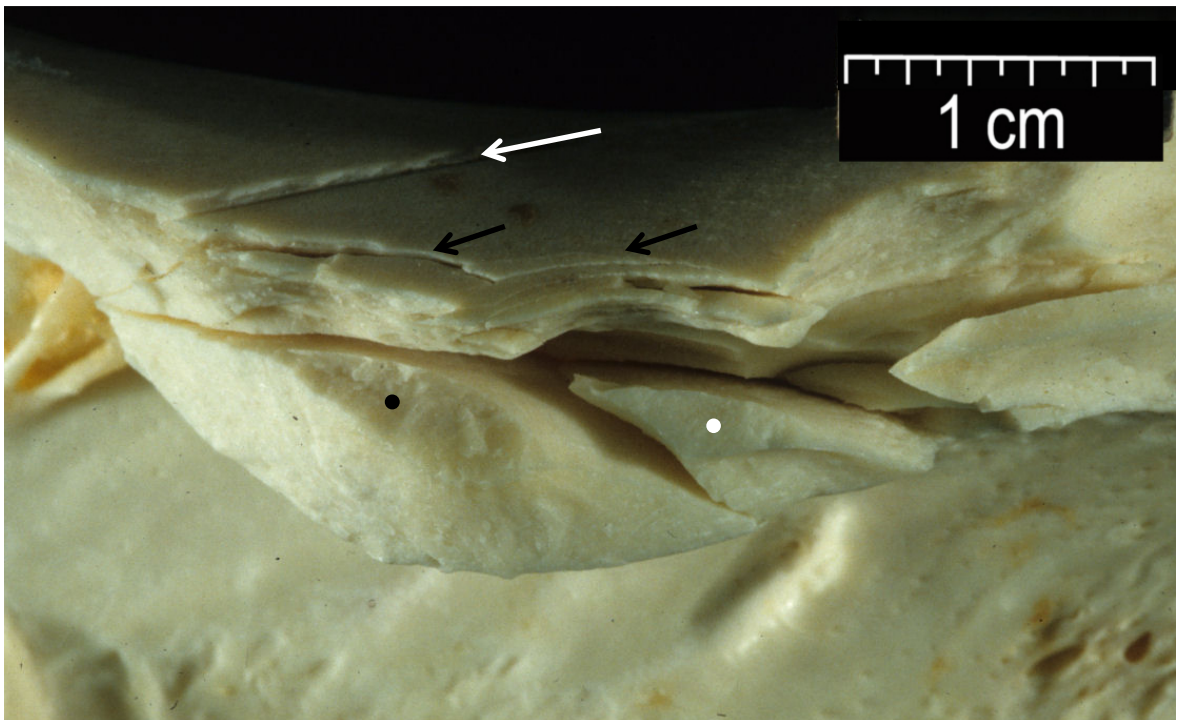


Fig. 2.17. Example of a large and complete cone produced on a cow bone by hammerstone impact (dot). The apex of this cone is clearly visible. Also note the incipient flakes (black arrows) above the cone at the cortical surface as well as impact shatter fragments adjacent to the cone (white dot). A radiating crack (white arrow) is visible on the cortical surface on the left side of the image.

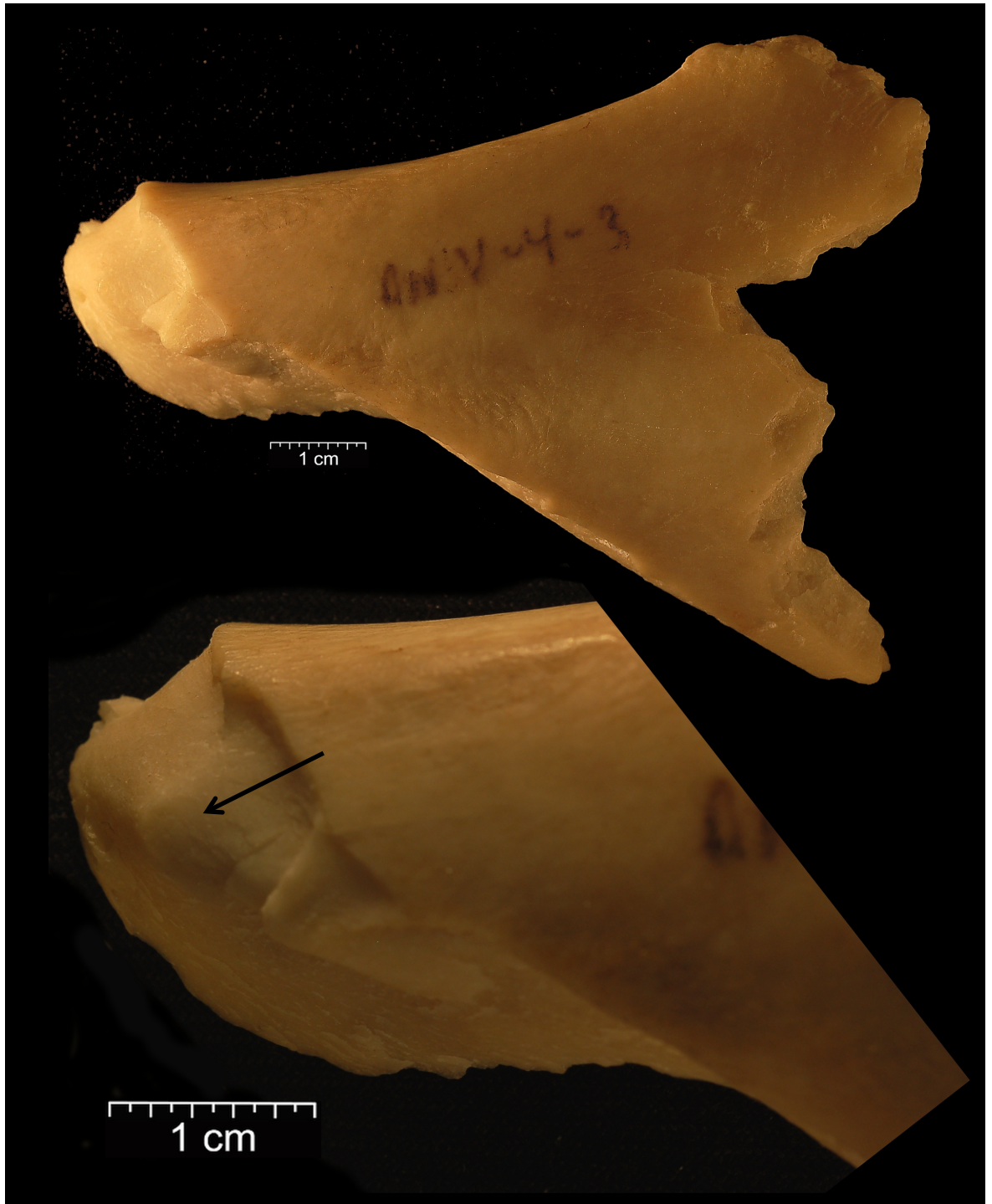


Fig. 2.18. Example of a large and nearly complete cone produced on a cow bone by hammerstone impact after being fed to hyaenas. The upper image shows the cone (on the left) created by hammerstone impact while the right part of the fragment displays carnivore damage including tooth marks and very small notches. Although not shown here, feathering on the fracture surfaces adjacent to the cone clearly show the fracture originated at the cone. These fracture surfaces do not display any carnivore damage, but intersect fracture surfaces that do. This configuration of damages demonstrates that the hammerstone breakage occurred subsequent to carnivore gnawing. The lower image shows a close-up of the cone. The apex of the cone is clearly visible (arrow).

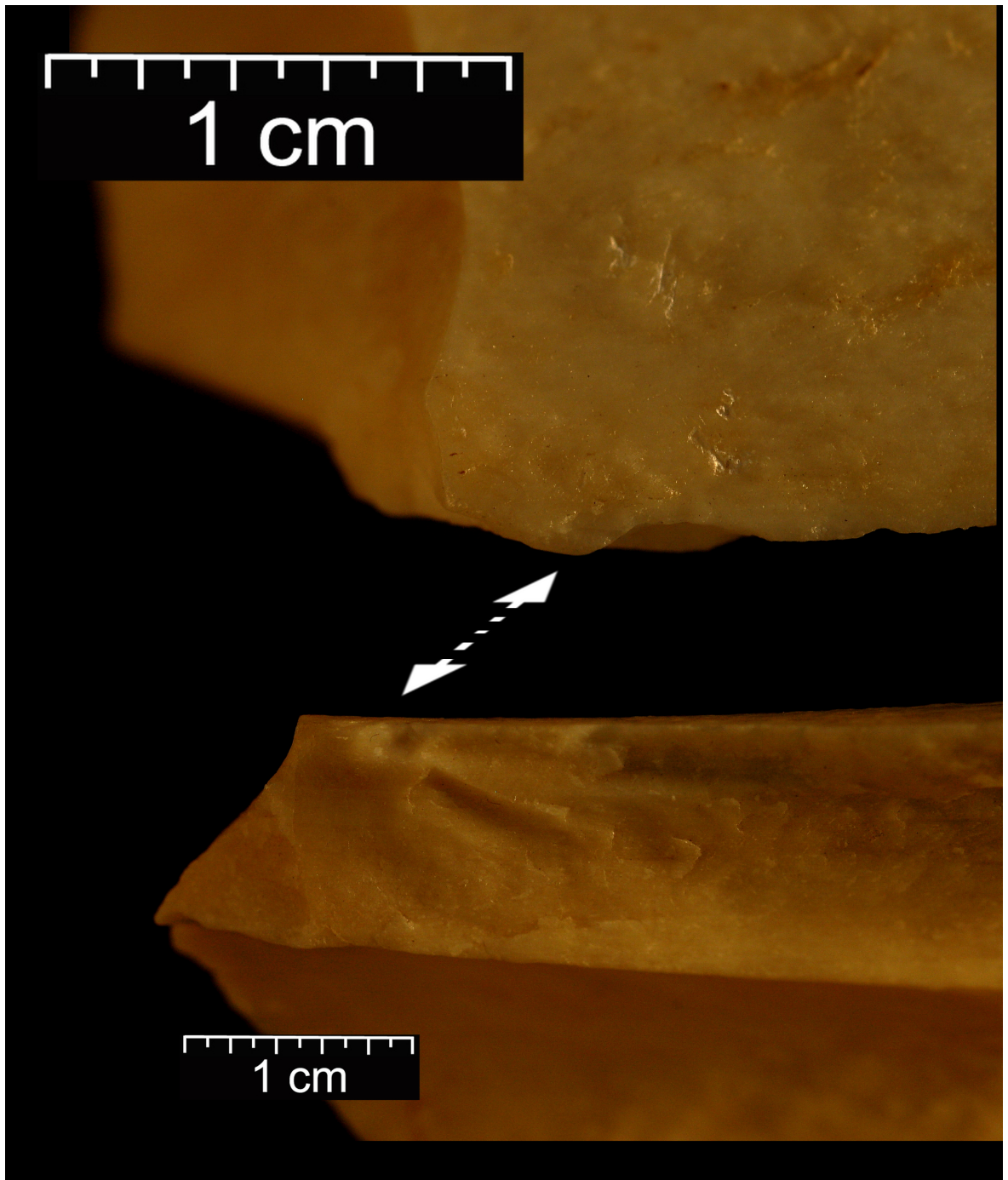


Fig. 2.19. Example of a very small cone (a dimple/dome) produced on a cow bone by hammerstone impact. The upper image shows the percussion mark created by hammerstone impact and the lower image shows the cone. Note also the outline of a partial cone on the fracture surface profile immediately to the left of the cone below the arrow in the lower image as well as this cone surface in the upper image. Also visible are several fracture features. A lateral stress fracture feature, in this case a groove, begins just right of the small dimple above the partial cone proper and extends as it broadens, paralleling the cortical surface, to a length of about 2cm. An errailure scar is visible just below the start of the lateral stress feature. Feathering or fringe, whose convex end point back to the fracture origin are somewhat visible below the lateral stress feature and extend beyond it on this fracture surface. This loading point would not have been identified were it not for careful inspection of this and adjacent fracture surfaces.

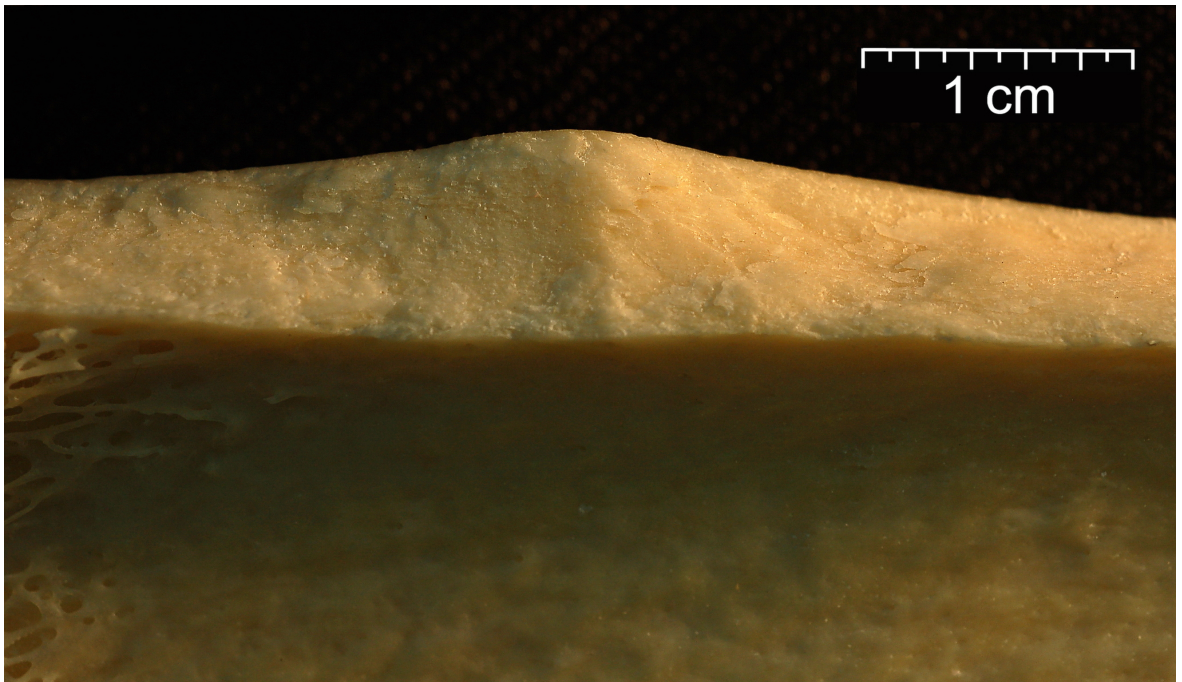


Fig. 2.20. Example of a small cone produced on a cow bone by hammerstone impact. In this example the indicators that this protuberance is a cone created by impact loading are the barely visible hackle marks that emanate from the cone apex, and the slight dimple-like features located about 1cm on either side of the cone center.

less well defined cone-like features (Cotterell and Kaminga 1987; Quinn 2007). Cones and partial cones are characterized by a) greater fracture angles than the bulbar scars sometimes produced by static loading, b) the frequent presence of a distinctive cone apex, c) relatively broad and thin terminations, and d) the frequent lack of an associated flake scar. If present, “bulbs” on pressure flakes are always part of associated flake scars, which tend to be shallower, less pronounced, and the overall flake scar much narrower (Figs. 2.14 and 2.15) than the pronounced cones produced by impact (Figs. 2.16 – 2.21). As a descriptive term here, cones refer exclusively to a feature that is clearly related to hertzian fracture. It should also be noted that in bone bulbar scars are particularly difficult to identify where multiple flake scars are present. In contrast, cones and partial cones are more readily identifiable.

Although cones, partial cones, and cone scars are not *unequivocally diagnostic* of impact-loading they are certainly *characteristic* of impact-loading, particularly when

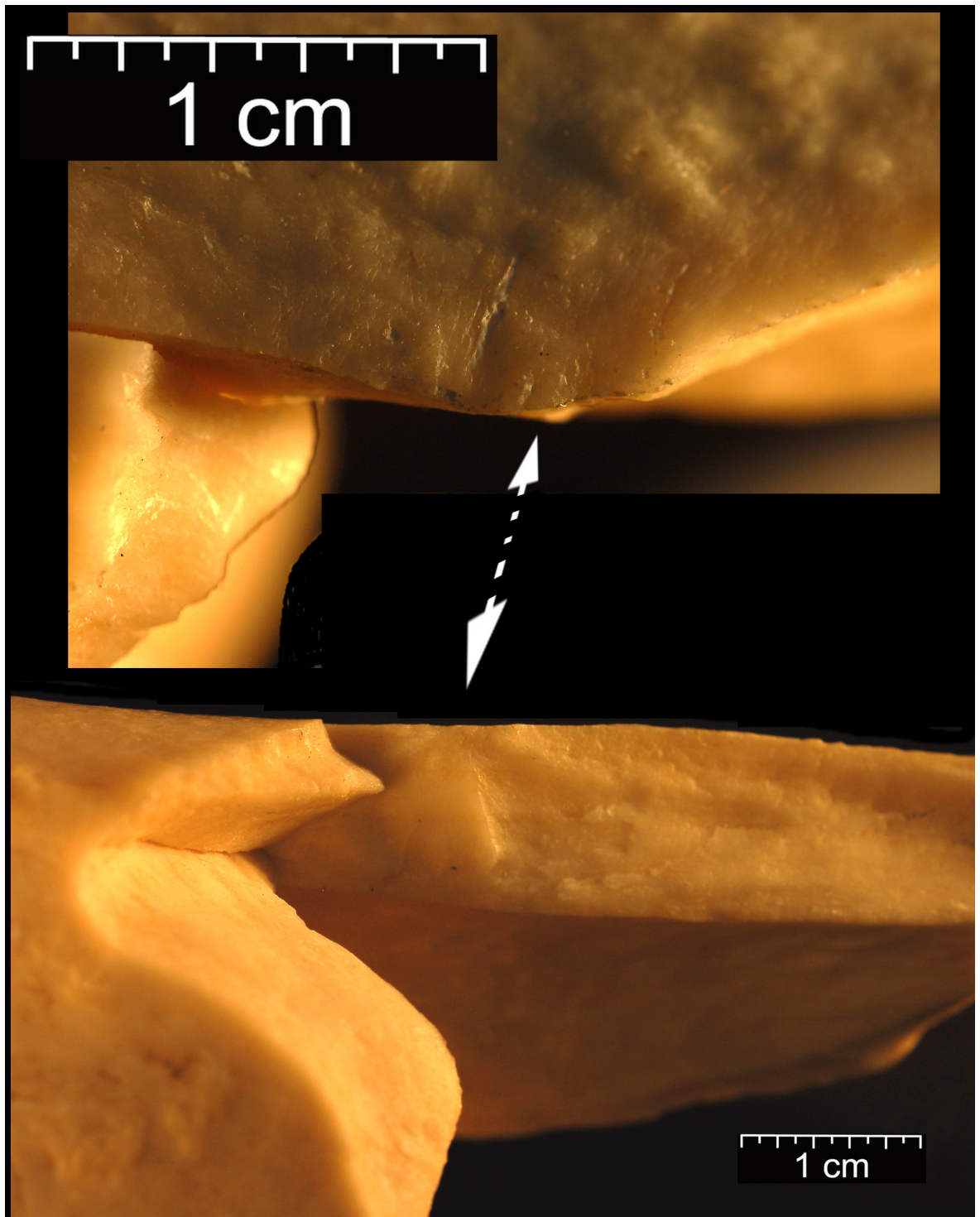


Fig. 2.21. Example of a moderate-size cone produced on a cow bone by hammerstone impact. The upper image shows the percussion mark created by hammerstone impact and the plan view of the cone. The lower image shows the cone. The arrow points to the same location in each image. Also visible is a lateral stress fracture feature, in this case a groove, that begins just right of the partial cone proper and extends as it broadens, paralleling the cortical surface, to a length of about 4cm.

associated with other fracture features (i.e., radiating fractures, radiating fracture front movement directions, lateral stresses, and incipient flakes; see below). Examples of cones and partial cones produced in cow bones broken with hammerstone and anvil are shown in Figures 2.16 – 2.22. Impact fracture often produces many small (length ~4cm or less), thin flakes each bearing a partial cone on the dorsal surface and a cone scar on the ventral surface (Fig. 2.16). These are incipient flakes (see below) that became detached from the nucleus, the larger bone fragment. Partial cones on larger fragments have a variety of manifestations (Figs 2.17 – 2.21). Some are large and have a clear “cone appearance”. Others even though attached to the larger fragment, are highly fractured and can only be defined by re-fitting (in the case of experimentally fractured bone) to the conjoin piece with the corresponding flake scar. Cones produced by impact often appear as a singular feature with no associated flake scar or incipient flakes (Figs. 2.18 – 2.21).

In some cases these cones are barely perceptible and attention is drawn to their presence only by their position opposite an impact fracture feature and/or the presence of fracture front features indicating front movements in opposite directions (Figs. 2.19 – 2.20). Sometimes these partial cones and scars have the appearance of dimples or very small domes and are not found within a flake scar or beneath a notch. These smaller partial cones seem to be found predominately on the side of the bone that lay on the anvil. Because of the high levels of force applied by impact-loading multiple fracture surfaces are often created. One consequence is the creation of diagnostic small fragments with multiple fracture surfaces that display multiple fracture angles and a complex suite of radiating front movement directions. These are referred to as impact shatter fragments (Fig. 2.22). Static-loading simply lacks the necessary force to create so many small and closely spaced fracture surfaces on a small fragment.

Dimple/Dome: This is a new fractographic feature observed on bone fractured experimentally in this study with hammerstone and anvil. Because this feature’s appearance grades into that of a cone, dimple/domes are termed cones here. They are

separated in this discussion to emphasize just how subtle some loading points appear. Dimples, and on the opposite fracture face their positive counterpart, the dome, are found on the on fracture surfaces immediately below the impact point or above the anvil. These circular to oblong features are small, often quite shallow, and usually appear without larger, more readily visible features like a flake scar or notch, (Fig. 2.19). They typically have a maximum dimension of approximately 1–5mm. Because of their small size and subtlety of expression, this feature is rarely readily identifiable without careful scrutiny of fracture surfaces and fracture front movement directions. In most cases there is little outward difference in the topography of adjacent fracture surfaces. Similarly the fracture line on the cortical surface above a dimple/dome usually displays no or a very minor change in shape. In many cases this feature is found only after careful inspection of the fracture surfaces opposite an impact fracture feature. In other cases this feature is found only after diverging fracture fronts indicate the presence of a loading point. This feature seems to be associated with anvil loading. It seems likely that dimple/dome formation is related to the intersection of and/or rebound of shock and stress waves emanating from both the impact point and anvil surface. Like cones, this feature is diagnostic of impact.



Fig. 2.22. Example of an impact shatter fragment produced experimentally. The large number of separate fracture surfaces (at least six on this specimen) is characteristic of impact shatter pieces. Note also the cone with a well-defined apex on the uppermost fracture surface.

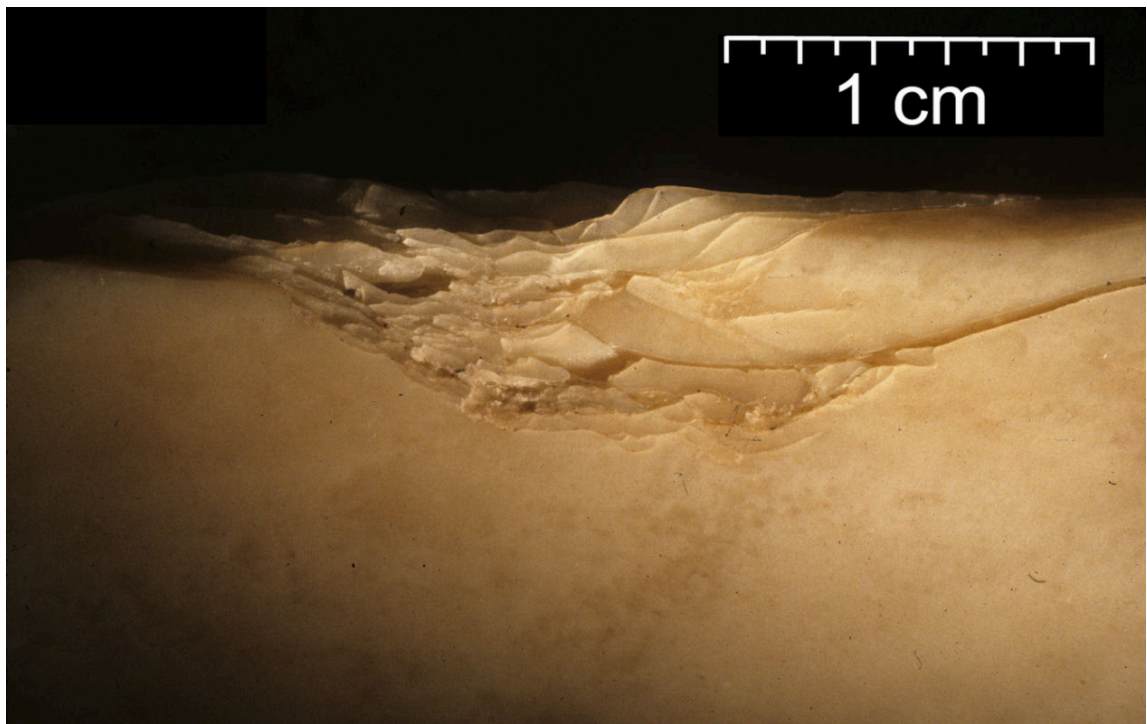


Fig. 2.23. Example of incipient flakes (aka ring cracks, aka concentric fracture lines) produced experimentally by hammerstone impact on cow bone. Note the large number of individual flakes and fracture lines. This complexity is a reflection of the multiple fracture surfaces created by high-energy loading.

Ring Crack: Another frequent consequence of impact-loading is the creation of ring cracks (aka incipient flakes, aka concentric fracture lines) on the cortical surface. As noted above, ring cracks form just outside of an indenter in hertzian fractures in the area of high tensile stress (Figs. 2.23 and 2.24). As the indenter moves further into the material, the surface contact area increases expanding the zone of tensile stress thereby creating multiple ring cracks, small flakes, and sometimes a collar form around the main crack (Lawn and Marshall 1979). According to fractographic literature studies (e.g., Frechette 1990) multiple concentric fracture lines and the flakes they define are indicative of impact-loading. Under certain conditions a few may form without impact, e.g., by static-loading on tooth cusps during mastication (Kim et. al 2008). Nevertheless, incipient flakes are much more common, better expressed (i.e., display more concentric fracture lines), and are associated with cones, partial cones, notches, and/or flake scars in materials subject to high velocity impact-loading (Ball and McKenzie 1994).

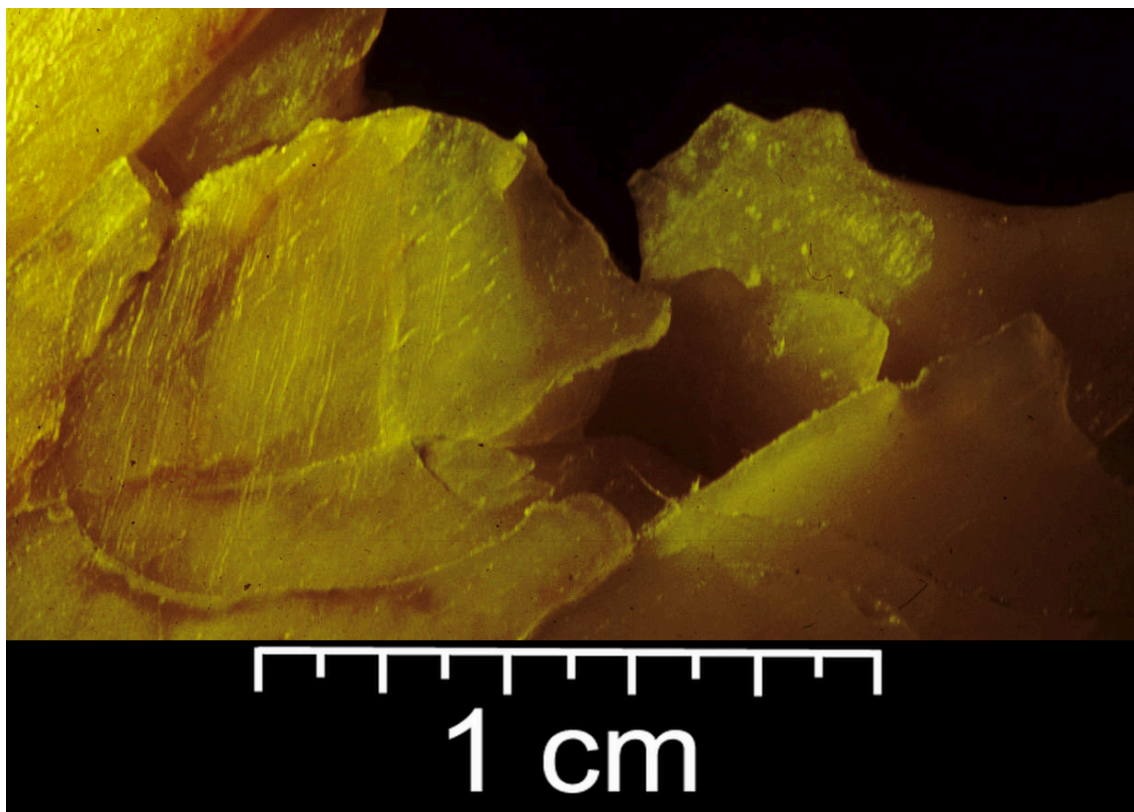


Fig. 2.24. Example of a percussion mark (striae) produced experimentally by hammerstone impact on a cow bone. Note also the incipient flakes, and the large number of fracture lines and small, irregularly shaped shatter pieces.

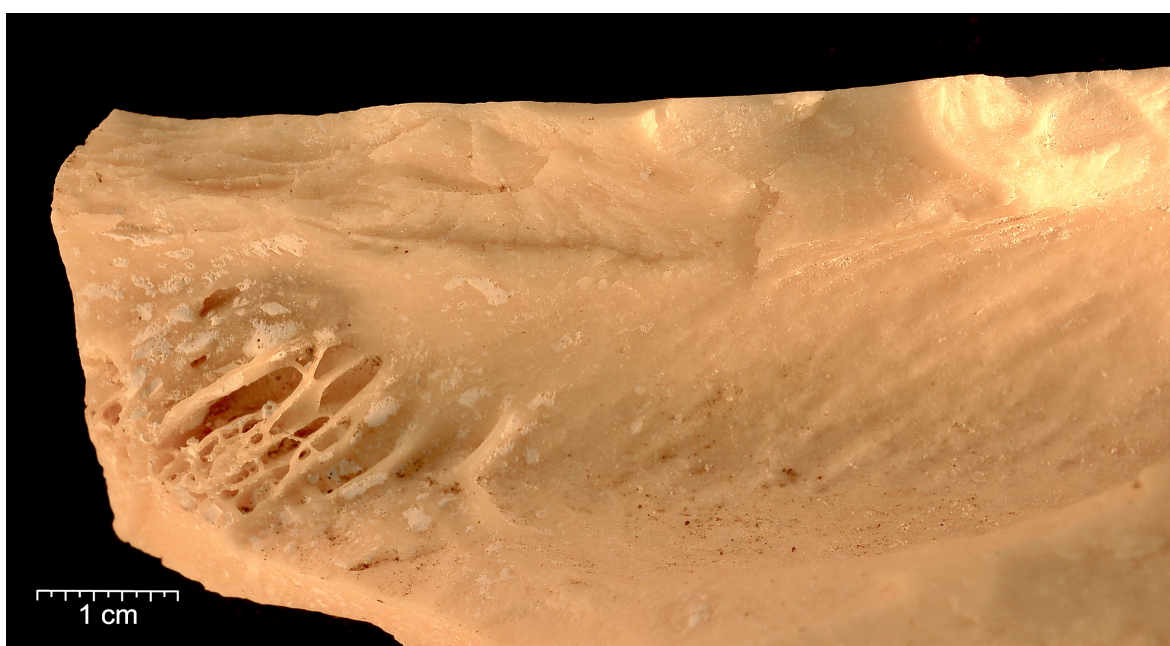


Fig. 2.25. Example of complex flake scars created by experimental hammerstone breakage of cow bone. At least three larger flake scars and numerous hinge terminations are visible. The large number of small flakes reflects the greater surface area that is created by impact-loading. The tiers of hinge terminations are large flakelettes. It is also important to note that this impact event did not produce a single definable notch, but instead produced multiple small notches each truncating the other. Note also the hackle marks in the larger left flake scar that point up to the loading point on the cortical surface.

In the archaeological bone fracture literature the ring cracks and flakes lying between ring cracks are referred to as concentric (Bonnichsen 1979) or incipient flakes (Capaldo and Blumenschine 1994) that form a series of concentric fracture lines on the cortical surface immediately adjacent to percussion notches. Like the fractographic studies, this experimental bone fracture literature also suggests that concentric fracture lines (aka incipient flakes) are diagnostic of hammerstone-induced bone fracture. Well-defined incipient flakes with numerous concentric fracture lines are rarely produced by carnivore gnawing. This is probably because static-loading by teeth cusps precipitates wedging where the compressive and tensile forces are strictly limited to and defined by the tooth cusp.

Flake Scars and Flakelettes: Both static and impact loading can remove small pieces from the nucleus material thereby creating flakes and flake scars. As noted above, flake scars produced by carnivore chewing are typically small and narrow with a steep fracture angle (Figs. 2.14 and 2.15). Both the flake and corresponding scar have a rather simple appearance being comprised of just one flake/scar. Bulbar scars, if present, appear as a separate component of the flake scar. In contrast, the flakes and corresponding scars produced by impact are typically larger and have a more complex, more irregular appearance being comprised of multiple flake scars and numerous hinge terminations (Figs. 2.25 – 2.27). In part, the multiple flake scars below an impact point reflect the removal incipient flakes. Thus, the fracture surface below a percussion notch has a more complex, multi-faceted appearance than the smaller, more regular appearing notch and flake created by carnivore teeth. This difference in flake production is ultimately due to the greater force and area of application in percussion compared to the static-loading of narrow, pointed carnivore teeth.

Flakelettes are a cascade of small flakes, with hinge terminations, are frequently created just below impact-loading points (Cotterell and Kamminga 1987; Figure 2.25). They are typically located just below the cortical surface, but whose appearance grades

into larger flake scars. Although a cascade of flakelettes seems diagnostic of impact fracture, both static– and impact–loading can create a crushed area at or just below the indenter contact area and it is often difficult to differentiate crushing from minute flaking.

Notches: Definitions of notches given here follow the description of carnivore and percussion notches presented by Capaldo and Blumenschine (1994). A notch is defined as a concave interruption of a fracture line at a loading point. A loading point notch is a particular type of fracture line created when application of force by the indenter causes the underlying bone to collapse forming a fracture line with a concave outline. Flake scars are normally formed below the notch. Notches have an oblong, almost linear, to semi–circular shape and are usually easily identified. They may define a loading point even when the fracture surface is poorly preserved or obscured by adhering sediment. Its length is the distance between inflection points that denote the intersections of the notch and the adjacent fracture lines. Notch width is the perpendicular distance between a line connecting the two inflection points and the most concave part of the notch.

If bounded by adjacent fracture lines it is possible to measure notch length and width. Notch length (breadth in Capaldo and Blumenschine 1994) is the distance between inflection points that denote the intersections of the notch and the adjacent fracture lines. Notch depth is the perpendicular distance between a line connecting the two inflection points and the most concave part of the notch (Figure 2.23). Capaldo and Blumenschine (1994) established, using notch and flake scar measurement, that hammerstone impact creates longer and shallower notches with larger flake scars than the semi–circular, arcuate notches and small flake scars created by carnivore gnawing. Importantly, impact notches often have a more irregular shape than the arcuate notches created by carnivore teeth.

Hackle Marks (aka, striae or whisker lances): These are linear features on the flake scar or flake surface that emanate and fan out from where the indenter contacts the material (Figs. 2.14, 2.16, 2.20, 2.25, and 2.28). Hackle marks are frequently visible on bone flakes and flake scars although larger ones are difficult to differentiate from steps that also point

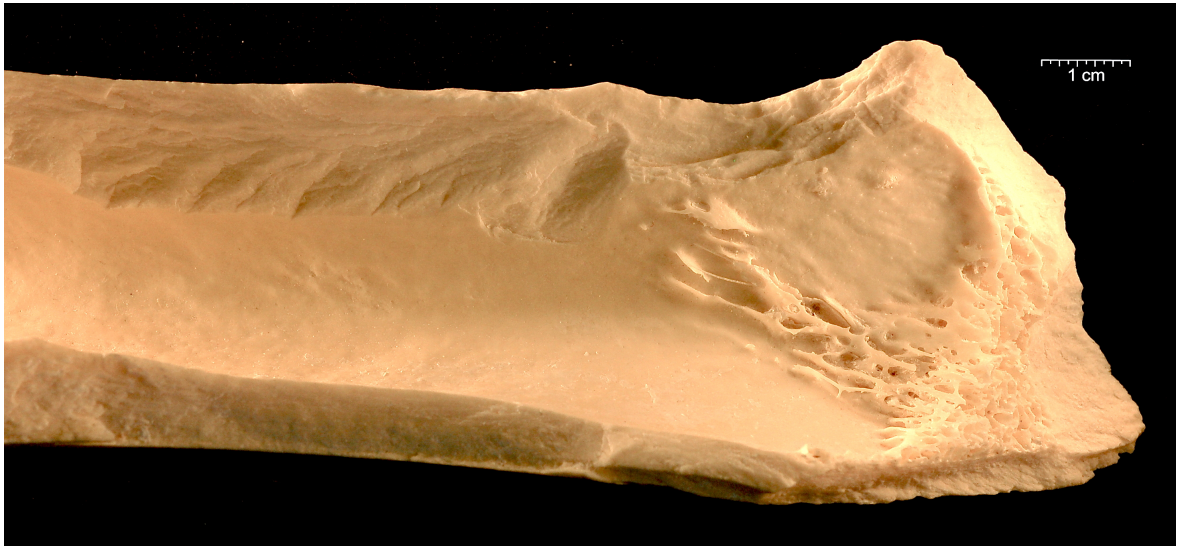


Fig. 2.26. Example of complex flake scars created by experimental hammerstone breakage of cow bones. Numerous hinge terminations indicative of smaller flakes are visible within and adjacent to the large flake scar. The large number of small flakes removed as well as the breadth and depth of the notch created in this single impact event reflects the greater surface area that is created by impact-loading. Note also the clearly defined chevrons or feathering on the upper fracture surface adjacent to the notch that point back to the load point origin, the flake scar and notch (see the schematic diagram of chevrons in Fig. 2.32).



Fig. 2.27. An example of damages created on a cow bone, first by experimental hammerstone fracture and then feeding of the broken bones to hyaenas. The complex flake scar (upper) is opposed by a loading point devoid of a flake scar (lower); both load points were created by experimental hammerstone fracture. Numerous hinge terminations indicative of smaller flakes as well as incipient flakes are visible within and adjacent to the large flake scar (upper load point). The lower loading point is defined by feathering features that diverge from the area immediately opposing the upper load point. Tooth marks overlies the lower load point and other tooth marks are visible on the medullary wall.

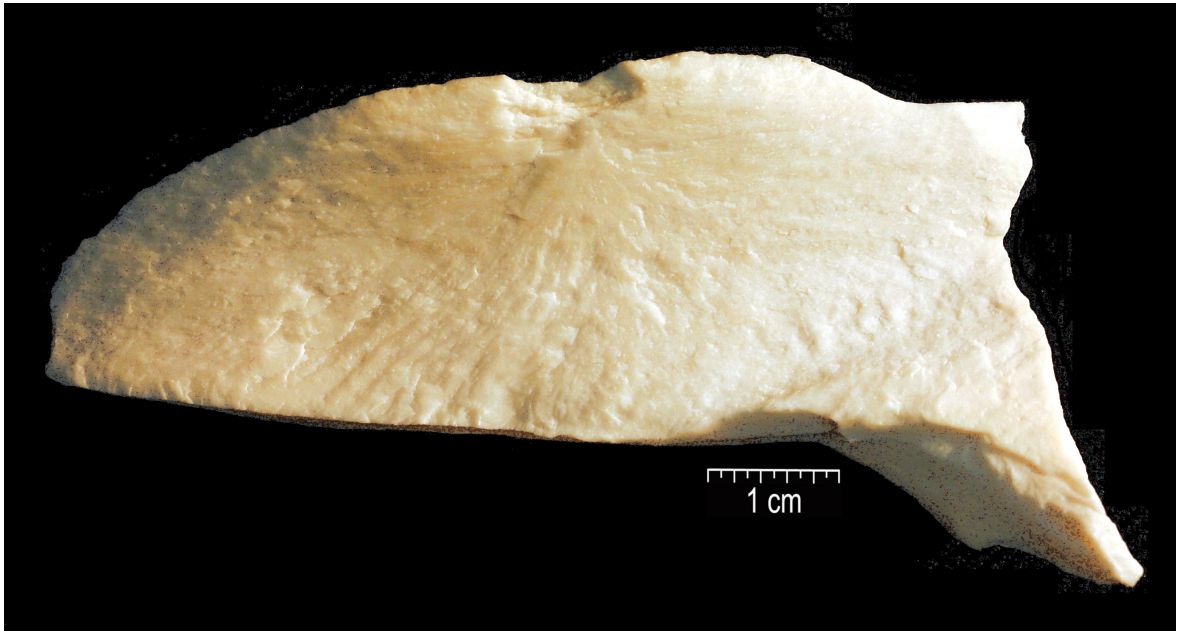


Fig. 2.28. An example of hackle marks on a cortical flake created during by experimental hammerstone fracture. Hackle marks are the linear features that point to the location of fracture initiation, in this case denoted by the small flake scar just below the cortical surface. Here hackles present a fan-shaped appearance. Hackles are clearly related to chevrons and feathering features found outside of the loading point on adjacent fracture surfaces.

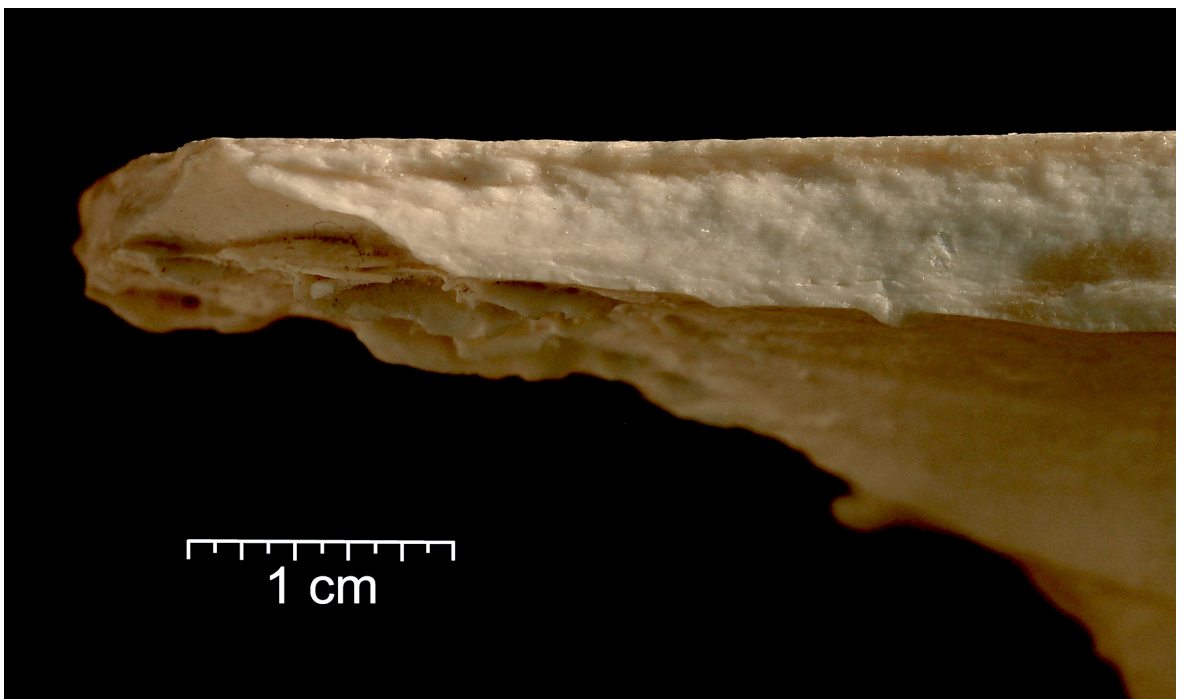


Fig. 2.29. An example a lateral stress feature created by experimental hammerstone fracture. In this case the lateral stress feature is expressed as a groove on the fracture surface adjacent to the loading point denoted by the flake scar on the left side of the specimen. Note also that the flake scar fracture angle is considerably less than the near 90° angles created by static loading with carnivore teeth.

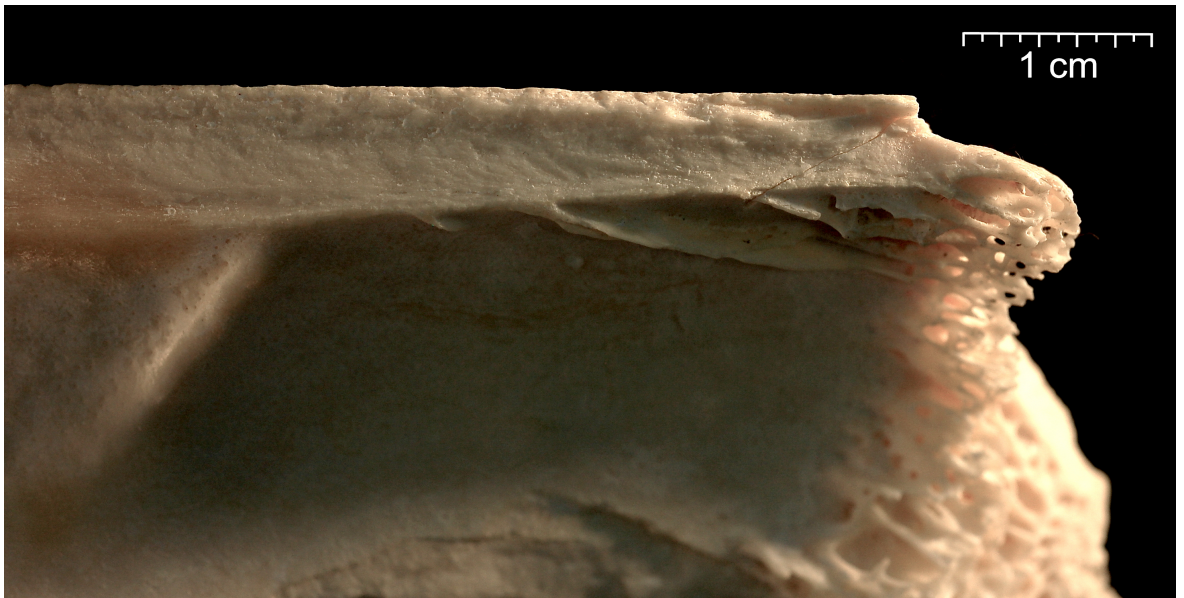


Fig. 2.30. An example a lateral stress feature emanating from the partial cone loading point (right side of specimen) created by experimental hammerstone fracture. In this case the lateral stress feature begins as a groove on the fracture surface adjacent to the loading point but quickly transitions into a ridge. The cone on the right is also outlined by incipient flake crack running diagonally downward to the right. Note again that the cone fracture angle is considerably less than the near 90° angles created by static loading with carnivore teeth. Feathering is slightly expressed below the middle part to the lateral stress feature.



Fig. 2.31. An example a lateral stress feature emanating from the loading point (angular indentation) created by experimental hammerstone fracture. In this case the lateral stress feature is a groove beginning at the cortical surface, which presents a cone-like outline. Unlike most impact loading points, the loading point fracture angle on this specimen is close to 90°. Loading points like this that lack a flake scar, notch, cone, and which present a steep fracture angle seem to be associated with loading on the anvil.

to the fracture origin. Although hackle marks are commonly produced on brittle materials under high tensile stresses occurring under both dynamic– and static–loading, their expression is likely more pronounced on impact fractured material. Hackle marks are clearly related to other features that indicate fracture front movement, i.e., chevron and feathering. As defined here, hackle marks are usually associated with a flake or flake scar. They often grade into the chevrons located on fracture surfaces immediately adjacent to the loading point. Several analysts (e.g., Bonnicksen 1979; Johnson 1985; Diez et al. 1999; Pickering and Egeland 2005) have used the presence of hackle marks to define impact fracture, but the frequencies of hackle marks in various assemblages have not been quantified.

Lateral Stress Feature: This is a new fractographic feature observed on bone fractured experimentally in this study with hammerstone and anvil. This feature has the appearance of a small ridge, groove, or crack and is found on the fracture surface immediately adjacent to the loading point just below the cortical surface (Figs. 2.29 – 2.31, 2.19, and 2.21). If both adjacent fracture surfaces are present lateral stress features usually appear in pairs, one just outside each side of the loading point. In some cases the ridge/groove angles up towards the cortical surface at the edge of the loading point fracture surface, following the same angle as the edge of the cone or flake scar to the cortical surface. In other cases, after an initial slightly upward orientation at the edge of the loading point, this feature seems to parallel the cortical surface. The length of lateral stress features may only be a few millimeters at the juncture with the loading point fracture surface, but expands to several millimeters (2–10mm) as it extends onto the adjacent fracture surface. This feature is best expressed on fracture surfaces longitudinal to the bone’s long axis. It seems clear that lateral stress features are related to tensile stresses just outside of the indenter contact area. The location of this feature suggests that it may be a truncated hertzian cone similar to that identified by Subhash et al. (2008). It may also be the expression of an incompletely formed annular (incipient) flake whose propagation was

either a) interrupted by the formation of a major fracture surface adjacent to the loading point moving along the bone's longitudinal axis, or b) represents initial formation of the longitudinal crack. Additionally, the location of lateral stress features near the cortical surface suggests that the interface between the circumferential lamellae and cortical haversian or primary bone below may play some role in fracture development. That is, fracture propagation may proceed more easily through the sheath-like circumferential lamellae and be arrested by the denser bone below. In composite polymers or ceramics, for example, lateral cracks may form at the interface between the surficial coating or outer layer and the underlying material/layer.

Feathering, Fringe, Chevrons or Plumes: Fracture fronts moving rapidly through a brittle material often create a chevron pattern in which the point of the chevron's "V" points back to the origin (e.g., Hull 1999). Each arm of the "V" is actually curvilinear with the concavity pointing to the fracture origin and opposite the direction of fracture propagation (Figs. 2.32, 2.15, 2.26, 2.27, 2.30). Chevrons are related to hackles and vertically oriented hackle marks on flakes and flake scars. This relationship can often be seen at the edges of the loading zone where hackles can be seen to turn and become curvilinear. In most cases only one arm of the "V" is apparent creating a plume feature, but again the concavity of the arm indicates fracture origin and direction. Chevrons and plumes are also referred to as twist hackle. Like hackle marks at the loading point, twist plumes can be produced under both impact- and static-loading, but they are particularly well pronounced on material fractured by impact-loading. This feature is particularly useful in locating the fracture origin (loading point) and can thus focus attention on an area of the cortical and fracture surface where loading point features may be found. Although Bonnichsen and Will's (1979) discussion of the use of micro-step fractures to determine the direction of fracture propagation is not sufficiently detailed to assess fracture front movement, it is clear that Bonnichsen was referring to chevrons and plumes.

Determination of fracture front movement direction for each fracture surface is a critical part of the fractographic approach. Assessment of fracture propagation directions yields information about the fracture event(s) on a number of levels. First, and foremost perhaps, determining the direction of front movement often leads to the identification of loading points that would not otherwise be noted. The importance of determining the direction of fracture front movement in the identification of small cones has been noted above. Similarly, tracing fracture origination directions on fracture surfaces back to the same location on the specimen often reveals the presence of a fracture surface or feature initially overlooked. On many specimens, for example, tracing fracture origination direction of two fracture surfaces to the same location revealed the presence of small flake scars separating the fracture lines (Fig. 2.33). While neither of these bits of fracture information — the small flake scars or the fracture origination direction — are important by themselves, their configuration allows definition of the flake scars as the likely loading point thereby forcing greater scrutiny of this location for other fracture features that might provide support for the definition of a loading point. In this manner, and others like it, assessment of fracture front movement allowed the identification of fracture features that would have otherwise gone unnoticed. Similarly, the configuration of surficial damages, fracture features, the number of fracture lines, and fracture front directions are important in the identification of hammerstone shatter and carnivore lever-ups.

Because carnivores typically begin gnawing at the softer epiphyseal ends of long bones, often where much soft tissue remains after muscle mass removal (by whatever agent), they commonly create what are here called lever-ups. Lever-up specimens typically have two relatively long fracture lines that, for much of their length, run parallel to each other. On one end of the specimen the long, roughly parallel fracture lines are separated by one or more fracture lines with associated carnivore toothmarks. On the other end, the long and roughly parallel fracture lines may intersect to form a point, or may be separated by an irregular fracture line. Fracture front movement of one or both long,

parallel fracture lines emanates from the end with carnivore damage. Examples of carnivore lever-up pieces showing how their identification is aided by determination of fracture front movement directions are shown in Fig. 2.34.

Radiating Fractures: These are fracture lines (cracks) that radiate out from the loading point but do not fragment the specimen into separate pieces. According to the fractographic and fracture mechanics literature (e.g., Quinn 2007), their creation requires the high forces associated with impact-loading. Although not defined as fracture lines, Johnson (1985) has noted the importance of radiating fractures in identifying impact-fractured bone. Radiating cracks created by hammerstone impact are illustrated in Figs. 2.17 and 2.35).

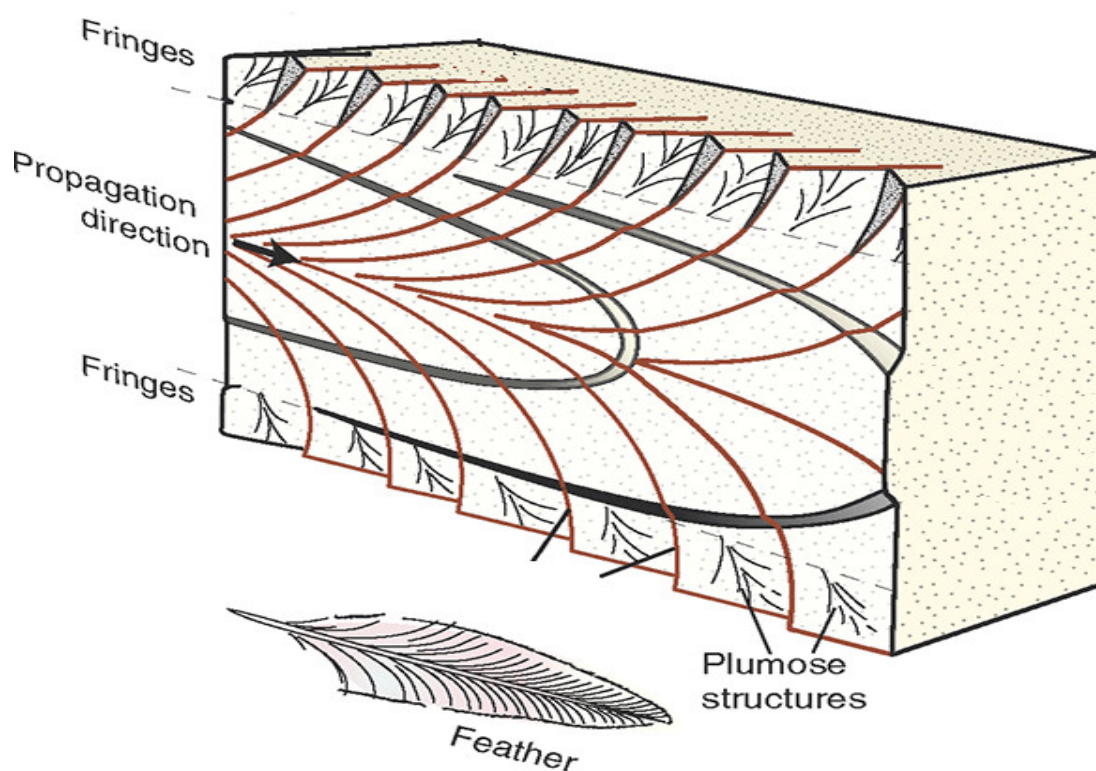


Fig. 2.32. Schematic diagram showing the chevrons and associated fringe fracture features whose convex side point back to the fracture point of origin and reveals the direction of fracture front movement. The broad arc features that intersect the chevron arms are called arrest lines. Chevrons, fringe, and arrest lines can have various appearances. Often for example, only the upper or lower part of the chevron arms are present in which case they are difficult to distinguish from arrest lines. Similarly, fringe at the edges of fracture surfaces frequently merge imperceptibly with chevron arms. Regardless of their specific appearance, these “feathering” features indicate the direction of fracture origin and direction of fracture front movement.

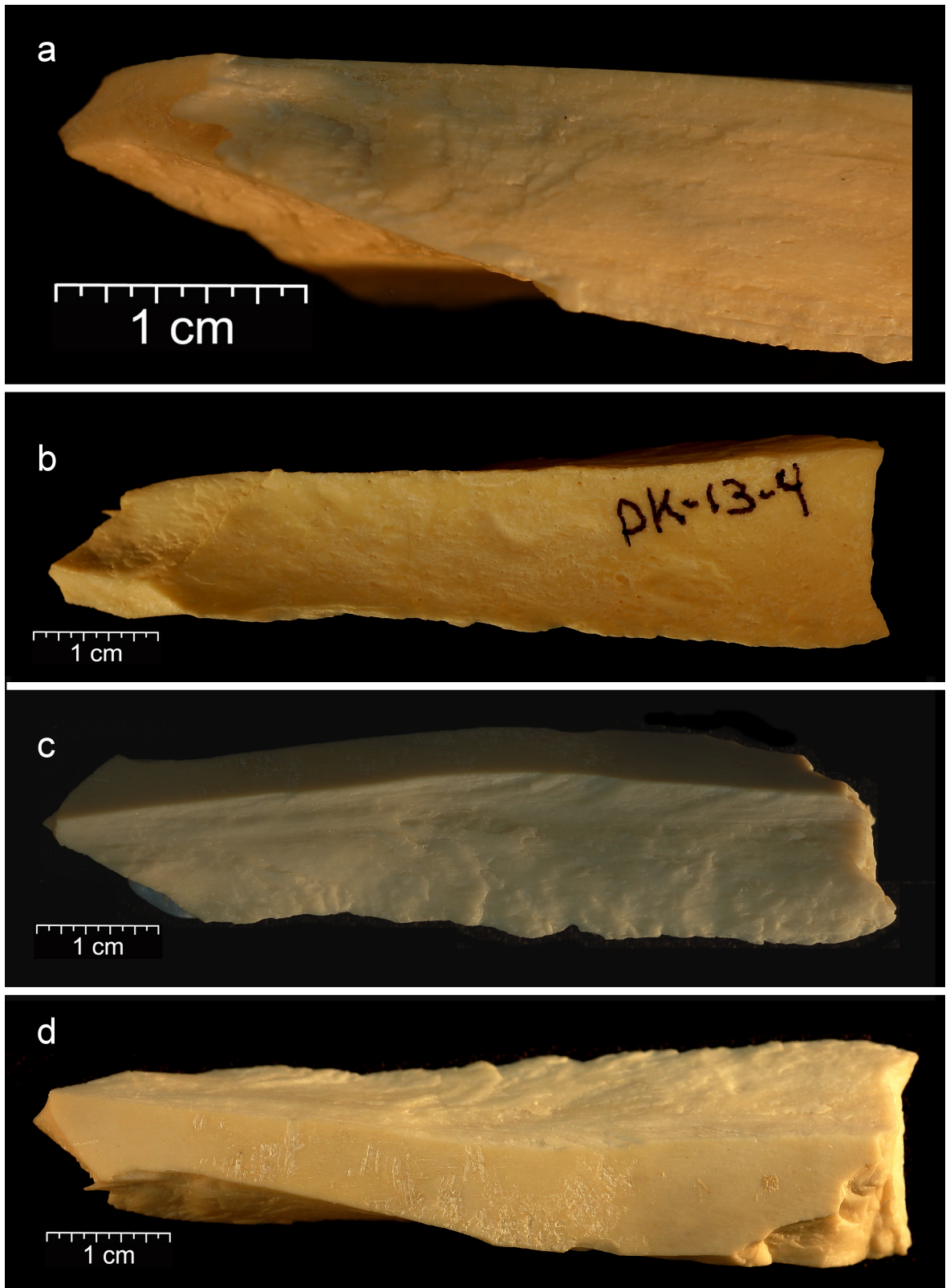


Fig. 2.33. Example of how determination of fracture front movement directions are critical to the fractographic approach. cursory examination did not allow definition of a loading point on this specimen. Close examination of the adjacent fracture surfaces (a and c), revealed that the chevrons on each pointed back to the load point. A slight dimple is visible (a) just before the feathering begins. Closer inspection of these surface revealed that they have hackle marks, a partial cone outline, and a slight notch, indicating that this was the loading point. Determining fracture front movement directions frequently permits definition of loading points and fracture agency. Percussion marks (d) are also visible.

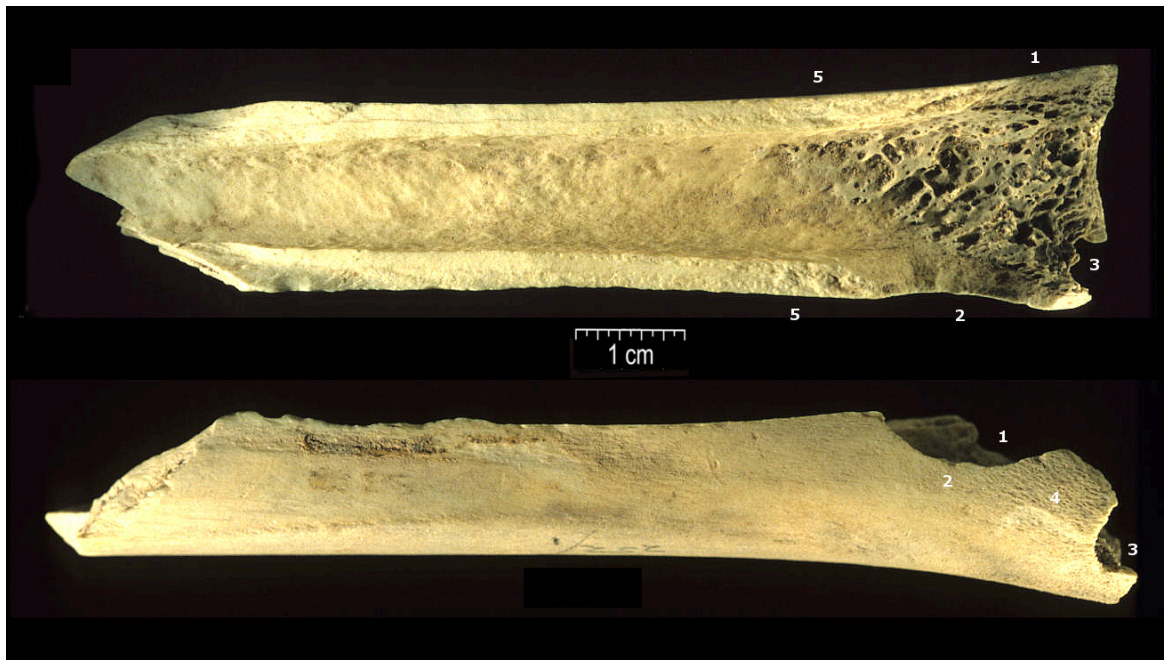


Fig. 2.34. Paired images (fracture, cancellous, and medullary wall surfaces above; cortical surface below) of a carnivore lever-up piece from AHD showing how the configuration of damages and fracture features aid in identifying loading points and fracture agent. Numbers 1-3 indicate the locations of paired tooth notches and number 4 is located above a series of tooth scores. Feathering (half chevrons) on the two roughly parallel and longitudinal fracture surfaces indicate the fractures emanated from the location of the carnivore damage.



Fig. 2.35. An example a radiating cracks emanating from the loading point denoted by the (barely visible) percussion mark and complete cone created by experimental hammerstone fracture.

Typically radiating cracks have an oblique or transverse orientation. Carnivore-induced fracture will create transverse and oblique fractures originating at the loading point, but rarely create radiating cracks in which the bone is not split into separate pieces. This is due to the slow and lower application of force in static-loading as well as the size and shape of the indenter. Because of their larger contact area hammerstone loads are spread out over a larger area instantaneously, whereas the smaller, pointed, and oblong contact area of carnivore teeth concentrate loads over a smaller, more linear-shaped area. That is, whereas hammerstone impact requires instantaneous energy dissipation across an area devoid of pre-existing cracks (save micro-flaws and zones of weakness inherent in bone), carnivore-induced fractures are likely initiated by wedging in which stresses are built up in a small, localized, and linear-shaped area prior to failure thus precluding the formation of radiating cracks.

Fracture (Plane) Angle: Bonnichsen (1979) and others (Morlan 1984; Johnson 1985; Villa and Mahieu 1991) noted that the fracture to cortical surface angle is important in distinguishing dry and green fractures. Fracture of fresh (green) bone tends to produce oblique and acute fracture plane angles whereas in dry, mineralized bone fracture planes tend to display a 90° angle. Additionally, Bonnichsen (1980, pers. com.) suggested that carnivore-induced fractures also tend to create 90° or near 90° fracture surface angles. Radchenko and Kobenko (2000) observed that impact-loading initiation face angles created on composites also tend to be near 45°.

Alcantara et al. (2006) provided experimental documentation that fracture planes created by carnivore-induced bone fractures have fracture plane angles approaching 90° whereas more oblique or acute angles are created by impact-loading. The explanation for this pattern may be because carnivores cause wedging fractures in which teeth forced into bone causes a very small area deform plastically allowing crushed bone to fill the void, thereby initiating a crack. As noted in studies of lithic flake production (Cotterell and Kamminga 1987), wedging tends to create nucleus edge angles near 90°. The more oblique

and acute impact-initiated fracture angles may represent the extension of one of the similarly angled faces of the hertzian cone or associated flakes. This difference in fracture plane angles created by hammerstone- and carnivore induced fractures has been recently applied to assess the relative frequency breakage patterns in Plio-Pleistocene assemblages (Pickering et al. 2005; Dominguez-Rodrigo and Barba 2007b).

Fracture Orientation: Recording the orientation of individual fracture lines relative to the bone's long axis, e.g., transverse, oblique, and longitudinal, avoids problems associated with characterizing the shape of a specimen with multiple fractures. Alcantara et al. (2006), Pickering et al. (2005), and Dominguez-Rodrigo and Barba (2007b) used this system in their analyses of fracture plane angles.

There are suggestions that hammerstone- and carnivore-induced fracture orientations may differ, at least at the assemblage level. Johnson (1985), for example, notes that carnivore chewing from limb bone ends reduces overall bone strength and continued chewing tends to create rectilinear fragments. These are fragments in which the dominant fracture line direction is longitudinal to the long axis. Johnson's description of these carnivore-created rectilinear pieces seems to match what are here called leverup pieces. And, in spite of not being diagnostic of percussion fracture, curved, or spiral fractures seem to be associated with this mode of fracture and assemblages created by hominins (Johnson 1985; Villa and Mahieu 1991).

Note that time constraints did not allow assessment of either fracture orientations or fracture angles. An attempt was made to measure fracture angles. Fracture angle measurement was abandoned because the fracture angle frequently changes within a load point and because most fracture lines also exhibit more than one angle. Future work will address this issue. The above discussions of fracture orientations and angles are included because of their likely importance in differentiating carnivore- from hammerstone-broken bone.

Indenter (Tooth and Percussion) Marks: The cortical surface of bone may preserve two features, notches and indenter marks, which provide important, often conclusive, data for ascertaining fracture agent. The definition of percussion marks follows that given by Blumenschine and Selvaggio (1988). Tooth mark definitions follow Binford (1981). [Loading marks, i.e., tooth marks and percussion marks, are sometimes associated with notches and provide further, often conclusive, data for ascertaining fracture agent. Tooth marks may appear as pits or scores on the cortical surface of compact bone while punctures and furrows are typically restricted to epiphyses and near epiphyses with thin compact bone.] Bonnichsen (1979, pers. comm. 1980) noted but did not describe the impact scars that were created in his hammerstone fracture experiments. Blumenschine and Selvaggio (1988) provided a description noting they may appear as either small patches of microstriae, or small, irregularly shaped depressions with a somewhat crushed appearance that may or may not contain linear or irregularly shaped patches of microstriae (Figs. 2.19, 2.21, and 2.33d).

Tooth pits (Fig. 2.36) are circular to oblong or slightly irregular depressions in which at least part of the bone appears compressed. At low magnification, minute cortical pieces at the cortical surface–depression wall juncture may appear crushed, pushed down, or torn and oriented toward the base of the depression. A tooth pit may have a linear aspect, as it becomes a tooth score. Pitting may be concentrated on epiphyseal ends and on broken bones near the exposed medullary cavity due to carnivore’s attempt to extract marrow or lever pieces back to expose more of the marrow cavity (pers. observ.). Tooth pits are distinguished from hammerstone impact marks by their regular shape and a lack of microstriae on the pit walls (Blumenschine & Selvaggio, 1988).

A tooth score is a broad, u-shaped groove in which the groove walls appear compressed or torn (Haynes, 1981; Shipman, 1981). Striae are usually absent in the groove, but if present they are poorly defined and do not extend the entire length of the

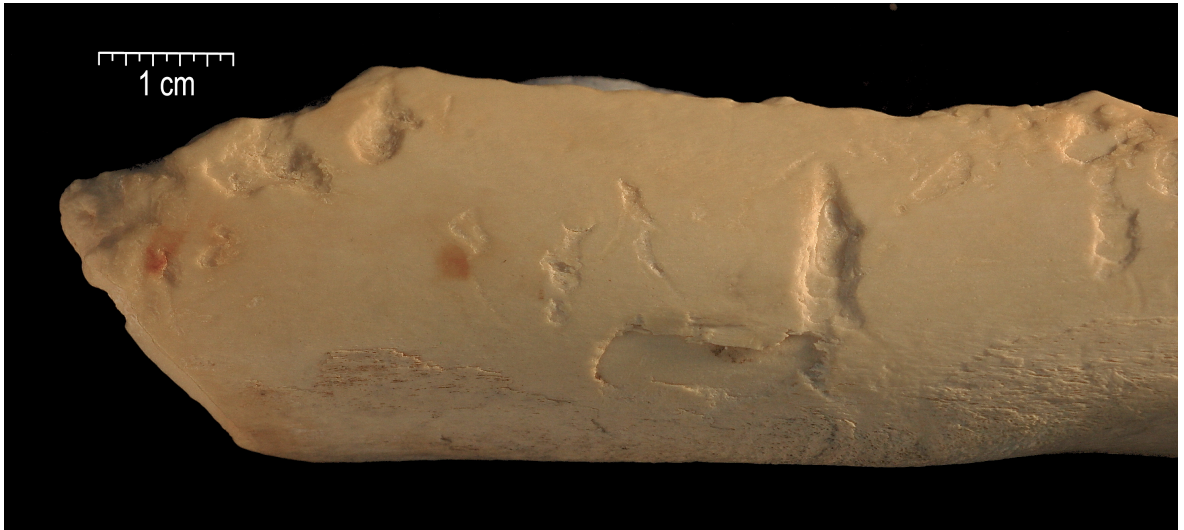


Fig. 2.36. Diagnostic tooth pits and scores created by Denver Zoo hyaenas. Note that although many tooth marks shown here have regular edges where they intersect the cortical surface, many do not.

score. Scores often begin as a pit or an oblong depression and end in a shallow lineation (also called a “tail”).

2.6 Synopsis

The above carnivore bite force and impact force calculations, and review the fracture mechanics and fractographic literature has shown that a) hammerstones create orders of magnitude greater loads than can be created by carnivore gnawing, b) the hierarchical construction and material properties of bone plays a significant role in fracture development, c) static- and impact-loading differ in their fracture mechanics, and d) differences in the fracture mechanics of static- and impact loading creates discernable differences in the appearance of fracture surfaces and overall fracture patterning.

Previous zooarchaeological fracture studies casually note that carnivore teeth and hammerstone-impact load bones differently, but have not stated just what the difference between static- and impact-loading means. The review presented here demonstrates just how vast these differences are, both in terms of applied load as well as aspects of indenter size and shape. Hammerstones load bone via impact with large indenters creating a minimum of ~10300N of force, while carnivores with smaller, statically-applied teeth create an observed maximum bite-force of ~4500N.

The review of the fracture mechanics literature revealed important concepts that aid in understanding fracture, particularly differences in fracture development under impact- and static loading conditions. The following are particularly important:

- 1) Under static-loading the applied forces, and thus energy transfer, are lower and the rate of loading much slower than with impact-loading in which the energy imparted to the material is instantaneous.
- 2) Impact-loading creates shock waves in the material while static-loading does not. The interaction of shock waves with existing (i.e., bone surface) and developing (i.e., fracture surfaces) surfaces causes multiple fractures to occur simultaneously.
- 3) Because impact-loading imparts more energy to the material, greater work is done and more fracture surfaces are created than with static loading.
- 4) Finally, the importance of examining each specimen in its entirety – its fracture surfaces, fracture features, overall shape, associated damages, and their configuration relative to one another – cannot be over-emphasized. An a priori decision to examine just obvious notches and indenter marks (tooth and percussion) – as is common in zooarchaeological analyses – is a very narrow approach that ignores much information and severely limits our ability to understanding bone fracture and identify fracture agency. By definition the fractographic approach outlined here forces the examination of the specimen in its entirety.

The fracture mechanics principles and fractographic features outlined above indicate that the four assemblages under consideration should display fragmentation patterns and frequencies of select fracture features dependent on the amount of force applied to the bones. The specific expectations for the assemblages are stated in the next chapter.

- CHAPTER 3 -
***Research Framework: Hypotheses for Fracture Patterns and Features
Among the Four Assemblages***

3.1 Introduction

The previous chapter's fracture mechanics and fractographic overview of differences in static and impact loading which should result in different fracture patterns are summarized here in terms of specific expectations for the modern Amboseli Hyaena Den (AHD) and Experimental (EXP) control assemblages, and the Plio-Pleistocene fossil assemblages from Olduvai Gorge, Tanzania, FLK-NN2, and FLK-Zinj. Not all fracture feature and pattern differences that the fracture mechanics and fractographic literature indicate should result from static- vs. impact loading are examined here. Only those related to fragmentation and fracture features associated with loadpoints (LDPTs) are examined.

Given this knowledge of fracture mechanics and fractographic features created by static and impact loading extremes, we should expect bone assemblages created by carnivores and hammerstone impact to exhibit discernable differences in the frequencies of some specific fracture features and fracture patterns. The following expectations assessed in this study are structured by a) the fracture mechanics and fractographic principles and features outlined above, b) the agents *known* to create the AHD and EXP assemblages, i.e., hyaenas and hammerstone-fracture, respectively, and c) *interpretations* of the agents responsible for the FLK-NN2 and FLK-Zinj assemblages presented by previous analysts (e.g., Bunn and Kroll 1986; Potts 1988; Oliver 1994; Blumenshine 1995; Dominguez-Rodrigo et al. 2007; Egeland 2007). That is, while the overall goal of this research is to determine if specific fracture features can define carnivore- and hammerstone-induced fracture, enough work has been done on both fossil assemblages to warrant statement of which fossil assemblage should be most similar and/or dissimilar to the known carnivore and hammerstone created assemblages, AHD and EXP. Thus, both the lack of tools as well as characteristics of the faunal assemblage, including a lack of cut and percussion marks,

abundance of tooth marks, and patterns of limb bone preservation, indicate FLK–NN2 was accumulated by carnivores (Potts 1988; Egeland 2007). Similarly, although percussion mark and notch frequencies presented by previous analysts are low, all agree that hominins were responsible for a large, but unknown amount of bone fracture at FLK–Zinj.

3.2 Hypotheses to Test

Given the principles of fracture mechanics and the fractographic features resulting from static and impact loading extremes outlined in Chapter 2, several hypotheses for differences in the four study assemblages may be stated:

- 1) The most general, hypothesis is that if these interpretations are correct, then analyses presented here should show the FLK–Zinj fracture feature frequencies and associations to be most similar to those observed in the hammerstone–broken EXP assemblage. Similarly, the carnivore-accumulated assemblages, AHD and FLK–NN2, are expected to show more similarities in fracture features than they are with the EXP and FLK–Zinj assemblages.
- 2) Because of the vast differences in loads imparted by carnivore gnawing and hammerstone impact, assemblages created by carnivores should be less fragmented, the specimens larger and more complete than in assemblages fragmented mainly by hammerstone processing for marrow. Limb specimens from AHD and FLK–NN2 are expected to be more complete than those from either FLK–Zinj or the EXP assemblages.
- 3) Similarly, because high loads create more fracture surfaces, the AHD and FLK–NN2 assemblages should exhibit fewer fractures than the hammerstone created EXP assemblage as well as the FLK–Zinj assemblage.
- 4) The frequencies of loading points (defined by the presence of flake scars – FLKSs, notches – NTCHs, cones – FLKOs, percussion marks – PMs, tooth marks – TMs, and those defined on the basis of fracture features – FRFEs), alone or in combination are

expected to be less in the AHD and FLK–NN2 assemblages than in the EXP and FLK–Zinj assemblages. This is because carnivores typically attack the epiphyseal ends before the limb shaft which leaves fewer identifiable load points than hammerstone–induced fracture that is typically directed at the shafts where load points are more readily preserved.

- 5) Because hertzian fracture is characteristic of impact loading, it is hypothesized that load points defined on the basis of cones or partial cones (FLKOs) should be more frequent in the EXP and FLK–Zinj assemblages than in either the AHD or FLK–NN2 assemblages. The same is true for the cone or partial cone fracture feature (CO).
- 6) Ring cracks, aka incipient flakes (IF) have been shown to be diagnostic of impact fracture (Capaldo and Blumenshine 1994) and consequently should exhibit greater frequencies in the EXP and FLK–Zinj assemblages than those observed in the AHD and FLK–NN2 assemblages.
- 7) Similarly, impact loading imparts considerable energy to the material that must be dissipated via the creation of fracture surfaces. Consequently, one type of fracture line – the radiating crack (RC) – located at the loading point should be more frequent in the EXP and FLK–Zinj assemblages than in either the AHD or FLK–NN2 assemblages.
- 8) The fractographic literature indicates that hackle marks (HK) are commonly created on the flakes and flake scars created by impact loading. Zooarchaeological analyses have also used hackle marks to define impact fracture. Consequently the eighth hypothesis is that more loading points that display hackle marks are expected in the EXP and FLK–Zinj assemblages than in the AHD and FLK–NN2 assemblages.
- 9) The fractographic feature lateral stress features (LS, defined here for the first time), seems to be mechanically related to the creation of hertzian cones. These shallow ridges or grooves that emanate from impact loading points are expected to be

infrequent in the AHD and FLK–NN2 assemblages, but characteristic of loading points in the EXP and FLK–Zinj assemblages.

- 10) Since the fractographic literature indicates that finer scale fracture features (5 through 9 above) are better–expressed on materials broken by impact loading than static loading, the tenth hypothesis is that the overall frequency of fracture features should be greater in EXP and FLK–Zinj than that of the AHD and FLK–NN2 assemblages.
- 11) If the fracture features noted above (cones, lateral stress, incipient flakes, hackle marks, and ring cracks) are in fact indicative of impact fracture, then they should be frequently and directly associated with percussion marks.

Although, the above hypotheses will be tested and assessed in this study, it is important to realize that this is not a “cookbook” approach to the study of bone fracture. That is while some features are frequently indicative of static or impact loading, it is the configuration of features and damages that provide the most valuable information and, moreover, frequently force attention to an otherwise overlooked diagnostic feature or damage. Too much valuable information will be lost by focusing only on obvious loading points. Rather, the analytical methodology advocated here attempts to understand the fracture evidence of individual fragments within the context of bone as a material, the vast difference in static and impact loads. Moreover, even when specific diagnostic features are absent, these data provide a framework – a constellation of fracture features – for understanding bone fracture and placing them in the context of patterns that can be ascribed to specific agents. That is, with an appreciation of the hierarchical structure of bone, fracture mechanics, and fractography – particularly as they relate to the large differences in force applied by static – and impact–loading – it is possible to make a *subjective but informed assessment* of fracture agent based on a suite of fracture features even where diagnostic damages are lacking.

- CHAPTER 4 - ***Materials and Methods***

4.1 Introduction

The experimental (EXP), actualistic (AHD), and fossil assemblages (FLK-NN2 and FLK-Zinj) examined in this study are first briefly described. The damage and fracture attributes coded for each assemblage are defined. Attributes include a subset of the bone damages and fracture attributes reviewed in Chapter 2 - Fractography and Fracture Mechanics), as well as commonly examined tool mark and carnivore damage types. The damages and fracture attributes coded for each bone examined are defined and the rationale explained in the second section of this chapter.

4.2 Materials: Assemblage Descriptions

One experimental, one actualistic, and two fossil assemblages were examined. The actualistic, carnivore accumulated assemblage studied is the Amboseli Hyaena Den (AHD) assemblage collected by Hill (1981, 1983, 1984, 1989) in Amboseli National Park, Kenya. Bones broken by the author using hammerstone and anvil constitute the experimental assemblage (EXP). Some of these experimental bones were also fed to hyaenas at the Denver Zoo to assess what damages might be used to define whether hominins or carnivores had first access to the bones. These experiments resulted in little more than tooth marking of the bones. Both of the fossil assemblages are from Bed I, Olduvai Gorge, Tanzania. The FLK-NN2 assemblage is a small assemblage that previous research has indicated is mainly a hyaena accumulation (Bunn 1982; Potts 1988; Egeland 2007b). The FLK level 22, aka FLK-Zinj, assemblage is a large assemblage that all analysts agree hominins played a large role in forming (Bunn 1982; Bunn and Kroll 1986; Blumenshine 1987, 1995; Capaldo 1997; Dominguez-Rodrigo et al. 2007a; Oliver 1994; Potts 1988) although the mode of carcass acquisition is debated.

H.T. Bunn (pers. comm.) kindly provided a list of catalogue numbers and the corresponding taxonomic and skeletal identifications for the FLK-NN2 and FLK-Zinj

assemblages. A. Hill and R. Potts (pers. comm.) kindly provided a list of catalogue numbers and the corresponding taxonomic and skeletal identifications for the AHD assemblage. In this study, only bovid, suid, and equid material are considered. Specimens <20mm in maximum dimension from each assemblage were examined (if present) and coded, but most analyses are restricted to specimens >20mm.

Table 4.1 is a list of abbreviations used in this study. Taxa, element, and element portion codes follow Gifford and Crader (1977). The taxonomic and skeletal identifications as well as age, and size class assignments for the FLK-NN2 and FLK-Zinj specimens are derived from Bunn (1982, p. 477-499; 1990 pers. comm.). The AHD material was identified by A. Hill (1990, pers. comm.). Age data were not collected for the AHD assemblage. Element, portion, and side identifications were first made by the author and then crosschecked with lists provided by Bunn (pers. comm.) and Hill (pers. comm.).

Size class categories developed by Brain (1981) and refined by Bunn (1982) are used here:

- 0 – indeterminate size
- 1 – < 50 lb. (23 kg.); e.g., Thomson's gazelle
- 2 – 50 – 250 lb. (23 – 113 kg.); e.g., impala, warthog
- 3 – 250 – 750 lb. (113 – 340 kg.); e.g., topi, wildebeest, zebra
- 3a – 250 – 400 lb. (113 – 181 kg.); e.g., adult topi
- 3b – 400 – 750 lb. (181 – 340 kg.); e.g., wildebeest, zebra
- 4 – 750 – 2000 lb. (340 – 907 kg.); e.g., eland, buffalo
- 5 – 2000 – 6000 lb. (907 – 2722 kg.); e.g., hippo, rhino, giraffe
- 6 – >6000 lb. (>2722 kg.); e.g., elephant

For the purposes of this study, size 1 and 2 specimens were grouped together (size class 1-2) as were size 3 and 4 specimens (size class 3-4).

EXP material was assigned a two-part catalogue number. The first part refers to the experiment number (which refers to one element) and the second to the fragment number. The AHD catalogue number consists of a letter code for element and a number. The FLK-Zinj and FLK-NN2 catalogue schemes are variable. Catalogue numbers normally appear on specimens found in the wooden trays on museum shelves, but rarely on specimens in

Table 4.1. List of abbreviations used in this study.

ASSEMBLAGE

EXP	–	Experiments conducted at Denver Zoo
AHD	–	Amboseli Hyaena Den, Amboseli National Park, Kenya
FLK–NN2	–	FLK North North Level 2, Olduvai Gorge, Tanzania
FLK–ZINJ	–	FLK level 22 (FLK –“Zinjanthropus”), Olduvai Gorge, Tanzania

ELEMENT

FEM	–	femur
HUM	–	humerus
LBSF	–	long bone indeterminate (shaft fragment)
MCM	–	main metacarpal
MTM	–	main metatarsal
METM	–	metatarsal/metacarpal
RAD	–	radius
RUL	–	radius–ulna
TIB	–	tibia
ULN	–	ulna

PORZION

CO	–	complete bone
COD	–	complete juvenile shaft plus distal epiphysis
COP	–	complete juvenile shaft plus proximal epiphysis
COS	–	complete juvenile shaft
DS	–	distal articular end
DSE	–	distal shaft minus epiphysis
DSH	–	distal articular end plus shaft
PSE	–	proximal shaft minus epiphysis
PSH	–	proximal articular end plus shaft
PX	–	proximal articular end
SH	–	shaft

LOADING POINTS

LDPT	–	loadpoint
FLKS	–	loadpoint defined by flake scar
FLKO	–	loadpoint defined by a cone or partial cone
FRFE	–	loadpoint defined by other fracture features
NTCH	–	loadpoint defined by a notch
LMRK	–	loadpoint defined by a loading (indenter) mark

FRACTURE FEATURES

CO	–	cone or cone fragment
LS	–	lateral stress
IF	–	incipient flake (aka ring crack, aka concentric fracture lines)
Bsc	–	bulbar scar
HK	–	hackle marks
FR	–	fringe (aka chevrons, aka plumes)
RC	–	radiating cracks
#FLNs	–	number of fracture lines

LOAD MARKS

PM	–	percussion mark
TM	–	tooth mark

ASSEMBLAGE MEASUREMENTS

NISP	–	number of identified specimens
MNE	–	minimum number of elements
MNI	–	minimum number of individuals

variously labeled fragment bags (Samples I and F, see below). Still, many identifiable specimens (particularly those from FLK-Zinj) either lack numbers or the numbers are illegible. Catalogue numbers on specimens that matched those given by Bunn (1982 and pers. comm. 1990) were accepted. FLK-NN2 and FLK-ZINJ specimens with illegible or missing numbers were not automatically assigned arbitrary laboratory numbers. Rather, an attempt was made to determine the specimen number by comparing the element identification and specimen dimensions with the list of specimen numbers and corresponding identifications, descriptions, and dimensions provided by Bunn (1982; pers. comm.).

Specimens identified to taxa and element from AHD (n=487), FLK-Zinj (n=551), and FLK-NN2 (n=124) are located on shelves in wooden trays within the vertebrate paleontology range at the Kenya National Museum. Most of these have catalogue numbers, although many are illegible. A sample of larger bone fragments from FLK-Zinj (n=538) some of which have been identified to taxa and element by Bunn (1982), is not found on the Olduvai Gorge shelves with the identified material, but is stored in bags in another part of the vertebrate paleontology range. The sample of small (most <40mm in length) indeterminate fragments from FLK-Zinj (n=838), few of which can be identified beyond a mammal long bone shaft fragment (see Bunn 1982) is stored with the larger bone fragments. Although the FLK-Zinj fragment and indeterminate bags are variously labeled, few specimens are numbered. The small, fragmentary, and unidentifiable material in the AHD and EXP assemblages was assigned to the fragment category (n=429 and 139, respectively).

The maximum length, width, and thickness (in millimeters) of all specimens from each assemblage were recorded. These measurements are particularly useful in identifying specimens examined by Bunn (1982) and Blumenschine (1995). Bunn (1982; 1990, pers. comm.) also recorded the maximum length, width, and thickness of specimens >40mm

maximum length from FLK-Zinj and FLK-NN2. Both sets of measurements were compared to ensure the same specimen was examined, to check unclear catalogue numbers, and locate otherwise “missing” specimens.

4.2.1 Hammerstone Fracture Experiments (EXP)

Hammerstone fracture and a few carnivore feeding experiments were conducted at the Denver Zoo to a) aid in the development of a fracture and damage coding key, b) assess damage patterns created in different hominin and carnivore access sequences, and c) create an assemblage fracture patterns created by known agents for comparison to the other studied assemblages. Thirty fresh adult cow bones were obtained from a Denver meat processing plant. Only very small scraps of flesh remained on the bones. Most scraps of flesh (tendons and bits of muscle) were located at the proximal and distal metaphyses with occasional quite small bits of muscle on the shaft. Some bones were obviously from large mature bulls while others were from smaller mature animals, likely cows. A few bones were from sub-adults, displaying incomplete epiphyseal fusion. Three hyaenas and two lions were used in the feeding experiments (Fig. 4.1, Table 4.2). All specimens are in the possession of the author.

Four types of experiments were conducted:

- 1) breakage/gnawing by carnivores only (C),
- 2) breakage by hammerstone then presentation to carnivores (HC),
- 3) breakage/gnawing by carnivores then hammerstone breakage (CH),
and
- 4) breakage/gnawing by carnivores then hammerstone breakage then another episode of carnivore breakage/gnawing (CHC).

A smooth and round granitic cobble weighing approximately 1.6kg and a larger flat cobble were used as the hammerstone and anvil in the impact fracture experiments. The goal in these impact fracture experiments was to expose the marrow cavity to allow removal of largely intact marrow pieces relatively “uncontaminated” with small flake fragments (sharp slivers). Previous experience (pers. observ.) indicated that the difficulty of removal, contiguity, and state of contamination of marrow varies by elements and initial

blow location. Mid-shaft blows often leave sharp fragments in the main marrow body and, moreover, create proximal and distal portions from which the marrow is often difficult to remove, often requiring an implement (e.g., stick, knife, spoon) or (in a procedure not unlike trying to get ketchup out of a bottle) by pounding the broken end in hopes of the marrow falling out as a unit. Blows struck at or just below the metaphysis, however, tend to yield less contamination of the main marrow body (cancellous bone absorbs some of the impact energy) while at the same time creating a larger marrow piece. Moreover, larger, more contiguous pieces of sliver-free marrow may be removed by either prying loose long fragments still held together by the periosteum, or by addressing less forceful blows at the ends of fracture lines to open up the marrow cavity. Therefore, most bones were initially struck not at the mid-shaft, but near the base of the metaphysis. [As an aside, this experience suggests that there may be reason to believe the location of hammerstone blows may vary with post-processing behaviour, e.g., cooking.] When possible, less forceful blows were then used to split the mid-shaft. A plastic spoon and/or a five-inch long knife were used to remove as much marrow as possible from each bone before being fed to the carnivores.

Five carnivores, three adult hyaenas (two females and one male) and an adult male and female lion (Table 4.2) were presented whole and hammerstone-broken bones. Most, but not all, large fragments created by hammerstone-induced fracture were presented to the carnivores when they remained tightly attached to the proximal end plus shaft (PSH) and/or distal end plus shaft (DSH) halves. Zoo safety concerns and fear of loss in the pens meant that the small, disassociated flakes, cones, impact shatter fragments, and slivers resulting from hammerstone breakage were not presented to the hyaenas. Some larger fragments not firmly attached to the proximal or distal end were also removed before feeding. Carnivore access times ranged from 16 to 108hrs (Table 4.3). There was some loss of small limb shaft fragments in all experiments, either due to carnivore consumption

or loss in the enclosure yards. Carnivore gnawing produced very few fragments. Regardless of the timing of hammerstone breakage (before or after feeding), all but a few fragments are the result of impact fracture.

Details of the 30 experiments including experiment type, number of fragments created in each stage, and the time carnivores had access to the bones are summarized in Table 4.2. The NISP and MNI values are given in Table 4.3.

Bones were degreased at the Illinois State Museum using a propane-fueled burner and a turkey-fryer pot. Each large piece and groups of smaller fragments (placed in separate gauze bags) were boiled in water with $\frac{1}{4}$ to $\frac{1}{2}$ a cup of Biz detergent. Grease was periodically skimmed from the surface. Boiling times varied depending on bone size and grease content. Bones were removed from the bags and allowed to dry outside in the sun. After drying the specimens were catalogued, identified to elements and portion (PSH, DSH, and SH) and the maximum length, width, and thickness recorded.

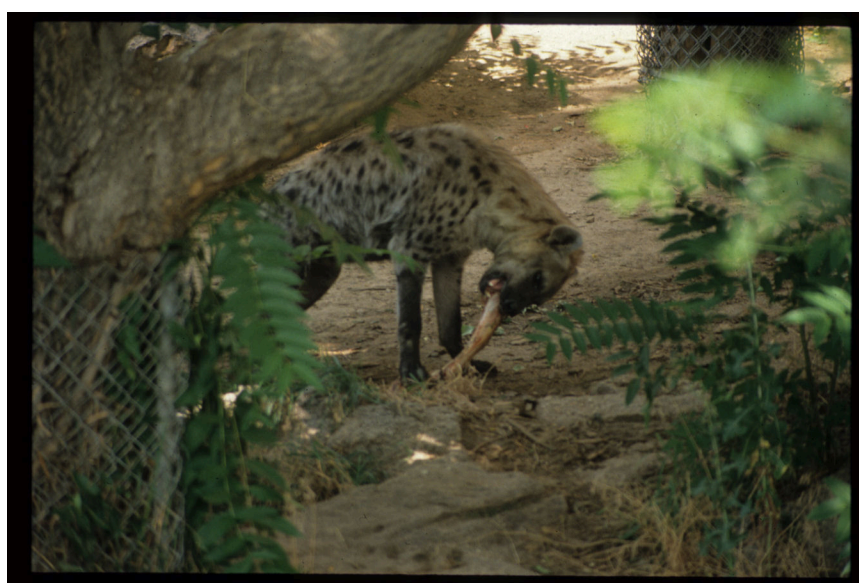


Fig. 4.1. One of the Denver Zoo hyenas gnawing a cow bone.

Table 4.2. Denver Zoo carnivores used in feeding experiments.

Taxa	Name	Sex	Age	Weight (kg)
<i>Crocuta crocuta</i>	Bearries	female	2	50
<i>Crocuta crocuta</i>	Morticia	female	12–13	59
<i>Crocuta crocuta</i>	Igor	male	7–8	43
<i>Panthera leo</i>	Yambio	male	unknown	181
<i>Panthera leo</i>	Lucy	female	unknown	132

Table 4.3. Summary of fracture experiments. CO = complete; PSH = proximal end plus shaft; DSH = distal end plus shaft; SH = shaft.

EXP. #	EXP. ^a	ELEMENT	STAGE 1				STAGE 2				RECOVERED ^{b,c,e}				total					
			AGENT		START ^d		AGENT (cvre hrs of access time)		START ^d		CO		PSH			DSH				
			cvre hrs of access time)	CO	PSH	SH	DSH	total	CO	PSH	SH	DSH	total	CO		PSH	SH	DSH		
EXP-1	CH	rt. femur	hyaena (108)	1	1	1	1	1	1	H/A	1	1	1	0	1	8	6	1	10	(8)
EXP-2	C	l. tibia	hyaena (22)	1	1	1	1	1	1	na	1	1	1	1	1	1	1	1	1	1
EXP-3	C	l. radius-ulna	hyaena (22)	1	1	1	1	1	1	na	1	1	1	1	1	1	1	1	1	1
EXP-4	CH	rt. humerus	hyaena (26)	1	1	1	1	1	1	H/A	1	1	1	1	1	1	1	1	1	1
EXP-5	CHC	l. radius-ulna	hyaena (21)	1	1	1	1	1	1	H/A	1	1	1	1	1	1	1	1	1	1
EXP-6	CH	l. humerus	hyaena (87)	1	1	1	1	1	1	H/A	1	1	1	1	1	1	1	1	1	1
EXP-7	C	rt. humerus	hyaena (65)	1	1	1	1	1	1	na	1	1	1	1	1	1	1	1	1	1
EXP-8	C	rt. femur	lion (35)	1	1	1	1	1	1	na	1	1	1	1	1	1	1	1	1	1
EXP-9	C	rt. tibia (+tarsals)	lion (37)	1	1	1	1	1	1	na	1	1	1	1	1	1	1	1	1	1
EXP-10	HC	l. humerus	H/A	1	1	1	1	1	1	hyaena (22)	1	1	1	1	1	1	1	1	1	1
EXP-11	HC	rt. tibia(+1 tarsal)	H/A	1	1	1	1	1	1	hyaena (22)	1	1	1	1	1	1	1	1	1	1
EXP-12	HC	rt. femur	H/A	1	1	1	1	1	1	hyaena (16)	1	1	1	1	1	1	1	1	1	1
EXP-13	HC	rt. tibia	H/A	1	1	1	1	1	1	hyaena (16)	1	1	1	1	1	1	1	1	1	1
EXP-14	HC	l. radius-ulna	H/A	1	1	1	1	1	1	hyaena (16)	1	1	1	1	1	1	1	1	1	1
EXP-15	HC	l. radius-ulna	H/A	1	1	1	1	1	1	hyaena (17)	1	1	1	1	1	1	1	1	1	1
EXP-16	HC	rt. humerus	H/A	1	1	1	1	1	1	hyaena (17)	1	1	1	1	1	1	1	1	1	1
EXP-17	HC	rt. tibia(+tarsals)	H/A	1	1	1	1	1	1	hyaena (17)	1	1	1	1	1	1	1	1	1	1
EXP-18	HC	l. radius-ulna	H/A	1	1	1	1	1	1	hyaena (17)	1	1	1	1	1	1	1	1	1	1
EXP-19	HC	rt. femur	H/A	1	1	1	1	1	1	hyaena (17)	1	1	1	1	1	1	1	1	1	1
EXP-20	HC	l. tibia	H/A	1	1	1	1	1	1	hyaena (17)	1	1	1	1	1	1	1	1	1	1
EXP-21	HC	rt. radius-ulna	H/A	1	1	1	1	1	1	hyaena (24)	1	1	1	1	1	1	1	1	1	1
EXP-22	HC	rt. tibia (+ 1 tarsal)	H/A	1	1	1	1	1	1	hyaena (24)	1	1	1	1	1	1	1	1	1	1
EXP-23	HC	rt. humerus	H/A	1	1	1	1	1	1	hyaena (24)	1	1	1	1	1	1	1	1	1	1
EXP-24	C	rt. Humerus	hyaena (48)	1	1	1	1	1	1	na	1	1	1	1	1	1	1	1	1	1
EXP-25	C	rt. Humerus	hyaena (24)	1	1	1	1	1	1	na	1	1	1	1	1	1	1	1	1	1
EXP-26	C	l. radius-ulna	hyaena (48)	1	1	1	1	1	1	na	1	1	1	1	1	1	1	1	1	1
EXP-27	CH	l. radius-ulna	hyaena (56)	1	1	1	1	1	1	H/A	1	1	1	1	1	1	1	1	1	1
EXP-28	C	l. humerus	hyaena (24)	1	1	1	1	1	1	na	1	1	1	1	1	1	1	1	1	1
EXP-29	C	rt. radius-ulna	hyaena (48)	1	1	1	1	1	1	na	1	1	1	1	1	1	1	1	1	1
EXP-30	CH	l. tibia (+tarsals)	hyaena (24)	1	1	1	1	1	1	H/A	1	1	1	1	1	1	1	1	1	1

a: C = carnivore only; CH = carnivore then hammerstone; HC = hammerstone then carnivore; CHC = carnivore then hammerstone then carnivore

b: The ulna and tarsals were not counted.

c: The first number in the SH and total columns are the total number of pieces and the number in parentheses indicates specimens >20mm in length. Many fragments created during H/A fracture remained tightly attached to larger pieces. Only larger attached fragments of the PSH and DSH portions could be confidently counted.

d: Note that shaft pieces created in hammerstone and anvil (H/A) breakage, but not attached to larger PSH and DSH ends were not presented to carnivores (to meet zoo concerns and possible loss of fragments). Those shaft pieces presented to the carnivores were created during H/A fracture but remained tightly attached to larger PSH and DSH pieces.

e: Most shaft pieces created during H/A fracture and attached to larger pieces when presented to carnivores were disassociated from larger pieces after carnivore access.

f: In the final stage, both the PSH and DSH were presented to hyaenas, but after 17 hours of access time no further damage resulted.

g: Specimens were largely undamaged after feeding to lions and were not coded.

h: 5 shaft fragments still attached to either the proximal or distal pieces after hammerstone breakage. Proximal piece split through articular surface. Carnivore gnawing resulted in loss of 3 large shaft fragments disassociation of 3 distal fragments and complete splitting of proximal end.

i: All 18 shaft fragments remained attached to the proximal or distal pieces. The number of fragments were counted after becoming disassociated during degreasing.

Table 4.4. Experimental (EXP) assemblage number of identified specimens (NISP), minimum number of elements (MNE), and minimum number of individuals (MNI) for all bovid, suid and equid limb bones identified to element with a maximum dimension ≥ 20 mm. Element abbreviations: HUM = humerus; RAD = radius; ULN = ulna; MCM = metacarpal; FEM = femur; TIB = tibia; MTM = metatarsal; METM = metapodial; LBSF = long bone shaft fragment. Portion abbreviations: CO = complete element, PSH = proximal end plus shaft; DSH = distal end plus shaft, SH = shaft. The numbers of bones <20 mm are given in parentheses. for all bovid, suid and equid limb bones identified to element with a maximum dimension ≥ 20 mm. The numbers of bones <20 mm are given in parentheses.

ELEMENT PORTION	SzCls CND	SzCls 1-2			SzCls 3-4			Total SzCls 1-4			Total NISP	
	NISP	NISP	MNE	MNI	NISP	MNE	MNI	NISP	MNE	MNI		
HUM	CO				1			1				
	PSH				2			2				
	SH				14			14				
	DSH				8			8				
	total	0	0	0	0	25	8	9	25	8	9	25
RAD	CO				0			0				
	PSH				9			9				
	SH				7			7				
	DSH				5			5				
	total	0	0	0	0	21	7	7	21	7	7	21
ULN	CO				1			1				
	PSH				4			4				
	SH				3			3				
	DSH				0			0				
	total	0	0	na	na	8	na	na	8	na	na	8
MCM	CO											
	PSH											
	SH											
	DSH											
	total	0	0	0	0	0	0	0	0	0	0	0
FEM	CO				0			0				
	PSH				5			5				
	SH				9			9				
	DSH				4			4				
	total	0	0	0	0	18	4	4	18	4	4	18
TIB	CO				0			0				
	PSH				6			6				
	SH				19			19				
	DSH				6			6				
	total	0	0	0	0	31	6	6	31	6	6	31
MTM	CO											
	PSH											
	SH											
	DSH											
	total	0	0	0	0	0	0	0	0	0	0	0
METM	PSH											
	SH											
	DSH											
	total	0	0	na	na	0	na	na	0	na	na	0
	LBSF	44 (22)	0	na	na	108 (14)	na	na	108 (14)	na	na	152 (36)
TOTAL	<i>CO</i>	0	0		2			2			2	
	<i>PSH</i>	0	0		26			26			26	
	<i>SH</i>	44 (22)	0		160 (14)			207 (36)			251 (36)	
	<i>DSH</i>	0	0		23			23			23	
	TOTAL	44 (22)	0	na	na	211 (14)	na	na	258 (36)	na	na	302 (36)
TOTAL ID	<i>CO</i>	0	0		2			2				
	<i>PSH</i>	0	0		26			26				
	<i>SH</i>	0	0		52			52				
	<i>DSH</i>	0	0		23			23				
	TOTAL	0	0	0	0	103	25	9	103	25	9	103

4.2.2 Amboseli Hyaena Den (AHD)

The Amboseli Hyaena Den (AHD), a spotted hyaena (*Crocuta crocuta*) communal and natal den, is located in the open grassland of the now dry bed of Lake Amboseli, Amboseli National Park, Kenya (Fig. 4.2). The assemblage was collected and described by Hill (1981, 1983, 1984, 1989) and is currently housed at the Paleontology Department, National Museum of Kenya (NMK), Nairobi. Formed by the collapse of the calcrete duricrust the den remains in use today. Although not excavated, bones on the 20 x 4m open-air depression that forms the den floor were mapped and collected by Hill in 1975 and 1977. Permission to study the AHD collection by NMK and A. Hill was generously accompanied by Hill's original specimen identification list.

The assemblage is comprised of over 2017 specimens 1048 of which are limb pieces. Of these limbs and limb fragments, 976 representing at least eight mammalian taxa and 35 individuals (Table 4.5) were located in this study. Wildebeest, (*Connochaetes taurinus*), and zebra (*Equus burchelli*), are most common in terms of NISP (n=136) and MNI followed by Grant's gazelle (*Gazella granti*) and Thomson's gazelle (*Gazella thomsoni*). The breakdown of the assemblage by element, portion, and size class with their corresponding NISP, MNE, and MNI values are provided in Table 4.5. Because it is a surface collection and no sieving was conducted (dry or water), small specimens, particularly those <20mm in maximum dimension, are likely under-represented.



Fig. 4.2. Hyaena cub emerging from one of the Amboseli Hyeana Den entrances. Photo by D. Schreier (<http://www.flickr.com/photos/dlsimages/5128664742/in/set-72157624531287760/>).

Table 4.5. Number of identified specimens (NISP) and minimum number of individuals (MNI) (in parentheses) by element for the Amboseli Hyaena Den (AHD) assemblage.

TAXA	HUM	RAD	ULN ^a	MCM	FEM	TIB	MTM	METM	LBSF	Total
<i>C. taurinus</i>	25 (9)	28 (11)	2	19 (11)	6 (4)	25 (9)	28 (14)	3	0	136 (14)
<i>E. burchelli</i>	18 (8)	12 (8)	2	6 (5)	1 (1)	7 (3)	17 (9)	1	0	64 (9)
<i>G. granti</i>	4 (3)	6 (3)	0	2 (1)	1 (1)	7 (4)	1 (1)	0	0	21 (4)
<i>B. taurus</i>	2 (2)	2 (1)	1	2 (2)	1 (1)	0 (0)	0 (0)	0	0	8 (2)
<i>E. asinus</i>	0 (0)	0 (0)	0	0 (0)	0 (0)	0 (0)	4 (3)	0	0	4 (3)
<i>G. thomsoni</i>	0 (0)	1 (1)	1	2 (1)	0 (0)	2 (1)	1 (1)	0	0	7 (1)
Capridae	1 (1)	0 (0)	0	0 (0)	0 (0)	0 (0)	0 (0)	0	0	1 (1)
<i>P. aethiopicus</i>	0 (0)	0 (0)	0	0 (0)	0 (0)	1 (1)	0 (0)	0	0	1 (1)
indet. bovid	1	0	0	20	0	0	15	52	0	88
indet. mammal	14	53	1	3	11	59	2	11	492	646
TOTAL	65	102	7	54	20	101	68	67	492	976 (35)

a: ULN used to calculate RAD MNE and MNI.

Table 4.6. Amboseli Hyaena Den (AHD) assemblage number of identified specimens (NISP), minimum number of elements (MNE), and minimum number of individuals (MNI) for all bovid, suid and equid limb bones identified to element with a maximum dimension ≥ 20 mm. Element abbreviations: HUM = humerus; RAD = radius; ULN = ulna; MCM = metacarpal; FEM = femur; TIB = tibia; MTM = metatarsal; METM = metapodial; LBSF = long bone shaft fragment. Portion abbreviations: CO = complete element, PSH = proximal end plus shaft; DSH = distal end plus shaft, SH = shaft. The numbers of bones <20 mm are given in parentheses.

ELEMENT PORTION ^a	SzCls CND	SzCls 1-2			SzCls 3-4			Total SzCls 1-4			Total NISP	
	NISP	NISP	MNE	MNI ^b	NISP	MNE	MNI ^b	NISP	MNE	MNI ^b		
HUM ^c	CO		1			12			13		13	
	PSH		0			0			0		0	
	SH		1			26			27		27	
	DSH		3			22			25		25	
	total	0	5	5	4	60	34	19	65	39	23	65
RAD ^d	CO		3			15			18		18	
	PSH		2			11			13		13	
	SH		2			61			63		63	
	DSH		0			8			8		8	
	total	0	7	6	4	95	29	20	102	35	24	102
ULN ^e	CO		0			2			2		2	
	PSH		0			0			0		0	
	SH		1			4 (1)			5 (1)		5 (1)	
	DSH		0			0			0		0	
	total	0	1	na	na	6	na	na	7 (1)	na	na	7 (1)
MCM ^f	CO		2			18			20		20	
	PSH		1			4			5		5	
	SH		1			20			21		21	
	DSH		0			8			8		8	
	total	0	4	4	2	50	26	18	54	30	20	54
FEM ^g	CO		1			3			4		4	
	PSH		0			1			1		1	
	SH		0			11			11		11	
	DSH		0			4			4		4	
	total	0	1	1	1	19	7	6	20	8	7	20
TIB ^h	CO		0			10			12		12	
	PSH		0			9			11		11	
	SH		1			55			55		56	
	DSH		0			16			22		22	
	total	1	10	8	6	90	25	12	100	33	18	101
MTM ⁱ	CO		1			34			35		35	
	PSH		0			11			11		11	
	SH		1			15			16		16	
	DSH		0			6			6		6	
	total	0	2	2	2	66	45	27	68	47	29	68
METM ^j	PSH					2			2		2	
	SH					60			60		60	
	DSH					5			5		5	
	total	0	0	na	na	67	na	na	67	na	na	67
	LBSF		8 (2)	0	na	na	484 (22)	na	na	484 (22)	na	na
TOTAL	CO		0			92			102		102	
	PSH		0			38			43		43	
	SH		9 (2)			732 (22)			737 (22)		746 (24)	
	DSH		0			69			78		78	
	TOTAL	9 (2)	30	na	na	937 (22)	na	na	967 (22)	na	na	976 (24)
TOTAL ID	CO		0			92			102		102	
	PSH		0			36			41		41	
	SH		1			188			193		194	
	DSH		0			64			73		73	
	TOTAL	1	29	26	7	380	166	28	409	192	35	410

a: CO portion includes complete juvenile shaft (COS), complete juvenile shaft with proximal epiphysis (COP), and complete juvenile shaft plus distal epiphysis (COD). PSH portion includes proximal shaft minus epiphysis (PSE) and proximal epiphysis (PX). DSH portion includes shaft minus epiphysis (DSE) and distal epiphysis (DS) portions.

b: MNI values calculated using taxonomic, element, portion, and size class identifications. Bones with taxonomic designations only to the mammal or bovid level, and those only to size class were not included in the MNI estimates.

c: Includes 18 Equid (7 CO, 7 DSH, 4 SH)

d: Includes 12 Equid (5 CO, 1 PSH, 4 DSH, 2 SH). ULN used to calculate RAD MNE and MNI.

e: Includes 2 Equid (1 CO, 1 SH)

f: Includes 6 Equid (4 CO, 2 SH)

g: Includes 1 Equid (SH)

h: Includes 1 SzCls 1-2 Suid (DSH) and 7 Equid (1 CO, 2 PSH, 1 SH, 3 DSH)

i: Includes 17 Equid (14 CO, 1 PSH, 1 DSH, 1 SH)

j: Includes 1 Equid (PSH).

4.2.3 FLK-NN2

M. D. Leakey (1971) reports that the fossil assemblage FLK-NN2, Olduvai Gorge, Tanzania (Figs. 4.3 and 4.4), was recovered from a fine-grained, buff-white tuff with clay patches in Bed I just below (approximately 30cm) the FLK-Zinj level (Fig. 4.5). These low gradient, likely (?) fluvial deposits formed near the edge of the shallow paleolake within a few hundred meters of freshwater (meteoric source) springs (Ashley, Tactikos, and Owen 2009; Ashley et al. 2010a, 2010b). The FLK-NN2 deposits are between 1.845 and 1.839 Ma, based on Deino's (Blumenschine et al. 2003) $^{40}\text{Ar}/^{39}\text{Ar}$ single-crystal dates of Tuffs IB (1.845 ± 0.002) and IC (1.839 ± 0.005) at the Naisuisui site, and their stratigraphic correlation with the FLK deposits (McHenry 2005; McHenry, Stollhofen, and Stanistreet 2013). No artifacts were found at FLK-NN2. Most of the fossils occurred in the clay patches near the base of the deposit, but unlike many of the archaeological sites from Bed I where the faunal and lithic material have limited vertical distribution (such as FLK Zinj), fossils at this site are dispersed throughout the one-foot thick tuff deposit. In comparison to other Bed I assemblages, the elements from FLK-NN2 are more complete. Although described as friable and poorly preserved (Leakey 1971), with the poorest cortical surface preservation of any Bed I site (Egeland 2007), most surfaces do in fact preserve considerable detail.

Bunn identified over 390 large mammal specimens in this assemblage, 138 of which are limb pieces (Bunn 1982, Table 4.36; Bunn 1990, pers. comm.). One hundred and twenty-four limb pieces were located and examined for this study (Tables 4.7 and 4.8). The limb assemblage is dominated by the large, extinct waterbuck *Kobus sigmoidalis* with nearly equal representation of size class 3 Alcelaphines and suids. Twenty-three of the 124 limb bones examined (19%) are complete. All but 14 specimens were identified to element. The limb assemblage consists almost entirely of size class 3 bovids. A minimum of nine bovid and two suid individuals are represented.

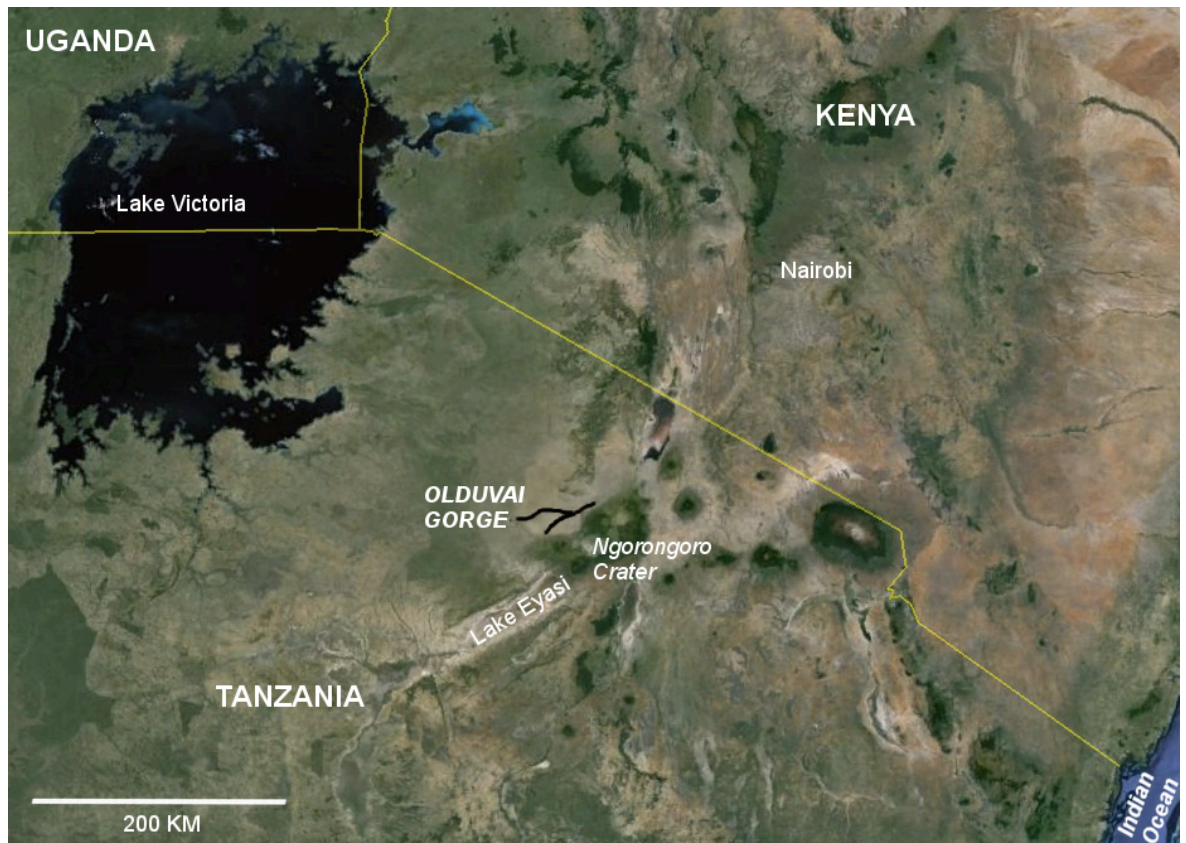


Fig. 4.3. Location of Olduvai Gorge, Tanzania (US Geographer Landsat image from Google Earth 2015).



Fig. 4.4. Olduvai Gorge, Tanzania ("Oldupai gorge" by Ingvar - [1]. Licensed under CC BY-SA 1.0 via Wikimedia Commons [https://commons.wikimedia.org/wiki/File: Oldupai_gorge.jpg#/media /File:Oldupai_gorge.jpg](https://commons.wikimedia.org/wiki/File:Oldupai_gorge.jpg#/media/File:Oldupai_gorge.jpg))

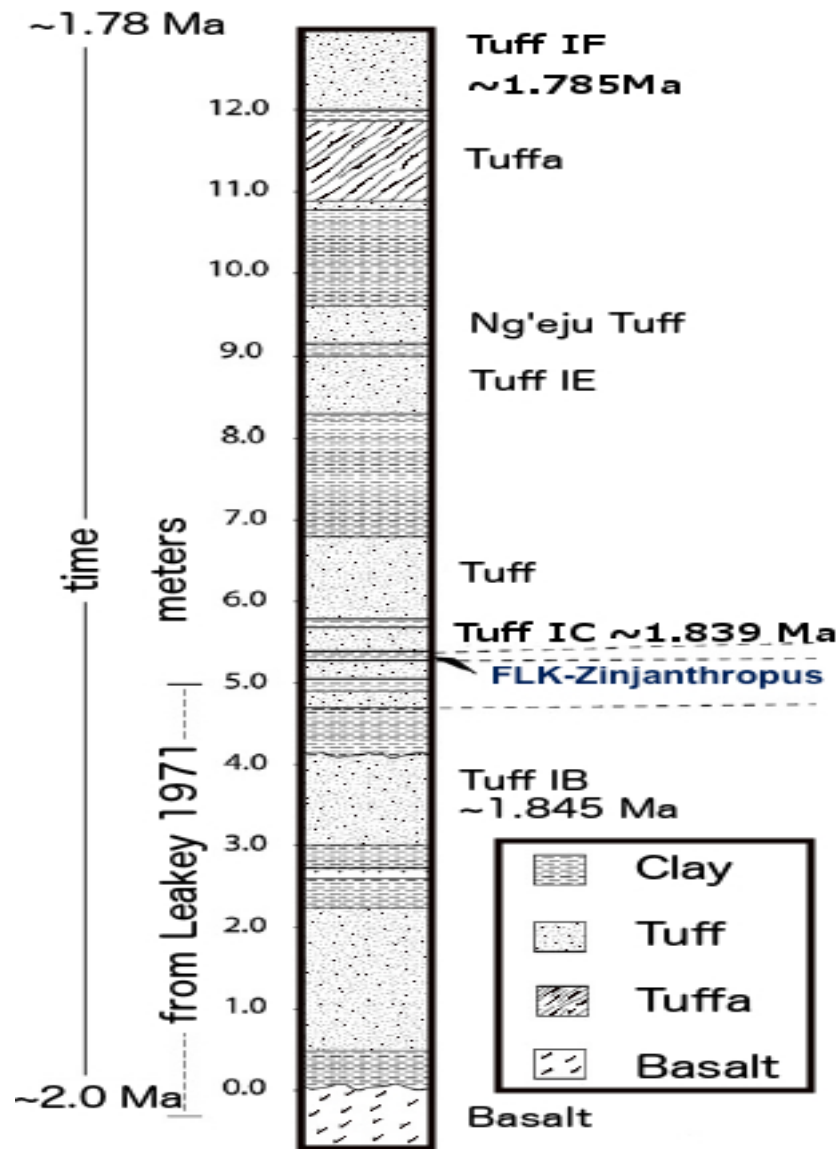


Fig. 4.5. Olduvai Gorge Bed I stratigraphy at FLK-Zinj (modified after Ashley et al. 2010a, Fig. 3).

Table 4.7. Number of identified specimens (NISP) and minimum number of individuals (MNI) (in parentheses) by element for the FLK-NN2 assemblage. Taxonomic identifications by Bunn (1982; 1990, pers. comm.). Element abbreviations: HUM = humerus; RAD = radius; ULN = ulna; MCM = metacarpal; FEM = femur; TIB = tibia; MTM = metatarsal; METM = metapodial; LBSF = long bone shaft fragment.

TAXA	HUM	RAD	ULN ^a	MCM	FEM	TIB	MTM	METM	LBSF	Total
Alcelaphini (szcls 3)	2 (2)	3 (2)	1	2 (2)	1 (1)	1 (1)	0 (0)	0	0	10 (2)
Hippotragini (szcls 3)	1 (1)	1 (1)	1	2 (2)	0 (0)	0 (0)	0 (0)	0	0	5 (2)
<i>Kobus sigmoidalis</i>	4 (2)	5 (3)	2	4 (2)	0 (0)	2 (2)	4 (3)	0	0	21 (3)
Reduncini (szcls 3)	0 (0)	0 (0)	0	0 (0)	0 (0)	1 (1)	0 (0)	0	0	1 (1)
Tragelaphini (szcls 3)	2 (1)	2 (1)	1	1 (1)	0 (0)	0 (0)	0 (0)	0	0	6 (1)
<i>Mesochoerus limnetes</i>	1 (1)	1 (1)	0	0 (0)	3 (2)	2 (1)	0 (0)	0	0	7 (2)
Suidae	1 (1)	0 (0)	0	0 (0)	0 (0)	2 (1)	2 (1)	0	0	5 (1)
indet. bovid	4 (3)	3 (1)	2	4 (1)	6 (2)	14 (3)	15 (5)	0	0	48 (5)
indet. mammal	4 (1)	1 (1)	0	0 (0)	1 (1)	1 (1)	0 (0)	0	14	21 (1)
Total	19	16	7	13	11	23	21	0	14	124 (10^b)

a: ULN used to calculate RAD MNE and MNI.

b: MNI does not include values derived from Suidae, indet. bovid, and indet. mammal.

Table 4.8. FLK-NN2 assemblage number of identified specimens (NISP), minimum number of elements (MNE), and minimum number of individuals (MNI) for all bovid, suid and equid limb bones identified to element with a maximum dimension ≥ 20 mm. Element abbreviations: HUM = humerus; RAD = radius; ULN = ulna; MCM = metacarpal; FEM = femur; TIB = tibia; MTM = metatarsal; METM = metapodial; LBSF = long bone shaft fragment. Portion abbreviations: CO = complete element, PSH = proximal end plus shaft; DSH = distal end plus shaft, SH = shaft. The numbers of bones <20 mm are given in parentheses. for all bovid, suid and equid limb bones identified to element with a maximum dimension ≥ 20 mm. The numbers of bones <20 mm are given in parentheses.

ELEMENT PORTION ^a	SzCls CND			SzCls 1-2			SzCls 3-4			Total SzCls 1-4			Total NISP
	NISP	NISP	MNE	MNI ^b	NISP	MNE	MNI ^b	NISP	MNE	MNI ^b			
HUM ^c	CO				2			2			2	2	
	PSH				0			0			0	0	
	SH	1			4			4			4	5	
	DSH				12			12			12	12	
	total	1	0	0	0	18	14	10	18	14	10	19	
RAD ^d	CO				4			4			4	4	
	PSH				7			7			7	7	
	SH				5			5			5	5	
	DSH				0			0			0	0	
	total	0	0	0	0	16	11	9	16	11	9	16	
ULN	CO				0			0			0	0	
	PSH				6			6			6	6	
	SH				1			1			1	1	
	DSH				0			0			0	0	
	total	0	0	na	na	7	na	na	7	na	na	7	
MCM	CO				8			8			8	8	
	PSH				2			2			2	2	
	SH				0			0			0	0	
	DSH				3			3			3	3	
	total	0	0	0	0	13	10	8	13	10	8	13	
FEM ^e	CO				3			3			3	3	
	PSH				1			1			1	1	
	SH				5			5			5	5	
	DSH				2			2			2	2	
	total	0	0	0	0	11	6	4	11	6	4	11	
TIB ^f	CO				3			3			3	3	
	PSH				2			2			2	2	
	SH				10			10			10	10	
	DSH				8			8			8	8	
	total	0	0	0	0	23	9	8	23	9	8	23	
MTM ^g	CO				3			3			3	3	
	PSH				14			14			14	14	
	SH				3			3			3	3	
	DSH				1			1			1	1	
	total	0	0	0	0	21	13	8	21	13	8	21	
METM	PSH												
	SH												
total	0	0	na	na	0	na	na	0	na	na	0		
LBSF		5 (2)	0	na	na	9	na	na	9	na	na	14 (2)	
TOTAL	CO	0	0			23			23			23	
	PSH	0	0			32			32			32	
	SH	6 (2)	0			37			37			43 (2)	
	DSH	0	0			26			26			26	
	TOTAL	6 (2)	0	na	na	118	na	na	118	na	na	124 (2)	
TOTAL ID	CO	0	0			23			23			23	
	PSH	0	0			32			32			32	
	SH	1	0			28			28			29	
	DSH	0	0			26			26			26	
	TOTAL	1	0	0	0	109	63	10	109	63	10	110	

proximal epiphysis (COP), and complete juvenile shaft plus distal epiphysis (COD). PSH portion includes proximal shaft minus epiphysis (PSE) and proximal epiphysis (PX). DSH portion includes shaft minus epiphysis (DSE) and distal epiphysis (DS) portions.

b: MNI values calculated using taxonomic, element, portion, and size class identifications. Bones with taxonomic designations only to the mammal or bovid level, and those only to size class were not included in the MNI estimates.

c: Includes 1 Suidae (CO).

d: Includes 1 Suidae (PSH).

e: Includes 3 Suidae (2 CO, 1 PSH).

f: Includes 4 Suidae (1 CO, 2 DSH, 1 FIB DSH).

g: Includes 2 Suidae (1 CO MT4, 1 PSH MT3).

4.2.4 FLK LEVEL 22 aka FLK-Zinj

FLK 22, more commonly known as FLK-Zinjanthropus (FLK-Zinj) owing to the discovery at the site of a nearly complete “*Australopithecus zinjanthropus*” (*A. boisei*) skull, is located on the right side of the main gorge near its side gorge junction Olduvai Gorge, Tanzania (Figs. 4.3 and 4.4) and was excavated by the Leakeys in 1959-1960 (Leakey 1971). The FLK-Zinj level consists of a grey-green silty clay of approximately 30cm in thickness (Leakey 1971) and lies in the middle of the Bed I sequence approximately 1m above Tuff 1B dated to 1.845my and just below Tuff 1C dated to 1.839my (Figure 4.5; Blumenschine et al. 2003). Artifacts and fossils were found at or within the top few centimeters of this clay deposit. The depositional environment is interpreted as low gradient, fluvial formed near the edge of the shallow paleolake. Recent work shows that the site formed within a few hundred meters of freshwater (meteoric source) springs (Ashley, Tactikos, and Owen 2009; Ashley et al. 2010a, 2010b). Further, Ashley and Liutkus, (2002) and Deocampo, (2002) argue that the dimensions and morphology of the shallow “channel” at FLK-Zinj is most consistent with the dimensions and sedimentological structure of a hippopotamus trail. Multiple lines of evidence indicate the site formed in grassy woodlands. A significant presence of C3 woody plants is indicated by stable isotope analysis of soil carbonates (Sikes 1994). Similarly, an Acacia woodland or gallery forest with some grassy patches is indicated by the faunal remains including the bovids (Kappelman 1984, Potts 1988) and their ecomorphology (Plummer and Bishop 1994), the micro-fauna (i.e., the Acacia rat, *Thallomys* (Jaeger 1976; Gentry and Gentry 1978)) as well as the habitat preferences of the fresh water snails and slugs (Hay 1973).

Approximately 25-30 Oldowan (mainly African) sites have been excavated over the last half century, but FLK-Zinj, often referred to and regarded as a “living floor”, remains the Oldowan site with the densest concentration of artifacts (approximately 2500 according

to Leakey 1971) and faunal remains (approximately 60,000 according to Bunn and Kroll 1986). Bunn (1982; Bunn pers. comm. 1990) identified over 2500 limb bones and fragments. Size class 3-4 bovids, primarily *Parmularius altidens* and *Kobus sigmoidalis*, as well as a large number that could not be assigned to species dominate the assemblage (Table 4.9). Element frequencies are given in Table 4.10. Only 12 limb bones are complete (including those from juveniles that may be missing one or both epiphyses).

Table 4.9. FLK-ZINJ number of identified specimens (NISP), minimum number of elements (MNE), and minimum number of individuals (MNI) for all bovid, suid and equid limb bones identified to element with a maximum dimension ≥ 20 mm. Element abbreviations: HUM = humerus; RAD = radius; ULN = ulna; MCM = metacarpal; FEM = femur; TIB = tibia; MTM = metatarsal; METM = metapodial; LBSF = long bone shaft fragment. Portion abbreviations: CO = complete element, PSH = proximal end plus shaft; DSH = distal end plus shaft, SH = shaft. The numbers of bones <20 mm are given in parentheses by element for the FLK-Zinj assemblage. Taxonomic identifications by Bunn (1982; 1990, pers. comm.).

TAXA	HUM		RAD		ULN		MCM		FEM		TIB		MTM		METM/LBSF		Total							
	NISP	MNE	NISP	MNE	NISP	MNE	NISP	MNE	NISP	MNE	NISP	MNE	NISP	MNE	NISP	MNE	NISP	MNE	MNI					
<i>Antidorcas recki</i>	12	5	5	4	3	1	1	14	4	3	15	6	3	29	10	7	25	9	5	117	40	7		
Antilopini	2	1	1				5	2	1		2	2	1	3	1	1	3	1	1	12	6	1		
<i>Parmularius altidens</i>	9	4	4	7	5	1	0	2	2	1	8	6	5	8	2	1	1	1	1	43	22	5		
<i>Comochaeates</i> sp.	1	1	1								2	1	1	3	2	1				6	4	1		
<i>Kobus sigmoidalis</i>	8	7	5	11	6	5	6	1	1	3	2	2	4	8	5	4	5	3	3	45	27	5		
<i>Tragelephus</i> sp.								2	1	1				1	1	1				3	2	1		
Suidae	1	1	1	1	1	1														1	1	1		
Equidae														1	1	1				3	3	1		
<i>Syncerus aequalis</i>								1	1	1				1	1	1				2	2	1		
szcls 2 indet. bovid	3	0	0	1	0	0		3	0	0	2	2	1	12	0	0	1	0	0	12	34	2	1	
szcls 2 indet. mammal	4	0	0								5	0	0	1	0	0				58	68	0	0	
szcls 3-4 indet. bovid	16	2	1	4	2	2		22	4	3	12	3	1	52	9	8	15	1	1	40	411	572	21	8
szcls 3-4 indet. mammal	32	0	0								21	0	0	22	0	0	1	0	0	896	76	0	0	
indet. mammal																					896	0	0	
Total SzCls 1-2	21	6	6	16	5	4	3	1	1	22	6	4	4	44	12	8	29	10	6	16	58	231	48	9
Total SzCls 3-4	67	15	12	31	17	14	7	1	1	30	10	8	47	13	9	95	20	16	23	40	411	751	82	23
TOTAL	88	21	18	47	22	18	10	2	2	52	16	12	69	21	13	139	32	24	56	1365	1878	130	32	

Table 4.10. FLK-Zinj assemblage number of identified specimens (NISP), minimum number of elements (MNE), and minimum number of individuals (MNI) for all bovid, suid and equid limb bones identified to element with a maximum dimension ≥ 20 mm. Element abbreviations: HUM = humerus; RAD = radius; ULN = ulna; MCM = metacarpal; FEM = femur; TIB = tibia; MTM = metatarsal; METM = metapodial; LBSF = long bone shaft fragment. Portion abbreviations: CO = complete element, PSH = proximal end plus shaft; DSH = distal end plus shaft, SH = shaft. The numbers of bones <20 mm are given in parentheses. for all bovid, suid and equid limb bones identified to element with a maximum dimension ≥ 20 mm. The numbers of bones <20 mm are given in parentheses.

ELEMENT PORTION ^a	SzCls CND	SzCls 1-2			SzCls 3-4			Total SzCls 1-4			Total NISP	
	NISP	NISP	MNE	MNI ^b	NISP	MNE	MNI ^b	NISP	MNE	MNI ^b		
HUM ^c	CO		0			1		1			1	
	PSH		3			3		6			6	
	SH		13			47		60			60	
	DSH		5			16		21			21	
	total	0	21	6	6	67	15	12	88	21	18	88
RAD ^d	CO					1		1			1	
	PSH		11			15		26			26	
	SH		4			46		50			50	
	DSH		1			4		5			5	
	total	0	16	6	5	66	16	12	82	22	17	82
ULN	CO		0			0		0			0	
	PSH		0			7		7			7	
	SH		3			11		14			14	
	DSH		0			0		0			0	
	total	0	3	na	na	18	na	na	21	na	na	21
MCM ^e	CO		1			1		2			2	
	PSH		5			9		14			14	
	SH		12			18		30			30	
	DSH		4			2		6			6	
	total	0	22	7	6	30	10	9	52	17	15	52
FEM	CO		1			0		1			1	
	PSH		1			4		5			5	
	SH		17			39		56			56	
	DSH		3			4		7			7	
	total	0	22	8	4	47	13	8	69	21	12	69
TIB ^f	CO		2			0		2			2	
	PSH		7			1		8			8	
	SH	1	32			88		120			121	
	DSH		3			6		9			9	
	total	1	44	12	8	95	19	10	139	31	18	140
MTM	CO	1	2			2		4			5	
	PSH		10			5		15			15	
	SH		15			12		27			27	
	DSH		2			4		6			6	
	total	1	29	10	9	23	6	6	52	16	15	53
METM	PSH		1			1		2			2	
	SH		10			39		49			49	
	DSH		5 (3)			0		5 (3)			5 (3)	
	total	0	16 (3)	na	na	40	na	na	56 (3)	na	na	56 (3)
	LBSF	896 (454)	58 (1)	na	na	411 (5)	na	na	469 (6)	na	na	1365 (460)
TOTAL	CO	1	6			5		11			12	
	PSH	0	38			45		83			83	
	SH	897 (454)	164 (1)			711 (8)		875 (9)			1772 (463)	
	DSH	0	23 (3)			36		59 (3)			59 (3)	
	TOTAL	898 (454)	231 (4)	na	na	797 (8)	na	na	1028 (12)	na	na	1926 (466)
TOTAL ID	CO	1	6			5		11			12	
	PSH	0	37			44		81			81	
	SH	1	96			261		357			358	
	DSH	0	18			36		54			54	
	TOTAL	2	157	49	9	346	79	12	503	128	21	505

a: CO portion includes complete juvenile shaft (COS), complete juvenile shaft with proximal epiphysis (COP), and complete juvenile shaft plus distal epiphysis (COD). PSH portion includes proximal shaft minus epiphysis (PSE) and proximal epiphysis (PX). DSH portion includes shaft minus epiphysis (DSE) and distal epiphysis (DS) portions.

b: MNI values calculated using taxonomic, element, portion, size class identifications, and application of the MNI calculations from Bunn 1982 to the material examined in this study. Bones with taxonomic designations only to the mammal or bovid level, and those only to size class were not included in the MNI estimates.

c: Includes 1 Equid HUM SH.

d: Includes 1 Equid RAD SH. ULN used to calculate RAD MNE and MNI.

e: Includes 1 Bovinae MCM PSH.

f: Includes 1 Bovinae and 1 Equid TIB SH.

4.3 Methods: Fragmentation, Damage, and Fracture Feature Coding

Each bone in each assemblage was examined to assess a) their completeness and fragmentation, b) the frequencies of loading points, c) the frequencies of select fracture features outlined in Chapter 2, c) other damages including percussion and tooth marks (pits, scores, and furrows) that have been used identify carnivore and hominin involvement, and d) the co-occurrence of fracture features with diagnostic percussion and tooth marks. Most of the fragmentation measures, loading point types, fracture features, and damages analyzed in this study were discussed Chapter 2. For methodological clarity, definitions these features and damages analyzed in this study are restated here.

4.3.1 Fragmentation

Fragmentation is a measure of the amount of processing to which an assemblage has been subjected. Two measures are presented here. One indication of fragmentation is specimen completeness as measured by length, width, and thickness. Another is the number of fracture lines on the assemblage specimens.

Because of the fragmentary nature of the assemblages examined, in this study a specimen's maximum dimension (usually length) is taken as a proxy measure of element completeness. Limb bone specimen lengths (in mm) were measured for 818 AHD, 211 EXP, 84 FLK-NN2, and 1416 FLK-Zinj limb specimens with a maximum dimension \geq 20mm.

Given that the greater the force applied to a material the greater the number of fractures and the greater for surface area created (an axiom of fracture mechanics, see Chapter 2), an overall assessment of the force applied to induce breakage may be examined via the number of fracture lines (#FLNs) in an assemblage. In this study the number of fracture lines on a bone serves as a proxy measure of fracture surface area.

A fracture line is defined as that segment of a specimen's total fracture surface that maintains a similar, unbroken linear direction between two bounding inflection points, i.e.,

where the fracture direction changes. Fracture line length is the distance (in mm) between inflection points. Typically, the fracture line is the fracture segment between inflection points on the cortical or medullary surfaces. These inflection points mark either an abrupt change in fracture direction or the intersection of two or more fractures and define the end of one fracture line and the beginning of another. This line must be clearly defined and should be expressed on the fracture surface from the cortical surface to medullary wall or cancellous bone. Minor undulations in the orientation of a fracture, as expressed on the cortical surface, are not counted. Short step fractures along a fracture line are not counted as separate fracture lines. Individual loading point flake scars and notches are counted as fracture lines except where the loading point has resulted in comminuted fracture with numerous ring cracks (aka incipient flakes), in which case the area of extreme fragmentation is counted as a single line.

Curvilinear fractures that spiral around the bone are coded as a single fracture line because the change in fracture direction is gradual and the fracture surface contains no breaks in appearance or a distinct intersection line at the spiral apex. The number of fracture lines was recorded for each specimen. Not counted are fractures that bisect a fracture line in which the direction of propagation (as indicated by chevrons, half-chevrons, or feathering) is the same on either side of the smaller fracture. These fractures are not counted because they did not contribute to opening the marrow cavity but occurred later. Dry breaks, chipped areas, and notches that did not precipitate the fracture on either side of the notch were not counted, but were coded as a separate damage, e.g, notch, carnivore-induced flake, chip, etc. Given the variability in fracture appearance from the cortical to fracture to medullary surfaces, it should be noted that there is a degree of subjectivity in the definition of individual fracture lines. The number of fracture lines and their attendant lengths should be treated as estimates.

Since it is likely that the potential number of fracture lines on a bone fragment is partially dependent on specimen and animal size, the mean #FLNS per unit (mm) specimen length (SPECL) for various specimen groupings are compared here. Complete elements, complete shafts, ulna, suidae (due to their relatively thicker compact bone compared to bovids and equids), and specimens of indeterminate (cnd) size class are excluded from this analysis. Determining whether or not the #FLNS to SPECL ratios were different between assemblages was determined by Student's t-Test (significance at 0.05).

4.3.2 Types of Load Points (LDPTs) and Fracture Features

Fractographic analysis is based on locating, identifying, and describing all loading points (LDPTs) regardless of whether or not the causal agent can be defined, as well as their spatial relationship and their overall “coherence” with other damages and fractographic features (see Chapter 2). LDPTs may be defined on the basis of one or more fracture features including those often found at the LDPT proper as well as fracture propagation directional indicators on adjacent fracture surfaces. Loading points are broadly defined as any one or combination of surficial damages resulting from indenter contact with bone and/or fracture features created during bone failure through the application of force by the indenter. Several types of LDPTs are defined on the basis of these indenter damages and fracture features. The suite of damages and fracture features employed to define LDPTs are largely based on features found on fractures of compact bone and thus fractures created by loading at the cancellous bone ends are less readily identifiable with these methods. Further, only LDPTs that created primary fractures are considered. That is, flake scars or other damages created on previously formed fracture surfaces are not counted.

Five main types of LDPTs were defined and tabulated based on their most obvious feature: flake scars (FLKSs), cones (FLKOs), notches (NTCHs), fracture features (FRFE), and loading marks (LMRKs). FLKSs, FLKOs, and FRFEs may also display NTCH or

LMRK components. NTCHs may be associated with LMRKs. Figure examples given in Chapter 2 reflect some of the range of variation in LDPT appearance, but are not always examples of the most obvious feature. Flake scars (FLKSs) are a fracture surface feature where part of the bone was removed by the indenter during fracture of the shaft (Figs. 2.14, 2.15, 2.25 – 2.27, 2.29, 2.33, and 2.34). The resultant scar may display a suite of fracture features including a bulb or bulbar scar, hackle marks, hinges, attached flakes, and micro-flakes. The size and complexity of flake scars are indicative of the size of the indenter and amount of force applied. Carnivores tend to produce simple, single flake scars with few separate flake scars or hinge fractures (Fig. 2.14) while those created by impact with large indenters (i.e., hammerstones) tend to be larger and more complex with hinge terminations, multiple flake scars, flakelettes (Figs. 2.17, and 2.25 - 2.27) and incipient flakes (IF; Figs. 2.17 and 2.23) on the cortical surface. Flake scars are usually associated with notches.

As noted in Chapter 2, a notch (NTCH) is defined as a concave interruption of a fracture line where an indenter contacted and fractured bone. Notches have an oblong, almost linear, to semi-circular shape and are usually easily identified. Its length is the distance between inflection points that denote the intersections of the notch and the adjacent fracture lines. Notch width is the perpendicular distance between a line connecting the two inflection points and the most concave part of the notch.

If bounded by adjacent fracture lines it is possible to measure notch length and width. Notch length (breadth in Capaldo and Blumenschine 1994) is the distance between inflection points that denote the intersections of the notch and the adjacent fracture lines. Notch depth is the perpendicular distance between a line connecting the two inflection points and the most concave part of the notch.

Load points where a cone or partial cone fracture feature (CO, see below) is present define FLKOs (Figs. 2.16 – 2.22, 2.30 and 2.35). As noted in Chapter 2, it is widely accepted that cones are characteristic of impact fracture. FLKOs are created by a cone of

compressive force that propagates rapidly through a solid material creating an area of great tensile stress just outside the contact radius that begins extending downward and outward through the material causing the cone-shaped fracture.

A fourth LDPT type is defined by the presence of fracture features, FRFE. If FLKs, FLKOs, and NTCHs were absent or initially unrecognized due to their very subtle expression, but the fracture surface displays any one of several fracture features (i.e., IF, RC, BSc, CO, HK, LS, and/or FR, see below) indicative of loading then the load point was coded as FRFE (Fig. 2.33). Other fracture surface irregularities, i.e., dimples/domes, although usually coded as FLKOs sometimes defined FRFE LDPTs if converging fracture front indicators pointed to a particularly subtle cone or dimple/dome. The fifth type of LDPT is defined by the presence of one or more loading marks (LMRKs), usually a tooth mark (TM) or percussion mark (PM), in a location near a fracture line bearing other evidence of loading.

Several fracture features may be associated with a LDPT. These include incipient flakes (IF; aka concentric or ring cracks), radiating cracks or fracture lines (RC), cones, or fragments thereof (CO), bulbar scar (BSc), hackle marks (HK), lateral stress (LS), and indicators of diverging fracture front movement directions including fringe/feathering (FR). These fracture features, although sometimes cited as evidence of impact fracture have not been quantified. In this study the presence or absence of each of these fracture features on each LDPT was coded for all specimens identified to size class and element in each assemblage.

Incipient flakes (aka ring cracks or concentric fracture lines) are small arcuate fracture lines concentric to the point of indenter contact. As noted in Chapter 2, incipient flakes form just outside of an indenter in hertzian fractures in the area of high tensile stress (Figs. 2.23 and 2.24). According to fractographic literature studies (e.g., Frechette 1990) as well as experimental studies of bone fracture (Capaldo and Blumenshine 1994) multiple

concentric fracture lines and the flakes they define are indicative of impact-loading. Incipient flakes are usually, but not always associated with notches.

Cones are created by instantaneous application of force by an indenter that cause a cone of compressive force to propagate through a solid material forming an area of great tensile stress just outside the contact radius that begins extending downward and outward through the material causing the cone-shaped fracture. In bone complete cones are usually very small fragments unidentifiable to element (Figs. 2.16 and 2.22) although they sometimes occur on identifiable pieces (Figs. 2.17 and 2.18). Usually only partial cones are preserved (Figs. 2.19 – 2.21).

Radiating cracks are fracture lines (cracks) that radiate out from the loading point (Figs 2.17 and 2.35) and seem to require higher levels of force associated with impact loading (Quinn 2007). Typically radiating cracks are oriented transverse or oblique to the bone long axis. Although not quantified by Bonnicksen (1979) or referred to specifically by Johnson (1985), it is clear both recognized that radiating cracks may be indicative of impact fracture.

Lateral stress is a new fracture feature associated with loading points defined here for the first time. This feature has the appearance of a small ridge, groove, or crack and is found on the fracture surface immediately adjacent to the loading point just below the cortical surface (Figs. 2.29 – 2.31, 2.19, and 2.21). As noted in Chapter 2, location of lateral stress feature suggests that it may be a truncated hertzian cone similar to that identified by Subhash et al. (2008). It may also be the expression of an incompletely formed incipient flake whose propagation was either a) interrupted by the formation of a major fracture surface adjacent to the loading point moving along the bone's longitudinal axis, or b) represents initial formation of the longitudinal crack.

Bulbar scars (Figs. 2.14, 2.15) are a concave fracture feature located near the cortical interface of flake scars. As defined here, they are always part of the flake scar. Although

bulbar scars are commonly held to be characteristic of impact fracture Cotterell and Kaminga (1987) note that what sometimes appear to be percussion bulbs as well as flakes can be created by (static) pressure flaking.

Hackle marks are linear features on the flake scar or flake surface that emanate and fan out from where the indenter contacts the material (Figs. 2.14, 2.16, 2.20, 2.25, and 2.28). Hackle marks are clearly related to other features that indicate fracture front movement, i.e., chevron and feathering. They often grade into the chevrons located on fracture surfaces immediately adjacent to the loading point. Hackle marks are commonly produced on brittle materials under high tensile stresses occurring under both dynamic- and static-loading, but according to the fractographic literature (see Chapter 2) their expression is likely more pronounced on impact fractured material. Several analysts (e.g., Bonnicksen 1979; Johnson 1985; Diez et al. 1999; Pickering and Egeland 2005) have used the presence of hackle marks to define impact fracture, but the frequencies of hackle marks in various assemblages have not been quantified.

Fringe or feathering and chevrons are curvilinear fracture features with the concavity pointing to the fracture origin and opposite the direction of fracture propagation (Figs. 2.32, 2.15, 2.26, 2.27, 2.30). Like hackle marks at the loading point, twist plumes can be produced under both impact- and static-loading, but they are particularly well pronounced on material fractured by impact-loading. This feature is particularly useful in locating the fracture origin (loading point) and can thus focus attention on an area of the cortical and fracture surface where loading points and other fracture features may be found.

All large mammal specimens (excluding carnivores) identified to size class with a maximum dimension $\geq 20\text{mm}$ specimens were coded for the presence of these LDPTs and associated fracture features and indenter (tooth and percussion) marks. Fragments identified to size class but not to element, i.e. long bone shaft fragments (LBSFs) are included only where stated. Between assemblage differences in the frequencies of LDPTs

and fracture features were assessed with χ^2 (significance level at 0.05) and Principle Component Analysis.

4.3.3 Fragments and Damages Diagnostic of Fracture Agent

Although the primary agent responsible for bone fracture in the EXP and AHD assemblages is known, and all analysts agree hominins played a major role in accumulation of the FLK-Zinj assemblage and that FLK-NN2 was a carnivore accumulation, the above fracture feature analyses are tabulated without reference to agency. To proceed, however, it is necessary to analyze damages long-recognized as diagnostic of fracture agency, i.e., percussion marks, tooth marks, percussion notches, and tooth notches, and their co-occurrence with LDPT fracture features on individual specimens. (Cut marks are not discussed here as they do not relate to bone fracture.)

There are two classes of tooth marks, pits and scores, created when a tooth is pressed or pressed and dragged along the bone surface (Figs. 2.27 and 2.36). For the present study tooth furrows are defined as scores that penetrate cancellous bone. Tooth pits are circular to oblong or slightly irregular depressions in which at least part of the bone appears compressed. At low magnification, minute cortical pieces at the juncture with the depression walls may appear pushed down, oriented toward the base of the depression. A tooth pit may have a linear aspect as it becomes a tooth score. Pitting may be concentrated on epiphyseal ends and on broken bones near the exposed medullary cavity due to carnivore's attempt to extract marrow or lever pieces back to expose more of the marrow cavity (pers. observ.). Tooth pits are distinguished from hammerstone impact marks by their regular shape and a lack of micro-striae on the pit walls (Blumenschine & Selvaggio, 1988). A tooth score is a broad, u-shaped groove in which the groove walls appear compressed or torn (Haynes, 1981; Shipman, 1981). Striae are usually absent in the groove, but if present they are poorly defined and do not extend the entire length of the

score. Scores often begin as an oblong depression and end in a shallow lineation (also called a “tail”).

Other processes, notably insect or larvae feeding, mosses, fungi and bacteria, are known to create marks somewhat similar in appearance to tooth marks (Dominguez-Rodrigo and Barba 2006, 2007b; Fernández-Jalvo et al. 2010; Kaiser 2000). Bioerosion marks created by fungi and bacteria are characterized as having irregular edges where the pit or groove intersects the cortical bone surface as well as a more irregular overall shape than those produced by carnivore teeth. Insect feeding creates a variety of marks, from u-shaped grooves with regular groove edges, to star-shaped marks likely created by termites.

It is often quite difficult to identify the agent responsible for individual marks – including tooth marks when multiple linear marks with highly variable appearances are present. Due to the variety of lineations on the outer bone surfaces in many of the specimens in the FLK-Zinj assemblage it was difficult to confidently define tooth marks unless the following conditions were met: Pits and scores define carnivore activity only if (a) the two co-occur on the same area of bone, or (b) one or the other occur in large numbers so that there is little doubt that potential mimics could not have produced the marks, or (c) the mark is particularly clear and not subject to misidentification, and/or (d) they are associated with other more diagnostic carnivore-induced damages such as furrows, punctures and lever-up breaks. Nevertheless, more confidence is placed on identification of tooth marks on fracture surfaces, medullary walls, and cancellous bone surfaces (FMC) because fewer marks are present and fewer processes are known to modify these surfaces.

Tooth notches may be differentiated from hammerstone-impact notches. Like flake scars, indenter size and amount of applied force tends to be reflected in the size, shape and complexity of the resultant notch. As demonstrated by Capaldo and Blumenshine (1994) the length and depth of tooth notches tend to be equidimensional usually with a regular

semi-circular to ovate outline (Fig. 2.14). Identification of tooth notches is based visual assessment of notch outline, length/depth ratio, and associated damages (e.g., associated tooth score or pit, crushing, absence of ring cracks, lack of complexity in flake scar appearance). Tooth notches created on the diaphysis are typically semi-circular to oblong in outline. The notch depth and length dimensions are variable, but the length/depth ratio is usually smaller in tooth notches than in notches created by hammerstone impact. Percussion notches typically have a larger length/depth ratio and more irregular shape than tooth notches (Figs. 2.17, 2.23, 2.26, and 2.35). Moreover, hammerstone-induced notches frequently display features (including ring cracks, radiating fracture lines, and micro-flaking just under the notch lip) not associated with tooth notches (Figs. 2.17 and 2.23).

Percussion marks are the scars created by hammerstone contact with the cortical bone surface. Percussion marks may appear as either small patches of microstriae, or small, irregularly shaped depressions with a somewhat crushed appearance that may or may not contain linear or irregularly shaped patches of microstriae (Blumenshine and Selvaggio 1988; Figs. 2.19, 2.21, and 2.33d). Hammerstone impact marks have a much more variable and irregular appearance than tooth marks.

As well, two types of fragments are diagnostic of agent, carnivore lever-ups and hammerstone-impact shatter. A carnivore lever-up (LVRUP; Fig. 2.33) is defined on the basis of the presence of two relatively long fracture lines that, for much of their length, run roughly parallel to each other and do not cross the longitudinal axis. On one end of the specimen the long, roughly parallel fracture lines are separated by one or more fracture lines with associated carnivore toothmarks. On the other end, the long and roughly parallel fracture lines may intersect to form a point, or may be separated by an irregular fracture line often with a profile approximating a hinge termination. Fracture front movement of one or both long, parallel fracture lines emanates from the end with carnivore damage. Carnivore gnawing on shaft cylinder or proximal or distal end plus shaft, usually on pieces

where the medullary cavity is largely exposed creates LVRUP pieces. Hammerstone shatter fragments (Fig. 5.22) refer to specimens whose fracture line complexity indicates all fracture lines were created simultaneously (i.e., it exhibits a number of short fracture lines with numerous fracture line movement directions). Definitive percussion fracture features (e.g., percussion marks, flake scars, cones, dimples, lateral stress features, etc.) may be present.

The co-occurrence of different surficial damages with one another as well with fracture features may provide information for a) the degree to which both carnivores and hominins played roles in creating the assemblages b) the sequence of carnivore and hominin access to represented carcasses, and c) the definition of fragment types diagnostic of hominin- or carnivore-induced breakage. Moreover, the co-occurrence of diagnostic damages with fracture features provides a method to assess the diagnostic potential of the fracture features discussed here. Frequencies of diagnostic damages are first tabulated followed by an analysis of their co-occurrence. Finally, the co-occurrences of the various combinations of damages with fracture features are analyzed as a means to assess the diagnostic potential of the fracture features discussed here.

- CHAPTER 5 - *Results*

5.1 Introduction

According to the fracture mechanics literature (see Chapter 2, framed as expectations in Chapter 3 Research Framework), if very different levels of force were applied to bones in the four assemblages examined here, then the assemblages should show different levels of fragmentation and distinctive fracture features. Specifically, the AHD assemblage broken by hyaena chewing should be distinctly different in these respects from the hammerstone-broken EXP assemblage. Similarly, if (as interpreted by Bunn 1982; Potts 1982, 1988; Egeland 2007) FLK-NN2 is mainly a hyaena accumulation, its level of fragmentation and fracture feature expression should be most similar to the AHD. If hominins played the major role in breakage of the FLK-Zinj assemblage, then it should display patterns of fracture and fragmentation similar to the EXP assemblage and different from both the AHD and FLK-NN2 assemblages.

Results are divided into three sections to assess these propositions. In the first section, *Fragmentation*, inter-assemblage differences in fragmentation are analyzed by examining specimen dimensions and the number of fracture lines per specimen. Fractographic data and analyses, the goal of which is to determine if specific fracture patterns and features may differentiate breaks created by carnivore chewing and hammerstone impact, are presented in the second section, *Fractographic Analysis*. By way of chi-square for independence (χ^2 , 0.05 significance) and principal component analysis (PCA), this section assesses inter-assemblage differences in frequencies of a) undifferentiated load points, b) 15 load point types (defined by the presence of flake scars, cones or cone fragments, fracture features, notches, and load marks either singly or in combination), and c) specific fracture features, i.e., cones, bulbar scars, hackle marks, fringe, and lateral stress, associated with the load points.

Data and analyses in these first two sections are wholly descriptive, without reference modifying or breakage agent. In the third section (*Fracture Agency: Estimating Hominin and Carnivore Fracture in the FLK-Zinj Fossil Assemblage*), damages accepted as referable to either carnivore or hammerstone breakage, i.e., tooth and percussion marks, are first tabulated. The co-occurrence of these diagnostic marks with fracture features is then analyzed. This analysis serves as a means of crosschecking the features that fractographic analyses suggested may differentiate fractures created by carnivore chewing and hammerstone impact. In turn, these data allow definition of specimens broken by carnivores or percussion (but which lacking diagnostic tooth or percussion marks) thereby improving the estimates of fracture agency for the two fossil assemblages FLK-Zinj and FLK-NN2.

As noted in the Methods, only long bones, but not the ulna, are considered. For each of the four assemblages, each skeletal part was assigned an animal size class: size class 1-2, size class 3-4, and indeterminate (after Bunn 1982). For many analyses the size class 1-2 and 3-4 material was combined to form size class 1-4. All assemblages are dominated by size class 3-4 material.

5.2 Fragmentation

Fragmentation in carnivore and zooarchaeological assemblages is largely a measure of how much force was applied to bones and thus the amount of processing to which an assemblage was subjected although trampling, geological, and diagenetic processes may play a role. Two measures of fragmentation are presented here. One indication of fragmentation is specimen completeness, here measured by length. Another is the number of fracture lines on the assemblage specimens.

5.2.1 Specimen Completeness: Length

The mean specimen length for each assemblage by size class are provided in Table 5.1 and summarized graphically with their 95% confidence intervals in Figure 5.1. The lengths of 818 AHD, 211 EXP, 84 FLK-NN2, and 1416 FLK-Zinj specimens were

Table 5.1. Mean specimen length (mm) of all long bone specimens ≥ 20 mm (excluding complete elements, ulnae, and suids) by size class. FLK-N2 specimens are the largest, FLK-Zinj specimens are the smallest, and the AHD specimens are second smallest, but are close in size to the EXP material. Note that size class 3-4 specimens dominate all assemblages.

	Count	Mean	Minimum	Maximum	Std. Dev.	Std. Error
AHD	szcls cnd	7	32.143	20	66	17.639
	szcls 1-2	18	100.222	38	185	40.297
	szcls 3-4	801	66.403	18	265	40.748
	szcls 1-4	819	67.147	18	265	41.015
	Total	826	66.850	18	265	40.994
EXP	szcls cnd	25	27.680	20	53	7.707
	szcls 1-2	-	-	-	-	-
	szcls 3-4	193	87.668	19	262	62.068
	szcls 1-4	193	87.668	19	262	62.068
	Total	218	80.789	19	262	61.500
FLK-NN2	szcls cnd	2	64.500	60	69	6.364
	szcls 1-2	-	-	-	-	-
	szcls 3-4	88	119.023	29	280	52.796
	szcls 1-4	88	119.023	29	280	52.796
	Total	90	117.811	29	280	52.826
FLK-ZINJ	szcls cnd	440	28.236	17	140	9.143
	szcls 1-2	215	50.660	19	182	24.003
	szcls 3-4	777	59.489	20	276	31.387
	szcls 1-4	992	57.576	19	276	30.151
	Total	1432	48.561	17	276	28.958

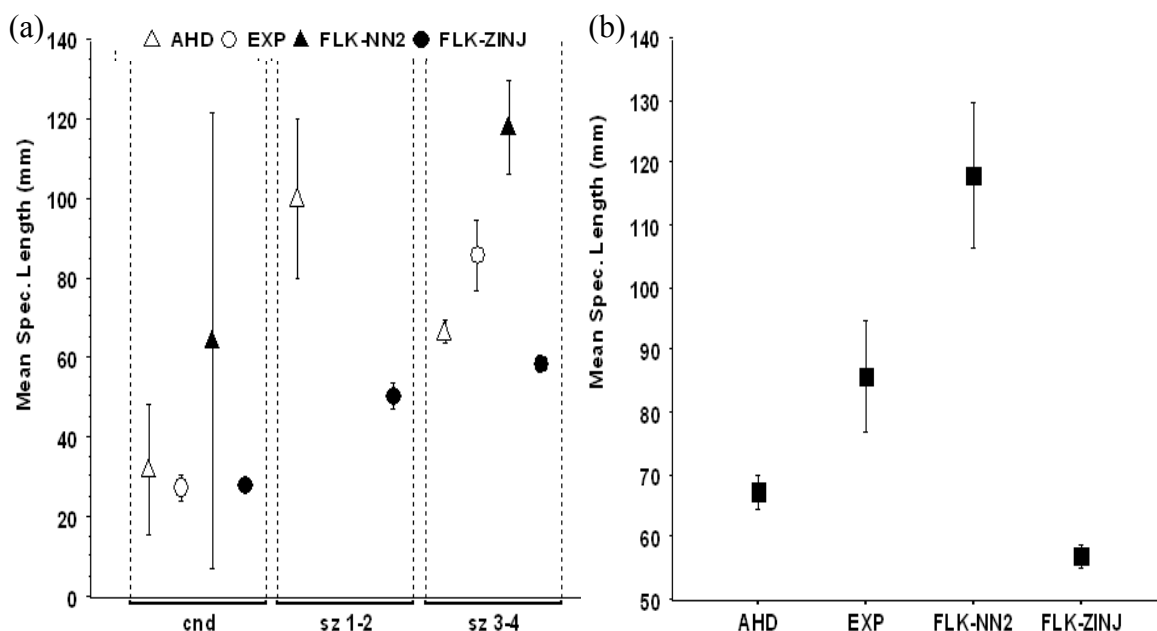


Fig. 5.1. Mean specimen length (mm) of all limb specimens ≥ 20 mm (excluding complete specimens, ulnae, and suids) for (a) indeterminate (cnd), 1-2, and 3-4 size classes, and (b) size class 1-4 (size classes 1-2 plus 3-4) in each assemblage. FLK-N2 specimens are the largest, FLK-Zinj specimens are the smallest, and the AHD specimens are second smallest, but are close in size to the EXP material. Note that size class 3-4 specimens dominate all assemblages. Bars indicate 95% confidence intervals.

measured for this analysis. In each assemblage the size class 3-4 specimens are dominant. Size class 1-2 material is absent from both the EXP and FLK-NN2 assemblages. Only FLK-Zinj includes a significant number of specimens that could not be assigned to a size class, but most are likely size class 3-4. ANOVA tests were conducted (significance level 0.05) to compare the mean specimen length of each assemblage (except for comparison of size class 1-2 material which is present only in the AHD and FLK-Zinj assemblages for which an independent Student t-test which was used) and the probabilities for each comparison are given in Table 5.2.

The mean lengths of specimens that could not be assigned to size class (end or indeterminate) are smallest in the EXP and FLK-Zinj assemblages, 27.7mm and 28.2mm,

Table 5.2. ANOVA p-values (except for (b) which are t-test values) for differences in the mean specimen length for all bovid and equid specimens ≥ 20 mm (excluding complete elements and ulnae). Statistically significant differences are in bold.

ASSEMBLAGE COMPARISON	Mean Diff.	Std. Error	p-value	95% CI	
				Lower	Upper
<i>a) CND (SzCls 0) (f-value = 10.68)</i>					
AHD vs. EXP	4.463	3.947	0.671	-5.71	14.64
AHD vs. FLK-NN2	-32.357	7.4	<0.0001	-51.44	-13.28
AHD vs. FLK-Zinj	3.906	3.516	0.683	-5.16	12.97
EXP vs. FLK-NN2	-36.82	6.782	<0.0001	-54.31	-19.33
EXP vs. FLK-Zinj	-0.556	1.898	0.991	-5.45	4.34
FLK-NN2 vs. FLK-Zinj	36.264	6.541	<0.0001	19.4	53.13
<i>b) SzCls 1-2 (t-value = 8.845)</i>					
AHD vs. FLK-Zinj	53.209	-	<0.0001	41.34	65.06
<i>c) SzCls 3-4 (f-value = 72.793)</i>					
AHD vs. EXP	-21.265	3.265	0.000	-29.66	-12.87
AHD vs. FLK-NN2	-52.619	4.572	0.000	-64.38	-40.86
AHD vs. FLK-Zinj	6.914	2.05	0.004	1.64	12.19
EXP vs. FLK-NN2	-31.354	5.237	0.000	-44.82	-17.89
EXP vs. FLK-Zinj	28.179	3.274	0.000	19.76	36.6
FLK-NN2 vs. FLK-Zinj	59.534	4.579	0.000	47.76	71.31
<i>d) SzCls 1-4 (f-value = 87.242)</i>					
AHD vs. EXP	-20.522	3.161	<0.0001	-28.65	-12.39
AHD vs. FLK-NN2	-51.876	4.432	<0.0001	-63.27	-40.48
AHD vs. FLK-Zinj	9.571	1.865	<0.0001	4.78	14.37
EXP vs. FLK-NN2	-31.354	5.082	<0.0001	-44.42	-18.29
EXP vs. FLK-Zinj	30.093	3.108	<0.0001	22.1	38.08
FLK-NN2 vs. FLK-Zinj	61.447	4.394	<0.0001	50.15	72.75
<i>e) TOTAL (SzCls 0-4) (f-value = 142.025)</i>					
AHD vs. EXP	-13.939	2.876	<0.0001	-21.33	-6.55
AHD vs. FLK-NN2	-50.961	4.193	<0.0001	-61.74	-40.18
AHD vs. FLK-Zinj	18.289	1.65	<0.0001	14.05	22.53
EXP vs. FLK-NN2	-37.022	4.733	<0.0001	-49.19	-24.86
EXP vs. FLK-Zinj	32.228	2.746	<0.0001	25.17	39.29
FLK-NN2 vs. FLK-Zinj	69.25	4.105	<0.0001	58.7	79.8

respectively, with the AHD mean only slightly larger at 32.1mm. With the exception of FLK-NN2 (represented by only two specimens), the mean lengths of indeterminate size class specimens from the assemblages are not significantly different (Table 5.2; Fig. 5.1a). Specimens that could not be assigned to animal size class are not considered in subsequent analyses because of their low frequencies in most assemblages.

The mean lengths of AHD and FLK-Zinj size class 1-2 specimens are 100.2mm and 50.7mm, respectively. The mean lengths of AHD and FLK-Zinj size class 1-2 specimens are clearly different (Table 5.2; $p < 0.0001$), and the 95% confidence intervals do not overlap (Fig. 5.1a).

For size class 3-4 fragments, the FLK-NN2 assemblage displays the greatest mean specimen length of 119.0mm, followed by EXP with 87.7mm, and AHD with a mean length of 67.2mm. With a mean length of 59.5mm, the FLK-Zinj specimens are the smallest of the assemblages. These mean specimen lengths are significantly different from one another ($p < 0.0001$; Table 5.2) and the 95% confidence intervals do not overlap (Fig. 5.1a). When all specimens are combined (size class 0-4 = indeterminate size class + size class 1-2 + and size class 3-4) the assemblages show the same ranking of mean lengths (FLK-NN2 = 117.8mm; EXP = 80.8mm; AHD = 66.9mm; FLK-Zinj = 48.6mm), and again all means are significantly different ($p < 0.0001$; Table 5.2). The same is true of both size class 3-4 and 1-4 material.

Note that for both size class 1-2 and 3-4 the mean length of the AHD material is greater than that of FLK-Zinj material. Overall then, FLK-NN2 material is larger than that of EXP, which is larger than the AHD material, which is larger than that from FLK-Zinj. This analysis of mean specimen lengths indicate that the AHD assemblage is less complete and more fragmented than EXP while the FLK-Zinj limb material is the least complete and most fragmented. FLK-NN2 specimens have the greatest mean length and are therefore the most complete.

5.2.2 Number of Fracture Lines per Specimen Length (#FLNs per SPECL)

A total of over 6000 fracture lines were measured in the four assemblages. Since it is likely that the potential number of fracture lines on a bone fragment is partially dependent on specimen and animal, element, and fragment size, the mean #FLNS per unit (mm) specimen length (SPECL) for various specimen groupings are compared here. The frequency, means, and range of the mean number of fracture lines per unit (mm) specimen length for shafts (SH), proximal ends plus shafts (PSH) and distal ends plus shaft (DSH) for each assemblage are provided in Table 5.3. This grouping by element portion is not used in subsequent analyses, but it is worth noting that when all specimens assigned to size class are considered (size class 1-4) the shaft fragments display the greatest number of fracture lines in all assemblages. Data are summarized in this manner because most specimens categorized as DSH and PSH specimens include considerable amounts of the shaft. Data are analyzed by size class. The cell plot with 95% confidence intervals shown in Figure 5.2 summarizes these data by size class. ANOVA tests were conducted (significance level $p < 0.05$) to compare the mean #FLNs per SPECL for size class 3-4 material in each assemblage. Independent Student t-test was used to compare size class 1-2 material (which is present only in the AHD and FLK-Zinj assemblages). The probabilities for each comparison are given in Table 5.4.

The size class 3-4 material displays a progressively greater #FLNs per SPECL from FLK-NN2 (0.05) to EXP (0.07) to AHD (0.09) to FLK-Zinj (0.10), and none of the means overlap at the 95% confidence interval. ANOVA statistics (Table 5.4) show that the AHD and FLK- Zinj material are not dissimilar (0.0690) and likewise that the EXP material and FLK-NN2 material are not dissimilar (0.0630). In both cases, however, the differences approach significance. All other comparisons of the mean #FLNs per SPECL are significantly different between assemblages for the size class 3-4 long bone specimens. The difference between the mean #FLNs per SPECL for size class 1-2 material in the AHD

(0.07) and in FLK-Zinj (0.1) assemblages is considerably greater than for the size class 3-4

bones (Table 5.2, Fig. 5.2b). However, AHD has very few specimens (n=18).

Table 5.3. Mean number of fracture lines per unit specimen length (mm) of long bone specimens ≥ 20 mm (excluding complete elements and ulnae) by size class and element portion. PSH = proximal end plus shaft; SH = shaft; DSH = distal end plus shaft. Note that in most cases the shaft displays the greatest number of fracture lines per unit specimen length.

			Count	Mean	Minimum	Maximum	Std. Dev.	Std. Error
SzCls 1-2	AHD	PSH	4	0.05100	0.024	0.073	0.020543	0.010271
		SH	5	0.09980	0.075	0.159	0.034201	0.015295
		DSH	8	0.05975	0.016	0.105	0.033388	0.011805
		Total	17	0.06947	0.016	0.159	0.035767	0.008675
	FLK-ZINJ	PSH	28	0.10646	0.011	0.263	0.059688	0.011280
		SH	160	0.13021	0.020	0.273	0.044150	0.003490
		DSH	12	0.08500	0.011	0.176	0.049789	0.014373
		Total	200	0.12418	0.011	0.273	0.048413	0.003423
SzCls 3-4	AHD	PSH	28	0.07179	0.008	0.133	0.032841	0.006206
		SH	701	0.09566	0.020	0.261	0.040248	0.001520
		DSH	58	0.05909	0.010	0.200	0.042731	0.005611
		Total	787	0.09211	0.008	0.261	0.041456	0.001478
	EXP	PSH	20	0.04920	0.025	0.100	0.019116	0.004275
		SH	74	0.07723	0.038	0.250	0.032492	0.003777
		DSH	23	0.05396	0.017	0.224	0.039964	0.008333
		Total	117	0.06786	0.017	0.250	0.034373	0.003178
	FLK-NN2	PSH	17	0.04212	0.016	0.094	0.021877	0.005306
		SH	32	0.06272	0.021	0.120	0.025847	0.004569
		DSH	17	0.04076	0.018	0.081	0.018223	0.004420
		Total	66	0.05176	0.016	0.120	0.025164	0.003097
	FLK-ZINJ	PSH	34	0.08744	0.038	0.333	0.059110	0.010137
		SH	663	0.10070	0.023	0.400	0.042596	0.001654
		DSH	30	0.06347	0.019	0.151	0.028818	0.005261
		Total	727	0.09854	0.019	0.400	0.043673	0.001620
SzCls 1-4	AHD	PSH	32	0.06919	0.008	0.133	0.032078	0.005671
		SH	706	0.09569	0.020	0.261	0.040190	0.001513
		DSH	66	0.05917	0.010	0.200	0.041488	0.005107
		Total	804	0.09163	0.008	0.261	0.041452	0.001462
	EXP	PSH	20	0.04920	0.025	0.100	0.019116	0.004275
		SH	74	0.07723	0.038	0.250	0.032492	0.003777
		DSH	23	0.05396	0.017	0.224	0.039964	0.008333
		Total	117	0.06786	0.017	0.250	0.034373	0.003178
	FLK-NN2	PSH	17	0.04212	0.016	0.094	0.021877	0.005306
		SH	32	0.06272	0.021	0.120	0.025847	0.004569
		DSH	17	0.04076	0.018	0.081	0.018223	0.004420
		Total	66	0.05176	0.016	0.120	0.025164	0.003097
	FLK-ZINJ	PSH	62	0.09603	0.011	0.333	0.059651	0.007576
		SH	823	0.10644	0.020	0.400	0.044439	0.001549
		DSH	42	0.06962	0.011	0.176	0.036734	0.005668
		Total	927	0.10407	0.011	0.400	0.045938	0.001509

Table 5.4. ANOVA (*c*, and *d*) and Student's t-test (*a*, because only two assemblages can be compared) p-values for differences in the mean number of fracture lines (#FLNs) per specimen length (SPEC1) for all specimens ≥ 20 mm (not including complete elements, ulnae, and suidae). Significant differences are in are bold.

ASSEMBLAGE COMPARISON	Mean Diff.	Std. Error	p-value	95% CI	
				Lower	Upper
<i>a) SzCls 1-2 (t-value = -4.588)</i>					
AHD vs. FLK-Zinj	-0.054000	-	<0.0001	-0.07800	-0.03100
<i>b) SzCls 3-4 (f-value = 38.294)</i>					
AHD vs. EXP	0.024610	0.004105	<0.0001	0.01405	0.03517
AHD vs. FLK-NN2	0.040439	0.005312	<0.0001	0.02678	0.05410
AHD vs. FLK-Zinj	-0.005223	0.002133	0.0690	-0.01071	0.00026
EXP vs. FLK-NN2	0.015830	0.006376	0.0630	-0.00057	0.03223
EXP vs. FLK-Zinj	-0.029833	0.004121	<0.0001	-0.04043	-0.01924
FLK-NN2 vs. FLK-Zinj	-0.045662	0.005324	<0.0001	-0.05935	-0.03197
<i>c) SzCls 1-4 (f-value = 50.816)</i>					
AHD vs. EXP	0.024134	0.004239	<0.0001	0.01323	0.03503
AHD vs. FLK-NN2	0.039964	0.005488	<0.0001	0.02585	0.05408
AHD vs. FLK-Zinj	-0.011335	0.002069	<0.0001	-0.01665	-0.00601
EXP vs. FLK-NN2	0.015830	0.006593	0.0770	-0.00112	0.03278
EXP vs. FLK-Zinj	-0.035469	0.004198	<0.0001	-0.04626	-0.02467
FLK-NN2 vs. FLK-Zinj	-0.051298	0.005457	<0.0001	-0.06533	-0.03727

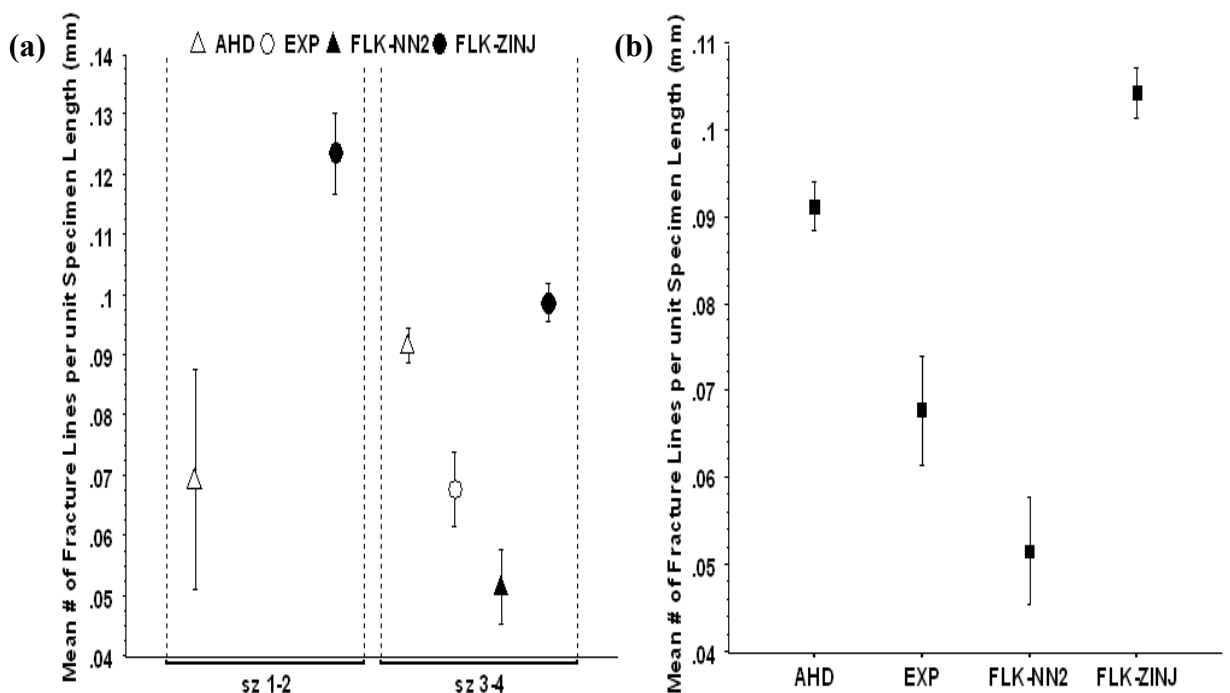


Figure 5.2. Plot of mean number of fracture lines per unit specimen length (mm) for limb specimens ≥ 20 mm by (a) 1-2 and 3-4 size classes and (b) size classes 1-4. Bars indicate 95% confidence interval. Note that the ratio is greatest for the FLK-Zinj material and least for FLK-NN2.

Comparison of the mean #FLNs per unit SPECL (mm) for size class 1-4 specimens (size class 1-2 and 3-4) indicates significant differences between all but the EXP (0.07) vs. FLK-NN2 (0.05) assemblage comparisons and no overlap in 95% confidence intervals (Table 5.3, Fig. 5.2a, Table 5.4). FLK-Zinj displays a significantly greater mean #FLNs per unit SPECL (0.1) than either AHD (0.09) or FLK-NN2 (0.05). The hammerston-broken EXP assemblage #FLN to SPECL ratio is less than that of AHD, but greater than FLK-NN2 and is much less than that of FLK-Zinj.

While differences in the mean #FLNs per SPECL is not always significant and overlap in 95% confidence intervals occur in a few comparisons, patterns are clear:

- 1) FLK-NN2 has the lowest ratio of FLNs to specimen length while FLK-Zinj has the highest.
- 2) In most cases the FLK-NN2 assemblage has fewer #FLNs per SPECL than either AHD or FLK-Zinj. These differences are significant.
- 3) The FLK-NN2 and EXP assemblages are more similar to each other than they are to either the AHD or FLK-Zinj assemblages.

5.3 Fractography: Load Point Frequencies, Types, and Fracture Features

Fractographic results are described by examining the frequencies, types, and fracture features associated with loading points (LDPTs). Loading points were broadly defined in Chapter 2 as any damage created through the application of force by the indenter causing the bone to fracture. The fractographic literature (see Chapter 2) suggests that different types of loading points (LDPTs) and fracture features (FRACFEATs) are produced with the application of different levels of force. To explore how this may or may not be true for bone fracture, each specimen from each assemblage was examined for LDPTs. If present, the LDPTs were classified according to the features observed and tallied.

A LDPT may be identified on the basis of one or more cortical surface damages or fracture features on the fracture surface. Fifteen types of LDPTs were defined in this study based on the presence of flake scars (FLKSs), cones or cone fragments (FLKOs), notches (NTCHs), load marks (aka indenter marks; LMRKs), and fracture features (e.g., lateral

stress, hackle marks, ant fringe; FRFEs), alone or in various combinations. These abbreviations are used in all subsequent tables referring to LDPT types. In the first analysis the overall frequency of LDPTs in the assemblages is assessed. This is followed by an analysis of the frequencies of specific LDPT types in the four assemblages. Finally, the frequencies of fracture features (i.e., incipient flakes, IF; radiating cracks, RC; lateral stress, LS; cones, CO; hackle marks, HK; fringe, FR; bulbar scars, Bsc) associated with LDPTs are analyzed.

5.3.1 Number of LDPTS

Table 5.5 shows the frequencies that each type of LDPT occurs on each skeletal part, for each specimen for which a size class can be determined, as well as a combined frequency for both large and small animals (size class 1-2 plus size class 3-4). The tallies are presented both as overall scores, i.e., the number of LDPT types, and the total number of LDPTs, and as frequencies, i.e., the average number of LDPTs per individual specimen. The average number of LDPTs per specimen was calculated in three ways. Table 5.5 shows the overall average using all specimens including the ulnae and isolated LMRKs (i.e., those located some distance from the LDPT and those for which various fractographic features did not allow the definition of a LDPT that caused fracture). Table 5.6 gives the average number of LDPTs per specimen excluding isolated LMRKs as well as long bone shaft fragments not identified to element (LBSFs). Because of their lack of marrow and overall geometry, the ulnae are also excluded in a third calculation (Table 5.7).

The LDPT frequencies for all size class 1-2 and 3-4 AHD, FLK-NN2, EXP, and FLK-Zinj specimens are given in Table 5.5. When all size class 1-4 specimens (including long bone shaft fragments, LBSFs) are considered, the total number of LDPTs is 351 in the AHD assemblage, 293 in EXP, 32 in FLK-NN2, and 1173 in the FLK-Zinj assemblage. What is immediately striking is the greater number of LDPTs per NISP in the EXP (293/195; 1.50) and FLK-Zinj (1173/1005, 1.17) assemblages compared to that of AHD (351/840, 0.42) or FLK-NN2 (32/93, 0.34). On average the EXP and FLK-Zinj limbs

specimens have 2.3 to 4.2 times the number of LDPTs per NISP than FLK-NN2 and AHD. The same patterns hold true for size class 1-2 and size class 3-4 materials. The AHD size class 1-2 specimens display less than half the number LDPTs per NISP (0.65) as that for FLK-Zinj (1.42). For size class 3-4 material FLK-Zinj and EXP display 1.1 and 1.50 LDPTs per NISP, respectively, while for AHD and FLK-NN2 the frequencies are much lower 0.41 and 0.34, respectively.

The above cursory examination of LDPT frequencies may be misleading for a variety of reasons, however. First, isolated LMRKs should be excluded from LDPT frequency comparisons because of the different level of difficulty in identifying or inferring when a LMRK, particularly the two under consideration here – percussion marks (PM) and tooth marks (TM) – caused fracture. That is, while by definition a percussion marks is a LDPT that reflects an attempt to initiate fracture, not all percussion marks are related to a fracture event – as indicated by the location of many some distance from a fracture surface. PMs located more than about 4cm from a fracture (regardless of whether or not a LDPT could be defined on the basis of fracture surface features) were coded as isolated. Similarly, not all tooth marks – and likely many fewer – are created as part of a carnivore’s attempt to gain access to the marrow cavity. Many (most?) are related to flesh removal or chewing and not necessarily breakage. A TM not directly associated with a fracture was coded as an isolated LMRK. When isolated LDPTs are removed the frequencies of LDPTs on AHD and FLK-NN2 specimens remains virtually identical (0.42 and 0.33, respectively), while those for EXP and FLK-Zinj specimens are considerably smaller, 1.10 and 0.86, respectively (Table 5.6). The pattern remains the same, however; the EXP and FLK-Zinj specimens display considerably more LDPTs per specimen than the AHD and FLK-NN2 material.

As noted by Faith (2007) LDPT frequencies may also be influenced by specimen size. That is, the small size of LBSFs (too small to preserve an anatomical landmark) would seem to reduce the chances of observing a LDPT as well as make it unlikely that all

LDPT types and many fracture features would be preserved. Thus, both long bone shaft fragments should also be excluded when calculating LDPT frequencies (Table 5.6). Even when the unidentified LBSFs are excluded from the total (size class 1-4), the AHD and FLK-NN2 assemblages still display fewer LDPTS per specimen (0.61 and 0.36, respectively) than the EXP and FLK-Zinj material (1.74 and 1.27, respectively). The scatter plot of the number of LDPTs (excluding isolated LMRKs) vs. the identified element NISP (Fig. 5.3) shows just how different the AHD and FLK-NN2 assemblages are from EXP and FLK-Zinj. The data fall into two groups; the EXP and FLK-Zinj assemblages have similarly steeper regression line slopes than the shallow slopes of AHD and FLK-NN2.

caption for Table 5.5: Load point (LDPT) frequencies observed on all long bones \geq 20mm in length for a) the Amboseli Hyaena Den (AHD), b) Experimental (EXP), c) FLK-NN2, and d) FLK-Zinj. LDPT abbreviations: FLKS = flake scar, PCON = partial/complete cone, FRFE = fracture feature, NTCH = notch, isolated LMRK = load mark not associated with fracture, FLKS + NTCH = flake scar with associated notch, FLKS + LMRK = flake scar with associated load mark, FLKS + NTCH + LMRK = flake scar with associated notch and load mark, PCON + NTCH = partial/complete cone with associated notch, PCON + LMRK = partial/complete cone with associated load mark, PCON + NTCH + LMRK = partial/complete cone with associated notch and load mark, FRFE + NTCH = fracture feature with associated notch, FRFE + NTCH + LMRK = fracture feature with associated notch and load mark, NTCH + LMRK = notch and associated load mark. Note that overall LDPT frequencies are considerably smaller in AHD and FLK-NN2 than in the EXP and FLK-Zinj assemblages where they comprise a significant proportion of the observed LDPTs. Also note that LDPT types defined by isolated LMRKs, and those with a PCON, or FRFE component were observed much less often in AHD and FLK-NN2 than in the EXP and FLK-Zinj assemblages.

Table 5.5a. AHD load point (LDPT) frequencies.

SzCls	ELEMENT														LDPT Total	LDPTS/NISP		
		NISP	FLKS	FLKO	FRFE	NTCH	isolated LMRK	FLKS+NTCH	FLKS+LMRK	FLKS+NTCH+LMRK	FLKO+NTCH	FLKO+LMRK	FLKO+NTCH+LMRK	FRFE+NTCH			FRFE+LMRK	FRFE+NTCH+LMRK
SzCls 1-2	HUM	4							6								6	1.50
	RAD	4						1									1	0.25
	ULN	1															0	0.00
	MCM	2							1								1	0.50
	FEM	0																
	TIB	8								1	2						3	0.38
	MTM	1									2						2	2.00
	METM	0																
	LBSF	0																
	TOTAL	20							1	1	11						13	0.65
ID ONLY	20							1	1	11						13	0.65	
SzCls 3-4	HUM	48	4	3	1	1	12	2	6				1		4	34	0.71	
	RAD	80	3	1	2		14	5	21				2	2	2	52	0.65	
	ULN	3							1					1		2	0.67	
	MCM	32		2		2	3	2	13					1		23	0.72	
	FEM	16	3				1	1	2							7	0.44	
	TIB	80	5		4	1	12	4	18					3	2	49	0.61	
	MTM	32	2		1		4	2	6					1	7	23	0.72	
	METM	67	2	1			5	8	8					2	1	2	29	0.43
	LBSF	462	33	5		3	1	23	20	28	1			2	3	119	0.26	
	TOTAL	820	52	12	5	9	2	74	44	103	1			3	12	1	20	338
ID ONLY	358	19	7	5	6	1	51	24	75				3	10	1	17	219	0.61
SzCls 1-4	HUM	52	4	3	1	1	12	2	12				1		4	40	0.77	
	RAD	84	3	1	2		14	5	22				2	2	2	53	0.63	
	ULN	4							1					1		2	0.50	
	MCM	34		2		2	4	2	13					1		24	0.71	
	FEM	16	3				1	1	2							7	0.44	
	TIB	88	5		4	1	12	5	20					3	2	52	0.59	
	MTM	33	2		1		4	2	8					1	7	25	0.76	
	METM	67	2	1			5	8	8					2	1	2	29	0.43
	LBSF	462	33	5		3	1	23	20	28	1			2	3	119	0.26	
	TOTAL	840	52	12	5	9	2	75	45	114	1			3	12	1	20	351
ID ONLY	378	19	7	5	6	1	52	25	86				3	10	1	17	232	0.61

Table 5.5b. EXP load point (LDPT) frequencies.

SzCls	ELEMENT													LDPT Total	LDPTS/NISP				
		NISP	FLKS	FLKO	FRFE	NTCH	isolated LMRK	FLKS+NTCH	FLKS+LMRK	FLKS+NTCH+ LMRK	FLKO+NTCH	FLKO+LMRK	FLKO+NTCH+LMRK			FRFE+NTCH	FRFE+LMRK	FRFE+NTCH+LMRK	NTCH+LMRK
SzCls 1-2	HUM	0																	
	RAD	0																	
	ULN	0																	
	MCM	0																	
	FEM	0																	
	TIB	0																	
	MTM	0																	
	METM	0																	
	LBSF	0																	
	TOTAL	0																	
ID ONLY	0																		
SzCls 3-4	HUM	25	6	6	5	8	3	9	3	9	1	2					52	2.08	
	RAD	21	3	2	1	26	1	13	11	6		3					66	3.14	
	ULN	7				1	3	1	1	2						1	9	1.29	
	MCM	0																	
	FEM	18	5	1	4	5	3	4	2	6		7					37	2.06	
	TIB	31	6	3	10	23	5	4	3	11		13					78	2.52	
	MTM	0																	
	METM	0																	
	LBSF	93	8	14	3	13	1	2		5		5					51	0.55	
	TOTAL	195	28	26	23	1	78	14	33	21	37	1	30	1	1	1	1	293	1.50
ID ONLY	102	20	12	20	1	65	13	31	21	32	1	25	1	1	1	1	242	2.37	
SzCls 1-4	HUM	25	6	6	5	8	3	9	3	9	1	2					52	2.08	
	RAD	21	3	2	1	26	1	13	11	6		3					66	3.14	
	ULN	7				1	3	1	1	2						1	9	1.29	
	MCM	0																	
	FEM	18	5	1	4	5	3	4	2	6		7					37	2.06	
	TIB	31	6	3	10	23	5	4	3	11		13					78	2.52	
	MTM	0																	
	METM	0																	
	LBSF	93	8	14	3	13	1	2		5		5					51	0.55	
	TOTAL	195	28	26	23	1	78	14	33	21	37	1	30	1	1	1	1	293	1.50
ID ONLY	102	20	12	20	1	65	13	31	21	32	1	25	1	1	1	1	242	2.37	

Table 5.5c. FLK-NN2 load point (LDPT) frequencies.

SzCIs	ELEMENT												LDPT Total	LDPTS/NISP				
		NISP	FLKS	FLKO	FRFE	NTCH	isolated LMRK	FLKS+NTCH	FLKS+LMRK	FLKS+NTCH+ LMRK	FLKO+NTCH	FLKO+LMRK			FLKO+NTCH+LMRK	FRFE+NTCH	FRFE+LMRK	FRFE+NTCH+LMRK
SzCIs 1-2	HUM	0																
	RAD	0																
	ULN	0																
	MCM	0																
	FEM	0																
	TIB	0																
	MTM	0																
	METM	0																
	LBSF	0																
	TOTAL	0																
ID ONLY	0																	
SzCIs 3-4	HUM	16	1				1	3								5	0.31	
	RAD	12	1				4	2								7	0.58	
	ULN	7														0	0.00	
	MCM	5												1	1	0.20		
	FEM	8				1	4								5	0.63		
	TIB	19	1				1	2	2						6	0.32		
	MTM	17		1			2	3	1						7	0.41		
	METM	0																
	LBSF	9	1												1	0.11		
	TOTAL	93	4	1		1	12	5	8					1	32	0.34		
ID ONLY	84	3	1		1	12	5	8					1	31	0.37			
SzCIs 1-4	HUM	16	1				1	3								5	0.31	
	RAD	12	1				4	2								7	0.58	
	ULN	7														0	0.00	
	MCM	5																
	FEM	8				1	4								5	0.63		
	TIB	19	1				1	2	2						6	0.32		
	MTM	17																
	METM	0																
	LBSF	9	1												1	0.11		
	TOTAL	93	4	1		1	12	5	8					1	32	0.34		
ID ONLY	84	3	1		1	12	5	8					1	31	0.37			

Table 5.5d. FLK-Zinj load point (LDPT) frequencies.

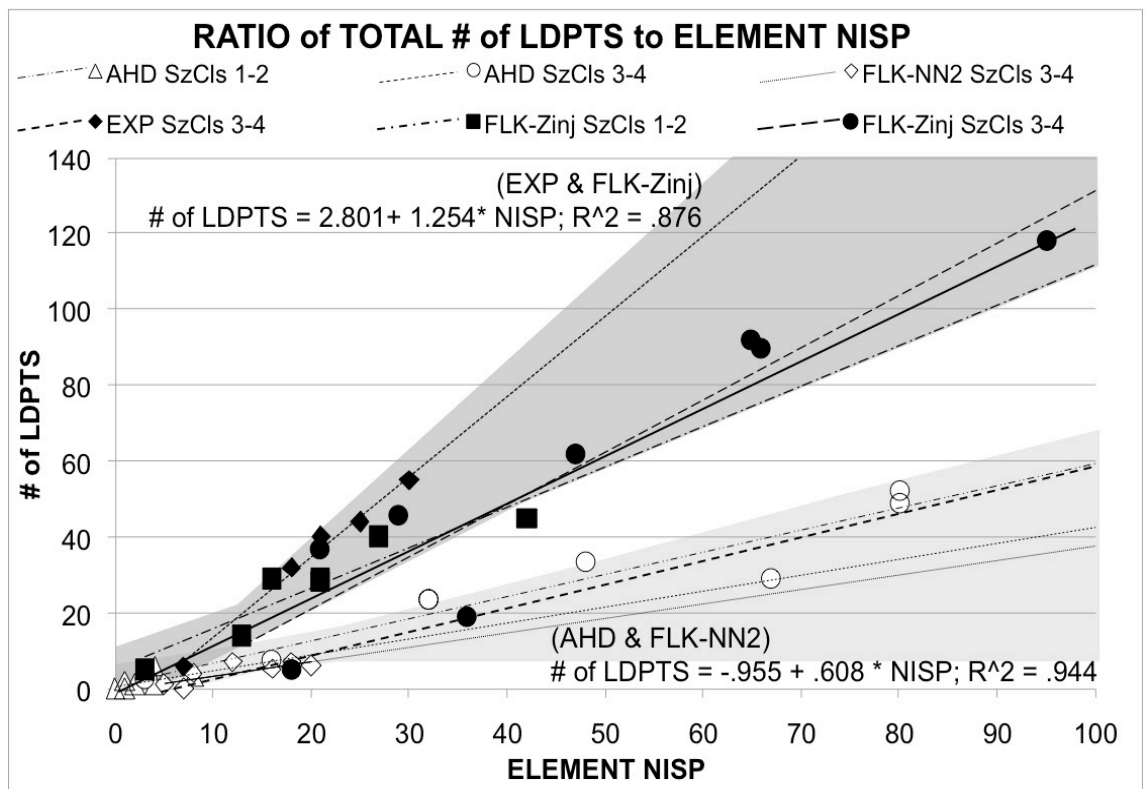
SzCIs	ELEMENT	NISP	FLKS	FLKO	FRFE	NTCH	isolated LMRK	FLKS+NTCH	FLKS+LMRK	FLKS+NTCH+ LMRK	FLKO+NTCH	FLKO+LMRK	FLKO+NTCH+LMRK	FRFE+NTCH	FRFE+LMRK	FRFE+NTCH+LMRK	NTCH+LMRK	LDPT Total	LDPTS/NISP
SzCIs 1-2	HUM	21	4	2	2	4	7	5	4	1	1	1						31	1.48
	RAD	16	3	2	10	6	4	3	7									35	2.19
	ULN	3			1	1	2	1										5	1.67
	MCM	21	7	3		11	8	2	3	2	1		1					38	1.81
	FEM	21	9	5	2	7	6		1	4			1					35	1.67
	TIB	42	12	2	3	1	23	9	6	8		1		2			1	68	1.62
	MTM	27	4	4	3	3	19	8	3	10	1	1	2	1	2		1	62	2.30
	METM	13	1	1	1		3	2	3	2	2		1		1			17	1.31
	LBSF	57	6	3			1	2	5	1		4						22	0.39
	TOTAL	221	46	20	22	4	73	45	30	37	3	15	6	2	8		2	313	1.42
ID ONLY	164	40	17	22	4	72	43	25	36	3	11	6	2	8		2	291	1.77	
SzCIs 3-4	HUM	66	10	7	3	1	18	25	19	11	2	8	1	1	2			108	1.64
	RAD	65	9	11	9		44	8	10	20		11	1	2	11			136	2.09
	ULN	18			2		9	1							1		1	14	0.78
	MCM	29	4	4	4	3	17	12	5	4	3		1	5	1			63	2.17
	FEM	47	11	13	11		23	10	5	5	5			1				84	1.79
	TIB	95	23	10	12	1	43	15	10	20	9	5	1	9			3	161	1.69
	MTM	21	3	5	6	1	21	3	5	9	3			1	1			58	2.76
	METM	37	3	2	2		10	7	3	1	1				1			30	0.81
	LBSF	406	34	18	1		50	3	66	3	31							206	0.51
	TOTAL	784	97	70	50	6	235	84	123	73	5	68	7	6	31	1	4	860	1.10
ID ONLY	378	63	52	49	6	185	81	57	70	5	37	7	6	31	1	4	654	1.73	
SzCIs 1-4	HUM	87	14	7	5	1	20	29	26	16	2	12	2	2	3			139	1.60
	RAD	81	12	13	19		50	12	13	27		11	1	2	11			171	2.11
	ULN	21			3		10	3	1						1		1	19	0.90
	MCM	50	11	7	4	3	28	20	7	7	5	1	1	6	1			101	2.02
	FEM	68	20	18	13		30	16	5	6	9			2				119	1.75
	TIB	137	35	12	15	2	66	24	16	28	9	6	1	11			4	229	1.67
	MTM	48	7	9	9	4	40	11	8	19	4	1	2	2	3		1	120	2.50
	METM	50	4	3	3		13	9	6	3	2	1	1		2			47	0.94
	LBSF	463	40	21	1		51	5	71	4	35							228	0.49
	TOTAL	1005	143	90	72	10	308	129	153	110	8	83	13	8	39	1	6	1173	1.17
ID ONLY	542	103	69	71	10	257	124	82	106	8	48	13	8	39	1	6	945	1.74	

Table 5.6. The total number of LDPTs excluding isolated LMRKs and the corresponding LDPTs per NISP frequencies for each assemblage.

SzCIs	ELEMENT	AHD			EXP			FLK-NN2			FLK-Zinj		
		NISP	total LDPTS (no isolated LMRKS)	total non-LMRK LDPTS/NISP	NISP	total LDPTS (no isolated LMRKS)	total non-LMRK LDPTS/NISP	NISP	total LDPTS (no isolated LMRKS)	total non-LMRK LDPTS/NISP	NISP	total LDPTS (no isolated LMRKS)	total non-LMRK LDPTS/NISP
SzCIs 1-2	HUM	4	6	1.50	0			0			21	29	1.38
	RAD	4	1	0.25	0			0			16	29	1.81
	ULN	1	0	0.00	0			0			3	4	1.33
	MCM	2	1	0.50	0			0			21	27	1.29
	FEM	0			0			0			21	28	1.33
	TIB	8	3	0.38	0			0			42	45	1.07
	MTM	1	2	2.00	0			0			27	43	1.59
	METM	0			0			0			13	14	1.08
	LBSF	0			0			0			57	21	0.37
	TOTAL	20	13	0.65	0			0			221	240	1.09
	ID ONLY	20	13	0.65	0			0			164	219	1.34
SzCIs 3-4	HUM	48	33	0.69	25	44	1.76	16	5	0.31	66	90	1.36
	RAD	80	52	0.65	21	40	1.90	12	7	0.58	65	92	1.42
	ULN	3	2	0.67	7	6	0.86	7	0		18	5	0.28
	MCM	32	23	0.72	0			5	1	0.20	29	46	1.59
	FEM	16	7	0.44	18	32	1.78	8	4	0.50	47	61	1.30
	TIB	80	49	0.61	31	55	1.77	19	6	0.32	95	118	1.24
	MTM	32	23	0.72	0			17	7	0.41	21	37	1.76
	METM	67	29	0.43	0			0			37	20	0.54
	LBSF	462	118	0.26	93	38	0.41	9	1	0.11	406	156	0.38
	TOTAL	820	336	0.41	195	215	1.10	93	31	0.33	784	625	0.80
	ID ONLY	358	218	0.61	102	177	1.74	84	30	0.36	378	469	1.24
SzCIs 1-4	HUM	52	39	0.75	25	44	1.76	16	5	0.31	87	119	1.37
	RAD	84	53	0.63	21	40	1.90	12	7	0.58	81	121	1.49
	ULN	4	2	0.50	7	6	0.86	7	0		21	9	0.43
	MCM	34	24	0.71	0			5	0		50	73	1.46
	FEM	16	7	0.44	18	32	1.78	8	4	0.50	68	89	1.31
	TIB	88	52	0.59	31	55	1.77	19	6	0.32	137	163	1.19
	MTM	33	25	0.76	0			17	0		48	80	1.67
	METM	67	29	0.43	0			0			50	34	0.68
	LBSF	462	118	0.26	93	38	0.41	9	1	0.11	463	177	0.38
	TOTAL	840	349	0.42	195	215	1.10	93	31	0.33	1005	865	0.86
	ID ONLY	378	231	0.61	102	177	1.74	84	30	0.36	542	688	1.27

Table 5.7. The total number of LDPTs excluding the ulnae and isolated LMRKs and the corresponding LDPTs per NISP frequencies for each assemblage.

SzCls	AHD			EXP			FLK-NN2			FLK-Zinj		
	NISP	total LDPTS	LDPTS /NISP	NISP	total LDPTS	LDPTS /NISP	NISP	total LDPTS	LDPTS /NISP	NISP	total LDPTS	LDPTS /NISP
SzCls 1-2												
TOTAL	19	13	0.68	0			0			218	236	1.08
ID ONLY	19	13	0.68	0			0			161	215	1.34
SzCls 3-4												
TOTAL	817	334	0.41	188	209	1.11	84	31	0.37	766	620	0.81
ID ONLY	355	216	0.61	95	171	1.80	77	30	0.39	360	464	1.29
SzCls 1-4												
TOTAL	836	347	0.42	188	209	1.11	84	31	0.37	984	856	0.87
ID ONLY	374	229	0.61	95	171	1.80	77	30	0.39	521	679	1.30



Assemblage Regression Solutions and R2 values:

AHD #LDPTS = 0.595*NISP + 0.396; R2 = 0.954

FLK-NN2 #LDPTS = 0.382*NISP + 0.405; R2 = 0.631

EXP #LDPTS = 2.117*NISP + (-7.366); R2 = 0.988

FLK-Zinj #LDPTS = 1.281*NISP + (-0.391); R2 = 0.901

Fig. 5.3. Plot of total number of loadpoints (LDPTs) vs. number of identified specimens (NISP) for identified elements in the four assemblages. Does not include specimens with only isolated LMRKs. Each point represents the LDPT to NISP ratio for an element of each size class for each assemblage (data from Tables 5.5 and 5.6). The heavy solid line shows the regression line for the combined EXP and FLK-Zinj samples and the heavy dashed line shows the regression line for the combined AHD and FLK-NN2 samples. The darker and lighter shadings indicate the 95% confidence intervals for the combined EXP and FLK-Zinj, and AHD, and FLK-NN2 combined samples, respectively. These data show that the AHD and FLK-NN2 assemblages have many fewer LDPTS per NISP than the EXP and FLK-Zinj assemblages.

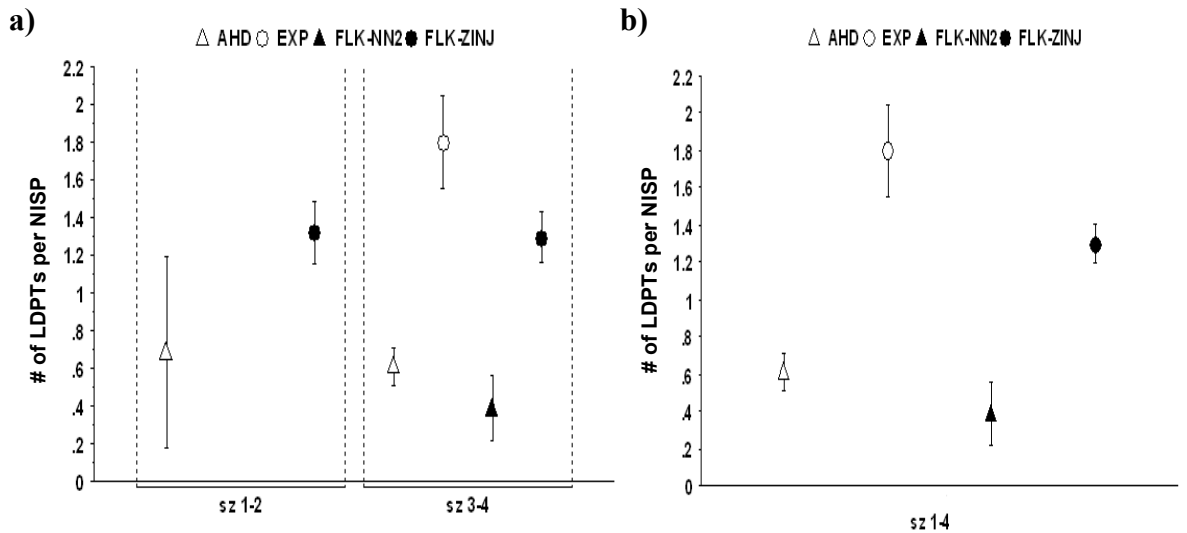


Fig. 5.4. Point plot of frequency of loadpoints (LDPTs) per number of identified specimens (NISP) in Amboseli Hyaena Den (AHD), Experimental (EXP), FLK-NN2, and FLK-Zinj long bone assemblages (excluding specimens not identified to element - LBSFs, as well as the ulna, and isolated LMRKs) for (a) size class 1-2 and 3-4 specimens, and (b) size class 1-4 specimens >20mm in maximum dimension. Bars indicate 95% confidence intervals.

LDPT frequencies may also be influenced by specimen geometry. The ulna's shape i.e., its shaft is not cylindrical, and perhaps more importantly, its lack of much marrow, would seem to mitigate against the creation of LDPTs as well as make it unlikely that all LDPT types and many fracture features would be preserved. This exclusion of the ulnae, LBSFs, and specimens with just an isolated LMRK lowers the size class 1-4 AHD NISP to 374 specimens with 229 LDPTs. For the FLK-NN2 material the NISP falls to 77 with 30 LDPTs. The NISP for the EXP material becomes 95 with 171 LDPTs. The greatest change is seen in the FLK-Zinj material because of the large number of fragments that could not be assigned to an animal size class (LBSFs). Excluding the ulnae, LBSFs, and specimens with just an isolated LMRKs results in a size class 1-4 FLK-Zinj NISP of 521 with 679 LDPTs. Again, however, the number of LDPTs per NISP for AHD and FLK-NN2 for specimens identified to element is considerably smaller than that of EXP and FLK-Zinj, i.e., 0.61 and 0.39 vs. 1.80 and 1.30, respectively (Table 5.7). The point plot of the size class 1-2, 3-4, and 1-4 means (Fig. 5.4) shows just how different the AHD and FLK-NN2 assemblages are compared to the EXP and FLK-Zinj limb material.

Statistical analysis of these frequencies (Table 5.5 and Table 5.8, rows labeled “*Total – No LBSF/ULN*”) indicates that there is no difference in the frequency of LDPTs per NISP in the AHD and FLK-NN2 assemblages, while both tend to display statistically fewer LDPTs than observed in either the EXP or FLK-Zinj assemblages. For example, for neither the large animal limb (size class 3-4) nor the combined small and large animal limb samples (size class 1-4) are the AHD and FLK-NN2 LDPT frequencies statistically different ($\chi^2_6 = 5.733$, $p = 0.4537$, and $\chi^2_6 = 5.399$, $p = 0.4937$, respectively). In contrast, the LDPT frequencies in the AHD and FLK-NN2 are significantly smaller than those observed for the EXP and FLK-Zinj assemblages (size class 3-4: AHD vs. EXP: $\chi^2_7 = 100.534$, $p < 0.00001$; AHD vs. FLK-Zinj: $\chi^2_7 = 70.192$, $p < 0.00001$; FLK-NN2 vs. EXP: $\chi^2_5 = 64.996$, $p < 0.00001$; FLK-NN2 vs. FLK-Zinj: $\chi^2_7 = 43.631$, $p < 0.00001$; size class 1-4: AHD vs. EXP: $\chi^2_7 = 118.042$, $p < 0.00001$; AHD vs. FLK-Zinj: $\chi^2_7 = 90.295$, $p < 0.00001$; FLK-NN2 vs. EXP: $\chi^2_7 = 64.996$, $p < 0.00001$; FLK-NN2 vs. FLK-Zinj: $\chi^2_7 = 50.892$, $p < 0.00001$). The LDPT frequencies for the total size class 1-2 AHD and FLK-Zinj while not significantly different, are nearly so ($\chi^2_5 = 10.926$, $p = 0.0529$). The EXP and FLK-Zinj LDPT frequencies are significantly different (size class 3-4: $\chi^2_7 = 20.419$, $p = 0.0047$; size class 1-4: $\chi^2_7 = 20.574$, $p = 0.0045$). Finally, as is evident in Table 5.6 and Figure 5.5, this pattern is not due to gross differences in LDPT frequencies on specific elements. Rather, the LDPT frequencies of all elements are always greater in the EXP and FLK-Zinj assemblages compared to AHD and FLK-NN2.

For size class 1-4 elements, the 95% confidence intervals for the AHD and FLK-NN2 LDPT means overlap, but rarely overlap with those of FLK-Zinj or EXP (Fig. 5.5c). Statistical analysis provided in Table 5.8 confirms this pattern. Note, for example, that for all size class 3-4 and the combined size class 1-4 limbs there is no difference in the number

Table 5.8. Probabilities (χ^2) for difference in assemblage loadpoint frequencies (excluding isolated loadmarks). Significant differences (at 0.05) are in bold. Those approaching significance are in italics. Abbreviations given in Table 3.1.

	SITE / ELEMENT	EXP	FLK-NN2	FLK-ZINJ
<i>S_zCIs 1-2</i>	AHD			
	HUM	-	-	0.1057
	RAD	-	-	0.2039
	ULN	-	-	0.2482
	MCM	-	-	0.6351
	FEM	-	-	-
	TIB	-	-	0.2178
	MTM	-	-	0.8787
	METM	-	-	-
	LBSF	-	-	-
	<i>Total - No LBSF/ULN</i>	-	-	<i>0.0529</i>
<i>Total</i>	-	-	0.1563	
<i>S_zCIs 3-4</i>	AHD			
	HUM	0.0017	0.2359	0.0004
	RAD	0.0006	0.7345	0.0005
	ULN	0.7363	0.1074	0.2691
	MCM	-	0.9283	0.0351
	FEM	0.0216	0.1404	0.1127
	TIB	<0.0001	0.5077	0.0015
	MTM	-	-	0.0702
	METM	-	-	0.8920
	LBSF	<0.0001	0.7146	<0.0001
	<i>Total - No LBSF/ULN</i>	<0.0001	0.4537	<0.0001
<i>Total</i>	<0.0001	0.6483	<0.0001	
<i>S_zCIs 3-4</i>	EXP			
	HUM	-	0.0015	0.0820
	RAD	-	0.1489	0.2427
	ULN	-	0.2818	0.3384
	MCM	-	-	-
	FEM	-	0.0080	0.1598
	TIB	-	0.0003	0.0999
	MTM	-	-	-
	METM	-	-	-
	LBSF	-	0.0795	<i>0.0564</i>
	<i>Total - No LBSF/ULN</i>	-	<0.0001	0.0047
<i>Total</i>	-	<0.0001	0.0067	
<i>S_zCIs 3-4</i>	FLK-NN2			
	HUM	-	-	0.0003
	RAD	-	-	0.3279
	ULN	-	-	0.3962
	MCM	-	-	0.2928
	FEM	-	-	<i>0.0521</i>
	TIB	-	-	0.0362
	MTM	-	-	0.1806
	METM	-	-	-
	LBSF	-	-	0.5713
	<i>Total - No LBSF/ULN</i>	-	-	<0.0001
<i>Total</i>	-	-	0.0014	

Table 5.8. continued.

		EXP	FLK-NN2	FLK-ZINJ
SzCls 1-4	AHD			
	HUM	0.0015	0.1638	<0.0001
	RAD	0.0004	0.7486	<0.0001
	ULN	0.6983	0.1653	0.6642
	MCM	-	0.9266	0.0068
	FEM	0.0216	0.1404	0.0658
	TIB	<0.0001	0.5748	0.0006
	MTM	-	0.5139	0.1578
	METM	-	-	0.4716
	LBSF	<0.0001	0.7146	<0.0001
	<i>Total - No LBSF/ULN</i>	<0.0001	0.4937	<0.0001
	<i>Total</i>	<0.0001	0.7397	<0.0001
EXP				
HUM	-	0.0015	0.0325	
RAD	-	0.1489	0.0604	
ULN	-	0.2818	0.3679	
MCM	-	-	-	
FEM	-	0.0080	0.1617	
TIB	-	0.0003	0.0981	
MTM	-	-	-	
METM	-	-	-	
LBSF	-	0.0795	0.0559	
<i>Total - No LBSF/ULN</i>	-	<0.0001	0.0045	
<i>Total</i>	-	<0.0001	0.0244	
FLK-NN2				
HUM	-	-	0.0002	
RAD	-	-	0.3354	
ULN	-	-	0.2801	
MCM	-	-	0.2294	
FEM	-	-	0.0192	
TIB	-	-	0.0286	
MTM	-	-	0.0962	
METM	-	-	-	
LBSF	-	-	0.5705	
<i>Total - No LBSF/ULN</i>	-	-	<0.0001	
<i>Total</i>	-	-	0.0002	

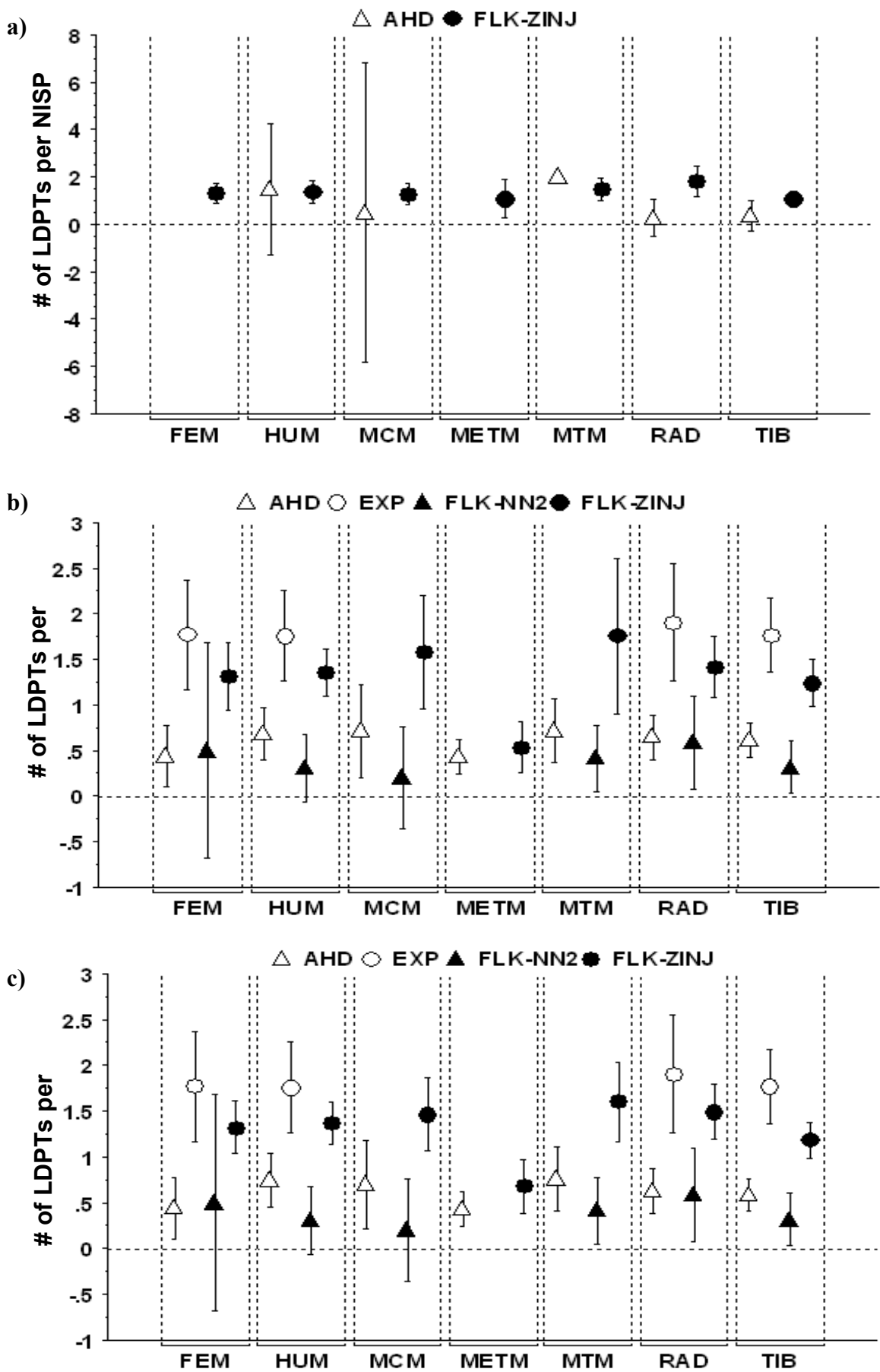


Fig. 5.5. Point plot of mean number of loadpoints (LDPTs) per element, excluding isolated loadmarks (LMRKs) for size class (a) 1-2, (b) 3-4, and (c) 1-4 specimens. Bars indicate 95% confidence intervals.

of LDPTs per specimen in the AHD and FLK-NN2 assemblages (size class 3-4: $\chi^2_6 = 5.733$, $p = 0.4537$; size class 1-4: $\chi^2_7 = 5.399$, $p = 0.4937$). Similarly, the size class 3-4 EXP and FLK-Zinj limb elements do not display statistically different LDPT frequencies although the overall frequencies are significantly different ($\chi^2_7 = 20.419$, $p < 0.0001$). Only the EXP size class 1-4 humerii display a statistically greater number of LDPTs per NISP than observed in the FLK-Zinj assemblage ($\chi^2_5 = 12.172$, $p = 0.0325$), but again the overall frequencies are significantly different ($\chi^2_7 = 20.574$, $p, 0.0045$)

Regardless of the sample or sub-sample considered (all specimens, size class 1-2, 3-4, 1-4 or 0-4, with or without isolated LMRKs, LBSFs, or ulnae) show the same pattern, i.e., the AHD and FLK-NN2 assemblages display significantly fewer LDPTs per specimen than the EXP and FLK-Zinj assemblages. As argued above, however, the most conservative sample is that which excludes isolated LMRKs, LBSFs, and the ulnae. This is the sample used in most of the following analyses.

5.3.2 LDPT Types

For each assemblage, Table 5.9 shows the frequency with which each type of LDPT occurs on each skeletal part (expressed as both the number of LDPTs per NISP and as a percentage of the total number of LDPTs), for each specimen for which a size class can be determined (size class 1-2 and 3-4), as well as a combined frequency for both large and small animals (size class 1-4). In all assemblages, larger sized animals dominate, and the whole assemblage results are only slightly moderated by the inclusion of the smaller sized animal bones. Figure 5.6 shows the number of each LDPT type per NISP with their 95% confidence intervals by size class for each assemblage.

The AHD size class 3-4 specimens are dominated by three LDPT types (Table 5.9): 0.208% of all specimens are comprised of those that display a flake scar, notch, and load mark (FLKS+NTCH+LMRK), 23.6% display a flake scar and notch (FLKS+NTCH), and 11.1% are comprised of those that exhibit a flake scar and load mark (FLKS+LMRK). As

Table 5.9. Number of loadpoint (LDPT) types per number of identified specimens (NISP) and percentage of the total number of LDPTs for all specimens (excluding shaft fragments, the ulna and those with only an isolated LMRK). LDPT frequencies and NISP values are given in Table 5.5. Loadpoint type abbreviations given in Table 3.1.

		AHD		FLK- NN2		EXP		FLK-Zinj	
		#/ NISP	% LDPTs	#/ NISP	% LDPTs	#/ NISP	% LDPTs	#/ NISP	% LDPTs
SzCIs 1-2	FLKS	0.000	0.0	—	—	—	—	0.248	18.6
	FLKO	0.000	0.0	—	—	—	—	0.106	7.9
	FRFE	0.000	0.0	—	—	—	—	0.130	9.8
	NTCH	0.000	0.0	—	—	—	—	0.025	1.9
	FLKS+NTCH	0.053	7.7	—	—	—	—	0.255	19.1
	FLKS+LMRK	0.053	7.7	—	—	—	—	0.149	11.2
	FLKS+NTCH+LMRK	0.579	84.6	—	—	—	—	0.224	16.7
	FLKO+NTCH	0.000	0.0	—	—	—	—	0.019	1.4
	FLKO+LMRK	0.000	0.0	—	—	—	—	0.068	5.1
	FLKO+NTCH+LMRK	0.000	0.0	—	—	—	—	0.037	2.8
	FRFE+NTCH	0.000	0.0	—	—	—	—	0.012	0.9
	FRFE+LMRK	0.000	0.0	—	—	—	—	0.050	3.7
	FRFE+NTCH+LMRK	0.000	0.0	—	—	—	—	0.000	0.0
	NTCH+LMRK	0.000	0.0	—	—	—	—	0.012	0.9
SzCIs 3-4	FLKS	0.054	8.8	0.039	10.0	0.211	11.7	0.175	13.6
	FLKO	0.020	3.2	0.000	0.0	0.126	7.0	0.144	11.2
	FRFE	0.014	2.3	0.013	3.3	0.211	11.7	0.131	10.1
	NTCH	0.017	2.8	0.000	0.0	0.000	0.0	0.017	1.3
	FLKS+NTCH	0.144	23.6	0.156	40.0	0.126	7.0	0.222	17.2
	FLKS+LMRK	0.068	11.1	0.065	16.7	0.316	17.5	0.158	12.3
	FLKS+NTCH+LMRK	0.208	34.3	0.104	26.7	0.200	11.1	0.194	15.1
	FLKO+NTCH	0.000	0.0	0.000	0.0	0.000	0.0	0.014	1.1
	FLKO+LMRK	0.000	0.0	0.000	0.0	0.337	18.7	0.103	8.0
	FLKO+NTCH+LMRK	0.000	0.0	0.000	0.0	0.011	0.6	0.019	1.5
	FRFE+NTCH	0.008	1.4	0.000	0.0	0.000	0.0	0.017	1.3
	FRFE+LMRK	0.025	4.2	0.000	0.0	0.263	14.6	0.083	6.5
	FRFE+NTCH+LMRK	0.003	0.5	0.000	0.0	0.000	0.0	0.003	0.2
	NTCH+LMRK	0.048	7.9	0.013	3.3	0.000	0.0	0.008	0.6
SzCIs 1-4	FLKS	0.051	8.3	0.039	10.0	0.211	11.7	0.198	15.2
	FLKO	0.019	3.1	0.000	0.0	0.126	7.0	0.132	10.2
	FRFE	0.013	2.2	0.013	3.3	0.211	11.7	0.131	10.0
	NTCH	0.016	2.6	0.000	0.0	0.000	0.0	0.019	1.5
	FLKS+NTCH	0.139	22.7	0.156	40.0	0.126	7.0	0.232	17.8
	FLKS+LMRK	0.067	10.9	0.065	16.7	0.316	17.5	0.155	11.9
	FLKS+NTCH+LMRK	0.227	37.1	0.104	26.7	0.200	11.1	0.203	15.6
	FLKO+NTCH	0.000	0.0	0.000	0.0	0.000	0.0	0.015	1.2
	FLKO+LMRK	0.000	0.0	0.000	0.0	0.337	18.7	0.092	7.1
	FLKO+NTCH+LMRK	0.000	0.0	0.000	0.0	0.011	0.6	0.025	1.9
	FRFE+NTCH	0.008	1.3	0.000	0.0	0.000	0.0	0.015	1.2
	FRFE+LMRK	0.024	3.9	0.000	0.0	0.263	14.6	0.073	5.6
	FRFE+NTCH+LMRK	0.003	0.4	0.000	0.0	0.000	0.0	0.002	0.1
	NTCH+LMRK	0.045	7.4	0.013	3.3	0.000	0.0	0.010	0.7

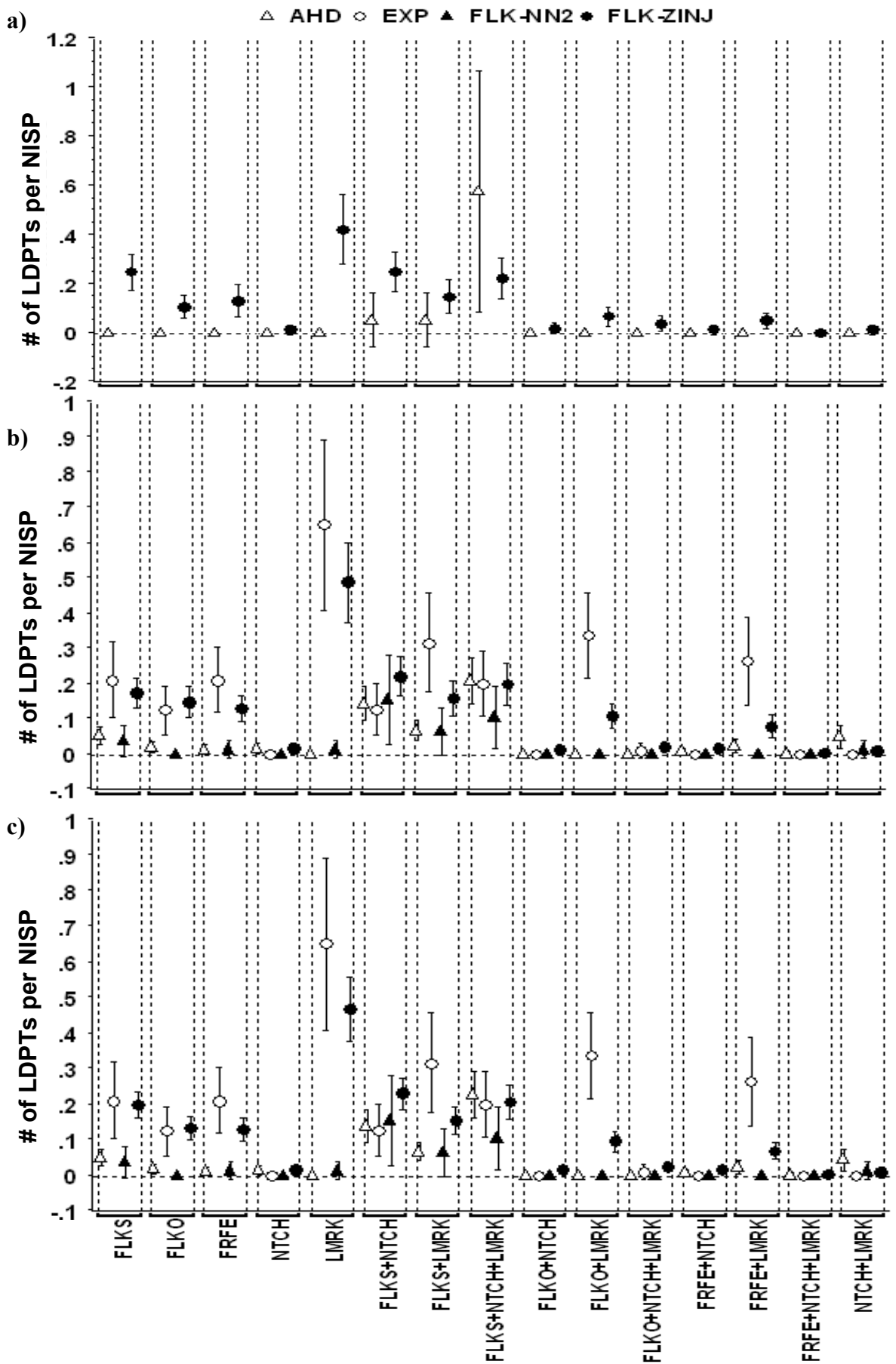


Fig. 5.6. Point plot of the mean number of loadpoint (LDPTs) types per number of identified specimens (NISP) for (a) size class 1-2, (b) size class 3-4, and (c) size class 1-4 specimens (except long bone shaft fragments and the ulnae). Bars represent 95% confidence intervals. Loadpoint type abbreviations given in Table 3.1.

the frequency of smaller animal bones is quite low, the proportions for the size class 1-4 material are nearly the same: The FLKS+NTCH+LMRK type comprise 37.1%, the FLKS+NTCH type 22.7%, and the FLKS+LMRK type 10.9% of all observed LDPTs. For the entire assemblage, only two of the other 11 types comprise more than 7% of the LDPTs (FLKS, 8.3%; NTCH+LMRK, 7.4%). Nine types were very uncommon: FRFE+LMRK = 3.9%, FLKO = 3.1%, NTCH = 2.6%, FRFE = 2.2%, FRFE+NTCH = 1.3%, and FRFE+NTCH+LMRK = 0.4%. Three LDPT types, FLKO+NTCH, FLKO+LMRK, and FLKO+NTCH+LMRK were not observed in the AHD assemblage.

The proportions of the various LDPT types are largely the same for the FLK-NN2 assemblage. Size class 1-4 specimens are dominated by three LDPT types: 40.0% of all LDPTs are comprised of those that display flake scar and notch (FLKS+NTCH), 26.7% display a flake scar, notch, and load mark (FLKS+NTCH+LMRK), and 16.7% are comprised of those that exhibit a flake scar associated with a load mark (FLKS+LMRK). Only three other types are present in the FLK-NN2 assemblage, FLKS (10%), FRFE (3.3%), and NTCH+LMRK (3.3%). Eight types were not observed, notably of those with a FLKO.

The percentage LDPT types are more evenly distributed in the EXP limb specimens compared to the AHD and FLK-NN2 assemblages. Six types comprise more than 10% of all observed LDPTs (Table 5.9): FLKO+LMRK = 18.7%; FLKS+LMRK = 17.5%; FRFE+LMRK = 14.6%; FLKS = 11.7%; FRFE = 11.7%; FLKS+NTCH+LMRK = 11.1%. The FLKO and FLKS+NTCH types both contributed 7.0% to the LDPT total while FLKO+NTCH+LMRK represent 0.6% of all observed LDPTs. Five types were not observed in the EXP assemblage, NTCH, FLKO+NTCH, FRFE+NTCH, FRFE+NTCH+LMRK, and NTCH+LMRK.

Like the EXP assemblage, the size class 1-4 FLK-Zinj LDPT types are more evenly distributed with six types contributing more than 10% to the LDPT total: FLK+NTCH = 17.8%; FLK+NTCH+LMRK = 15.6%; FLKS = 15.2%; FLKS+LMRK = 11.9%; FLKO =

10.2%; FRFE = 10.0%. Only two of the remaining eight LDPT types have percentages greater than 5%, FLKO+LMRK (7.1%) and FRFE+LMRK (5.9%). Six LDPT types contributed less than 2% to the total number of LDPTS. The LDPT type proportions are largely the same for the size class 3-4 material, but are slightly more variable in the size class 1-2 material.

Considering the size class 1-4 material, there are several patterns in these data. First, as indicated above, while a few LDPT types (i.e., FLKS+NTCH+LMRK, FLKS+NTCH, and FLKS+LMRK) dominate the AHD and FLK-NN2 assemblages, other types contribute significantly to total number of LDPTs observed in the EXP and FLK-Zinj assemblages. The second pattern in LDPT type frequencies is the complete or near absence of LDPT exhibiting a FLKO component in both the AHD (3.1%) and FLK-NN2 (0.0%) assemblages compared to those for the EXP (26.3%) and FLK-Zinj (20.3%). Thirdly, like types with a FLKO component, those with defined on the basis of fracture features (FRFE), comprise much greater proportions in the EXP (26.3%) and FLK-Zinj (16.9%) assemblages than in either AHD (7.9%) or FLK-NN2 (3.3%). These patterns are also seen when the frequencies of each LDPT type per assemblage NISP are plotted with their 95% confidence intervals (Fig. 5.6). LDPT types FLKO, FRFE, FLKO+LMRK and FRFE+LMRK are more frequently observed on EXP and FLK-Zinj specimens than on the AHD and FLK-NN2 specimens and their 95% confidence intervals do not overlap.

To test if these differences in the frequencies (% NISP) of 14 LDPT types between the assemblages are significant, χ^2 tests were performed (Table 5.10). Comparisons of the LDPT frequencies for AHD and FLK-Zinj size class 1-2 material are hampered by low AHD sample size. Thus, while Figure 5.6a shows that the 95% confidence intervals of the frequency of FLKS, FLKO, FRFE, LMRK, and FLKS+NTCH types per NISP do not overlap, none are significantly different and only the FLKS means approach a statistically significant difference (Table 10; $\chi^2_{7} = 5.6845$, $p = 0.0583$). The FLKS+NTCH+LMRK

Table 5.10. Chi-square probabilities (upper cell value), values (middle cell value), and degrees of freedom (lower cell value) for difference in loadpoint type frequencies between assemblages (excluding longbone shaft fragments and the ulna, and specimens with only an isolated loadmark). Significant differences (at 0.05) are in bold. Those approaching significance are in italics.

	<i>SzCls 1-2</i>	<i>SzCls 3-4</i>			<i>SzCls 1-4</i>			
	FLK-ZINJ	EXP	FLK-NN2	FLK-ZINJ	EXP	FLK-NN2	FLK-ZINJ	
<i>FLKS</i>	AHD	0.0583 5.6845 2	0.0006 17.4940 3	0.8458 0.3350 2	<0.0001 23.0642 2	0.0003 19.0104 3	0.8727 0.2722 2	<0.0001 36.3378 2
	EXP	-	-	0.0547 7.6131 3	0.2508 4.1008 3	-	0.0547 7.6131 3	0.0942 6.3883 3
	FLK-NN2	-	-	-	0.0186 7.9711 2	-	-	0.0058 10.3140 2
	AHD	0.1366 2.2154 1	<0.0001 21.0585 1	0.2141 1.5433 1	<0.0001 32.6995 3	<0.0001 22.5642 1	0.2263 1.4639 1	<0.0001 33.2171 3
	EXP	-	-	0.0012 10.4558 1	0.8502 0.7970 3	-	0.0012 10.4558 1	0.9003 0.5830 3
	FLK-NN2	-	-	-	0.0092 11.5335 3	-	-	0.013 10.7781 3
<i>FRFE</i>	AHD	0.5575 2.0724 3	<0.0001 48.1567 2	0.9405 0.0057 1	<0.0001 32.8300 2	<0.0001 51.0196 2	0.9787 0.0007 1	<0.0001 33.6563 3
	EXP	-	-	0.0012 13.5060 2	0.1336 4.0263 2	-	0.0012 13.5060 2	0.2048 4.5849 3
	FLK-NN2	-	-	-	0.0166 8.2012 2	-	-	<i>0.0535</i> 7.6618 3
	AHD	0.6252 0.2387 1	0.2021 1.6273 1	0.2506 1.3197 1	0.4926 1.4162 2	0.2141 1.5438 1	0.2632 1.2519 1	0.5910 1.0520 2
	EXP	-	-	-	0.5132 1.3341 2	-	-	0.5244 1.2911 2
	FLK-NN2	-	-	-	0.5822 1.0818 2	-	-	0.5925 1.0468 2
<i>LMRK (isolated)</i>	AHD	0.3381 5.6845 5	<0.0001 118.924 5	0.2334 1.4202 1	<0.0001 100.931 7	<0.0001 125.008 5	0.2149 1.5383 1	<0.0001 106.201 7
	EXP	-	-	<0.0001 27.6982 5	0.3029 9.4865 8	-	<0.0001 27.6982 5	0.1135 12.9512 8
	FLK-NN2	-	-	-	0.0022 22.3403 7	-	-	0.0025 21.9969 7

Table 5.10. continued.

	<i>SzCls 1-2</i>		<i>SzCls 3-4</i>		<i>SzCls 1-4</i>			
	FLK-ZINJ	EXP	FLK-NN2	FLK-ZINJ	EXP	FLK-NN2	FLK-ZINJ	
<i>FLKS +NTCH</i>	AHD	0.2310 2.9307 2	0.6056 1.8430 3	0.2484 5.4033 4	0.2259 5.6611 4	0.6128 1.8097 3	0.2346 5.5588 4	0.0320 10.5567 4
	EXP	-	-	0.6584 1.6044 3	0.5912 2.8034 4	-	0.6584 1.6044 3	0.5126 3.2769 4
	FLK-NN2	-	-	-	0.3650 4.3151 4	-	-	0.1782 6.2942 4
		-	-	-	-	-	-	-
<i>FLKS +LMRK</i>	AHD	0.8332 0.8679 3	< 0.0001 28.5975 4	0.3672 2.0037 2	0.0054 12.6637 3	< 0.0001 29.9021 4	0.3492 2.1042 2	0.006 12.4629 3
	EXP	-	-	0.0261 11.0372 4	0.0044 15.1420 4	-	0.0261 11.0372 4	0.0029 16.1276 4
	FLK-NN2	-	-	-	0.4482 2.6534 3	-	-	0.4234 2.8004 3
		-	-	-	-	-	-	-
<i>FLKS +NTCH +LMRK</i>	AHD	0.0209 11.5655 4	0.7891 2.4158 5	0.4994 4.3560 5	0.7013 2.9915 5	0.9032 2.1718 6	0.5461 4.9818 6	0.5718 4.7843 6
	EXP	-	-	0.0877 4.8669 2	0.7814 1.7512 4	-	0.0877 4.8669 2	0.7879 1.7154 4
	FLK-NN2	-	-	-	0.5024 3.3413 4	-	-	0.4283 3.8386 4
		-	-	-	-	-	-	-
<i>FLKO +NTCH</i>	AHD	0.5485 0.3600 1	-	-	0.0259 4.9653 1	-	-	0.0161 5.7946 1
	EXP	-	-	-	0.2481 1.3341 1	-	-	0.2241 1.4779 1
	FLK-NN2	-	-	-	0.2983 1.0818 1	-	-	0.2736 1.1984 1
		-	-	-	-	-	-	-
<i>FLKO +LMRK</i>	AHD	0.2397 1.3826 1	< 0.0001 107.335 3	-	< 0.0001 37.3822 2	< 0.0001 112.788 3	-	< 0.0001 35.6089 2
	EXP	-	-	< 0.0001 25.9592 3	< 0.0001 23.6516 3	-	< 0.0001 25.9592 3	< 0.0001 32.7815 3
	FLK-NN2	-	-	-	0.0151 8.3913 2	-	-	0.0231 7.5388 2
		-	-	-	-	-	-	-
<i>FLKO +NTCH +LMRK</i>	AHD	0.3921 0.7325 1	0.0530 3.7452 1	-	0.0083 6.9710 1	0.0470 3.9453 1	-	0.0021 9.4696 1
	EXP	-	-	0.3666 0.8153 1	0.5563 0.3461 1	-	0.3666 0.8153 1	0.3856 0.7528 1
	FLK-NN2	-	-	-	0.2174 1.5216 1	-	-	0.1611 1.9640 1
		-	-	-	-	-	-	-

Table 5.10. continued.

	<i>SzCls 1-2</i>		<i>SzCls 3-4</i>			<i>SzCls 1-4</i>		
	FLK-ZINJ	EXP	FLK-NN2	FLK-ZINJ	EXP	FLK-NN2	FLK-ZINJ	
FRFE +NTCH	AHD	0.6252 0.2387 1	0.3687 0.8082 1	0.4182 0.6553 1	0.3245 0.9707 1	0.3812 0.7669 1	0.4304 0.6218 1	0.326 0.9646 1
	EXP	-	-	-	0.2053 1.6045 1	-	-	0.2241 1.4779 1
	FLK-NN2	-	-	-	0.2540 1.3012 1	-	-	0.2736 1.1984 1
	AHD	0.3202 0.9880 1	<0.0001 38.6287 2	0.4131 1.7680 2	0.0166 8.2019 2	<0.0001 41.0654 2	0.4324 1.6768 2	0.0168 8.1710 2
	EXP	-	-	0.0005 15.2902 2	0.0001 18.0809 2	-	0.0005 15.2902 2	<0.0001 27.6127 2
	FLK-NN2	-	-	-	0.0662 5.4316 2	-	-	0.0822 4.9968 2
FRFE +NTCH +LMRK	AHD	-	0.6045 0.2682 1	0.641 0.2174 1	0.9921 0.0001 1	0.6139 0.2546 1	0.6497 0.2063 1	0.8136 0.0556 1
	EXP	-	-	-	0.6071 0.2645 1	-	-	0.6691 0.1826 1
	FLK-NN2	-	-	-	0.6434 0.2144 1	-	-	0.7004 0.1480 1
	AHD	0.6252 0.2387 1	0.347 3.29927 3	0.7928 1.0348 3	0.1109 6.0146 3	0.3723 3.1282 3	0.818 0.9308 3	0.0816 6.7151 3
	EXP	-	-	0.2653 1.2410 1	0.3720 0.7969 1	-	0.2653 1.2410 1	0.3377 0.9192 1
	FLK-NN2	-	-	-	0.6971 0.1515 1	-	-	0.7805 0.0776 1

LDPT type is significantly more frequent in the AHD size class 1-2 material ($\chi^2 = 11.5655$, $p = 0.0209$), although the 95% confidence intervals overlap considerably with those of FLK-Zinj.

In contrast, the size class 3-4 and 1-4 LDPT type frequencies indicate that the AHD and FLK-NN2 assemblages are more similar to each other than they are to the EXP and FLK-Zinj assemblages, which are in turn similar. For example, the 95% confidence intervals for all AHD and FLK-NN2 LDPT types for both size class 3-4 and 1-4 material overlap and for no LDPT type are the frequencies significantly different (Fig. 5.6, Table

5.10). Likewise, the EXP and FLK-Zinj material are not significantly different. Only the FLKS+LMRK, FLKO+LMRK, and FRFE+LMRK means are significantly different (size class 3-4: $\chi^2_3 = 15.1420$, $p = 0.0044$; $\chi^2_3 = 23.6516$, $p < 0.0001$; $\chi^2_2 = 08.0809$, $p < 0.0001$; size class 1-4: $\chi^2_4 = 16.1276$, $p = 0.0029$; $\chi^2_4 = 32.7815$, $p < 0.0001$; $\chi^2_4 = 26.6127$, $p < 0.0001$, respectively), but only for the FLKO+LMRK and FRFE+LMRK LDPT types do the 95% confidence intervals not overlap. Again, χ^2 test shows all of these LDPT means (comparing EXP vs. AHD, EXP vs. FLK-NN2, FLK-Zinj vs. AHD, and FLK-Zinj vs. FLK-NN2) are significantly different or nearly so, usually with p values of <0.0001 . Similarly, most of the other LDPT types with FLKO and FRFE component (i.e., FLKO+NTCH, FLKO+NTCH+LMRK, FRFE+NTCH, and FRFE+NTCH+LMRK) frequencies are low in the AHD (0.004 and 0.016, respectively) and FLK-NN2 (0.000 and 0.000, respectively) assemblages. In contrast the frequencies of LDPTs with FLKO and FRFE components are higher in EXP (0.000 and 0.135, respectively) and FLK-Zinj (0.015 and 0.042, respectively).

In summary, the AHD and FLK-NN2 assemblages show more similarities to each other and numerous statistically significant differences with the EXP and FLK-Zinj assemblages that are, in turn, rather similar. Considering all size class 3-4 and 1-4 pairwise χ^2 comparisons, for example, none of the 21 AHD vs. FLK-NN2 LDPT types display a significant difference, while only six of the 28 pairwise comparisons of the EXP and FLK-Zinj LDPT types display a significant difference. In contrast, 17 of the 28 AHD vs. FLK-Zinj LDPT frequency comparisons and 13 of 26 AHD vs. EXP LDPT frequencies are significantly different. Seven of the 28 FLK-NN2 vs. FLK-Zinj and 12 of the 18 EXP vs. FLK-NN2 frequency comparisons are statistically different. Further, there is patterning in of specific types of LDPTs frequencies in AHD and FLK-NN2 compared to EXP and FLK-Zinj, with a few LDPT types being absent or nearly so in the AHD and FLK-NN2 while often comprising a significant proportion of the LDPTs in the EXP and FLK-Zinj

assemblages. Specifically, LDPTs with FLKO or FRFE components are typically absent or occur in very low frequencies in the ADH and FLK-NN2, but occur frequently in the EXP and FLK-Zinj assemblages. In the AHD assemblage, for example, the FLKO+NTCH, FLKO+LMRK, FLKO+NTCH+LMRK, and FRFE+NTCH+LMRK types were not observed or were observed only once and just seven specimens displayed isolated FLKOs. The FLK-NN2 assemblage lacks any specimens with a FLKO component and only one bone displays a FRFE LDPT. In the size class 3-4 sample the frequencies of LDPT types FLKO, FRFE, FLKO+LMRK, and FRFE+LMRK (Table 5.10) are 3 to 16 times greater in EXP (0.126, 0.211, 0.337, 0.263, respectively) and FLK-Zinj (0.147, 0.128, 0.108, 0.078, respectively) compared to AHD (0.020, 0.014, 0.000, 0.025, respectively) and FLK-NN2 (0.000, 0.013, 0.000, 0.000, respectively).

Given the lack or very low frequencies of certain LDPT types, the number of types was reduced to better assess between-assemblage differences in the frequencies the main LDPT components, FLKS, FLKO, FRFE, and NTCH. Treating FLKS, FLKO, FRFE, and NTCH as the main LDPT components and summing their frequencies clarifies differences in the LDPT types in the AHD and FLK-NN2 assemblages compared to EXP and FLK-Zinj. For example, for three LDPTs, a FLKS, a FLKS+NTCH+LMRK, and a FRFE+NTCH on a femur would tally as 2 FLKSs, 2 NTCHs, and 1 FRFE. Table 5.11 lists the frequencies of FLKs, FLKOs, FRFEs, or NTCHs observed in each assemblage. Here the frequencies of each component are expressed as the number per NISP, the number per NISP with a LDPT, and the percentage of the total number LDPTs. The frequency of each LDPT component per the number of specimens with a LDPT (columns 9, 13, 17, and 21 in Table 5.11), their ranges, standard errors, and standard deviations are given in Table 5.12. The frequencies of LDPT components (per specimens with a LDPTS) with their 95% confidence intervals are given in Figure 5.7. Chi-square probabilities for the LDPT type frequency comparisons are shown in Table 5.13.

In terms of their contribution to the total number of LDPTs in the size class 3-4 sample (Table 5.12, Fig. 5.7), the FLKS and NTCHs dominate the AHD (77.8% and 70.3% of all LDPTs, respectively) and FLK-NN2 (93.3% and 70.1%, respectively, or 1.28 and 1.40 FLKS per specimen with a LDPT, Table 5.12) limb material. The FLKS type also dominates the EXP and FLK-Zinj size class 3-4 material (47.4% and 58.3%, or 1.01 and 1.15 FLKS per specimen with a LDPT, respectively) but at significantly lower proportions than in AHD or FLK-NN2 (Table 5.13; EXP vs. AHD: $\chi_1^2 = 38.4678$, $p < 0.0001$; EXP vs. FLK-NN2: $\chi_1^2 = 21.7246$, $p < 0.0001$; FLK-Zinj vs. AHD: $\chi_1^2 = 24.4773$, $p < 0.0001$; FLK-Zinj vs. FLK-NN2: $\chi_1^2 = 14.4784$, $p < 0.0001$). NTCH LDPTs are the second most frequent type in FLK-Zinj (38.5% of LDPTs, or 0.76 per specimen with a LDPT) but are the least frequent type in the EXP assemblage (18.7% or 0.40 per specimen with a LDPT). Both are significantly smaller than either the AHD or FLK-NN2 frequencies (FLK-Zinj vs. AHD: $\chi_1^2 = 59.9900$, $p < 0.0001$; FLK-Zinj vs. FLK-NN2: $\chi_1^2 = 11.6171$, $p = 0.0007$; EXP vs. AHD: $\chi_1^2 = 132.644$, $p < 0.0001$; EXP vs. FLK-NN2: $\chi_1^2 = 34.5766$, $p < 0.0001$). The greatest difference between the AHD and FLK-NN2 assemblages compared to the EXP and FLK-Zinj material is in the proportion of FLKO and FRFE LDPT types. The FLKO and FRFE types comprise negligible proportions in AHD (3.2% and 8.4%, or 0.05 and 0.05 per specimen with a LDPT, respectively) and FLK-NN2 (0.0% and 3.3%, or 0.0 and 0.05 per specimen with a LDPT, respectively) assemblages compared to the FLK-Zinj and EXP assemblages, which include a sizable number of FLKOs (22.4% and 26.3%, or 0.44 and 0.56 per specimen with a LDPT, respectively) and FRFEs (17.4% and 26.3%, or 0.34 and 0.56 per specimen with a LDPT, respectively) (Table 5.11, Fig. 5.7). The FLKO frequencies in the AHD and FLK-NN2 are significantly smaller than in EXP and FLK-Zinj (AHD vs. EXP: $\chi_1^2 = 43.6916$, $p < 0.0001$; AHD vs. FLK-Zinj: $\chi_1^2 = 39.5414$, $p = 0.0001$; FLK-NN2 vs. EXP: $\chi_1^2 = 10.1721$, $p = 0.0014$; FLK-NN2 vs. FLK-Zinj: $\chi_1^2 = 8.4943$, $p = 0.0036$). The FRFE frequencies in the AHD and FLK-NN2 are also significantly smaller

Table 5.11. Number of identified specimens (NISP, excluding ulna and long bone shaft fragments), total number of loadpoints (excluding isolated loadmarks), number of specimens with one or more loadpoint, and the FLKS, FLKO, FRFE, and NTCH frequencies for all size class 1-4 specimens identified to element.

	FLKS				FLKO				FRFE				NTCH							
	#	# per NISP	# per SPEC with LDPT	% of LDPTs	#	# per NISP	# per SPEC with LDPT	% of LDPTs	#	# per NISP	# per SPEC with LDPT	% of LDPTs	#	# per NISP	# per SPEC with LDPT	% of LDPTs				
				% NISP w/ LDPT				# of LDPTs per Spec. w/ LDPT												
AHD	1-2	19	13	8	0.68	1.63	42.1	1.63	13	0.68	1.63	100.0	0	—	—	—	12	0.63	1.50	92.4
	3-4	355	216	131	0.61	1.65	36.9	1.65	7	0.02	0.05	3.2	18	0.05	0.14	8.4	152	0.43	1.16	70.3
	Sum	374	229	139	0.61	1.65	37.2	1.65	7	0.02	0.05	3.1	18	0.05	0.13	7.8	164	0.44	1.18	71.7
FLK-NN2	1-2	0	—	—	—	—	—	—	—	—	—	—	—	—	—	—	—	—	—	—
	3-4	77	30	20	0.39	1.50	26.0	1.50	0	—	—	0.0	1	0.01	0.05	3.3	21	0.27	1.05	70.1
	Sum	77	30	20	0.39	1.50	26.0	1.50	0	—	—	0.0	1	0.01	0.05	3.3	21	0.27	1.05	70.1
EXP	1-2	0	—	—	—	—	—	—	—	—	—	—	—	—	—	—	—	—	—	—
	3-4	95	171	80	1.80	2.14	84.2	2.14	45	0.47	0.56	26.3	45	0.47	0.56	26.3	32	0.34	0.40	18.7
	Sum	95	171	80	1.80	2.14	84.2	2.14	45	0.47	0.56	26.3	45	0.47	0.56	26.3	32	0.34	0.40	18.7
FLK-Zinj	1-2	161	212	114	1.32	1.86	70.8	1.86	37	0.23	0.32	17.5	31	0.19	0.27	14.7	91	0.52	0.80	42.9
	3-4	360	465	236	1.29	1.97	65.6	1.97	104	0.29	0.44	22.4	81	0.23	0.34	17.4	179	0.50	0.76	38.5
	Sum	521	677	350	1.30	1.93	67.2	1.93	141	0.27	0.40	20.8	112	0.22	0.32	16.6	270	0.52	0.77	39.9

Table 5.12. Frequency of FLKS, FLKO, FRFE, and NTCH loading point components per specimen with one or more loading point.

			Count	Mean	Min.	Max.	Std. Dev.	Std. Error	
SzCls 1-2	FLKS	AHD	8	1.625	1	4	1.061	0.375	
		EXP	-	-	-	-	-	-	
		FLK-NN2	-	-	-	-	-	-	
		FLK-ZINJ	114	1.228	0	4	0.863	0.081	
	FLKO	AHD	8	0.000	0	0	0.000	0.000	
		EXP	-	-	-	-	-	-	
		FLK-NN2	-	-	-	-	-	-	
		FLK-ZINJ	114	0.325	0	2	0.540	0.051	
	FRFE	AHD	8	0.000	0	0	0.000	0.000	
		EXP	-	-	-	-	-	-	
		FLK-NN2	-	-	-	-	-	-	
		FLK-ZINJ	114	0.272	0	3	0.584	0.055	
	NTCH	AHD	8	1.500	1	4	1.069	0.378	
		EXP	-	-	-	-	-	-	
		FLK-NN2	-	-	-	-	-	-	
		FLK-ZINJ	114	0.798	0	3	0.843	0.079	
SzCls 3-4	FLKS	AHD	131	1.282	0	6	1.025	0.090	
		EXP	80	1.013	0	4	1.049	0.117	
		FLK-NN2	20	1.400	0	4	0.883	0.197	
		FLK-ZINJ	236	1.148	0	7	1.064	0.069	
	FLKO	AHD	131	0.053	0	1	0.226	0.020	
		EXP	80	0.563	0	3	0.672	0.075	
		FLK-NN2	20	0.000	0	0	0.000	0.000	
		FLK-ZINJ	236	0.441	0	4	0.672	0.044	
	FRFE	AHD	131	0.137	0	2	0.226	0.020	
		EXP	80	0.563	0	3	0.672	0.075	
		FLK-NN2	20	0.050	0	1	0.000	0.000	
		FLK-ZINJ	236	0.343	0	2	0.672	0.044	
	NTCH	AHD	131	1.160	0	6	1.044	0.091	
		EXP	80	0.400	0	2	0.587	0.066	
		FLK-NN2	20	1.050	0	4	0.945	0.211	
		FLK-ZINJ	236	0.758	0	6	0.979	0.064	
	SzCls 1-4	FLKS	AHD	139	1.302	0	6	1.026	0.087
			EXP	80	1.013	0	4	1.049	0.117
			FLK-NN2	20	1.400	0	4	0.883	0.197
			FLK-ZINJ	350	1.174	0	7	1.002	0.054
FLKO		AHD	139	0.050	0	1	0.219	0.019	
		EXP	80	0.563	0	3	0.672	0.075	
		FLK-NN2	20	0.000	0	0	0.000	0.000	
		FLK-ZINJ	350	0.403	0	4	0.634	0.034	
FRFE		AHD	139	0.129	0	2	0.358	0.030	
		EXP	80	0.563	0	3	0.793	0.089	
		FLK-NN2	20	0.050	0	1	0.224	0.050	
		FLK-ZINJ	350	0.320	0	3	0.567	0.030	
NTCH		AHD	139	1.180	0	6	1.044	0.089	
		EXP	80	0.400	0	2	0.587	0.066	
		FLK-NN2	20	1.050	0	4	0.945	0.211	
		FLK-ZINJ	350	0.771	0	6	0.936	0.050	

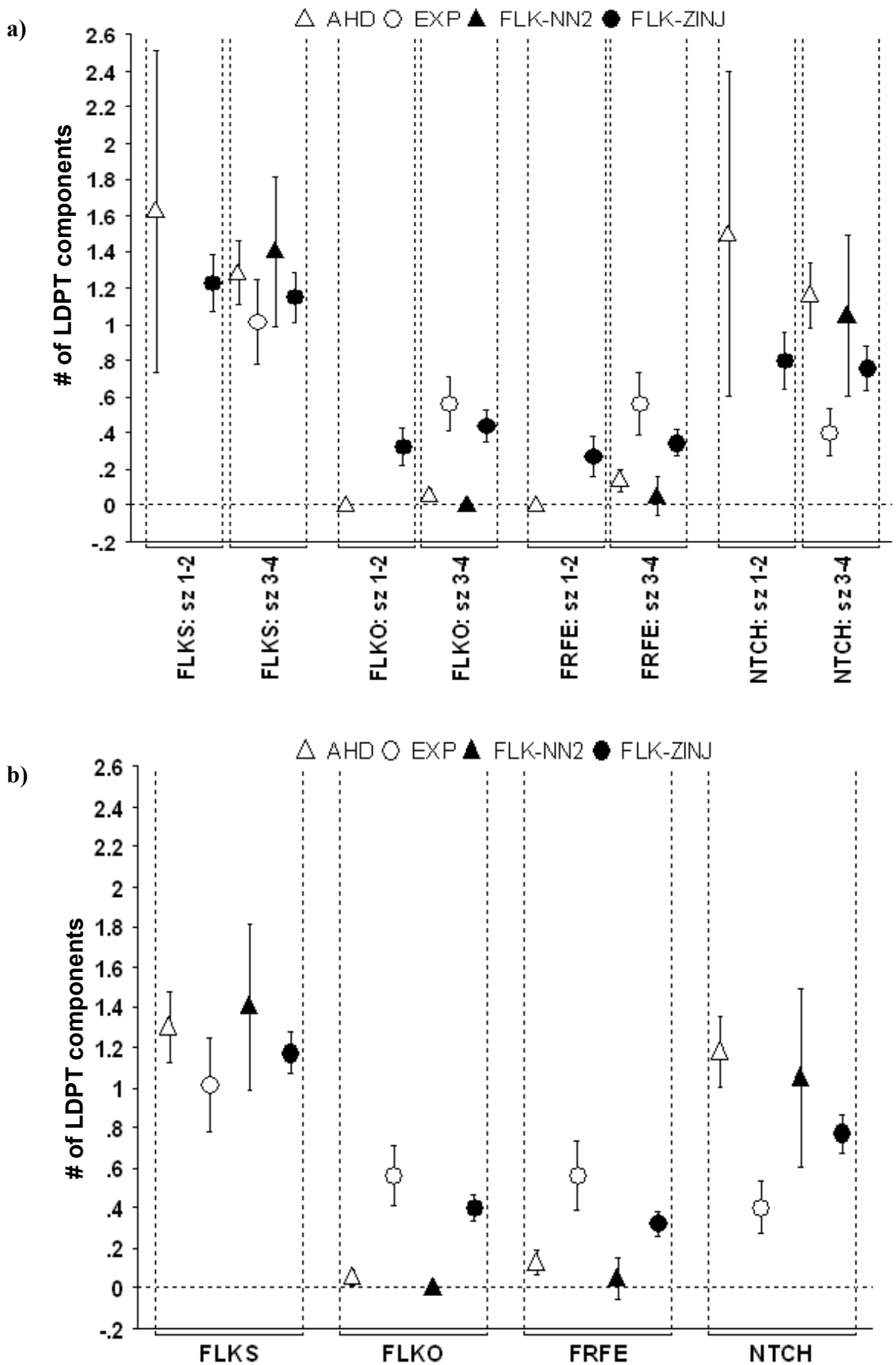


Fig. 5.7. Point plot of mean number of FLKSs, FLKOs, FRFEs, and NTCHs for size class (a) 1-2, 3-4, and (b) 1-4 specimens identified to element with one or more loadpoint. Bars indicated 95% confidence intervals.

Table 5.13. Chi-square (χ^2) probabilities (upper cell value) and values (lower cell value) for difference in loadpoint component frequencies (number of LDPTs with the component / number of LDPTs) between assemblages (excluding long bone shaft fragments and the ulna). Degrees of freedom for all tests is 1. Significant differences (at 0.05) are in bold. Those approaching significance are in italics.

		<i>SzCls 1-2</i>	<i>SzCls 3-4</i>			<i>SzCls 1-4</i>		
		FLK-ZINJ	EXP	FLK-NN2	FLK-ZINJ	EXP	FLK-NN2	FLK-ZINJ
<i>FLKS</i>	AHD	0.0108 6.4928	<0.0001 38.4678	0.0473 3.9360	<0.0001 24.4773	<0.0001 43.4532	0.0622 3.479	<0.0001 25.3887
	EXP	—		<0.0001 21.7246	0.0141 6.0226		<0.0001 21.7246	0.0016 9.9751
	FLK-NN2	—			0.0001 14.4784			0.0003 12.9901
<i>FLKO</i>	AHD	0.0994 2.7154	<0.0001 43.6916	0.3171 1.0007	0.0001 39.5414	<0.0001 46.8265	0.3316 0.9425	<0.0001 19.3681
	EXP	—		0.0014 10.1721	0.2971 1.0875		0.0014 10.1721	0.1212 2.4018
	FLK-NN2	—			0.0036 8.4943			0.0052 7.8047
<i>FRFE</i>	AHD	0.1376 2.2047	<0.0001 22.6451	0.3364 0.9240	0.0017 9.8004	<0.0001 25.1289	0.3712 0.7996	<0.0001 80.9201
	EXP	—		0.0057 7.6387	0.0126 6.2287		0.0057 7.6387	0.0033 8.6415
	FLK-NN2	—			0.0443 4.0457			<i>0.0533</i> 3.7332
<i>NTCH</i>	AHD	0.0005 12.0343	<0.0001 132.644	0.9668 0.0017	<0.0001 59.9900	<0.0001 109.636	0.8539 0.0339	<0.0001 69.0506
	EXP	—		<0.0001 34.5766	<0.0001 22.0668		<0.0001 34.5766	<0.0001 26.6782
	FLK-NN2	—			0.0007 11.6171			0.0010 10.7597

than either the EXP or FLK-Zinj assemblages (AHD vs. EXP: $\chi_1^2 = 22.6451$, $p < 0.0001$; FLK-NN2 vs. EXP: $\chi_1^2 = 7.6387$, $p = 0.0057$; AHD vs. FLK-Zinj: $\chi_1^2 = 9.8004$, $p = 0.0017$; FLK-NN2 vs. FLK-Zinj: $\chi_1^2 = 4.0457$, $p = .0443$). When both size classes (1-2 and 3-4) are combined (size class 1-4) there is little change in the proportions and the pattern remains that same – FLKO and FRFE LDPTs make a negligible contribution the total number of

LDPTS in the AHD and FLK-NN2 assemblages, but constitute a considerable proportion of the LDPTs observed in the EXP and FLK-Zinj limb material.

To summarize, all LDPT types in the AHD and EXP assemblages are significantly different with FLKS and NTCH types being more frequent in AHD than in EXP and the FLKO and FRFE being much more frequent in EXP than in AHD (Table 5.13). None of the AHD and FLK-NN2 type frequencies is significantly different. For AHD and FLK-Zinj pairwise comparisons, all but one (size class 1-4 FLKS) are significantly different where, as with the EXP assemblage, FLKS and NTCH types being more frequent in AHD than in FLK-Zinj and the FLKO and FRFE being much more frequent in FLK-Zinj than in AHD. None of the AHD and FLK-NN2 type frequencies is significantly different. Six of the eight FLK-NN2 vs. EXP LDPT type comparisons are significantly different with both the FLKO and FRFE LDPT types being significantly greater in the EXP assemblage while NTCHs are more frequent in FLK-NN2. Only the FLKS LDPT frequencies are not significantly different in the EXP and FLK-NN2 assemblages. Tests for differences in LDPT type frequencies between FLK-NN2 and FLK-Zinj show more mixed results. Only three of the eight frequencies are significantly different, i.e., both size class 3-4 and 1-4 FLKO frequencies are significantly greater in FLK-Zinj and the size class 1-4 NTCH frequencies are significantly greater in FLK-NN2. Thus, the frequencies of LDPT types in AHD and FLK-NN2 are clearly similar to each other but are usually significantly different from the frequencies observed in the EXP and FLK-Zinj assemblages which are in turn most similar to each other. The greater frequencies of FLKO and FRFE LDPTs in both the EXP and FLK-Zinj assemblages compared to the AHD and FLK-NN2 are notable.

This pattern is particularly clear when the mean LDPT type frequencies for all specimens identified to size class that display one or more LDPT are plotted with their 95% confidence intervals (Fig. 5.7a). Again, the mean number of FLKOs in the assemblages falls into two groups. The 95% confidence intervals of the low FLKO AHD and FLK-NN2 means overlap and are statistically similar ($\chi_1^2 = 0.9425$, $p = 0.3316$), but

neither overlap with the EXP and FLK-Zinj confidence intervals, whose means are not significantly different ($\chi^2_1 = 2.4018$, $p = 0.1212$). The pattern is the same for the FRFE means and confidence intervals. The pattern is largely the same for the size class 1-4 sample. Although the EXP and FLK-Zinj FLKO and FRFE means are significantly different for size class 1-4, their 95% confidence intervals clearly overlap (Fig. 5.7b).

That the FLKS, FLKO, FRFE, and NTCH LDPT component frequencies in the four assemblages form two distinct groups, with AHD and FLK-NN2 assemblages similar to each other but distinct from the EXP and FLK-Zinj assemblages, is clearly illustrated by principal component analysis (Figs. 5.8 and 5.9). Principal component analysis reduces a number of variables to a fewer number of components that can be plotted in 2-dimensions. Eigenvalues indicate the amount of variance accounted for by the components. Acceptable eigenvalues for the first two components are those that account for most variability in the data. The eigenvectors or bi-plot vectors (in this case FLKS, FLKO, FRFE, and NTCH) represent the original variable axes and show which variables create the most separation of the components. The eigenvectors are a visualization of the loadings. Loadings show just how much a particular variable influences a particular component. Eigenvectors are useful in determining how the variables interact to create the observed data distribution.

Here PCA is used to visually summarize the above analyses in a single graph. The AHD and FLK-NN2 LDPT assemblages characterized by high frequencies of FLKS and NTCH components show considerable overlap, but do not overlap with the EXP and FLK-Zinj assemblages characterized by lesser proportions of LDPTs with FLKS and NTCH components, but significant number of FLKO and FRFE LDPT types. Principal components (PC) 1 and 2 explain 72.6 and 13.5% of the variability, respectively, and the correlations for the LDPT types are clearly patterned with highly positive correlations for PC 1 FLKO and FRFE LDPT components that comprise the bulk of the EXP and FLK-Zinj LDPT types, and highly negative correlations for NTCH LDPT types that form a significant proportion of the AHD and FLK-NN2 LDPTs (Fig. 5.9).

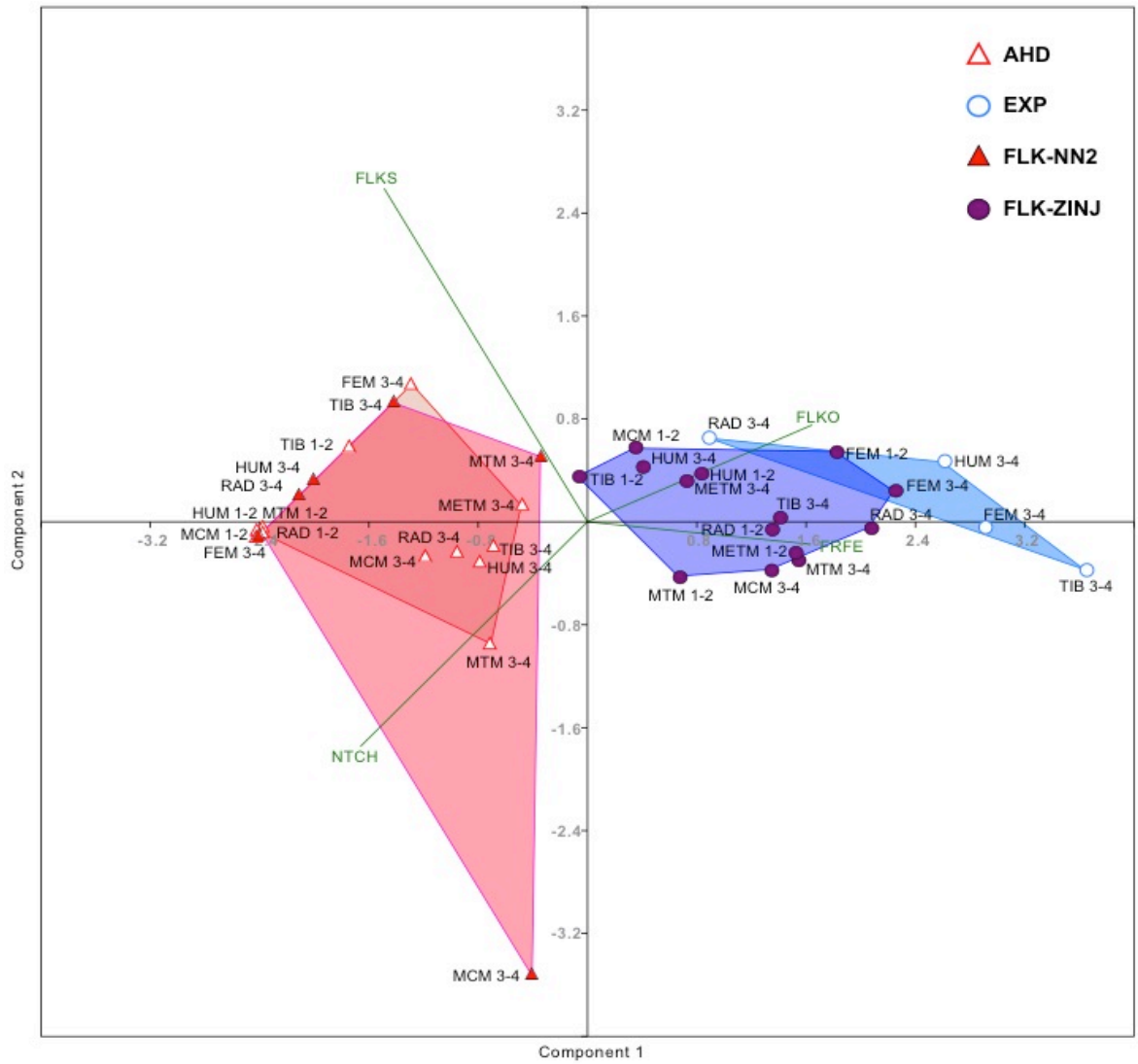


Fig. 5.8. Principal component analysis of loadpoint (LDPT) component frequencies in each assemblage. Each point represents the percent of the total number of LDPTs that display a FLKS, FLKO, FFRE, and/or NTCH for each size class 1-2 and 3-4 element. Eigen values and percent variance are PC1 :2.9056, 72.64; PC2: 0.5395, 13.49; PC3: 0.4089,10.223; PC4: 0.14560, 3.65.

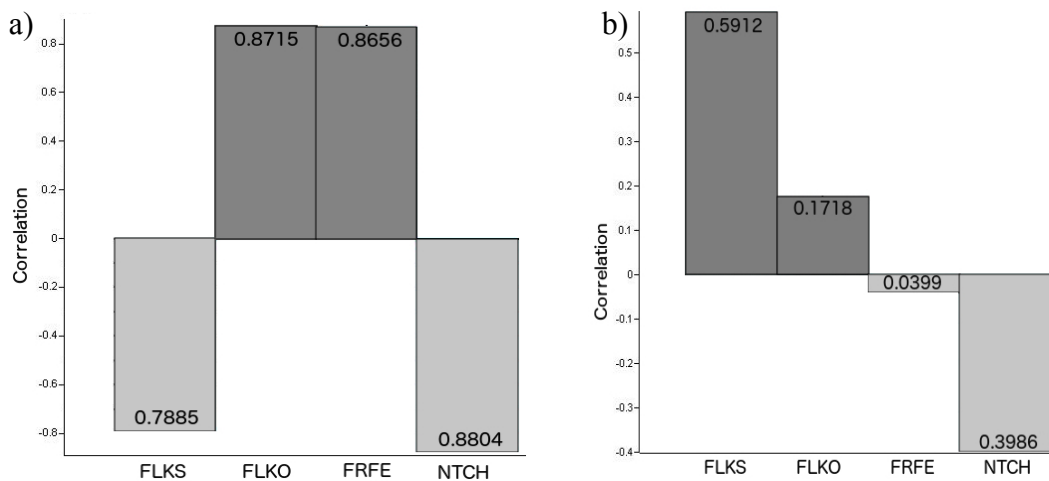


Fig. 5.9. Correlation value (loadings) histogram for FLKS, FLKO, FRFE, and NTCH loadpoints in (a) principal component 1 and (b) principal component 2.

5.3.3 LDPT Fracture Features

As indicated in the review of the fractographic literature (Chapter 2) a LDPT may display a suite of fracture features. Their expression is sometimes quite subtle, but often these fracture features aided in definition of a LDPT that would have otherwise been missed. Moreover, as indicated in the fractographic literature, some fracture features and in fact their overall frequencies, may relate to the amount of force applied. For example, hackle marks and incipient flakes have been proposed to be indicative of impact. The frequencies of fracture features, i.e., incipient flakes (IF), radiating cracks (RC), bulbar scars (BSc), cones, (CO), hackle marks (HK), lateral stress (LS), and fringe (FR), observed on FLKS, FLKO, FRFE, and NTCH LDPTs are considered here. The frequencies of these features observed on LDPTs coded for fracture features are given in Table 5.14. Again, the ulna and LBSFs are excluded from this analysis.

The total number of fracture feature observed on LDPTs in the size class 1-4 sample for each assemblage reveals that the assemblages fall into two groups. For the AHD large and small limb specimens 245 fracture features were observed on 229 LDPTs, or 1.07 per LDPT (Table 5.14). The average number of fracture features observed in the FLK-NN2 is similarly low, 0.800 (24 features on 30 LDPTs) and the differences are not great. The frequency of fracture features per LDPT is considerably greater in both the EXP (381/171 or 2.23 fracture features per LDPT) and FLK-Zinj size class 1-4 material (1214/666 or 1.82 fracture features per LDPT). The frequencies of fracture features on FLK-Zinj and EXP LDPTs are not significantly different. Overall then, the frequency of LDPTs that display one of the coded fracture features is significantly greater in the EXP and FLK-Zinj assemblages than in AHD and FLK-NN2 (Fig. 5.10).

When individual fracture features are examined a similar (Fig. 5.11), but more variable pattern, is evident. Incipient flakes (IF), for example, are present on 30.99% (53/171) and 7.36% (49/666) of the EXP and FLK-Zinj LDPTs, respectively. The IF frequencies observed on LDPTs in both the AHD, 3.06% (7/229), and FLK-NN2 3.33%

Table 5.14. continued.

SITE	SZCS	ELMNT	FLKS							FLKO							FRFE							NTCH							TOTAL LDPTs	TOTAL FRACTURE FEATURES							TOTAL FRFF		
			#	IF	RC	BSG	CO	HK	LS	FR	#	IF	RC	BSG	CO	HK	LS	FR	#	IF	RC	BSG	CO	HK	LS	FR	IF	RC	BSG	CO		HK	LS	FR							
		hum	21	16	20	2	1	1	0	5	6	2	5	1	0	0	5	0	3	0	FR	LS	HK	CO	BSG	RC	IF	RC	BSG	CO	HK	LS	FR	3	1	2	5	6	10	4	31
		rad	16	13	17	3	1	2	0	6	4	8	2	0	0	0	2	0	1	0	FR	LS	HK	CO	BSG	RC	IF	RC	BSG	CO	HK	LS	FR	4	1	4	2	7	10	14	42
		mcm	17	15	21	3	1	6	0	13	5	15	5	2	0	0	5	2	2	3	FR	LS	HK	CO	BSG	RC	IF	RC	BSG	CO	HK	LS	FR	5	1	6	5	15	8	19	59
		fem	21	16	16	1	0	4	0	5	6	10	9	0	0	0	9	3	6	5	FR	LS	HK	CO	BSG	RC	IF	RC	BSG	CO	HK	LS	FR	1	0	4	9	9	15	18	56
		tib	40	25	34	0	0	13	0	20	11	28	3	0	0	0	3	2	3	2	FR	LS	HK	CO	BSG	RC	IF	RC	BSG	CO	HK	LS	FR	1	1	14	3	25	17	33	94
		mtm	26	18	24	8	4	3	0	14	5	12	6	0	0	0	6	1	4	6	FR	LS	HK	CO	BSG	RC	IF	RC	BSG	CO	HK	LS	FR	8	4	4	7	16	11	24	74
		metm	10	5	5	0	0	1	0	4	1	3	4	1	1	0	4	2	2	3	FR	LS	HK	CO	BSG	RC	IF	RC	BSG	CO	HK	LS	FR	1	1	1	4	6	4	6	23
		Total ID	151	108	137	17	7	30	0	67	38	78	34	4	1	0	34	10	21	19	FR	LS	HK	CO	BSG	RC	IF	RC	BSG	CO	HK	LS	FR	23	9	35	35	84	75	118	379
		hum	66	51	65	3	6	21	0	31	19	8	17	1	2	0	17	10	9	4	FR	LS	HK	CO	BSG	RC	IF	RC	BSG	CO	HK	LS	FR	4	8	21	17	45	32	12	139
		rad	65	45	47	8	5	13	0	15	8	15	23	2	2	0	23	5	12	14	FR	LS	HK	CO	BSG	RC	IF	RC	BSG	CO	HK	LS	FR	10	8	13	23	25	28	38	145
		mcm	28	19	24	1	2	8	0	13	11	12	7	0	0	0	7	3	4	5	FR	LS	HK	CO	BSG	RC	IF	RC	BSG	CO	HK	LS	FR	2	2	9	7	21	19	25	85
		fem	47	31	32	0	1	4	0	11	16	23	19	0	0	0	19	7	9	13	FR	LS	HK	CO	BSG	RC	IF	RC	BSG	CO	HK	LS	FR	0	1	5	19	19	33	43	120
		tib	94	58	66	6	2	18	0	25	25	45	26	1	0	0	26	13	17	18	FR	LS	HK	CO	BSG	RC	IF	RC	BSG	CO	HK	LS	FR	8	2	21	27	40	55	80	233
		mtm	21	15	21	2	1	9	0	14	10	15	7	0	0	0	7	4	4	6	FR	LS	HK	CO	BSG	RC	IF	RC	BSG	CO	HK	LS	FR	2	2	9	7	18	21	28	87
		metm	33	12	13	0	0	3	0	3	3	4	3	0	0	0	3	2	1	3	FR	LS	HK	CO	BSG	RC	IF	RC	BSG	CO	HK	LS	FR	0	0	4	3	7	4	8	26
		Total ID	354	231	268	20	17	76	0	112	92	122	102	4	4	0	102	44	56	63	FR	LS	HK	CO	BSG	RC	IF	RC	BSG	CO	HK	LS	FR	26	23	82	103	175	192	234	835
		hum	87	67	85	5	7	22	0	36	25	10	22	2	2	0	22	10	12	4	FR	LS	HK	CO	BSG	RC	IF	RC	BSG	CO	HK	LS	FR	7	9	23	22	51	42	16	170
		rad	81	58	64	11	6	15	0	21	12	23	25	2	2	0	25	5	13	14	FR	LS	HK	CO	BSG	RC	IF	RC	BSG	CO	HK	LS	FR	14	9	17	25	32	38	52	187
		mcm	45	34	45	4	3	14	0	26	16	27	12	2	0	0	12	5	6	8	FR	LS	HK	CO	BSG	RC	IF	RC	BSG	CO	HK	LS	FR	7	3	15	12	36	27	44	144
		fem	68	47	48	1	1	8	0	16	22	33	28	0	0	0	28	10	15	18	FR	LS	HK	CO	BSG	RC	IF	RC	BSG	CO	HK	LS	FR	1	1	9	28	28	48	61	176
		tib	134	83	100	6	2	31	0	45	36	73	29	1	0	0	29	15	20	20	FR	LS	HK	CO	BSG	RC	IF	RC	BSG	CO	HK	LS	FR	9	3	35	30	65	72	113	327
		mtm	47	33	45	10	5	12	0	28	15	27	13	0	0	0	13	5	8	12	FR	LS	HK	CO	BSG	RC	IF	RC	BSG	CO	HK	LS	FR	10	6	13	14	34	32	52	161
		metm	43	17	18	0	0	4	0	7	4	7	7	1	1	0	7	4	3	6	FR	LS	HK	CO	BSG	RC	IF	RC	BSG	CO	HK	LS	FR	1	1	5	7	13	8	14	49
		Total ID	505	339	405	37	24	106	0	179	130	200	136	8	5	0	136	54	77	82	FR	LS	HK	CO	BSG	RC	IF	RC	BSG	CO	HK	LS	FR	49	32	117	138	259	267	352	1214

D) FLK-ZIN

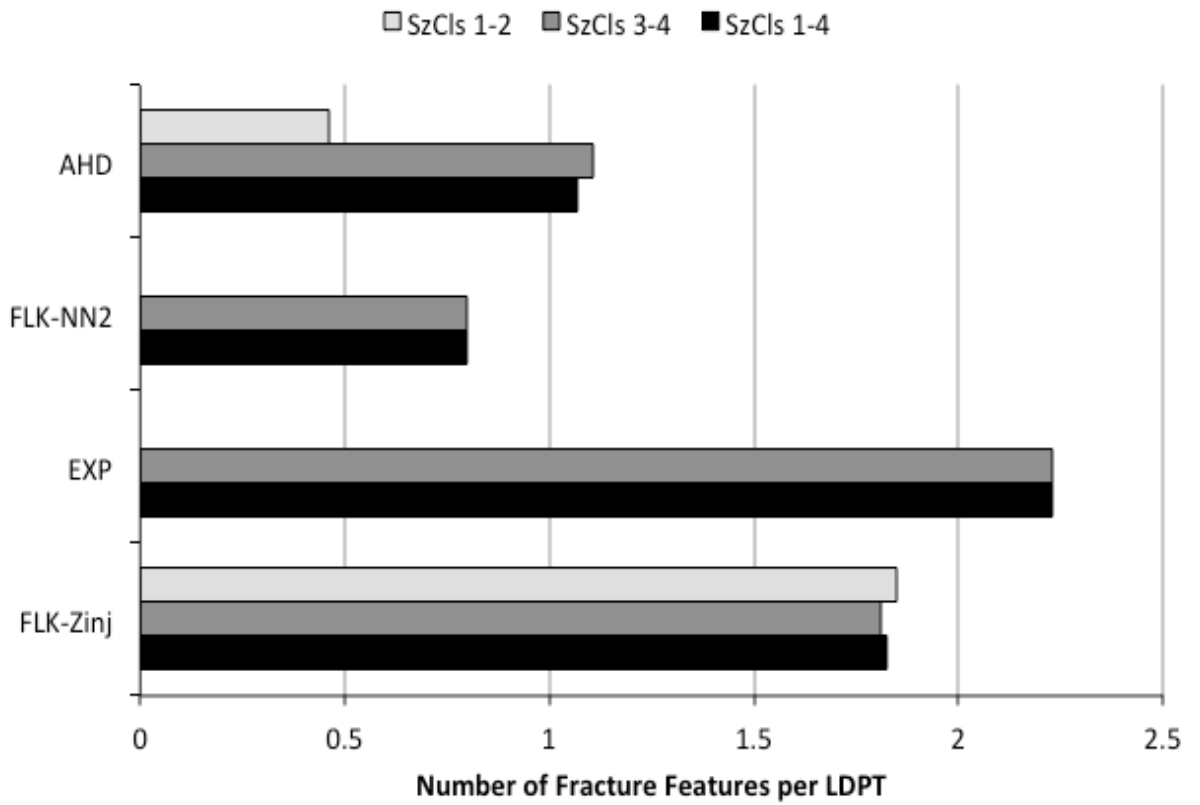


Fig. 5.10. Average number of fracture features (FRACFEAT) per loadpoint (LDPT) observed on size class 1-4 limb specimens excluding ulna and long bone shaft fragments.

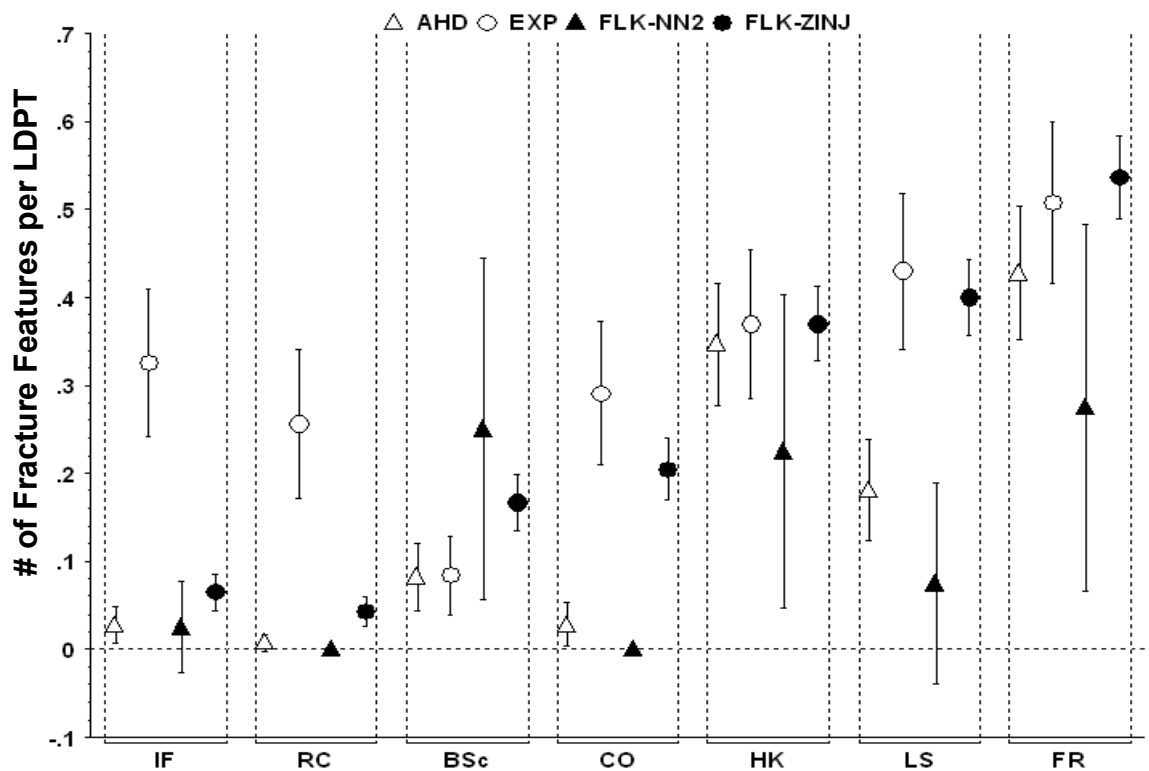


Fig. 5.11. Point plot of the number of fracture features (IF = incipient flake; RC = radiating crack; BSc = bulbar scar; CO = cone; HK = hackle; LS = lateral stress; FR = fringe) per size class 1-4 LDPT (excluding LBSF and the ulna) in each assemblage. Bars indicate 95% confidence intervals.

(1/30) assemblages are less than half that recorded for FLK-Zinj, 7.36% (49/666), and considerably less than EXP 68.83% (53/171). Similarly, the percentage of LDPTs associated with a radiating crack (RC) in the EXP and FLK-Zinj assemblages (25.15% and 4.80%, respectively) is almost 5 to 25 times that in the AHD and FLK-NN2 assemblages (0.87% and 0.00%, respectively). Differences in the frequency of LDPTs that display a cone or partial cone (CO) in AHD and FLK-NN2 compared to the EXP and FLK-Zinj assemblages are particularly pronounced; while 26.32% of EXP and 20.72% of FLK-Zinj LDPTs are associated with a cone or partial cone (CO), only 3.06% of the AHD LDPTs and no FLK-NN2 LDPTs display a this feature. The same pattern is seen for LDPTs that display lateral stress (LS). Comparison of lateral stress features (LS) reveals the same pattern: lateral stress features were observed on 41.52% of the EXP LDPTs and 40.09% of FLK-Zinj LDPTs, 2.5 to 6 times greater than observed in the AHD (16.59%) and FLK-NN2 (6.67%) assemblages.

No particular pattern is seen in the frequencies of fringe (FR) and hackle marks (HK). The expression of fringe (FR) in the FLK-NN2 assemblage (26.67%) is about half that observed in the EXP (50.29%) and FLK-Zinj (52.85%) material. About 41% of the AHD LDPTs are associated with FR on adjacent fracture surfaces, 10% less than that observed for the EXP and FLK-Zinj material. The percentages of hackle marks observed at LDPTs in the EXP (38.01%), FLK-Zinj (38.89%), AHD (34.06%), and FLK-NN2 (23.33%) do not appear different. The frequencies of bulbar scars (BSc) in the AHD and EXP assemblages are similar (8.73% and 10.53%, respectively), as are the frequencies in FLK-NN2 and FLK-Zinj (20.00% and 17.57%, respectively).

Figure 5.11 shows that although the number of IF, RC, CO, HK, LS, and FR features observed on LDPTs is greater for the EXP and FLK-Zinj, the 95% confidence intervals for only the RC, CO, and LS do not overlap with those of AHD and FLK-NN2. The HK and FR feature confidence intervals for the assemblages overlap considerably. The EXP incipient flake (IF) frequency is greater than any other assemblage. Fisher's exact test was

used to examine similarities and differences between the frequencies of different fracture features across the four assemblages (Table 5.15, Fisher's exact test, $p < 0.05$). The frequency of incipient flakes (IF) per LDPT in the AHD (0.031) assemblage is nearly identical to that observed for FLK-NN2 (0.033; $p > 0.9999$), but significantly smaller than both the EXP (0.310; $p < 0.0001$) and FLK-Zinj (0.074; $p = 0.0179$) material. The EXP IF frequency is significantly greater than that of FLK-NN2 ($p = 0.0007$) as well as that observed for the FLK-Zinj material ($p < 0.0001$). And, the FLK-NN2 IF frequency is not at all different from FLK-Zinj ($p = 0.7159$). Statistical comparison of the radiating crack (RC) frequencies mirrors the pattern that observed for IF frequencies although here the 95% confidence intervals do not overlap (Fig. 5.11).

While the frequency of LDPTs that display a bulbar scar (BSc) in the AHD assemblage (0.009) is significantly smaller than that of FLK-Zinj (0.09; $p = 0.0010$), the FLK-NN2 (0.200) vs. FLK-Zinj frequencies are not significantly different ($p = 0.8060$). Similarly, while the EXP BSc frequencies (0.105) are significantly smaller than those from FLK-Zinj ($p = 0.0266$), they are similar to the FLK-NN2 BSc frequency ($p = 0.0962$). The frequencies of LDPTs with HK in AHD (0.341), FLK-NN2 (0.233), EXP (0.380), and FLK-Zinj (0.389) are not statistically different.

The number of cones or partial cones (CO) on LDPTs in EXP (0.263) and FLK-Zinj (0.207) are significantly greater than in both AHD (0.031) and FLK-NN2 (0.000; EXP vs. AHD, $p < 0.0001$; EXP vs. FLK-NN2, $p < 0.0005$; FLK-Zinj vs. AHD, $p < 0.0001$; FLK-Zinj vs. FLK-NN2, $p = 0.0017$). In contrast, the EXP and FLK-Zinj CO frequencies are not dissimilar ($p = 0.1203$) and neither are those from AHD and FLK-NN2 ($p > 0.9999$). Similarly, the LS frequencies in AHD (0.166) and FLK-NN2 (0.067) are not dissimilar ($p = 0.1890$), but are significantly less than the frequencies in both the EXP (0.380) and FLK-Zinj (0.401) assemblages (for all comparison $p < 0.0001$). As well, there is no difference ($p = 0.6067$) in the frequencies of LDPTs that display fringe (FR) in EXP (0.503) and FLK-Zinj (0.529) but they are significantly different (FLK-Zinj vs. AHD, $p = .00017$;

FLK-Zinj vs. FLK-NN2, $p = 0.0079$; EXP vs. FLK-NN2, $p = 0.0180$), or nearly so (EXP vs. AHD, $p = 0.0672$), compared to the AHD (0.406) and FLK-NN2 (0.267) frequencies, In turn the AHD and FLK-NN2 FR frequencies are not significantly different ($p = 0.1662$).

Thus, the study assemblages form two groups based on their fracture feature frequencies. These analyses indicate that for the size class 1-4 material the fracture feature frequencies in the AHD and FLK-NN2 are similar to each other, but are usually significantly different from those of EXP and FLK-Zinj, which in turn are largely similar to each other. This pattern particularly evident for the CO and LS frequencies which are consistently similar in the AHD and FLK-NN2 assemblages and are always significantly smaller than the EXP and FLK-Zinj frequencies, which are in turn not at all dissimilar. The IF, RC, and FR frequencies show a similar but less consistent pattern. The frequencies of BSc and HK rarely show a significant difference between the assemblages.

Principal component analysis of IF, RC, BSc, CO, LS, HK, and FR frequencies in the assemblages makes the pattern described above considerably clearer (Fig. 5.12). Figure 5.13 shows the correlation values. The PC1 and PC2 axes explain 75% of the observed variability in fracture features (PC1 = 44%; PC2 = 31%). The AHD and FLK-NN2 assemblages cluster in nearly the same space with all but one PC1 value (that for AHD, size class 1-2 RAD which displays only one LDPT) being negative. In contrast, while the EXP and FLK-Zinj assemblages do not overlap, both show considerable clustering and all but one PC1 value (FLK-Zinj size class 1-2 HUM) is positive. The vectors (shown in green) show again that the CO, LS, and to a lesser degree the IF and RC frequencies distinguish the AHD and FLK-NN2 assemblages from the EXP and FLK-Zinj assemblages.

Table 5.15. Fisher's exact probabilities for difference in fracture feature frequencies (number of loadpoints with a feature / total number of loadpoints) in the AHD, EXP, FLK-NN2, and FLK-Zinj assemblages. Significant differences (at 0.05) in frequencies are in bold. Those approaching significance are in italics. Fracture feature abbreviations given in Table 3.1.

Size Class/ Site / Frac. Feat.		EXP	FLK-NN2	FLK-ZINJ	
SzCls 1-2	AHD				
	IF	—	—	0.3698	
	RC	—	—	>0.9999	
	BSc	—	—	0.6994	
	CO	—	—	0.1350	
	HK	—	—	0.2522	
	LS	—	—	0.0050	
FR	—	—	0.0035		
SzCls 3-4	AHD	IF	< 0.0001	>0.9999	0.2497
		RC	< 0.0001	>0.9999	0.0076
		BSc	0.6041	0.0971	0.0018
		CO	< 0.0001	>0.9999	< 0.0001
		HK	0.5240	0.3012	0.4425
		LS	< 0.0001	0.1858	< 0.0001
		FR	0.1235	0.1162	0.0392
	EXP	IF	—	0.0007	0.9289
		RC	—	0.0005	< 0.0001
		BSc	—	0.2163	< 0.0001
		CO	—	0.0005	0.0272
		HK	—	0.1501	0.2926
		LS	—	0.0001	>0.9999
		FR	—	0.0180	>0.9999
	FLK-NN2	IF	—	—	>0.9999
		RC	—	—	0.3857
		BSc	—	—	0.8055
		CO	—	—	0.0009
		HK	—	—	0.1216
		LS	—	—	< 0.0001
		FR	—	—	0.0134
SzCls 1-4	AHD	IF	< 0.0001	>.9999	0.0179
		RC	< 0.0001	>.9999	0.0046
		BSc	0.6064	0.0962	0.0010
		CO	< 0.0001	>.9999	< 0.0001
		HK	0.4607	0.3031	0.2064
		LS	< 0.0001	0.1890	< 0.0001
		FR	<i>0.0672</i>	0.1662	0.0017
	EXP	IF	—	0.0007	< 0.0001
		RC	—	0.0005	< 0.0001
		BSc	—	0.2163	0.0266
		CO	—	0.0005	0.1203
		HK	—	0.1501	0.8606
		LS	—	0.0001	0.7278
		FR	—	0.0180	0.6067
	FLK-NN2	IF	—	—	0.7159
		RC	—	—	0.3905
		BSc	—	—	0.8060
		CO	—	—	0.0017
		HK	—	—	0.1229
		LS	—	—	< 0.0001
		FR	—	—	0.0079

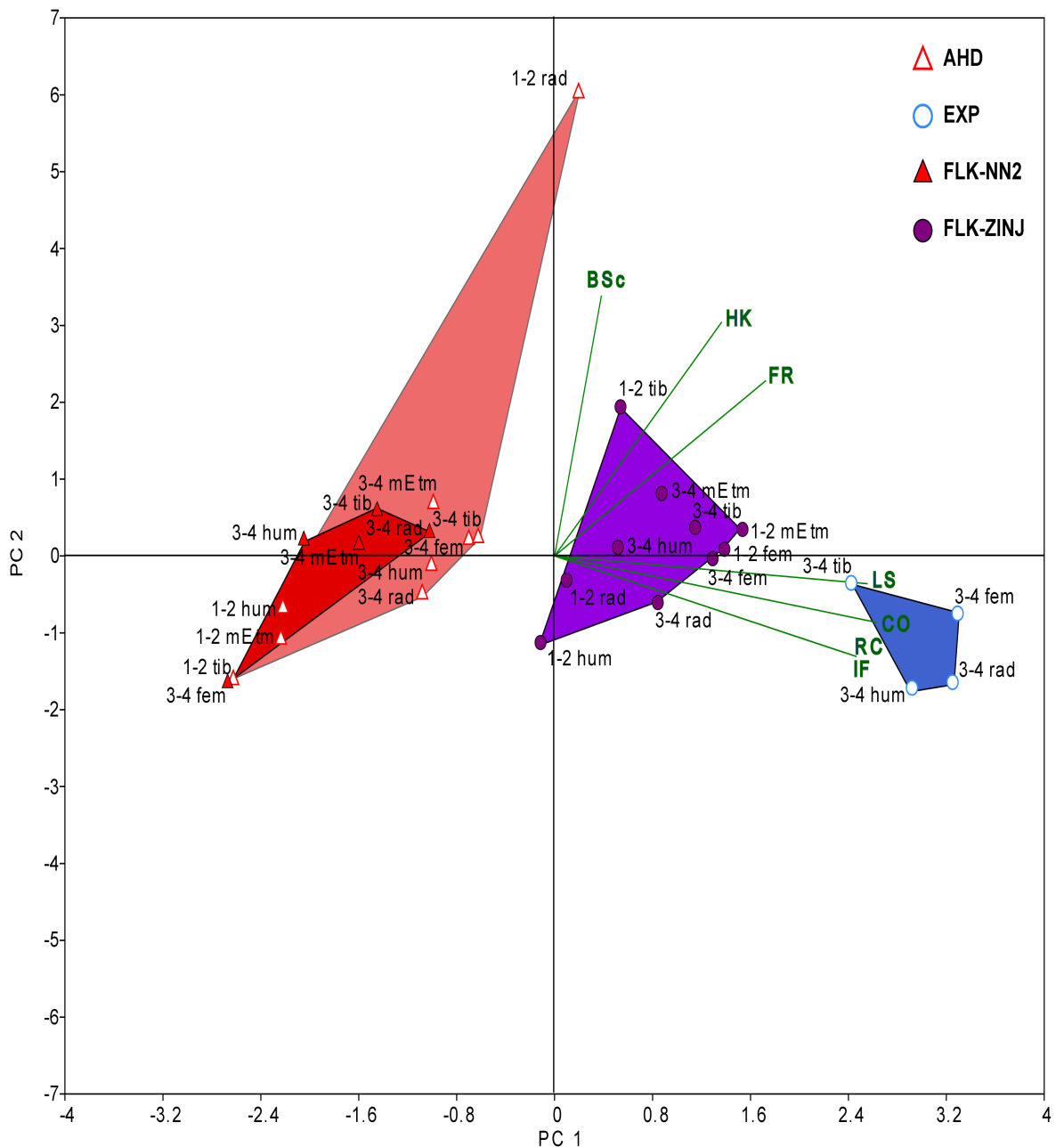


Fig. 5.12. Principal component analysis of the mean number of the seven fracture feature types (IF = incipient flake; RC = radiating crack; BSc = bulbar scar; CO = cone (usually partial); HK = hackle; LS = lateral stress; FR = fringe) observed on LDPTs on size class 1-2 and 3-4 elements (excluding ulna and long bone fragments; mEtm = MCM+MTM+METM). Vectors for each LDPT type, shown in green, indicate that the RC, IF, and particularly the LS and CO frequencies differentiate AHD and FLK-NN2 from the EXP and FLK-Zinj assemblages. Eigen values and percent variance are PC 1: 3.0565, 43.7; PC 2: 2.1515, 30.74; PC 3: 0.9677, 13.83; PC 4: 0.38275, 5.47; PC 5: 0.1960, 2.80; PC 6: 0.1456, 2.08; PC 7: 0.0999, 1.43.

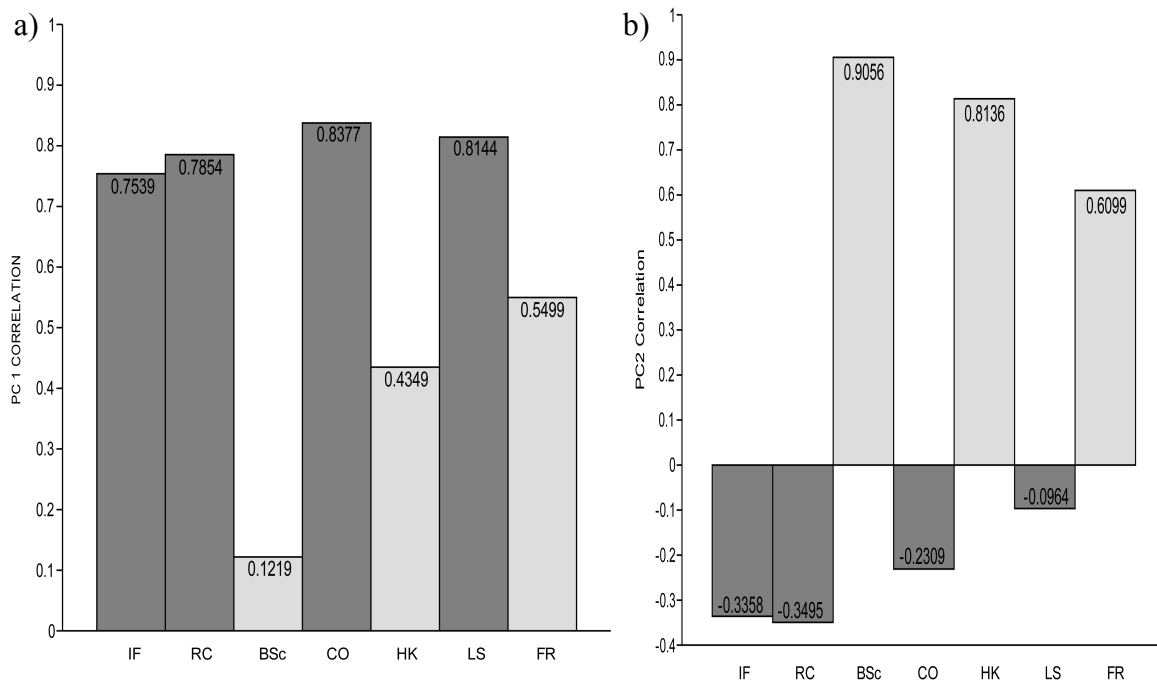


Fig. 5.13. Correlation value (loadings) histogram for seven fracture feature types (IF = incipient flake; RC = radiating crack; BSc = bulbar scar; CO = cone (usually partial); HK = hackle; LS = lateral stress; FR = fringe) observed on LDPTs on size class 1-2 and 3-4 elements in (a) principal component 1 and (b) principal component 2.

5.4 Carnivore and Hammerstone Damages: Fracture Agency and Overprinting

Because the primary purpose of this work is to establish whether or not individual or suites of fracture features (including LDPT types) described here can be used to defined bones fractured by carnivores and hammerstone impact, the above analyses were presented without reference to taphonomic agent. Other damages, notably percussion marks (PM) and tooth marks (TM), have been the focus of decades of experimental and actualistic research. Accordingly, although recent work (Dominquez and Barba 2007) has questioned some previous identifications in the FLK-Zinj assemblage (see Methods), these surficial damages are well defined and commonly used to identify humans and carnivores as agents in assemblage formation and their access sequence. In this section the fracture features that the above analyses indicate differentiate the AHD and FLK-NN2 assemblages from the EXP and FLK-Zinj assemblages, i.e., incipient flakes (IF), radiating cracks (RC), cones (CO), and lateral stress (LS), are analyzed with reference to the presence or absence of TM and PM. Here these fracture features are referred to as target features. Comparing the frequencies of LDPTs with these target features and an associated TM or PM permits

evaluation of whether or not the high frequencies of these features in the EXP and FLK-Zinj assemblages are causally related to carnivore gnawing or hammerstone impact. This analysis then allows the frequencies of carnivore and hammerstone breakage in the fossil assemblages to be estimated with reference to bone fracture.

This section is divided into three parts. First, the frequencies of specimens displaying carnivore damage are examined for each assemblage. In the second part of this section, the frequencies of percussion marks (PM) are analyzed. Finally, the frequencies of TMs and PMs directly associated with LDPTs displaying one or more of the target fracture features (CO, IF, RC, LS) for each assemblage are compared. In so doing, the relative strength of the target fracture features in defining hammerstone breakage may be assessed and used to estimate carnivore- and hominin-induced bone fracture in the fossil assemblages.

5.4.1 Carnivore Damage

First an overall assessment of carnivore damage frequencies (TM, TFLKS, TNTCH, TMRK, LVERUP, and CVRE BREAK) is presented for all size class 1-4-limb specimens (excluding the ulna and LBSF). Tooth mark frequencies are also examined using all size class 1-4 limb specimens including the ulna and LBSFs. Second, the ratio of specimens displaying a tooth mark to those exhibiting a carnivore break are assessed.

Table 5.16 and Fig. 5.14 present the frequencies of specimens that display diagnostic carnivore damage — tooth marks (TM), leverups (LVRUP), loadpoint damage (LDPT, i.e., TFLKS, TMRK, and TNTCH). Total carnivore damage reflects the sum of specimens that display either a carnivore TM, LDPT, or LVRUP. Also shown are the frequencies of specimens displaying evidence of carnivore-induced fracture (CVRE BREAK). Damages diagnostic of carnivore fracture include tooth marks (TMRK) at a loading point defined by the presence of a tooth notch (TNTCH) or tooth flake scar (TFLKS) singly or in combination and leverups (LVRUP). As noted in the Methods, the small size of FLKSs and NTCHs was used to define tooth flake scars (TFLKS), and notches (TNTCHs). The carnivore break frequency is the sum of specimens that display a leverup or a carnivore

load point. Also provided are frequencies of specimens that display a tooth mark on the fracture surface, medullary wall, or cancellous bone (FMC).

Table 5.16. Percentage of specimens (excluding the ulna and long bone fragments) that display carnivore damage in each assemblage. TM = tooth mark; LVRUP = carnivore leverup; CVRE LDPT = carnivore load point (tooth flake scar (TFLKS), tooth notch (TNTCH), and tooth loadmark (TMRK)). The total carnivore damage is the sum of specimens displaying either a tooth mark, carnivore loadpoint, or leverup. Also shown are the frequencies of specimens with a carnivore break, which is the sum of specimens exhibiting either a leverup or a carnivore loadpoint, and tooth marks located on the fracture surface, medullary wall, or cancellous tissue (FMC).

	NISP	TM	LVRUP	CVRE LDPT	TOTAL CVRE DMG	CVRE BREAK	TM on FMC
AHD	375	89.3	30.7	34.7	90.4	54.1	68.0
FLK-NN2	88	73.9	61.4	17.0	78.4	64.8	37.5
EXP	95	70.5	13.7	3.2	70.5	15.8	38.9
FLK-ZINJ	521	40.7	1.2	4.4	40.9	5.6	25.0

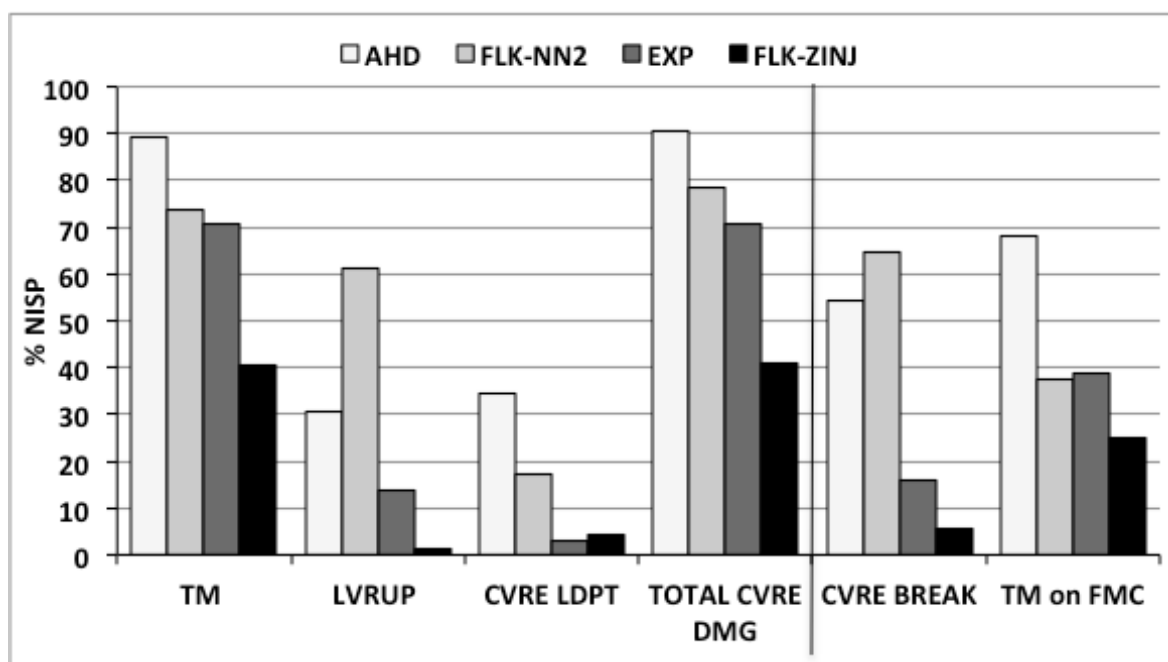


Fig. 5.14. Percentage of specimens (excluding the ulna and long bone shaft fragments) that display carnivore damage in each assemblage. TM = tooth mark; LVRUP = carnivore leverup; CVRE LDPT = carnivore load point (tooth flake scar (TFLKS), tooth notch (TNTCH), and tooth load mark (TMRK)). Note that while all assemblages display a high frequency of TMs, and overall carnivore damage, the frequencies of those that display a carnivore leverup loadpoint and break are considerably lower in the EXP and FLK-Zinj assemblages.

For the AHD, FLK-NN2, and EXP assemblages, over 70% of specimens display one or more tooth marks. The frequency (41%) is considerably less in the FLK-Zinj assemblage. All but the FLK-NN2 vs. EXP between-assemblage tooth mark frequency comparisons are statistically different (Fisher's exact test is used because only the summed frequencies are compared; $p < 0.0001$ for all comparisons except FLK-NN2 vs. EXP where $p = 0.6252$). The frequencies of leverup specimens significantly greater in the AHD (30.7%) and FLK-NN2 (61.4%) assemblages compared to those of EXP (13.7%) and FLK-Zinj (1.2%) (Fisher's exact test, $p < 0.0001$ for all comparisons except AHD vs. EXP where $p = 0.0007$). The frequencies of specimens with a carnivore load point are lower in all assemblages, less than 20% in all but AHD. Only the EXP and FLK-Zinj carnivore load point frequencies do not appear significantly different (Fisher's exact test: AHD vs. FLK-NN2, $p = 0.0013$; AHD vs. EXP, $p < 0.0001$; AHD vs. FLK-Zinj, $p < 0.0001$; FLK-NN2 vs. EXP, $p = 0.0021$; FLK-NN2 vs. FLK-Zinj, $p < 0.0001$; EXP vs. FLK-Zinj, $p = 0.7831$).

In estimating overall carnivore damage, however, here it seems reasonable to consider the long bone shaft fragments (LBSF), ulna, and complete elements. The reason is because tooth marks are small and may be preserved on specimens too small to preserve or evaluate load point or fracture damage. As well, the ulna, while not considered appropriate for evaluating fracture damages because of their unique geometry and lack of a true marrow cavity, should be included in evaluating tooth marks, in part because carnivores show a proclivity for gnawing the olecranon process of bovids.

Including these specimens does not appreciably alter the frequencies of carnivore tooth marks observed in the AHD (731/944) and FLK-NN2 (90/126) assemblages which remain over 70% (77.4 and 71.4%, respectively). For the EXP and FLK-Zinj material, however, the frequency of specimens displaying a tooth mark is much lower (78/201 or 38.8 and 289/1016 or 28.4%, respectively). Now, the frequencies of specimens with tooth marks in the AHD and FLK-NN2 assemblages are not statistically different (Fisher's exact test, $p = 0.1446$) while both frequencies are significantly different from those of the EXP

and FLK-Zinj assemblages (Fisher's exact test, $p < 0.0001$ for all comparisons). The EXP and FLK-Zinj tooth mark frequencies remain significantly different ($p = 0.0042$).

Tooth marks on the fracture surface, medullary wall, and/or cancellous tissue (FMC) reflect carnivore activity that occurred subsequent to bone fracture. Specimens with a tooth mark on the FMC occur in all assemblages. The AHD material displays a significantly greater frequency at 68.0% compared to the other assemblages ($p < 0.0001$ for all comparisons). The FLK-NN2 and EXP assemblages have roughly equivalent frequencies of post-fracture tooth marks, 37.5% and 38.9%, respectively, and are not significantly different ($p = 0.8797$). The frequency of specimens with a post-fracture tooth mark, 25% in the FLK-Zinj assemblage is significantly smaller than in other assemblages (AHD vs. FLK-Zinj, $p < 0.0001$; FLK-NN2 vs. FLK-Zinj, $p = 0.0187$; EXP vs. FLK-Zinj, $p = 0.0080$). Examples of tooth marks on FMC surfaces are illustrated in Figure 5.15.

As seen in Table 5.16 and Figure 5.14, there appears to be a dramatic difference in the ratio of all tooth-marked specimens to the number of specimens with evidence of carnivore-induced breakage in the AHD and FLK-NN2 assemblages compared to EXP and FLK-Zinj. That is, relative to the frequency of bones with evidence of carnivore-induced fracture, the number of tooth-marked specimens in the EXP and FLK-Zinj assemblages seems inordinately high compared to AHD and FLK-NN2. In AHD and FLK-NN2 the numbers of tooth-marked specimens per specimen that displays a carnivore break are 1.642 and 1.14, respectively. These values are 2.7 to 7 times less than that seen in EXP (4.467) or FLK-Zinj (6.839, Fig. 5.16). For AHD and FLK-NN2 the ratios are not significantly different (Fisher's exact test, $p = 0.0811$). Here again, Fisher's exact test is used because summary values are being examined. Similarly, the EXP and FLK-Zinj ratios are not significantly different (Fisher's exact test, $p = 0.2078$), but each is significantly different than the AHD and FLK-NN2 ratios (AHD vs. EXP, $p = 0.0005$; FLK-NN2 vs. EXP, $p < 0.0001$; AHD vs. FLK-Zinj, $p < 0.0001$; FLK-NN2 vs. FLK-Zinj, $p < 0.0001$).



Fig. 5.15. Examples of hammerstone-fractured bone with tooth marks on the fracture surface and/or medullary wall (FMC).

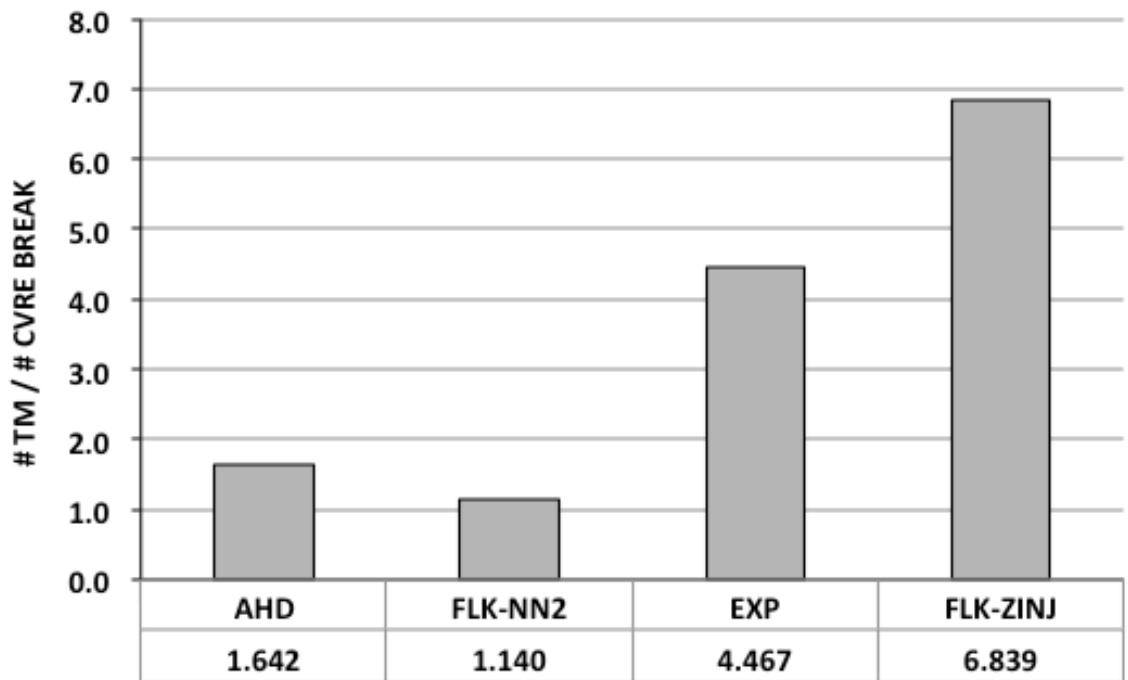


Fig. 5.16. Ratio of the frequency specimens displaying a tooth mark (TM) to specimens that exhibit a carnivore break (CVRE BREAK) for each assemblage. The AHD and FLK-NN2 ratios are not significantly different, but the EXP and particularly the FLK-Zinj ratios are significantly greater.

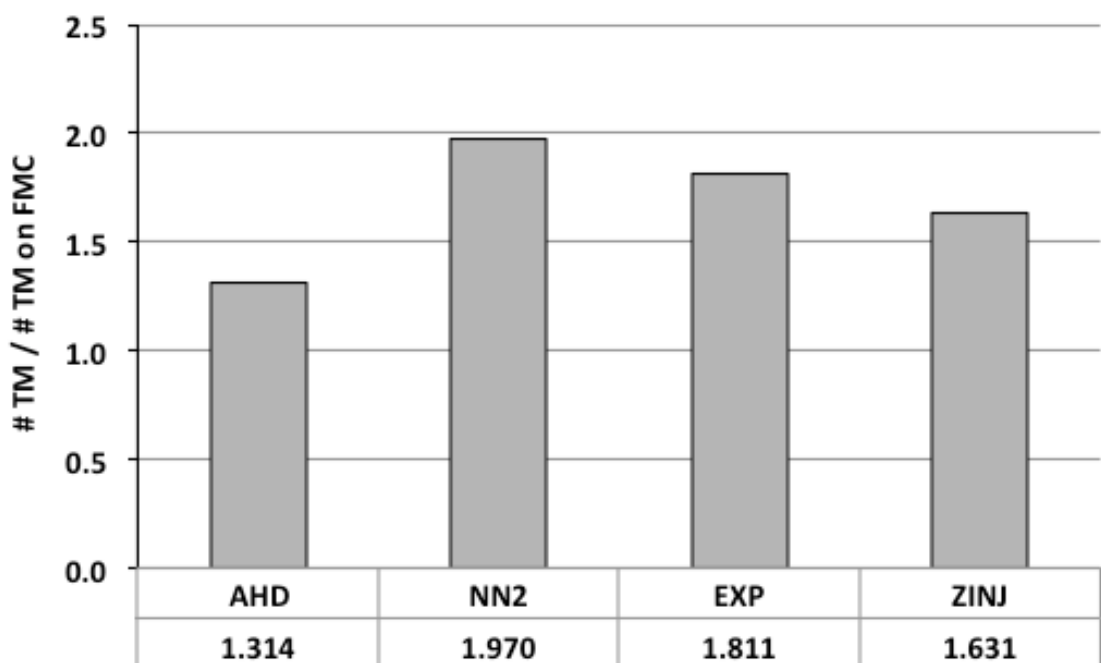


Fig. 5.17. Ratio of the frequency specimens displaying a tooth mark (TM) to specimens that exhibit a post-fracture TM on the fracture surface, medullary wall, and/or cancellous tissue for each assemblage. There are no significant differences in the ratios.

As shown in Fig. 5.17, the frequencies of specimens with a tooth mark per specimens with a post-fracture tooth mark (on the FMC surface) in the four assemblages appear quite similar, ranging from 1.970 for FLK-NN2 to 1.314 for AHD. There are no significant differences in the ratios (Fisher's exact test: AHD vs. NN2, $p = 0.0781$; AHD vs. EXP, $p = 0.1618$; AHD vs. FLK-Zinj, $p = 0.1291$; FNK-NN2 vs. EXP, $p = 0.8825$; FLK-NN2 vs. FLK-Zinj, $p = 0.4775$; EXP vs. FLK-Zinj, $p = 0.7288$).

5.4.2 Hammerstone Impact (Percussion) Damage

In this section the frequency of limb specimens (excluding the ulna and LBSFs) with percussion marks in the EXP and FLK-Zinj assemblages are analyzed. No percussion marks were observed in the AHD and FLK-NN2 assemblages. However, two LBSFs from AHD did display a small irregular depression with associated fine striae that could be mistaken for PMs.) The frequencies of PMs in the EXP and FLK-Zinj assemblages are given in Table 5.17 and illustrated in Fig. 5.18.

For the EXP assemblage, a total of 161 PMs were observed on 64 limb fragments, 71.1% of the total EXP limb NISP. In contrast the frequency of FLK-Zinj specimens with a PM (182 specimens, 388 individual PMs) is significantly less 34.9% (Fisher's exact test, $p < 0.0001$). Of the 161 EXP PMs, 63.4% ($n = 102$) are associated with a LDPT on 59 specimens while 36.6% ($n = 59$) occur as isolated marks (not directly associated with a LDPT) on five specimens. For the FLK-Zinj assemblage, fewer PMs, 54.9% ($n=213$), are associated with a LDPT, but the frequencies are not significant ($p = 0.0722$). Isolated mark frequencies display the opposite pattern. Consequently, the frequency of isolated PMs in FLK-Zinj is 45.1% (175 isolated PMs on 40 specimens), or 22.0% of the specimens with a PM, significantly greater than that observed for EXP, 36.6% of the PMs (59 isolated PMs on 5 specimens) and 7.8% of the specimens with a PM ($p < 0.0001$). Thus, while the EXP assemblage has more specimens that display a PM, the FLK-Zinj assemblage contains more specimens that display PMs not associated with a LDPT. Again, no percussion marks (PMs) were observed in the AHD and FLK-NN2 assemblages.

Table 5.17. Percussion mark frequencies in the four assemblages for a) those associated with a LDPT, b) isolated percussion marks, and c) the totals. The number in parentheses below each assemblage is the total site NISP (excluding the ulna and LBSFs).

	AHD (375)	FLK-NN2 (88)	EXP (95)	FLK-ZINJ (521)
a) PMs assoc. w/ LDPT				
#	0	0	102	213
% total PM	—	—	63.4	54.9
NISP	—	—	59	142
% NISP w/ PM	—	—	92.2	78.0
% Assemblage NISP			65.6	27.3
b) PMs not assoc. w/ LDPT (iso.)				
#	0	0	59	175
% total PM	—	—	36.6	45.1
NISP	—	—	5	40
% NISP w/ PM	—	—	7.8	22.0
% Assemblage NISP			5.6	7.7
c) Total				
#	0	0	161	388
% total PM	—	—	100.0	100.0
NISP	—	—	64	182
% NISP w/ PM	—	—	100.0	100.0
% Assemblage NISP			71.1	34.9

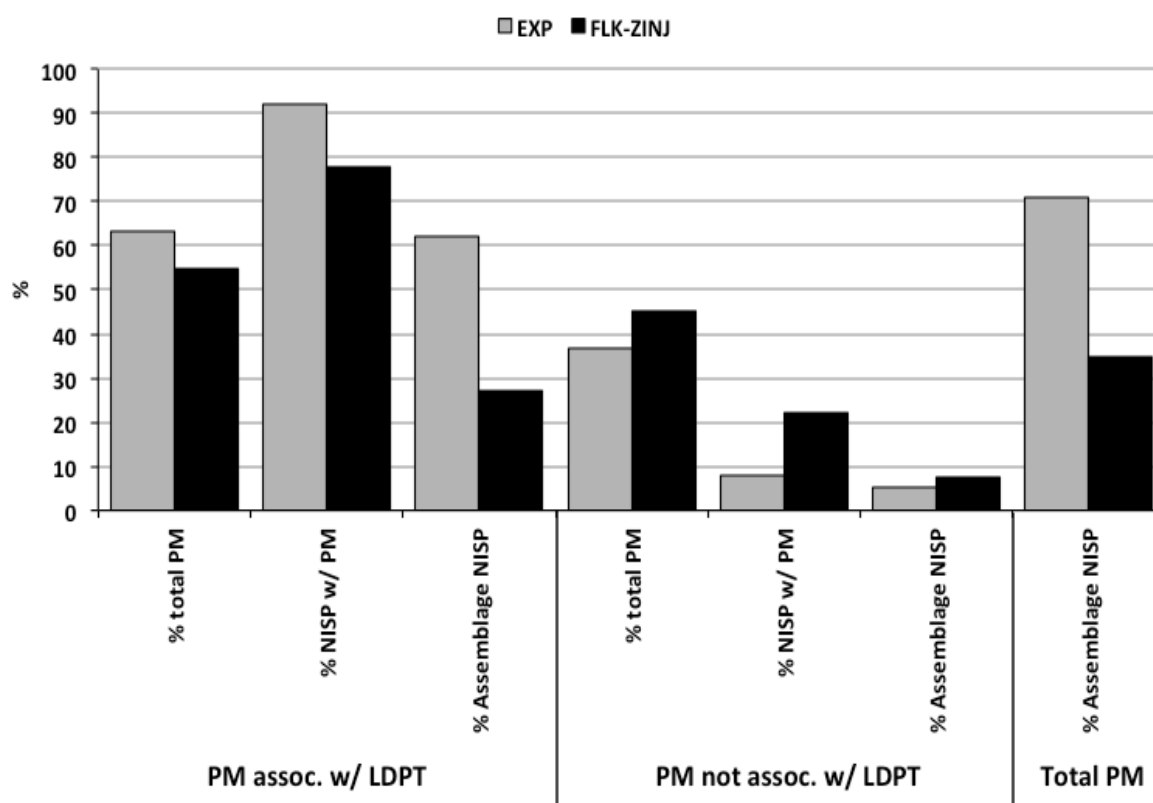


Fig. 5.18. Histogram showing the frequencies of percussion marks (PMs) associated with a loadpoint (LDPT) and isolated PMs, and the frequency of the total number of identified specimens (NISP) that display a PM for the EXP and FLK-Zinj assemblages.

5.4.3 Co-Occurrence of Percussion Marks and Tooth Marks

The frequencies of specimens in the EXP and FLK-Zinj assemblages that display both carnivore damage and a percussion mark (PM) are shown in Table 5.18 and graphically in Figure 5.20. There are three striking aspects to these frequencies. First, of the EXP specimens both broken by hammerstone and fed to Denver Zoo hyaenas over 50% display both a PM and carnivore damage. In contrast, the FLK-Zinj assemblage contains significantly fewer specimens (11.5%) that display both percussion and carnivore damage (Fisher's exact test, $p < 0.0001$). Second, while the zoo hyaenas were afforded several hundred hours of access time both prior to and following hammerstone breakage they created few load points ($n=1$, 1.1%) or breaks ($n = 8$, 8.9%). The FLK-Zinj frequency of specimens with a PM and evidence of carnivore breakage (0.8%) is significantly less than EXP ($p < 0.0001$). In contrast, the frequencies of specimens that display a PM and a carnivore LDPT in the two assemblages are not significantly different ($p = 0.5505$). Third, the frequency of tooth marks on the fracture, medullary, or cancellous surfaces (FMC) on EXP bones broken by hammerstone is significantly greater than that observed for FLK-Zinj (21.1% vs. 7.7%; $p < 0.0001$).

Table 5.18. Frequencies of specimens that display both a percussion mark (PM) and carnivore damage, including a carnivore tooth mark on the fracture surface, medullary wall, or cancellous tissue (TM on FMC), a tooth mark on any part of the specimen, or evidence of a leverup (LVRUP), or a carnivore load point (LDPT). Carnivore break is the sum of specimens that display a carnivore LVRUP or a LDPT. Any carnivore damage is the sum of specimens that display a TM, LVRUP or LDPT.

	PM & TM on FMC		PM & TM		PM & LVRUP		PM & CVRE LDPT		PM & CVRE BREAK		PM & any CVRE DMG	
	#	%	#	%	#	%	#	%	#	%	#	%
AHD	0	0.0	0	0.0	0	0.0	0	0.0	0	0.0	0	0.0
FLK-NN2	0	0.0	0	0.0	0	0.0	0	0.0	0	0.0	0	0.0
EXP	19	21.1	46	51.1	7	7.8	1	1.1	8	8.9	46	51.1
FLK-Zinj	40	7.7	60	11.5	0	0.0	4	0.8	4	0.8	60	11.5

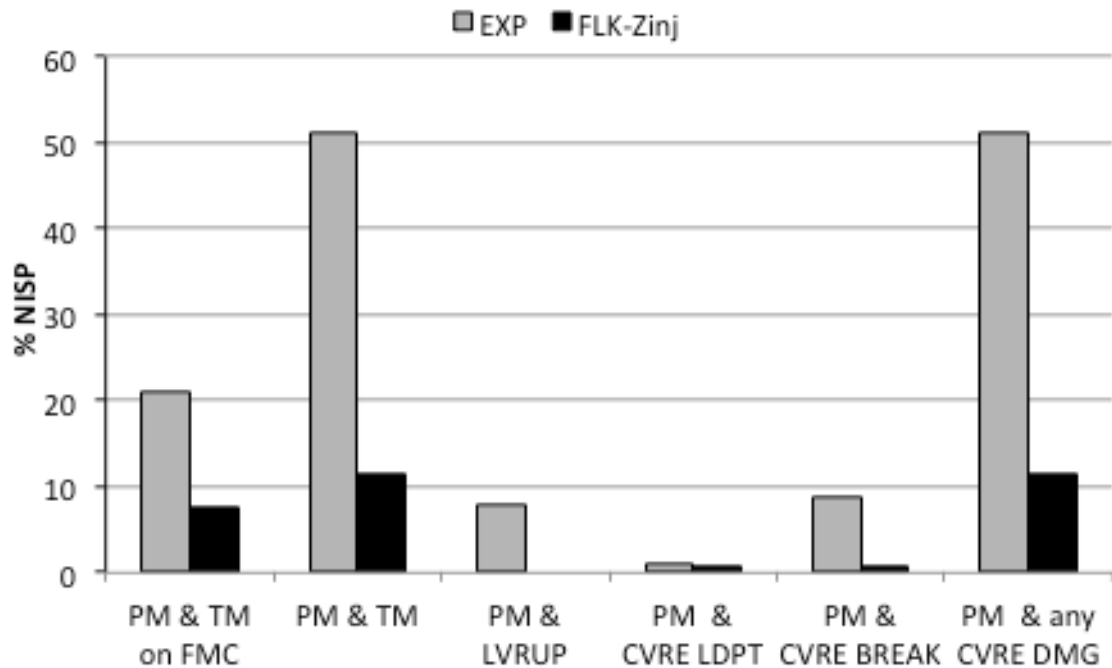


Fig. 5.19. Histogram of specimens that display both a percussion mark (PM) and carnivore damage, including a carnivore tooth mark on the fracture surface, medullary wall, or cancellous tissue (TM on FMC), a tooth mark on any part of the specimen, or evidence of a leverup (LVRUP), or a carnivore load point (LDPT). Carnivore break is the sum of specimens that display a carnivore LVRUP or a LDPT. Any carnivore damage is the sum of specimens that display a TM, LVRUP or LDPT.

5.4.4 Co-Occurrence of Percussion Marks or Tooth Marks at LDPTs with Incipient Flakes, Radiating Cracks, Cones, or Lateral Stress

In this section the frequency of bones which display TMs or PMs and which co-occur with cones, lateral stress, radiating cracks, and/or incipient flakes at LDPTs are analyzed. The frequencies of load points that exhibit one or more of these features in each assemblage and the number of specimens represented are given in Table 5.19.

A total of 48 LDPTs with cones, lateral stress, radiating cracks, and/or incipient flakes were observed on 44 specimens in the AHD assemblage. Only four LDPTs with these features were observed on four FLK-NN2 specimens. A total of 135 LDPTs with these fracture features were observed on 75 EXP specimens. For FLK-Zinj, 371 LDPTs with these fracture features were observed on 246 specimens. Overall, lateral stress (LS) is the most common feature observed, comprising 70.4% (38/54) of the LDPT features in AHD, 75.0% (3/4) of the FLK-NN2 features, 33.4% of EXP (71/212), and 56.7% of the target features observed in the FLK-Zinj assemblage (276/487). No specimens exhibit a

cone or partial cone feature in the FLK-NN2 assemblage, but seven specimens (15.9%, 7/44), or 14.6% (7/48) of the LDPTs, exhibit a cone. LDPTs with a cone or partial cone fracture feature are most frequent in the FLK-Zinj assemblage, occurring on 34.2% (127/371) of the LDPTs. In the EXP assemblage, cones (CO) occur on 33.3% (45/135) of the LDPTs with the examined features. LDPTs with incipient flakes are more common in the EXP assemblage than in FLK-Zinj, 38.5% (52/135) vs. 13.2% (49/371). One specimen exhibited a LDPT with an incipient flake in the FLK-NN2 assemblage. The differences in frequencies of these fracture features associated with tooth marks and percussion marks are striking. The frequency of AHD specimens with LDPTs associated with a CO, LS, RC, and/or IF feature as well as a TM, 59.1% (26/44; 28 LDPTs on 26 specimens), is significantly greater than that observed for FLK-NN2, 25% (1/4; one LDPT on one specimen; Fisher's exact test, $p < 0.0001$).

More importantly, the frequencies of LDPTs with these fracture features that co-occur with TM are significantly smaller in EXP and FLK-Zinj, 0.7% and 2.7% respectively ($p < 0.0001$ for all comparisons). As noted above, no percussion marks were observed in the AHD or FLK-NN2 assemblages. In contrast, PMs co-occur with 62.2% (84/135) of LDPTs with CO, LS, RC, and/or IF features observed in the EXP assemblage and 29.9% (111/371) of the FLK-Zinj assemblage. The frequencies of specimens with PM in both the EXP and FLK-Zinj assemblages are significantly greater than those that display TM at the LDPT with the fracture features ($p < 0.0001$ for both comparisons).

Additionally, although the presence of all fracture features was not coded, an additional 11 LDPTs representing 4 specimens from FLK-Zinj were coded for the presence cone or partial cone (coded as FLKO component for the LDPT types). Five of these are associated with percussion marks at the LDPT. None of these additional LDPTs are associated with tooth marks. No LDPTs in the other assemblages were coded for just the presence of cones or partial cones.

Table 5.19. Frequencies of LDPTs with cones or partial cones (CO), lateral stress (LS), radiating cracks (RC), and incipient flakes (IF) that co-occur with a percussion mark (PM) or tooth mark (TM) (at the LDPT) observed on limb fragments (excluding the ulna and LBSFs) in the four assemblages. Because, these features may co-occur on a single LDPT, both the frequency of LDPTs that exhibit one or more features as well as a the total number of times the features were observed are given. The first column for each assemblage (#) lists the total number of CO, LS, RC, and IF features that were observed on LDPTs with one or more of these features. The total number of times these features were observed on LDPTs is outside the parentheses in the totals while the number in parentheses is the actual number of LDPTs that exhibit one or more of the features. NISP values reflect the number of specimens that display one or more of the features and the number in parentheses is the actual NISP.

	AHD		FLK-NN2		EXP		FLK-ZINJ	
	#	NISP	#	NISP	#	NISP	#	NISP
<i>No TM or PM</i>								
CO	2	2	0	0	12	11	84	70
LS	17	16	2	2	30	17	198	129
RC	0	0	0	0	15	10	19	16
IF	2	2	1	1	18	17	25	22
total	21(20)	20 (18)	3 (3)	3 (3)	75 (50)	55 (21)	326 (250)	237 (146)
<i>TM assoc.</i>								
CO	5	5	0	0	0	0	1	1
LS	21	19	1	1	0	0	8	8
RC	2	2	0	0	1	1	1	1
IF	5	5	0	0	0	0	1	1
total	33 (28)	31 (26)	1 (1)	1 (1)	1 (1)	1 (1)	11 (10)	11 (10)
<i>PM assoc.</i>								
CO	0	0	0	0	33	27	42	37
LS	0	0	0	0	41	33	70	60
RC	0	0	0	0	28	20	15	14
IF	0	0	0	0	34	24	23	19
total	0 (0)	0 (0)	0 (0)	0 (0)	136 (84)	104 (53)	150 (111)	130 (90)
<i>Total</i>								
CO	7	7	0	0	45	38	127	108
LS	38	35	3	3	71	50	276	197
RC	2	2	0	0	44	31	35	31
IF	7	7	1	1	52	41	49	42
TOTAL	54 (48)	51 (44)	4 (4)	4 (4)	212 (135)	160 (75)	487 (371)	378 (246)

It is also useful to consider the frequency of specimens in which CO, LS, IF, and/or RC fracture features *not directly associated with a percussion or tooth loadpoint* (no TM or PM in Table 5.19), *but which do display a percussion or tooth loadpoint elsewhere on the specimen*. Although 21 AHD LDPTs with the target fracture features do not co-occur

with a tooth load point, 17 (89.5%) of these specimens display other diagnostic carnivore damage (i.e., a combination of TMRKs, TNTCHs, or TFLKSs). Of the 56 specimens represented by the 75 target LDPTs from EXP in which a PM or TMRK do not co-occur with the fracture features, 26 (43%) display PMs elsewhere on the specimen. No specimen from EXP or FLK-Zinj has a LDPT with these features and a carnivore LDPT elsewhere on the specimen. Of the 146 FLK-Zinj specimens that display CO, LS, IF, and/or RC fracture feature but lack an associated PM, 27 (18.5%) display a PM elsewhere on the specimen (either an isolated PM or a PM at a LDPT lacking a CO, LS, IF, and/or RC fracture feature). An additional 16 specimens conjoin with another fragment that exhibits a PM. Thus, 29.5% of the 146 specimens that do not have a LDPT in which a PM is associated with the target fracture features have a PM elsewhere on the specimen or conjoin with another percussion-marked specimen.

In total then, of the 146 FLK-Zinj specimens in which the LDPT is not directly associated with a PM, 32.2% (47) display a percussion damage elsewhere (27), conjoin with a specimen that has a percussion mark (16), or were coded for just a cone and have a percussion mark in direct association (4). Thus, 55.7% (137) of the FLK-Zinj specimens with a LDPTs with a CO, IF, LS, or RC are directly or indirectly associated with percussion damage.

5.4.5 Estimating Hominin and Carnivore Fracture Frequencies in the FLK-Zinj Fossil Assemblage

Given that 55.7% of the specimens with a LDPT and the target features also display percussion damage while significantly fewer, just 4%, are directly associated with tooth marks, it seems reasonable to assume that the majority of the remaining 99 specimens that display the target fracture features but are not directly associated with a percussion mark were in fact created by hammerstone fracture. An additional 51 specimens display percussion damage, but are not associated with a LDPT with a CO, LS, RC, or IF fracture feature. Thus, the frequencies of carnivore- and hammerstone-induced fractured bone in

the FLK-Zinj assemblage may be estimated by summing the a) 90 specimens with LDPTs that display the target fracture features directly associated with a percussion mark, b) 47 specimens where percussion marks are indirectly associated with the target LDPTs, b) 99 specimens that display a CO, LS, IF, and/or RC fracture feature but do not exhibit a PM, c) 51 specimens that lack a CO, LS, IF, and/or RC fracture feature, but which have a PM, and then, d) subtracting the target LDPTs associated with a tooth mark, 4 (0.04×99). Accordingly 53.9% (283/525) of the FLK-Zinj limb assemblage display evidence of hammerstone-induced fracture, and 5.7% were broken by carnivore chewing. *At a minimum his hammerstone breakage estimate using fractographic features in combination with percussion damage represents a 34% increase over that obtained by just using the presence of percussion marks* identified here. Fractographic analysis added another 95 hammerstone-fractured specimens to the 182 that display percussion marks. But again, many percussion marks would not have been identified on these 182 specimens were fractographic methods not used. Although it is difficult to know how comparable the samples are, this represents a 27% increase over Blumenschine's (1995) estimate and a 40% increase over that given by Dominguez-Rodrigo and Barba (2007b) based on percussion marks and/or hammerstone impact notches.

In contrast, fractographic analyses clearly demonstrate that FLK-NN2 assemblage limb bones were broken by carnivore chewing. Thus, fractographic analysis confirms previous interpretations (Bunn 1982; Potts 1988; Egeland 2007b) that FLK-NN2 is a carnivore-accumulated assemblage.

5.5 Synopsis

Several related analyses have been presented to determine whether or not certain fracture and fractographic features differentiate the modern hyaena assemblage and the likely carnivore fossil assemblage FLK-NN2 from the largely hammerstone broken EXP assemblage and the zooarchaeological assemblage FLK-Zinj. A synopsis of these analyses is given in Table 5.20, and is briefly summarized here.

This analysis began with an assessment of fragmentation in the assemblages. The mean specimen lengths for all assemblages are significantly different and, taken at face value (but see next chapter), fracture length does not differentiate the assemblages. The same is true for the number of fracture lines (#FLNs) to specimen length ratio where all but the EXP vs. FLK-NN2 ratios are significantly different.

Analysis of the number of LDPTs per NISP revealed clear and significant differences. Although overall the EXP and FLK-Zinj frequencies are significantly different many elements are not significantly different and, moreover, they are both significantly greater than either the AHD or FLK-NN2 assemblages. Here then the EXP and FLK-Zinj assemblages form a clear contrast to the AHD and FLK-NN2 assemblages. The frequencies of fifteen loadpoint types in the assemblages were compared. Overall, the AHD and FLK-NN2 assemblages are more similar to each other than they are to the EXP and FLK-Zinj assemblages, which in turn are similar. In particular, LDPTs with FLKO or FRFE components are typically absent or occur in very low frequencies in the ADH and FLK-NN2, but occur 3-16 times more frequently in EXP and FLK-Zinj.

Because many LDPT types are absent or occur in very low frequencies in all assemblages, but particularly AHD and FLK-NN2, the 15 types were collapsed into 4 types, flake scars (FLKS), notches (NTCH), cones/partial cones (FLKO), and those defined on the basis of less pronounced fracture features (FRFE). This analysis showed that FLKS frequencies were largely similar in all assemblages although AHD assemblage exhibits a significantly greater frequency than seen for the EXP material. The same is true of NTCHs, although in this case the frequency in the EXP assemblage is significantly less than in all other assemblages. Based on the FLKO frequencies, the assemblages clearly fall into two groups. The EXP and FLK-Zinj assemblages exhibit significantly greater frequencies than the AHD and FLK-NN2 assemblages in which FLKO LDPTs are absent or virtually so. The same pattern is seen for the FRFE LDPTs.

Principal component analysis makes the differences between the EXP and FLK-Zinj assemblages compared to the AHD and FLK-NN2 assemblages particularly clear.

The next analysis considered the frequencies of specific fracture features found at or immediately adjacent to LDPTs, i.e., incipient flakes (IF), radiating cracks (RC), hackle marks (HK), bulbar scars (BSc), cones/partial cones (CO), and lateral stress (LS). Overall, the total number of LDPTs that display one or more of these features is significantly greater in the EXP and FLK-Zinj assemblages, which are not significantly different, than in the AHD and FLK-NN2 assemblages. When the frequencies of individual fracture features are considered, no consistent pattern is apparent at first glance. For example, while incipient flakes are significantly more common in EXP and FLK-Zinj compared to the AHD assemblage, the FLK-NN2 frequency is not significantly different from either FLK-Zinj or AHD. Similarly, while radiating cracks are significantly more common in the EXP assemblage compared to the others, and while the FLK-Zinj frequency is significantly greater than that of AHD, the FLK-NN2 IF frequency is not significantly different from either FLK-Zinj or AHD. There is no difference in the frequency of hackle marks among the assemblages, and similarly while FLK-NN2 bulbar scar frequency is significantly greater than the AHD and EXP assemblages, which display similar frequencies, it is not significantly different from the FLK-Zinj frequency. The frequencies of LDPTs with pronounced fringe on adjacent fracture lines in the assemblages does not show a pattern either. The two features that distinguish the EXP and FLK-Zinj material from that of AHD and FLK-NN2 are cones/partial cones and lateral stress. For both fracture features the EXP and FLK-Zinj frequencies are significantly greater than those of AHD and FLK-NN2, which are not significantly different. Principal component analysis again makes the differences between the assemblages particularly clear. Lateral stress, cones, radiating cracks and lateral stress feature frequencies differentiate the EXP and FLK-Zinj assemblages from the AHD and FLK-NN2 material.

Table 5.20. Summary of analyses. For each analysis the assemblages are ordered from higher to lower frequencies. A greater than sign (>) indicates that the assemblage to the left exhibited a significantly greater frequency than the one to its immediate right. A greater than or equal to sign (\geq) indicates that while the assemblage on the left displays a greater frequency than the assemblage on the right, they are nearly equivalent in terms of their frequencies relative to the previous or subsequent assemblages. An equal sign (=) means that the frequencies are not significantly different.

Analysis	Results Summary
<i>Fragmentation</i>	
spec. lgth	•FLK-NN2 > EXP > AHD > FLK-Zinj
# fract. lines / spec. lgth	•AHD and FLK-Zinj relatively more similar with a smaller mean spec. lgth than the significantly larger FLK-NN2 & EXP means. •Does not distinguish AHD & FLK-NN2 from FLK-Zinj & EXP
<i>Fractography</i>	
# of LDPTs / NISP	•EXP \geq FLK-Zinj > AHD = FLK-NN2 •AHD & FLK-NN2 form 1 group with low frequencies. •EXP & FLK-Zinj form a 2nd group with high frequencies. •Distinguishes AHD & FLK-NN2 from EXP & FLK-Zinj.
15 LDPT Types	•Most of the LDPT types are absent or occur at very low frequencies in AHD & FLK-NN2. •Most
<i>LDPT Components</i>	
Flake Scar (FLKS)	•AHD \geq FLK-NN2 = EXP = FLK-Zinj •Does not distinguish the assemblages.
Cone/Partial Cone (FLKO)	•EXP \geq FLK-Zinj > AHD = FLK-NN2 •EXP frequency is significantly greater than that of FLK-Zinj but both have significantly greater frequencies than the AHD & FLK-NN2 frequencies, which are much lower & are not significantly different. •Distinguishes the EXP & FLK-Zinj assemblages from AHD & FLK-NN2.
Fracture Feature (FRFE)	•EXP \geq FLK-Zinj > FLK-NN2 = AHD •EXP & FLK-Zinj form a group with significantly greater frequencies than the group formed by AHD & FLK-NN2 which display much small frequencies which are not significantly different. •Distinguishes the EXP & FLK-Zinj assemblages from AHD & FLK-NN2.
Notch (NTCH)	•AHD = FLK-NN2 > FLK-Zinj = EXP •AHD & FLK-NN2, whose frequencies are not significantly different, are significantly different from both the EXP & FLK-Zinj frequencies, which are not significantly different. •Distinguishes the AHD & FLK-NN2 assemblages from EXP & FLK-Zinj.

Table 5.20. continued.

Analysis	Results Summary
<i>Fracture Features</i>	
# Fract. Feat. / LDPT	<ul style="list-style-type: none"> •EXP = FLK-Zinj > AHD ≥ FLK-NN2 •EXP & FLK-Zinj frequencies are not significantly different & therefor form a group whose frequencies are significantly different from those of AHD & FLK-NN2. •Distinguishes the assemblages.
Incipient Flake (IF)	<ul style="list-style-type: none"> •EXP > FLK-Zinj = FLK-NN2 = AHD •EXP frequencies are considerably & significantly greater than in the other assemblages. •FLK-Zinj frequencies are significantly greater than in AHD, but not significantly greater than in FLK-NN2. •The AHD & FLK-NN2 frequencies are not significantly different. •χ^2 does not distinguish assemblages, but Principal Component does.
Radiating Crack (RC)	<ul style="list-style-type: none"> •EXP > FLK-Zinj = FLK-NN2 = AHD •EXP frequencies are considerably & significantly greater than in the other assemblages. •FLK-Zinj frequencies are significantly greater than in AHD, but not significantly greater than in FLK-NN2. •The AHD & FLK-NN2 frequencies are not significantly different. •χ^2 does not distinguish assemblages, but Principal Component does.
Bulbar Scar (BSc)	<ul style="list-style-type: none"> •FLK-NN2 > FLK-Zinj > EXP = AHD •all means are significantly different. •Does not distinguish assemblages
Lateral Stress (LS)	<ul style="list-style-type: none"> •EXP = FLK-Zinj > AHD = FLK-NN2 •Distinguishes the assemblages.
Hackle Marks (HK)	<ul style="list-style-type: none"> •EXP = AHD = FLK-Zinj = FLK-NN2 •Does not distinguish the assemblages.
Cone (CO)	<ul style="list-style-type: none"> •EXP ≥ FLK-Zinj > AHD = FLK-NN2 •Distinguish the assemblages.
Fringe (FR)	<ul style="list-style-type: none"> •FLK-Zinj = EXP = AHD > FLK-NN2 •Does not distinguish the assemblages.

Table 5.20. continued.

Analysis	Results Summary
<i>Carnivore Damage</i>	
TM freq.	•AHD > FLK-NN2 = EXP > FLK-Zinj
LVRUP freq.	•FLK-NN2 > AHD > EXP > FLK-Zinj
LDPT freq.	•Distinguishes the assemblages •AHD > FLK-NN2 = EXP > FLK-Zinj
Total CVRE Damage	•Does not distinguish the assemblages •AHD ≥ FLK-NN2 > EXP ≥ FLK-Zinj
CVRE Break	•Distinguishes the assemblages •AHD ≥ FLK-NN2 > EXP ≥ FLK-Zinj
TM on FMC	•Distinguishes the assemblages •AHD > FLK-NN2 = EXP > FLK-Zinj
# TM / CVRE Break	•Does not distinguish the assemblages •FLK-Zinj > EXP > AHD = FLK-NN2
# TM / # TM on FMC	•TM seem much over-represented in FLK-Zinj •FLK-NN2 = EXP = FLK-Zinj = AHD •All display a similar ratio.
<i>Hammerstone Damage</i>	
PM assoc. w/ LDPT	•EXP > FLK-Zinj
Isolated PM	•FLK-Zinj > EXP
<i>Co-occurrence</i>	
<i>CVRE & HSTN</i>	
PM w/ TM on FMC	•EXP > FLK-Zinj
TM & PM	•EXP > FLK-Zinj
LVRUP & PM	•EXP > FLK-Zinj
CVRE LDPT & PM	•EXP = FLK-Zinj
CVRE Break & PM	•EXP > FLK-Zinj
Any CVRE Dmg. & PM	•EXP > FLK-Zinj
<i>Co-occurrence of TM or PM w/ Fract. Feat.</i>	
NISP w/ TM	•AHD ≥ FLK-NN2 > FLK-Zinj ≥ EXP
assoc. w/ LDPT w/ Fract. Feat.	•Most LDPTs with fracture features associated with TM in AHD •Very few LDPTs with fracture features associated with TM in EXP and FLK-Zinj
NISP w/ PM	•EXP > FLK-Zinj
assoc. w/ LDPT w/ Fract. Feat.	

The frequencies of damages diagnostic of carnivore chewing and hammerstone-induced bone breakage in the assemblages were then assessed. Overall, carnivore damage was significantly more common in the AHD assemblage while FLK-NN2 and EXP have similar frequencies and the FLK-Zinj assemblage displays the lowest frequency of total carnivore damage. Specimens with evidence of a carnivore break (carnivore LDPT, i.e., TFLKS, TNTCH, TFLKO, and/or a TM at the LDPT, or LVRUP damage) are significantly more frequent in the AHD and FLK-NN2 assemblages than in either the EXP or FLK-Zinj assemblages. Notably, the ratio of specimens with tooth marks to those broken by carnivores appears quite high in FLK-Zinj, as much as seven times greater than the AHD and FLK-NN2 material.

Percussion damage was observed only in the EXP and FLK-Zinj assemblages. While the overall PM frequency is significantly greater in the EXP assemblage, the frequency of specimens with one or more PM not associated with a LDPT (isolated PMs) is significantly greater in the FLK-Zinj assemblage.

Finally, in order to assess whether the fracture features that χ^2 and Principal component analyses indicated differentiate the EXP and FLK-Zinj assemblages from AHD and FLK-NN2 (i.e., incipient flake (IF), radiating crack (RC), lateral stress (LS), or cone (CO)) were created by carnivore or hammerstone-induced breakage, the frequencies of LDPTs with these fracture features and a PM or TM at the LDPT were tabulated. In both the EXP and FLK-Zinj assemblages negligible LDPTs with these fracture features were directly associated with tooth marks. In contrast, both assemblages have a significant proportion of LDPTs with these features that are directly associated with percussion marks. This association suggests that 1) lateral stress, incipient flakes, radiating cracks, and cones tend to be created by hammerstone impact, not carnivore chewing, and 2) the specimens in FLK-Zinj that display these fracture features but which do not display a PM at the loadpoint may be confidently interpreted as being created by hammerstone impact. Adding these specimens to those with a PM at the LDPTs that display the fracture features as well

as those that display a PM elsewhere on the specimen (but which are not associated with a target LDPT), and those that con-join with specimens with a PM indicates that 55% of the FLK-Zinj limb assemblage was broken by hammerstone impact. Thus, fractographic analysis increases the estimate of hammerstone breakage by at least 37 - 40% over that using percussion marks alone.

- CHAPTER 6 - *Discussion*

6.1 Introduction

There are three main goals to this study. The first goal has been to determine if a very limited suite of fracture patterns and fractographic features, which the material sciences literature indicates differ in materials broken by static and impact loading, can help define bones broken by the static loading of carnivore chewing from the impact loading that occurs when bones are broken by hammerstones. Four assemblages were used to assess the utility of fractographic principles and features to differentiate carnivore- from hammerstone-induced breaks.

Two of the assemblages are modern where the breakage agents are known, the Amboseli Hyaena Den and the Experimental assemblage created by hammerstone fracture (with some damages created carnivores prior or subsequent to hammerstone processing). These assemblages form the baseline for evaluating differences in the frequency and expression fracture patterns and features. The two Plio-Pleistocene fossil assemblages, FLK-NN2 and FLK-Zinj have been treated as the “unknowns”. However, previous work has shown that carnivores, likely hyaenas, were responsible for the FLK-NN2 assemblage (e.g., Bunn 1982; Potts 1988; Egeland 2007) and that at least part of the FLK-Zinj assemblage was accumulated and broken by hominins (e.g., Bunn and Kroll 1986; Oliver 1994; Blumenschine 1995; Dominguez-Rodrigo et al. 2007a). The overriding pattern demonstrated by fractographic analyses presented here is that breakage and damage patterns of the AHD and FLK-NN2 assemblages are similar to each other, but distinctly different from the EXP and FLK-Zinj assemblages, which in turn are similar to each other. Analyzing aspects of fragmentation and fracture patterns, particularly incipient flakes, radiating cracks, lateral stress, and cone fracture features associated with loading points, indicate one conclusion is that a fractographic approach holds promise for the understanding bone fracture and interpreting fragmented fossil assemblages.

Given these promising results, the second major goal of this work was addressed: Use the fractographic features that seem to differentiate the carnivore assemblages AHD and FLK-NN2 from FLK-Zinj and the largely hammerstone created EXP assemblage to refine the estimates of hominin involvement in the creation of the FLK-Zinj assemblage. Thus, a fractographic approach can also help us understand human behaviour and ecology.

Finally, it is incumbent that paleoanthropologists address the behavioural implications of their empirical work. The analyses addressing the first two goals simply constitute a methodological exercise. They are a means to establish baseline data – the extent of early hominin involvement in the creation of the FLK-Zinj fossil assemblage. The third goal of this work then, is to address the behavioural and socioecological implications of the newly estimated extent and character of hominin and carnivore involvement in the FLK-Zinj fossil assemblage. Did carnivores or hominins have first access to the animals represented? Were hominins securing and processing considerable amounts of meaty carcass parts, or were they scavengers of less meaty carnivore kills?

Following the introduction, this chapter has five main sections. In the first, 6.2 *Fragmentation Patterns*, and second sections 6.3 *Fractographic Patterns* each of the fragmentation and fractographic analyses presented above are discussed in terms of a) whether or not it meets the expectations outlined in Chapter 2 and b) the meaning the patterns and frequencies have for the assemblages studied. Assessing these patterns in terms of fracture agency is addressed in section 6.4 *Diagnostic Carnivore and Percussion Damage and Co-occurrence* and in section 6.5 that summarizes the co-occurrence of diagnostic damages with specific fracture features. Also presented in section 6.5 are revised estimates for early hominin involvement in the creation of the FLK-Zinj zooarchaeological assemblage. These discussions constitute a methodological exercise. Because of the important and broadly significant implications for early hominin behaviour and socioecology, in particular the meaning of early hominin entry into the carnivore guild, this study was driven by the need for accurate estimates the extent of hominin involvement

in the FLK-Zinj assemblage. In the final section, *6.6 Behavioural and Socioecological Implications for FLK-Zinj Hominins*, the socioecological implications of habitual carcass transport and meat-eating are explored.

6.2 Fragmentation Patterns

Fragmentation measures yielded mixed results, but discernable and explicable patterns are evident when previous conclusions about the fossil assemblages are acknowledged and fragmentation is recognized as a cumulative process. It was expected that greater levels of force application would create a greater degree of fragmentation. Accordingly, it was expected that the hammerstone-broken EXP assemblage would display greater fragmentation with shorter mean length and a greater number of fracture lines than the hyaena broken AHD assemblage. At first glance the fragmentation patterns, as measured by specimen length and the mean number of fracture lines per specimen length, do not appear to meet expectations. The mean length of size class 1-4 EXP fragments is significantly larger than the AHD pieces (85.9mm and 67.4mm, respectively, Table 5.1, Fig. 5.1b; ANOVA $p < 0.0001$, Table 5.2). Similarly, the EXP fragments displays a significantly smaller mean number of fracture lines per specimen length (0.07) than the hyaena-accumulated AHD assemblages (0.09, Table 5.3; ANOVA $p < 0.0001$, Table 5.4). By both measures FLK-Zinj is the most fragmented (mean length = 57.0mm, mean number of fracture lines per specimen length = 0.1) and FLK-NN2 the least fragmented of the assemblages (mean length = 118.0mm, mean number of fracture lines per specimen length = 0.05). So, the EXP assemblage is most similar to FLK-NN2 while the AHD is most similar to FLK-Zinj.

However, acknowledgment of site context (in this case the potential configuration of behaviours responsible for breakage) and acceptance of primary taphonomic agency assignments of previous studies of FLK-Zinj and FLK-NN2 makes assemblage comparisons more informative and brings them more into line with expectations. Previous research has indicated that hominins likely played a large taphonomic role in creating the

FLK-Zinj assemblage (e.g., Bunn and Kroll 1986; Oliver 1994; Blumenshine 1995; Dominguez-Rodrigo et al. 2007a), while FLK-NN2 has been interpreted as a likely carnivore accumulated assemblage (e.g., Bunn 1982; Potts 1988; Egeland 2007). Reasons for the dissimilarities in FLK-Zinj and EXP fragmentation as well as that of AHD and FLK-NN2 are broadly related to contextual aspects of the assemblages. More specifically, they reflect the nature of carnivore chewing over long time periods, as well as the fact that fragmentation is a cumulative process. Carnivores will often continue to fragment limb bones in order to gain access to as much marrow and cancellous tissue as possible. Because the AHD assemblage was accumulated by a large number of hyaenas (including infants and young) over a long period of time (Hill 1975, 1981), it is likely that there was some competition for bones and/or “boredom-related” bone chewing. More generally, unlike singular static loading events that may fracture bone, the fragmentation of carnivore chewed bones, and particularly that from large, long-occupied dens, is no doubt cumulative.

The second reason that these mean specimen length results are somewhat contrary to expectations is a reflection of the nature of experimental studies involving human-decision making. Breaking a limb bone open for marrow can be accomplished by one or many blows resulting in lesser or greater fragmentation. How does an experimenter decide how many blows are enough? In the archaeological assemblage, hunger may influence efforts to remove marrow and thus the degree of fragmentation. Planning and/or additional tool use may play a role in how much a bone is fragmented. For example, if the marrow is to be removed by another tool, e.g., a stick, or another actions, e.g., pounding the broken shaft vertically until marrow falls out, as done with the EXP hammerstone-broken bones, then only one blow may be necessary. Similarly, boredom or “nervous energy”, or desire for a snack when few unprocessed carcass parts are available may result in additional hammerstone-induced breakage. Like the carnivore den accumulations then (e.g., age and number of animals and length of occupation), human-decisions constitute a configurational aspect in the construction of analogues. Consequently, as argued elsewhere (Oliver 1986,

1989) it is often best to use analogues (and properly apply the principle of uniformitarianism) where patterns are produced by physical, immanent processes rather than those whose patterns may be structured by contextual (configurational) factors that are difficult to define for and project into the past (see Simpson 1970 for an exposition on the immanent and configurational aspects of uniformitarianism).

Note also should be made of the lower level of processing suggested by greater FLK-NN2 mean specimen length compared to AHD. Previous analyses have argued that carnivores accumulated the FLK-NN2 assemblage (Bunn 1982; Potts 1982, 1983; Egeland 2007). As such, the considerably different mean lengths of the AHD and FLK-NN2 specimens are interesting and suggest that there may be some species, behavioural and or ecological differences how the modern (AHD) and ancient (FLK-NN2) hyaenas accumulated bones. Whereas the AHD hyaenas clearly had the time and numbers to continue chewing and break more of the shaft in attempts to gain access to marrow, the FLK-NN2 hyaenas did not do much more than gnaw into the nutrient-rich epiphyses. Thus, more completeness in the FLK-NN2 assemblage may suggest fewer carnivores were present to modify bone for shorter periods of time or carcasses were not a scarce resource.

This seemingly odd juxtaposition of fragmentation values among the assemblages again highlights the role that site, behavioural, or experimental context plays in how taphonomic agents structure an assemblage. As argued above, while marrow removal may be the goal of both hyaena and hominin, it is difficult to mimic the decisions, and thus the consequent cumulative taphonomic patterns, made by one or more individuals when levels of competition, hunger, and time of site occupancy likely influence those decisions. Thus, the greater comminution of the AHD assemblage compared to FLK-NN2 is likely due to the former functioning as a clan and maternity den continuously for at least 10 years prior to excavation by Hill (1975) while FLK-NN2 seems to represent a short-lived burrow den (see Pokines and Kerbis Peterhans 2007). That is, at AHD, bones were exposed a large number of hyaenas of all ages for over a decade while it seem likely that the FLK-NN2

assemblage not only accumulated over a shorter time period (1-2 years?), but fewer hyaenas occupied the site. Similarly, while the hammerstone fracture experiments exposed the marrow cavity, they cannot replicate these same contextual variables (hunger, competition, and period of site occupancy) that structured the FLK-Zinj assemblage. More simply, when considering any measure of assemblage fragmentation, it is worth bearing in mind that force applied can be cumulative. As such, these data show that even for what seem to be the result of simple physical processes the configuration of processes and variables at work (particularly those with a strong behavioural and/or ecological component) will structure the resulting taphonomic pattern. When these contextual factors are considered, it remains notable both measures indicate that the FLK-Zinj assemblage is significantly more fragmented than AHD.

Other patterns are also worth noting. First, although not analyzed in detail here, the shaft fragments typically display slightly more fracture lines per mm than either the proximal (PSH) or distal (DSH) ends (Table 5.3). In part this likely reflects the difficulty in distinguishing between fracture and crushing in cancellous bone. Consequently it is difficult to count fracture lines on cancellous bone. Further, this is a reflection of the greater density of cortical bone of the shafts compared to the cancellous limb ends. Regardless of the force applied, cancellous bone tends to crush rather than produce distinct fracture lines. Fracture lines initiated in compact bone can propagate easily and multiple fracture lines may be created if enough force is applied and/or if pre-existing flaws or weaknesses are present.

Thus, the hypothesis should be re-phrased and the methods changed to adequately test the proposition that hammerstone-induced fracture creates greater fragmentation than carnivore chewing. First, the method should be altered to count and tabulate the number of fracture lines in compact bone of the shaft and those underlain by cancellous bone (at the metaphysis and epiphyseal ends). Counting which fractures are associated with cancellous bone cannot be accomplished using the current bone portion identifications because PSH

and DSH portions also include parts of the shaft. Second, several carnivore assemblages where the access time, group size, and length of occupation are known should be compared. Similarly, hammerstone-induced bone fracture experiments in which the intensity of processing is measured should be analyzed.

In summary, four points are notable. First, the FLK-Zinj assemblage, which all researchers agree has a large component of bones modified by hominins, displays shorter specimen length than the modern assemblage created by hyaenas, AHD. Second, specimens display a greater number of fracture lines in the FLK-Zinj assemblage than in that broken via hyaena bite-force, AHD. Third, differences in the measures for the two hyaena assemblages, AHD and FLK-NN2, and the two hominin modified assemblages, FLK-Zinj and EXP, indicate that although hyaena bite-force and hammerstone impact-force result in different levels of fragmentation, specific fragmentation values will be influenced by contextual factors, particularly cumulative nature of both carnivore and hominin bone processing. Finally, specimen size and the number of fracture lines may not be good measures of the amount of force applied to break bones and thus may not be a reliable measure to distinguish hammerstone and carnivore fractured bone because fragmentation is cumulative and because each agent gains access to the marrow cavity differently. Carnivore chewing of the epiphyseal ends, for example, creates many small fracture lines.

6.3 Fractographic Patterns

Fractographic analysis was restricted to features located at or immediately adjacent to where surficial damages, i.e., a percussion or tooth mark, and/or fracture features indicate the bone was subjected to loading that resulted in bone failure. Load points (LDPTs) are defined based on the presence flake scars (FLKSs), cones or cone fragments (FLKOs), notches (NTCHs), load or indenter marks (LMRKs), and the configuration of fracture features (i.e., incipient flakes (IF), radiating cracks (RC), bulbar scars (BSc), hackle marks (HK), cones/partial cones (CO), lateral stress (LS), and fringe (FR)),

fragment size, shape, and fracture lines (FRFEs), alone or in various combinations. The fractographic and fracture mechanics literature (Chapter 2) indicates that impact force can produce cones or cone fragments at the loading point while static loading does so only rarely. Also this literature suggested that more definable fracture features or a better expression of those features are created by impact compared to static loading. With a better expression of fracture features, some LDPTs, without the presence of FLKSs, FLKOs, or NTCHs, may be defined as FRFEs. It was therefore expected that the EXP assemblage should display more FLKO and FRFE load points than the AHD assemblage. And, if fragmentation in the FLK-Zinj was caused in large part by hammerstone-induced fracture, then it should also display a higher frequency of FLKO and FRFE LDPTs. If previous interpretations of FLK-NN2 as a carnivore (hyaena) accumulation are correct, it was expected that the assemblage should have resemble AHD more than either the EXP or FLK-Zinj assemblages.

For most analyses, the AHD and FLK-NN2 assemblages bear more similarities to each other and are significantly different from the EXP and FLK-Zinj material that, in turn, are largely similar. Overall, the EXP and FLK-Zinj material displays more LDPTs, LDPT types, and specific LDPT components (i.e., LDPTs defined on the basis of the presence of a cone/cone fragment – a FLKO, or other fracture features such as converging fracture lines associated with one or more other feature – a FRFE) as well as a significantly greater frequency of specific fracture features (i.e., incipient flakes, radiating cracks, cones/partial cones, and lateral stress) than that observed for the AHD and FLK-NN2 assemblages.

6.3.1 Loadpoint Frequencies, Types, and Components

On average an EXP size class 1-4 fragment (excluding the ULN and LBSFs) will display 1.8 LDPTs, three times the AHD frequency (0.61), nearly six times that seen in FLK-NN2 (0.29), but close to the 1.30 calculated for FLK-Zinj (Table 5.7, Figs. 5.3 and 5.4). The lower AHD LDPT frequencies are significantly different than the larger EXP and FLK-Zinj frequencies (χ^2 , $p < 0.0001$ for both comparisons), but not different to those

from FLK-NN2 (χ^2 , $p = 0.4937$; Table 5.8). FLK-NN2 is interpreted as a carnivore accumulated assemblage while the FLK-Zinj assemblage reflects a significant amount of hammerstone percussion. This is graphically shown in Fig. 5.5 where the LDPT to NISP ratios for identified elements in the EXP and FLK-Zinj assemblages overlap considerably, but are clearly separate from the AHD and FLK-NN2 assemblages whose ratios in turn overlap with each other.

In considering the lower frequency of LDPTs in the AHD and FLK-NN2 assemblages compared to those of EXP and FLK-Zinj, two aspects of how carnivores and hominins typically break into limb shafts are worth noting. First, the purpose here was to assess direct fracture of the limb shafts, not access to the marrow cavity gained via repetitive removal of cancellous bone at the epiphyses. While some LDPTs may be found epiphyses the suite of damages and fracture features employed to define LDPTs are largely based on features whose occurrence is restricted to compact bone on bone shafts. Thus, these LDPT frequency data do not reflect *overall* processing activity. Rather, they are a measure of effort to gain access to the marrow cavity directly via the shaft. As such, the differences in LDPT frequencies in part reflect the difference in how hammerstone-wielding hominins and carnivores gain access to the marrow cavity. Hominins using hammerstones tend to gain direct access to the marrow by breaking into the limb shaft first. Carnivores tend to chew at the epiphyseal ends first gradually opening up the marrow cavity, leaving relatively fewer definitive LDPTs on the compact bone of the shaft. This mode of access may create the lever-up fragment diagnostic of carnivore fracture (see below) in which definitive LDPTs are lacking.

Second, given that percussion-induced fracture often involves the use of a hammerstone and anvil, for any one percussive action two LDPTs may be formed on any one fragment that preserves both sides of the shaft. In contrast, opposing LDPTs are less likely to be created by carnivore chewing because most carnivore-induced fractures were initiated from the shaft ends exposed by previous gnawing of the metaphyses and

epiphyses, a process in which loading opposite sides of the shaft is not always necessary (i.e., gnawing of one side of an exposed shaft will create fracture). Also, even where a carnivore places the entire shaft between its carnassials, either may serve simply as an “anchor” and failure can be initiated on just one side. Where failure is initiated from one side only one LDPT may be created. And if opposing LDPTs are created they are less likely to be recognized using this method. This is because it seems likely that most are formed in areas underlain by cancellous tissue that may not preserve the fracture features examined here. Furthermore, it seems that many flakes and scars created by carnivore chewing are formed on already existing fractures.

The patterning in the frequencies of the 15 LDPT types and their four main components (flake scars - FLKS, cones/partial cones - FLKO, fracture features - FRFE, and notches - NTCH) in the assemblages further shows how similar are the EXP and FLK-Zinj fractures compared to those from AHD and FLK-NN2 which in turn are similar to each other. Several LDPT types observed in the EXP and FLK-Zinj assemblages were not observed or were present in very low frequencies in both the AHD and FLK-NN2 assemblages (Table 5.5 and Table 5.9). While all assemblages are dominated by LDPTs with FLKS or NTCH components, they are much less frequent in the EXP and FLK-Zinj assemblages in which LDPTs with FLKO or FRFE components each comprise between 16% and 26% of the observed LDPTs (Table 5.10 and Fig. 5.7). The significantly greater frequencies of LDPTs with a FLKO or FRFE component in EXP and FLK-Zinj compared to those in the AHD and FLK-NN2 assemblages (Table 5.12) indicates that these LDPT types, particularly FLKOs may be confidently used to identify bones broken by hammerstones. Principal component analysis shows just how useful these LDPT types are in separating the EXP assemblage created by hammerstone percussion and FLK-Zinj with which is similar from the modern hyaena den, AHD and FLK-NN2 (Fig. 5.9).

To summarize, the LDPT frequency, type, and component analyses reveal the following patterns that confirm expectations based on the fractographic literature. First, the

significantly greater number of LDPTs in the EXP and FLK-Zinj assemblages compared to those of the AHD and FLK-NN2 assemblages is in part a consequence of the method. The fracture features examined may define LDPTs created in the compact bone of the shaft as well as document differences in the nature of percussion breakage using hammerstone and anvil compared to static carnivore chewing. Hammerstone and anvil percussion focused exclusively on the shaft characteristically yields opposing LDPTs, whereas in the seemingly infrequent instances where carnivores attempt to break an unbroken shaft (and not as is typical attack the bone ends), tooth wedging on one side of the shaft may initiate fracture without creation of a discernable opposing LDPT. Further, because an individual impact fracture event creates a greater number of fragments than static loading (pers. observ. but not clearly demonstrated in the above analysis of specimen length or the number of fracture lines per specimen length), more fragments will include part of LDPT.

Second, the diversity of LDPT types is greater in the EXP and FLK-Zinj compared to the AHD and FLK-NN2 assemblages in which many types – particularly those with a FLKO or FRFE component – are absent or occur in negligible frequencies, but which occur 3-16 times more frequently in the EXP and FLK-Zinj assemblages. Third, in all assemblages the most common loading points have flake scar (FLKS) and notch (NTCH) components. This is because both static and impact loading can produce each LDPT component.

Fourth, the significantly greater frequencies of LDPTs that have either a FLKO or FRFE component in the percussed EXP assemblage compared to the carnivore accumulated AHD assemblage (52.6% and 10.9%, respectively; Table 5.12), supports the fractographic expectation that cones/partial cones as well as expression of finer-scale features (FRFE) should be greater in assemblages broken by percussion than in those broken by static carnivore chewing. Therefore, these LDPT types can be used to identify bones broken by impact force, i.e., by hammerstone percussion. Accordingly, overall similarity of the EXP and FLK-Zinj assemblages in terms of their overall number of

LDPTs (significantly greater than either AHD and FLK-NN2), their type (all 15 types present), and component frequencies (significantly greater frequencies of LDPTs with a FLKO or FRFE component than with AHD and FLK-NN2) supports previous work that indicating that hominins processed many bones for marrow at FLK-Zinj. Finally, the overall similarity of the AHD and FLK-NN2 assemblages in terms of their overall number of LDPTs (lower than either EXP and FLK-Zinj), their type (many not observed or rare), and component frequencies (FLKO and FRFE components are rare) supports previous work that interpreted the FLK-NN2 assemblage as being created by carnivores, likely hyaena.

6.3.2 Fracture Features

As noted in Chapter 2, LDPT expressions are often quite subtle and their presence is often revealed only by careful examination of fracture features (FRACFEAT) on the cortical and fracture surfaces. Moreover, many LDPTs, particularly FLKOs and FRFEs but FLKs and NTCHs as well, would go unrecognized by ignoring other, finer-scale fracture features. Fracture features particularly useful in identifying LDPTS include incipient flakes (IF), radiating cracks (RC), bulbar scars (BSc), cones or bulbs (CO), hackle marks (HK), lateral stress (LS), fringe/feathering (FR), and un-coded feature such as diverging fracture movement directions. Although some of these features, i.e., incipient flakes, radiating cracks, hackle marks, and bulbar scars have been noted before, they along with others introduced here, i.e., cones, lateral stress, and fringe, have not been explicitly used to help identify LDPTs, let alone quantified to assess differences in assemblages created by different agents. Data reported above demonstrates that a) these fracture features aid in LDPT identification, b) some previously recognized features are occur frequently on both carnivore and hammerstone fractured bone, but c) many fracture features define the fracture agent.

Data reported above support most expectations based on the fractographic and fracture mechanics literature. For example, fracture features are more common and better

expressed on bone broken by percussion (i.e., the EXP assemblage) than the static loading of carnivore chewing (i.e., the AHD assemblage). The hammerstone-broken EXP assemblage displays over twice the number of fracture features per LDPT (2.23 fracture features per LDPT) than observed in the AHD assemblage created by spotted hyaenas (1.07 fracture features per LDPT; Table 5.14, Fig. 5.10). The fractographic reasons for this difference include a) impact causes fracture fronts to move more rapidly than with static loading and greater fracture front speeds destabilize fracture front movement directions creating more fractographic features, b) static loads may be absorbed in a more restricted area than impact loading where the excessive load must be dissipated over a larger area thus creating more damage. The FLK-Zinj fracture feature frequencies per LDPT are nearly as high (1.81 fracture features per LDPT) as the EXP frequencies and are 1.6 to 2 times that observed for the AHD and FLK-NN2 material (0.8 fracture features per LDPT). This pattern indicates again that the FLK-Zinj assemblage includes a large number of hammerstone-broken bones while carnivore chewing fractured the FLK-NN2 limb bones.

Like their near equivalent FLKO LDPT, the cones/partial cones fracture feature (CO) is created almost exclusively by impact. Other fracture features, i.e., incipient flakes (IF), radiating cracks (RC), and lateral stress (LS) are also created significantly more often at impact LDPTs than on the static loading LDPTs of carnivore chewing. However, some recognized features supposedly diagnostic of impact-induced breakage, i.e., hackle marks (HK) and bulbar scars (BSc) occur frequently on both carnivore and hammerstone fractured bone. The lack of difference in the AHD and EXP HK means is somewhat surprising given that the fractographic and fracture mechanics literature indicates this feature is associated with the greater force produced by impact loading (Chapter 2). Hackles are often difficult to identify even in isomorphic material, however. It seems likely that this linear feature (that points to the loading point origination) observed at LDPTs in the four assemblages, despite their similarity to hackle marks, may have a different genesis. As such, the use of hackle marks to define hammerstone-broken bones by Bonnichsen

(1979) and others (e.g., Johnson 1985 and Hannus 1989, 1990) seems inappropriate, and others have pointed out that what are called hackle marks are created by carnivore-induced fracture (Haynes 1983a, 1983b). As with lithics, bulbar scars are often difficult to differentiate from the proximal to distal curvature of FLKSs and true bulbar scars are often appear similar to flake scar curvature created in pressure flaking (Cotterell and Kaminga 1987; Quinn 2007). Thus although sometimes cited as a damage indicative of hammerstone fracture (e.g., Bonnichsen 1979; Johnson 1985; Hannus 1989, 1990), the frequencies observed in this study indicates that bulbar scars, alone, are not diagnostic of impact fracture.

Some features are expected to vary between modern actualistic and experimental assemblages compared to fossil assemblages produced by the same agent. For example, it seems likely that higher frequency of incipient flakes (IF) and radiating cracks (RC) on the EXP material and the considerably lower values in the other assemblages may be explained by these features fragility. Both features are fractures in which both fracture faces remain attached. They should be more readily preserved on recent bone assemblages (i.e., the EXP material and even the AHD material) because periosteum or other soft tissue may bind fractured pieces together and because they have not been subjected to the all of the post-fracture taphonomic processes and diagenesis that effect the appearance of fossil assemblages.

Overall, as verified by chi-square, Fisher's exact test, and Principal component analysis (Fig. 5.13 and Fig. 5.14), incipient flakes, radiating cracks, cones/partial cones, and lateral stress features differentiate the hyaena gnawed AHD assemblage where the frequencies of these features are significantly lower than those from the hammerstone created EXP assemblage. The same pattern is seen in the comparison of the FLK-NN2 and FLK-Zinj fracture feature frequencies with those of FLK-Zinj being similar to the EXP assemblage but significantly different from those of FLK-NN2, which is in turn similar to

AHD. Thus, high frequencies of incipient flakes, radiating cracks, cones/partial cones, and lateral stress at LDPTs are indicative of hammerstone-induced fracture.

6.4 Diagnostic Carnivore and Percussion Damage and Co-occurrence

Since carnivore damage is present in both the EXP and FLK-Zinj assemblages it was necessary to assess whether or not the fracture features that are significantly more common in the EXP and FLK-Zinj assemblages tend to be associated with percussion or carnivore damage at the LDPT. This assessment first required tabulation of the frequencies of diagnostic carnivore and percussion damages in the assemblages. Carnivore damages tabulated comprise bones with tooth marks (TM), carnivore LDPTs (TFLKS and TNTCH), and fragments that display a leverup (LVRUP). Total carnivore damage includes specimens with a TM, including those with a TM on the fracture, medullary, or cancellous surfaces, or evidence of carnivore break (CVRE Break), the latter of which is the sum of specimens with a LVRUP or carnivore LDPT damage. Percussion marks, both isolated marks and those associated with a LDPT on a fracture surface, were tabulated for each assemblage. No percussion marks were observed in the AHD and FLK-NN2 assemblages. No PMs were expected in the AHD assemblage because it is a carnivore accumulation. The lack of PMs in the FLK-NN2 indicates again that hominins were not involved in formation of this assemblage.

6.4.1 Carnivore Damage

As with the fractographic analyses, the assemblages fall into two groups based on their carnivore damage frequencies: The AHD and FLK-NN2 assemblages are similar to each other and tend to display significantly higher frequencies of carnivore damage than from those of the EXP and FLK-Zinj assemblages, which in turn display largely similar frequencies of carnivore damage. For example, over 70% of specimens display one or more tooth marks in the AHD, FLK-NN2, and EXP assemblages. The frequency is significantly lower in the FLK-Zinj assemblage, where only 41% of the sample shows tooth marks (Table 5.16; (Fisher's exact test is used because only the summed frequencies

are compared; $p < 0.0001$ for all comparisons except FLK-NN2 vs. EXP where $p = 0.6252$). The frequencies of leverup specimens are significantly greater in the AHD (30.7%) and FLK-NN2 (61.4%) assemblages compared to those of EXP (13.7%) and FLK-Zinj (1.2%) ($p < 0.0001$ for all comparisons except AHD vs. EXP where $p = 0.0007$). The frequencies of specimens with a carnivore load point are lower in all assemblages, 34.7% of the AHD material, 17.0% of FLK-NN2, 3.2% of the EXP sample, and 4.4% of the FLK-Zinj material. Only the EXP and FLK-Zinj carnivore load point frequencies are not significantly different (AHD vs. FLK-NN2, $p = 0.0013$; AHD vs. EXP, $p < 0.0001$; AHD vs. FLK-Zinj, $p < 0.0001$; FLK-NN2 vs. EXP, $p = 0.0021$; FLK-NN2 vs. FLK-Zinj, $p < 0.0001$; EXP vs. FLK-Zinj, $p = 0.7831$). Frequencies of specimens with evidence of a carnivore break (i.e., TFLKS, TNTCH, TFLKO, and/or a TM at the LDPT, or LVRUP damage) are significantly higher in the AHD and FLK-NN2 assemblages (54.1% and 64.8% of the samples, respectively) than in either the EXP or FLK-Zinj assemblages (15.8% and 5.6% of the samples, respectively) ($p < 0.0001$ for all comparisons).

It is important to note, however, that in spite of their accepted use as a damage diagnostic of carnivore damage, tooth marks are sometimes difficult to differentiate from other lineations. The FLK-Zinj assemblage does have a considerable number of lineations that while superficially similar to TMs were not coded as such in this study. My notes contain numerous comments like “What are these marks? They don’t look like tooth marks, but what are they? There are not enough diagnostic tooth marks or fracture damages for them all to be tooth marks.” In many cases time constraints made it impossible to evaluate each and every mark on all specimens. In fact, as shown in Table 1.1, the estimates of carnivore tooth marks in the FLK-Zinj assemblage have varied considerably. Blumenshine (1995) reports tooth marks on 65% of the assemblage, while Dominguez-Rodrigo and Barba (2006), using experimental data showing that many marks with irregular edges and profiles are likely the result of bioerosion (by fungi and/or bacteria), report tooth marks on less than 16.8% of the assemblage. Using Dominguez-Rodrigo and

Barba's work with bioerosion and their refined tooth mark definitions, Parkinson (2013) reports tooth marked bone frequencies of 24.5%. The tooth mark frequencies for FLK-Zinj observed in this study, 40.7% of the NISP, lies between these high and low estimates, but did not take bioerosion into account. Despite the cautionary approach of this study, the tooth mark frequencies reported here appear too high. Consequently, the tooth mark to carnivore break ratio for FLK-Zinj is inordinately high compared to that of AHD and FLK-NN2 assemblages (Fig. 5.17). The comparably high EXP tooth mark to carnivore break ratio is due to the fact that because the zoo hyaenas were well-fed they did not break many bones but would attempt to remove remaining soft tissue. Sala et al. (2014) have also observed that captive wolves produce higher tooth mark frequencies than wild populations; higher tooth mark frequencies seem to be characteristic of captive carnivores.

Interestingly, however, the frequency of FLK-Zinj specimens with tooth marks on the fracture, medullary, or cancellous surfaces, 25%, is nearly identical to the overall tooth mark frequencies reported by Dominguez-Rodrigo and Barba (2006) and Parkinson (2013). It seems that the frequencies of TM on FMC surfaces may more accurately reflect overall carnivore damage than overall TM frequencies reported here for several reasons. First, the tooth mark to carnivore break ratio indicates that the tooth mark frequencies are too high. Second, tooth mark estimates given here were collected before the bioerosion study of Dominguez-Rodrigo and Barba (2006). Finally and critically, because there are fewer marks on these surfaces than on the cortical bone, more time was spent assessing each mark and assigning agency; it was possible to study each mark on these surfaces in detail and be more confident in identification of tooth marks.

Accordingly, the estimate of the carnivore involvement in modification of the FLK-Zinj assemblage likely ranges between 5.6%, the frequency of bones with evidence of carnivore breakage, and 25%, the frequency of specimens with tooth marks on the fracture, medullary, or cancellous surfaces. Given the ongoing issues with identification of tooth marks, the most conservative (and perhaps realistic) estimate of carnivore activity at FLK-

Zinj may in fact be the frequency of bones broken by carnivores. FLK-NN2 is certainly has a high degree of carnivore involvement based on its similarity in carnivore damage frequencies with those of AHD.

Further, as noted by Parkinson (2013) although the distribution of tooth marks does suggest some felid activity, there is little evidence that felids were responsible for most of the (over-estimated and incorrect) tooth marks. Blumenschine and colleagues (Blumenschine 1987, 1995; Capaldo 1997; Selvaggio 1998; Pante et al. 2012, 2015) have cited as evidence of scavenging of felid kills. Rather, the frequencies of tooth marks on fracture, medullary, and cancellous surfaces reported here indicate that most carnivore damages were inflicted at FLK-Zinj after marrow processing by early *Homo*. This finding lends further support to the use of fractographic features to diagnose fracture agency and the carcass access sequence.

6.4.2 Percussion Damage

An important finding of this study is that the frequency of FLK-Zinj limb specimens with percussion marks observed in this study, 34.9% of the NISP, is greater than that observed by Blumenschine (1995; 27.4%) and Dominguez-Rodrigo and Barba (2007b; 20.0%). This discrepancy may be explained by differences in methodologies. First, the method employed here required that each fracture surface be carefully examined. Consequently, it is likely that more time was spent examining each bone in this than in previous studies. Second, when a combination of fracture features or the number of fracture lines or the intersection of fracture lines or fracture shape suggested the presence of a loading point, the cortical surface of the suspected LDPT was examined carefully under a microscope. Third, as with the EXP assemblage, many PMs appear as very faint striae near the loading point, but lack the often-characteristic irregular or crushed depression. Consequently, this method allowed the identification of less obvious PMs. Regardless, all estimates of early hominin involvement with FLK-Zinj based on percussion

marks are well below 50%. The critical issue remains, *how was the remaining and largest portion of the limb bones broken.*

6.4.3 Co-Occurrence of Percussion Marks and Carnivore Damage

Carnivore access to previously hammerstone-broken bones as well as hammerstone breakage of bones previously gnawed by hyaenas resulted in the co-occurrence of percussion and carnivore damage on specimens in the EXP assemblage (Table 5.18, Fig. 5.20). Although the overall co-occurrence of tooth and percussion marks is over 50%, the frequencies of specimens with tooth marks on the FMC as well as those in which a percussion mark co-occurs with a carnivore LDPT or LVRUP are considerably lower. In all of the latter cases, the carnivore damage was inflicted following hammerstone breakage because carnivore marks overlay hominin-induced damage. The FLK-Zinj assemblage displays a similar pattern. About 9% of bones where both damages co-occur, tooth marks or carnivore LDPTs (40 specimens or 7.7% plus four specimens with carnivore LDPTs that do not display FMC TMs or 0.8%, respectively) are found on fracture surfaces created or exposed by hammerstone fracture. The LDPTs and LVRUPs are all overprinted on fracture surfaces created by percussion fracture. So, while overall 25% of the FLK-Zinj assemblage displays FMC TMs, these PM and carnivore co-occurrence data directly document carnivore scavenging of the hominin food remains at FLK-Zinj.

6.5 Co-Occurrence of Percussion Marks or Tooth Marks at LDPTs with Incipient Flakes, Radiating Cracks, Cones, or Lateral Stress and Estimates of Hominin Involvement in the FLK-Zinj Fossil Assemblage

As noted above (e.g., Table 1.1) although all analysts have noted the presence of hammerstone-broken bones in the FLK-Zinj assemblage, none of the frequency estimates even approach 50%. The critical issue remains; *can this estimate be improved using fractographic methods?* Certainly statistical analysis of the fractographic data indicates significant differences in fracture feature frequencies in the AHD and FLK-NN2 compared to those of EXP and FLK-Zinj. Can these features be directly related to percussion fracture? The co-occurrence of incipient flakes, radiating cracks, cones, and lateral stress

fracture features with carnivore damage and percussion marks were analyzed to determine if these features were created by carnivore activity or percussion fracture.

The answer to the above questions is yes; fracture features examined here are useful in diagnosing fracture agency. Incipient flakes, radiating cracks, cones/partial cones, and lateral stress overwhelmingly co-occur with percussion marks in the EXP and FLK-Zinj assemblages.

The damage frequency data define the boundary conditions for an accurate assessment of hominid and carnivore behaviours that created the FLK *Zinjanthropus* fossil assemblage. That is, these data quantify the degree of hominid and carnivore involvement in assemblage creation, as well as the nature of hominid-carnivore competitive interactions, including the sequence of access to carcass-parts. Moreover, data presented here provide a firm archaeological basis for exploring the socioecological implications of habitual animal food transport by early *Homo*.

The fractographic approach employed here has substantially improved the estimate of hammerstone-induced fracture in the FLK-Zinj assemblage. While hominins and carnivores both played a role in the modification of the FLK-Zinj assemblage, 54% of the assemblage was broken by hammerstone-wielding hominins. This is a minimal estimate because the fractographic method used here permitted the identification of percussion marks that would have otherwise been overlooked. This figure represents approximately a 34% increase over estimates based solely on the presence of percussion marks and constitutes 75% of the limb Minimum Number of Elements (MNE). The frequency of carnivore-modified bones is considerably lower, 25% (if the frequency of TMs on FMC surfaces is accepted as a better estimate than the likely too high overall TM frequency). Comparisons of types of carnivore damage, as well as the extent of hominid-induced damage, reveal other aspects of the character of hominid-carnivore competitive interactions. Most carnivore damage is minor, consisting of tooth pits and scores; more severe damages such as flaking, chipping, polish and furrowing are rare. The lack of tooth

marks, polish, and furrowing is consistent with the low frequency of carnivore-fractured bone (5.6% of the assemblage). Thus, not only is the overall extent of carnivore damage (25%) low, damage severity is slight.

Hominid and carnivore damage co-occurrence frequencies are also instructive in determining the access sequence. If early *Homo* was a habitual scavenger of meat-poor, skeletally-intact, carnivore-ravaged carcasses as argued by Blumenshine (1986, 1987, 1995) and others (e.g., Cavallo and Blumenshine 1989; Selvaggio 1994; Capaldo 1997; Pante et al. 2012, 2015; Pobiner 2015), then one might expect a high frequency of specimens to exhibit both carnivore and hominid damage. Only 11.5% of the limb assemblage displays both carnivore tooth marks and percussion damage suggesting that *hominins were not scavenging from carnivore-ravaged carcasses, and overall carnivore involvement in the FLK-Zinj assemblage was minimal*. Additionally, evidence for carnivore fracture on only about 9% of the previously hammerstone-fractured bones and those displaying tooth marks on the fracture, medullary, and cancellous bone surfaces created or exposed by hammerstone fracture indicates that in fact it was the carnivores who were scavenging the hominin food refuse. Thus, in conjunction with previous studies of cut marks and bone frequency patterns (Bunn 1981; Bunn 1982; Bunn and Kroll 1986; Potts and Shipman 1981; Potts 1982, 1988; Dominquez-Rodrigo and Barba 2007b), the hammerstone fracture frequency and carnivore hominin damage co-occurrence data presented here demonstrate that FLK Zinj was indeed a site of *habitual* carcass processing by early *Homo*, the refuse from which was later scavenged by carnivores.

The carnivore damage data may also give some indication of the type or size of carnivore involved. First, the comparative lack of carnivore-induced fractures and heavy pitting or scoring of epiphyseal ends suggest that the carnivore responsible for much of the damage may not have been a large, habitual bone-crushing animal like the hyaena, but rather a smaller carnivore that could make use of small meat scraps adhering to small bone fragments after hominin abandonment of their food refuse. The presence of micro-

mammals at FLK Zinj that Andrews and Evans (1983) have interpreted as the remains of genet scat also implies scavenging by small carnivores. Experimental studies have shown that rodents are one of the first scavengers of carcasses (Young et al. 2014). Thus, it seems reasonable to conclude that the abandoned food refuse not only acted as an attractant for medium to large carnivores, but also created a new microhabitat that attracted rodents, who in turn may have attracted other, smaller carnivores. That food refuse acts as an attractant for carnivores and rodents was certainly the case for many later archaeological sites (e.g., the Cherokee Sewer Site, Iowa, Semken, 1980, pers. comm., 1993; Quanhucun, China, Hu et al. 2014).

There are some similarities in the FLK Zinj limb bone fragmentation and that documented for modern hunter-gatherers, notably the Hadza (Bunn 1989; Oliver 1993). That is, FLK Zinj limb bones were not merely hit with hammerstone at the midshaft and the halves separated, as illustrated in earlier experimental studies of bone fracture (e.g., Bonnicksen, 1979; Johnson 1985) and as created in the EXP assemblage. Rather, bones can exhibit numerous impact marks along the shaft, fractures through the epiphyseal ends, or numerous impact marks at or near the epiphyseal end. During bone processing the Hadza frequently pound the epiphyseal ends to gain access to bloody, fat-rich cancellous tissue. This activity reduces some epiphyseal ends to unidentifiable fragments of cancellous bone (Oliver 1993). Thus, the presence of split epiphyseal ends, epiphyseal fragments, numerous impact marks, and impact marks at or near epiphyseal ends in the FLK Zinj assemblage suggests that the character of consumption behaviour undertaken by early *Homo* may have been similar to that of the modern Hadza. That is, the severity of the damages is more than required to remove marrow from the midshaft cavity alone. The severity of hammerstone-induced damage demonstrates concern with, and consumption of, the blood-rich cancellous ends. This intense processing may explain part of the loss of epiphyseal ends at FLK-Zinj noted previously by Bunn (1982; Bunn and Kroll, 1986).

Thus, hominin behaviour represented by FLK-Zinj indicates hominins were regularly acquiring meat-rich carcasses. As argued by others on the basis of much smaller percussion and cut mark frequencies (e.g., Bunn and Kroll 1986; Oliver 1994; Dominguez, Rodrigo et al. 2007a) as well as new studies of bovid age profiles which suggest hominin ambush hunting (Bunn and Gurtov 2014), data presented here demonstrate that Oldowan hominins were firmly established within the upper levels of the carnivore guild. Moreover, although meat-eating has been the over-riding concern of many paleoanthropologists, it is important to recognize another critical behaviour first emphasized by Isaac (1978a, 1978b) — *hominins habitually transported food to FLK-Zinj*. This behaviour is unique among primates.

Brantingham (1998) has also noted the importance of food transport in locating a carnivores position in the carnivore guild. His analysis of carnivore transport strategies using MNE head and limb frequencies for several carnivores and early hominins as represented by Plio-Pleistocene sites at Turkana and Olduvai Gorge indicates that early hominins had carved out niche space between the top carnivores and confrontational carnivores like hyaenas. Not only does this suggest early hominins were able to compete directly with large carnivores at kills, and had early access to meat-rich carcasses, it suggests that active hunting may have occurred. To fully appreciate the importance of data presented here and the importance of food transport the socioecological implications of carcass transport must be explored.

6.6 Socioecological Implications of Hominin Activity at FLK-Zinj

Early *Homo* was the primary agent of bone accumulation and modification at FLK Zinj. This seems clear from fractographic data given here, the co-occurrence of carnivore and hominin damages, and the resultant new estimates of hammerstone-fractured bone. Previous studies of cut mark frequencies (e.g., Bunn and Kroll 1986; Oliver 1994; Dominguez-Rodrigo and Barba 2007b), recent detailed analysis of tooth mark locations (Parkinson 2013), as well as new studies of bovid age profiles which suggest hominin

ambush hunting (Bunn and Pickering 2010; Bunn and Gurtov 2014) all indicate early *Homo* was the primary bone accumulation agent at FLK-Zinj.

Although it is now well documented that the early hominin diet included a substantial amount of animal tissue by about 1.8mya or earlier, the socioecological mechanisms that lay behind this novel behaviour have not been adequately explored. In particular it is not just the addition of animal tissue in the diet and entry of early hominins into the carnivore guild that is important. As first noted by Isaac (1978a, 1978b), *an equally notable and critical behaviour is the transport of food — a behaviour not exhibited by other primates*. Given that many carnivores transport food and that many of these live in environments similar to those inhabited, or at least frequented by, Plio-Pleistocene hominids, e.g., riparian woodlands, grassy woodlands, and open grasslands, it is reasonable to examine carnivore behaviour for insights into the biological and ecological mechanisms that determine food transport behaviour (Oliver 1994, and on which much of the following discussion is based). “Hominid dietary strategies must be understood within the larger context of carnivore behaviour and ecology...” (Lewis 1997: 257)

Carnivores are one of the few animals other than modern humans and birds that habitually transport food to a discrete location for consumption (Eisenberg 1981; see also Clutton-Brock 1991). Data on carnivore behaviour and biology, particularly food transport and intra- and interspecific competition behaviour (e.g., Ewer 1973; Kruuk 1972; Mech 1970; Rasa 1984; Rood 1986; Schaller 1972) may be particularly relevant. These data suggest that there are two major factors that work together to promote food transport to established dens or other protected locations: (1) the presence of altricial young, and (2) intensely competitive and dangerous interactions with other predators at food resources (i.e., carcasses). Moreover, the anti-predator behavioural responses that result from these two conditions, including the establishment of dens, food transport and various forms of group defense, are themselves a result of two environmental factors: (1) living in open to semi-open habitats with (2) high predator densities. Studies of carnivore sociality

frequently cite the need for anti-predator defensive strategies as a likely explanation for the evolution of carnivore sociality (Gittleman 1989; Treves and Palmqvist 2007). In fact, sociality in carnivores may have evolved as a response to the establishment of expansive grasslands in the late Pliocene (Martin 1989). The need for effective anti-predator defensive strategies, including denning and food transport, is particularly true for smaller species that cannot defend themselves individually from larger competitors (Ewer 1973; Kruuk 1972) and for species living in open habitats where vulnerability to predation increases due to a lack of cover (Lamprecht 1981). For larger carnivores, the explanation favoured for the evolution of sociality, is the increased hunting efficiency afforded by cooperative foraging behaviour (Gittleman 1989; Kruuk 1972; Lamprecht 1981; Schaller 1972).

As noted by many (e.g., Eisenberg 1981; Schaller and Lowther 1969; Lovejoy, 1981), the common social context for food transport and processing among many carnivores is the presence of young in the group, particularly altricial young. Because of their biological characteristics (limited strength, endurance and mobility, poorly developed senses and rapid post-natal growth rate), however, altricial young carry a high ecological cost to the infant, mother, and other group members. Specifically, altricial infants are highly vulnerable to predation and have high nutritional and energy demands to meet rapid post-natal growth rates that, in turn, act to create foraging and energetic problems for the mother and other group members. For human mothers, energetic costs to the mother during gestation and lactation are particularly high and require a high quality diet (Martin 1996, Leonard and Robertson 1994). Furthermore, the energetic costs of human mothers carrying their young are not only high; they impact hominin mobility patterns and ranging strategies (Watson et al. 2008; Wall-Scheffler and Meyers 2013). Among carnivores, specific solutions to these ecological, energetic, and social problems vary, but three broad options can be outlined: (1) infants may be carried on foraging trips; (2) infants may be sequestered in a secure location while other group members, including the mother, forage;

and (3) infants may be cared for by the mother and/or other care-givers at a secure location.

An extreme option, the one preferred by other mammals that do *not* bear altricial young, is the movement of young with the adults on daily foraging rounds. No carnivore transports their altricial young on foraging trips or hunts. Even the lion (*Panthera leo*) leaves its young in a protected location while it hunts (Schaller 1972). With adequate group size, however, lions have been known to carry infants to secured carcasses. For all smaller carnivores, foraging with altricial young would subject infants to increased risk of predation and either force the rest of the group to reduce the frequency, length or speed of its foraging trips, or force the mother to keep up thereby further increasing her nutritional and energetic demands. In this regard it is notable that among yellow baboons (*Papio cynocephalus*) living in open to semi-open habitats, mothers with clinging (precocial) infants often appear stressed during foraging trips with the troop and often lag behind, conditions that Altmann (1980) believes may increase both mother's and infant's vulnerabilities to predation. Reasons for this apparent stress are likely related to higher energy costs associated with load-carrying as well as increased wariness of potential dangers from predators.

Mothers that bear altricial young have to carry their infants, who, because of a lack of strength, endurance or fur, cannot cling. Recent studies have shown that for bipeds the energetic costs of load-carrying are high and impact group mobility and foraging strategies (Watson et al. 2008; Wall-Scheffler and Meyers 2013). Carrying infants increases a mother's energy requirements, biological stress, reduces versatility and speed, and therefore increases both mother and young's vulnerability to predation.

A second option is sequestering the infant alone in a protected location while other group members, including the mother, forage. For example, though spotted hyaena (*Crocuta crocuta*) mothers initially remain with their infants for several weeks, they gradually begin to leave them alone at the den for longer and longer periods of time, often

for several days. This option extracts a cost, however; Kruuk (1972) notes that this may be the time of greatest infant mortality, due largely to predation by other carnivores. Gittleman (1989) also draws attention to the fact that carnivores frequently prey on each other. In a study of life time reproductive success of leopards in the Sabi Sand Game Reserve, South Africa, for example, 45% of cubs were killed by other carnivores (lion, hyaena, banded mongoose, and honey badger; Balme et al. 2013). It is also interesting to note that when cubs are present, leopard mothers in Northern Tuli Game Reserve, Botswana significantly reduced the size of their core foraging area (Steyn and Funston 2009), presumably to afford more care and protection. Finally, studies of cheetahs, hyaenas, and wild dogs (Kruuk 1972; Caro, 1994; Laurenson 1994, Kelly and Durant 2000) have noted that cub survival is considerably higher in areas with lower densities of other carnivores.

Finally, the mother and perhaps other care-givers may remain with the infant while others forage. Most carnivores living in open to semi-open areas display variations of this latter behaviour (Eisenberg 1981; Ewer 1973; Gittleman 1989; Kingdon 1977; Kruuk 1972; Moehlman 1989; Rasa 1984; Schaller 1972). Several aspects of food transport among carnivores are worth noting. First, the sociobiological context of food transport among carnivores is to provision altricial young, and less often the mother and other helpers (typically the infant's elder siblings). The canids, in particular the wolf (*Canis lupus*), silver-backed jackal (*Canis mesonckas*), golden jackal (*Canis aureus*), and wild dog (*Lycaon pictus*), exemplify provisioning behaviour in carnivores (Eisenberg 1981; Ewer 1973; Moehlman 1987, 1989; Gittleman 1989) in the frequency of food brought not only to the infant, but also to the mother and other care-givers. Other carnivores, including the lynx (*Lynx rufus*), dwarf mongoose (*Helogale parvula*) and brown hyaena (*Hyaena brunnea*) also provision their infants. Among the dwarf mongoose, the alpha male sometimes brings insects and rodents to the termite mound-den and presents them to weaning infants (Rasa 1984). Although Kruuk (1972) did not observe Ngorongoro spotted

hyaenas (*Crocuta crocuta*) either regurgitating food or often transporting meaty parts to the den, Holekamp and Smale (1990) report, albeit low frequencies, spotted hyaena provisioning of young at Masai Mara National Reserve, Kenya. Food transport to dens and provisioning commonly occurs among both the brown and striped hyaenas (Owens and Owens 1979; Mills 1982, 1989; Kruuk 1972). Moreover, hyaena dens are known for their bone accumulations that likely represent provisioning (Hill 1975; Kingdon 1977; Holekamp and Smale 1990). As indicated above, lions seem to be the exception to this rule amongst the large carnivores by almost without exception moving their young to the kill. As the top predator, their size insulates lions from risks associated with transporting altricial young.

Second, among social carnivores this food transport behaviour apparently requires a daily division of the group into at least two functional units: an infant care-giving unit and a foraging unit. Altricial young are not taken foraging until they are at least able to keep up with adults, particularly among species in open to semi-open habitats with high predator densities (e.g., *L. pictus*, *C. aureus*, *C. mesomelus*, *H. brunnea*, *H. parvula*). Instead, the mother, and perhaps her helpers, remains with the altricial young at the rendezvous site, crèche, or den. Again, the canids are notable for having helpers that remain with the mother at the den (Ewer 1973; Kingdon 1977; Moelhman 1989), though non-mother care-givers also remain with dwarf mongoose infants (Rasa 1984; Rood 1986). Though it is rarely habitual, delayed consumption also occurs in several species, notably wolves and wild dogs, when excess food not eaten by the infants or mother is eaten by the members of the transport group. Although not provisioning behaviour, per se, several felids, including cheetahs (*Acinonyx jubatus*), bring live prey to their young for them to kill. In addition to "teaching" the young about hunting, this behaviour keeps the young in a controlled, protected setting, and presumably reduces the risk of predation. The presence of altricial young and their provisioning often impacts the foraging behaviour of others besides the mother. For example, when young are present among dwarf mongoose, the

foraging unit tends to return to the den earlier in the afternoon (Rasa 1984). Similarly, reduction in foraging distance occurs among wild dogs (Frame et al. 1979). Also, if pack size is adequate in wild dogs, care-givers are known increase pup survival (Courchamp et al. 2002). As noted above, load-carrying by bipeds likely have a significant impact mobility and foraging strategies as well.

Finally, interspecific killing among carnivores is known to account for a large portion of annual deaths in a number of species (Palomares and Caro 1999; Polis et al. 1989; Donadio and Buskirk 2006) and a large portion of these killings often occur in the context of food competition at a kill site. Studies by Kruuk (1972), Schaller (1972), van Lawick and van Lawick (1971) and others emphasize the great risks associated with interspecific competition for food at animal carcasses. Kruuk (1972), for example notes that most adult hyaena mortality in Ngorongoro occurred in during competition for food, particularly with lions. Most carnivores, particularly smaller carnivores, bolt down meat and/or retreat with carcass-parts to avoid this intense competition at animal carcasses and reduce their risk of injury and death. The ability to ingest so much food so quickly and the associated physiological changes in the stomachs of some carnivores, particularly the canids (e.g., Mech 1970), may be an evolutionary anti-predator response to this competition. In this regard, it is important to note that kleptoparasitism of carnivore kills by competitors (Kruuk 1972; Schaller 1968) has been shown to prohibit complete feeding and thus increases their energy expenditures by necessitating an increase in hunting time (Carbone et al. 1997). During Kruuk's study, lions obtained most of the food from hyaenas at their kills and wild dogs lost at least part of 60% of their kills to hyaenas. Wild dogs lost at least part of 86% of their kills to hyaenas in one Serengeti study (Fanshaw and Fitzgibbon 1993). Thus, competition at kill sites is not only dangerous and potentially fatal, it reduces food intake and increases energetic demands. Competition as kill sites therefore acts as a biological mechanism that promotes transporting food away from the carcass.

In summary, the conditions that seem to promote food transport among carnivores

are (1) altricial young, (2) living in open habitats to semi-open habitats characterized by (3) high predator densities. That is, the response to these biological and ecological boundary conditions is a suite of anti-predator behaviours. Altricial young, because of their vulnerability to predation, their high nutritional and energetic requirements and the consequent demands they make on their mother (and other care-givers), act as the biological force pulling food resources and other group members to the den or central place, while competition at food resources provides an impetus to retreat to more secure areas. The evolution of dens and food transport, therefore, appears to be a common and effective response to these conditions.

Early hominins apparently shared many of these same ecological and biological conditions. Using a limited set of biometric measurements and projected post-natal growth curves Stanley (1992) argued convincingly that early hominin infants were as altricial as modern humans. Even if they were not as altricial as modern human infants, post-natal growth curves (see Stanley 1992; Figs. 5 and 7) indicate they were closer to the modern human condition than that of precocial non-human primates. More recent work with *H. erectus* material, however, suggests that secondary altriciality may be a more recent evolutionary development (Dean et al 2001; Coqueugniot et al. 2004; Graves et al. 2010). These studies found more rapid dental development as well as a larger birth canal in *H. erectus* indicating that their life histories were accelerated compared to modern humans perhaps indicating birthing of infants less altricial than later hominin taxa (Dean et al. 2001; Coqueugniot et al. 2004; Graves et al. 2010). Still, it seems that early *Homo* infants (which because of some more australopithecine dental development and body proportions includes *H. habilis*, *H. rudolfensis*, *H. ergaster*) experienced a childhood phase in which they were dependent on others for food, had rapid brain growth, and slow somatic growth (Bogin 2006; Thompson and Nelson 2011). Moreover, even accepting that age of eruption estimates for *H. erectus* 1st molars are correct, the bulk of brain development would not be complete until about 4-5 years (Graves et al. 2010). Consequently, regardless of whether or

not early *Homo* was characterized by the same degree of altriciality of modern humans, *it seems likely that the young would spend a large portion of this development time dependent on adults for food, care, and protection*. The point is that regardless of whether or not early *Homo* infants were as altricial as modern humans, they were very likely more altricial than australopithecines. Regardless of how many years they were dependent on other group members, they were dependent for some period and, moreover, during this dependency did not possess either the physical, cognitive, or social characters to either forage as adults or encumber members of the foraging group.

Second, the ancient lakeshore habitats as well as the newly defined freshwater springs (Ashley et al. 2009) at Olduvai supported a diverse predator guild. Potts (1988), for example, notes that in the Bed I faunal assemblages the percentage of carnivore individuals (MNI) represented ranges from 1-21%. The bovids represented at FLK Zinj indicate that open-woodlands and grasslands dominated the area (Gentry and Gentry 1978; Kappleman 1984; Potts 1988), although ecomorphological (Plummer and Bishop 1994) and isotopic analyses (Sikes, 1994) indicate a more closed habitat at FLK Zinj. Though more wooded than previously thought, the presence of numerous open woodland to grassland taxa, e.g., alcelaphines and antilopines certainly suggest considerable open ground and habitat diversity nearby.

Finally, it seems certain that another biological constraint played a critical role in promoting animal food transport by early *Homo*. Unlike carnivores, primates lack the masticatory and digestive apparatus to gulp down large quantities of meat in a short period of time. Early *Homo* would not have the time to process and consume much animal tissue at kill sites in open settings where carnivores were numerous. Transport would not only reduce risks associated with confrontational scavenging or hunting in open habitats, it would allow the processing and consumption of more animal tissue.

Since early hominins shared the same fundamental biological and ecological boundary conditions that regulate carnivore's denning and food transport behaviours, these

mechanisms were likely as significant for early hominins. For bipeds, high energetic costs associated with carrying infants and their likely impact on mobility and foraging strategies are an additional consideration. Thus, there may have been similar evolutionary costs that precipitated development of socioecological "rules" for rearing altricial (or at least highly dependent) early *Homo* young in open, predator-rich habitats. These "rules" may include the following: (1) Groups will divide into two foraging sub-groups in order to (a) reduce predation risks to the infant and mother, and (b) reduce the mother's energy load. (2) Mother, infant and other care-givers will tend to remain in a core area where protected locations are present and/or risks of predation may be lower. (3) Non-caregivers will tend to forage in areas away from the caregivers so as (a) not to compete for food resources in refuge areas, (b) gain access to resources not available in the core area (e.g., animal carcasses), and (c) not attract carnivores to refuge areas. (4) Acquired carcass-parts will tend to be transported (a) away from the kill to avoid intense competition to (b) more wooded habitats or other refuge areas where predator densities are lower and physical means of protection are available (e.g., trees).

The above outline of socioecological explanations for the transported and processed bone and stone present at FLK Zinj and other Plio-Pleistocene sites may be tested with the archaeological data. For example, if early hominins had already expanded their habitat range dramatically over that of other hominids as argued by Foley (1989), Sikes and Ambrose (1993), and Plummer (2004), then the dual-unit foraging model outlined above suggests that there should be at least two different types of archaeological sites in the Plio-Pleistocene record both in terms of environmental setting and archaeological content. Specifically, Isaac's (1984) type C sites with large numbers of artefacts and bone indicative of intensive and/or repetitive occupation would have been located in more protected, wooded areas. In contrast, type B and particularly type A sites, with little fragmented bone or stone tool refuse suggestive of limited activities (Isaac, 1984), might be located in more open areas, removed from core, protected locations. Taken

as a whole the faunal, isotopic and pollen records suggest that early hominin responsible for FLK-Zinj occupied a grassy woodland while utilizing faunal resources from a variety of habitats.

Implicit in this model is that early hominins were exploiting resources across ecotonal boundaries where limited arboreal habits (e.g., sleeping?), lower predator densities, and refuge areas provided by semi-open woodlands to woodlands defined a core habitat occupied by all group members, but favoured at certain times of the year by those at particular risk to predation, e.g., altricial young and their care-takers. More open habitats apparently provided other resources, that because of increased risks and limited anti-predator defensive mechanisms, were transported to refuge areas. Finally, like other smaller carnivores today, the position and status of early hominins within the carnivore guild was likely dependent on the density and type of other carnivores on the landscape as well as overall food resource availability.

Finally, as argued by Isaac (1978a, 1978b), food transport would seem to imply sharing. Thus, the model given here may also provide a basis for exploring some of the socioecological mechanisms that promoted the evolution of sharing in humans.

- CHAPTER 7 - Conclusions

7.1 Introduction

This study has shown that an understanding of fracture mechanics and fractography, and quantification of select fracture features resulting from impact and static loading extremes, aids in diagnosing bone fracture. Specifically, although often cited as a reason why the fracture features created by carnivore chewing and hammerstone impact should differ, this is the first study to draw on the fracture mechanics and fractographic literature to explicitly state the fundamental differences between static and impact loading and resultant fracture features. This literature further suggested several fracture patterns and features should be characteristic of static loading created by carnivore chewing and hammerstone-impact. Impact fractures should create incipient flakes, bulbar scars, hackle marks, fringe/feathering, cones, lateral stress, and radiating cracks. The fundamental differences between static and impact loading and fracture mechanics axioms explain why impact and not static loading create these fracture features. These axioms structured the fractographic analyses of four assemblages — one created by carnivores (the Amboseli Hyaena Den), another by experimental hammerstone-impact, a fossil assemblage previously interpreted as a carnivore accumulation (FLK-NN2), and the FLK-Zinj fossil assemblage for which previous researches have documented both early *Homo* and carnivore involvement.

As the first quantified analysis of these fracture features, this study demonstrated that several characteristic fracture features, i.e., incipient flakes, cones, lateral stress, and radiating cracks are characteristic of hammerstone-impact. Some of these features were rarely observed in the modern and fossil carnivore accumulations. Quantification of these features demonstrated for the first time that Oldowan hominins were responsible for breakage over 50% of the FLK-Zinj limb assemblage. With this evidence that early *Homo* was the primary agent of bone accumulation, this study then explored the socioecological implications of habitual food transport from animal death/kill sites to processing sites like

FLK-Zinj. Based on environmental and biological constraints shared with certain social carnivores, it is argued that food transport by early *Homo* represents the intersection of two anti-predator defensive strategies — the need to avoid dangerous competitive interactions with carnivores at kill sites, and the need to reduce risks for altricial young and mothers. The above results are built on sequence conceptual and empirical arguments.

7.2 Static vs. Impact Loading, Fracture Mechanics, and Fractographic Features

While previous work by zooarchaeologists and taphonomists has acknowledged that static and impact loading are different, the differences have not been explicitly stated nor have the implications of these differences been explored. It has proven difficult to ascertain reasons why these loading modes should result in different fracture patterns and features, let alone be aware of which fracture features are likely characteristic of carnivore- and hammerstone-induced bone fracture without an understanding of the fundamental differences in these two modes of loading. This is the first zooarchaeological/taphonomic study to explain, as an axiom of fracture mechanics and fractography, that the fundamental difference between static and impact modes of breakage is in the amount of load each mode applies as well as material responses to loading extremes. This is the first study to list and compare carnivore bite-force estimates from the literature to estimates of hammerstone-impact load estimates. The bite-force (BF) of *P. leo* (3085 N) & *C. crocuta* (4510 N) are the highest recorded for extant carnivores (Table 2.1). Hammerstone impact-force was estimated with the formula $F=(1/2mv^2)/d$ (where m = mass, v = velocity, and d = distance of travel into the material before fracture). Using observed Oldowan hammerstone weights, impact velocities, and estimated travel distances (Tables 2.2 – 2.4) it was shown that hammerstone impact delivers forces of 6890 – 24704 N, 4.8 - 17.4 times that of the average adult hyaena, 1420 N. These estimates make it clear for the first time that impact loading with hammerstones creates loads orders of magnitude greater than even the greatest observed carnivore bite-force created by spotted hyaenas (Fig. 2.3). This

difference in applied loads is the primary reason why carnivore chewing and hammerstone-impact loading should result in characteristic fracture patterns and features.

Further review of the fracture mechanics and fractographic literature revealed other axioms relevant to differentiating carnivore- from hammerstone-induced bone fracture. Both the material response to static and impact loading extremes and the size and shape of the indenter play important roles in creation of fracture patterns and features. Static and impact fracture mechanics are fundamentally different. Static loads are applied gradually while impact loads are applied instantaneously, impart kinetic energy, and much greater loads. Static loads create *s* (secondary) waves and sequential crack formation. In contrast, impacts additionally generate *p* (primary) waves whose interaction with free surfaces and *s* waves causes simultaneous crack development (Fig. 2.11). Consequently, more damage and more complex fracture patterns are created by impact loading. Further, higher loads create higher crack velocities, which form more and better expressed features at the loading point (Figs. 2.8 – 2.10).

Also, there is a positive relationship between indenter size and resultant damage and feature expression. Small pointed indenters applied statically concentrate the load in a restricted area. This concentration of smaller loads means that the imparted energy can be dissipated locally. In contrast, large, broad indenters like hammerstones, in part because of their larger contact area, spread larger loads out over a greater area causing greater and more widespread damage. In impact loading the imparted energy cannot be dissipated locally. Fractographic studies demonstrate and bone fracture studies suggest that impact loading creates distinctive fracture features, including incipient flakes, cones, radiating cracks, bulbar scars, and feathering and a new feature, lateral stress, defined here. Thus, as outlined in Chapter 3, the fracture mechanics and fractographic literature suggested several specific fragmentation and fracture frequency patterns that should be observed among the four assemblages.

7.3 Fragmentation, Fracture Features, and Damages in the Study Assemblages

Fracture features, diagnostic percussion and tooth marks, as well as fragments diagnostic of agency were analyzed for each assemblage. All analyses showed that the AHD and FLK-NN2 assemblages tend to be similar to each other and significantly different than the EXP and FLK-Zinj assemblages, which are in turn similar.

Many, but not all, of the specific fragmentation and fracture feature frequency expectations for the four assemblages outlined in Chapter 2 were confirmed in this study:

1) The most general, expectation was that the carnivore accumulated Amboseli Hyaena Den assemblage and the hammerstone-broken experimental assemblage should consistently display different fragmentation and fracture frequencies. Moreover, if Oldowan hominins were responsible for much of the limb bone breakage at FLK-Zinj as indicated by previous analyses (e.g., Bunn and Kroll 1986; Potts 1988; Oliver 1994; Blumenschine 1995; Dominguez-Rodrigo et al. 2007a), then it should be most similar to the hammerstone-broken experimental assemblage. Similarly, if, as previous analyses have shown, FLK-NN2 was accumulated and modified by carnivores (Bunn 1982; Potts 1988; Egeland 2007), then it should be most similar to the carnivore-accumulated AHD assemblage. Most analyses confirmed this predicted pattern: The four assemblages formed two groups. The carnivore accumulated Amboseli Hyaena Den assemblage and the FLK-NN2 assemblage usually displayed fractographic similarities. The second group is comprised of the hammerstone-broken experimental assemblage and the Oldowan FLK-Zinj assemblage. Most fractographic analyses also showed that the AHD and FLK-NN2 assemblages are significantly different than the hammerstone-broken experimental assemblage and the FLK-Zinj assemblage.

2) Expectations concerning differences in the level of fragmentation in the four assemblages were not entirely met. Because of the fundamental differences between static and impact loading, it was expected that the hammerstone-broken EXP assemblage should display smaller bone fragment lengths than the carnivore-accumulated AHD assemblage.

Given previous analyses it was also expected that the FLK-NN2 and AHD assemblages should be more similar to each other than the EXP and FLK-Zinj assemblages. The mean lengths of size class 1-4 specimens in all assemblages were shown to be significantly different (Table 5.2). The AHD mean specimen length (67.4mm), while greater than that observed for the FLK-Zinj assemblage (57.0mm), is considerably smaller than that observed for both the FLK-NN2 (116.8mm) and EXP (79.0mm) assemblages (Fig. 5.1).

It was argued that reasons for the dissimilarities in FLK-Zinj and EXP fragmentation as well as that of AHD and FLK-NN2 are related to site context and the fact that fragmentation is a cumulative process. The AHD assemblage was accumulated by a large number of hyaenas (including infants and young) over a long period of time (Hill 1975, 1981), and it is likely that there was some competition for bones and/or “boredom-related” bone chewing. That is, unlike a singular static loading event, the fragmentation of carnivore chewed bones, and particularly that from large, long-occupied dens, is no doubt cumulative. The significantly smaller mean AHD specimen length compared to FLK-NN2 may suggest then that there are some species, behavioural and or ecological differences how the modern (AHD) and ancient (FLK-NN2) hyaenas accumulated bones. The AHD hyaenas clearly had the time and numbers to for multiple chewing episodes to reduce fragment size, while the FLK-NN2 hyaenas did not do much more than gnaw into the nutrient-rich epiphyses. Thus, more completeness in the FLK-NN2 assemblage may suggest fewer carnivores were present to modify bone for shorter periods of time or carcasses were not a scarce resource.

Further, the lack of similarity between the EXP and FLK-Zinj specimen lengths, is explained by contextual factors and the cumulative nature of fragmentation. A limb bone can be broken by one or many blows resulting in lesser or greater fragmentation. The number of blows delivered and thus the degree of fragmentation is likely dependent on a series of configurational variables including level of hunger, hominin skill, strength, age, and level of boredom.

3) Because of the fundamental differences between static and impact loading, it was also expected that the hammerstone-broken EXP assemblage and FLK-Zinj should display more fracture lines per specimen length than the carnivore-accumulated AHD assemblage and FLK-NN2. This fragmentation measure shows the same pattern (Tables 5.3 and 5.4, Fig. 5.2) as mean specimen length. The above explanations why this expectation was not met for fragment lengths also apply here.

4) As expected, the hammerstone-broken EXP assemblage and FLK-Zinj displayed significantly more loading points than the carnivore-accumulated AHD assemblage and FLK-NN2 (Tables 5.5 - 5.7; Figs. 5.3 and 5.4). Two related factors made it likely that the number of loading points would be greater in the hammerstone-broken EXP assemblage and FLK-Zinj than in the carnivore-accumulated AHD assemblage and FLK-NN2. Fractographic features used to define loading points in this study are better defined in the compact bone of limb shafts where hominins typically direct efforts to open the marrow cavity than on cancellous bone of the epiphyses or in the thinner compact bone of the metaphyses where carnivores focus much of their chewing. That this expectation was met indicates just how different hominin processing for marrow with hammerstones is compared to how carnivores access the marrow of larger animal limbs.

5) As expected, because fractographic studies have shown hertzian cones require the instantaneous application of high loads and are characteristic of impact fracture, loading points defined on the basis of cones or partial cones (FLKOs; Figs. 2.16 - 2.22, 2.30 and 2.35) were found to be significantly more frequent in the hammerstone-broken EXP assemblage and FLK-Zinj than in either the AHD or FLK-NN2 assemblages (Table 5.12 and 5.13; Figs. 5.7 and 5.8).

6) As noted in the fracture mechanics and fractographic literature, ring cracks, aka incipient flakes (IF), are formed when a material is instantaneously loaded by impact causing the area outside of the indenter to fail via tensile stress before, during, and after failure of the material immediately below the indenter. This study largely confirms the

finding of Capaldo and Blumenschine (1994) and the fractographic literature that incipient flakes are characteristic of impact fracture. The frequency of IF in the EXP assemblage is significantly greater than in all other assemblages and the FLK-Zinj frequency is significantly greater than in the AHD assemblage (Tables 5.14 and 5.15; Fig. 5.11). Although Capaldo and Blumenschine (1994) report no IF in the FLK-NN2 assemblage, one was observed in this study. The FLK-NN2 IF frequency, is not significantly different from that observed for FLK-Zinj, but the FLK-NN2 suffers from very low sample size. Moreover, Principal Component Analysis shows that the IF vector plays a major role in differentiating the AHD and FLK-NN2 assemblages from the hammerstone-broken EXP assemblage and FLK-Zinj (Fig. 5.12).

7) Similarly, the fracture mechanics and fractographic literature demonstrates that the energy created by large indenters that instantaneously apply large loads must be dissipated over a larger area creating more damage than is the case with smaller indenters applied in a static manner. As expected, one consequence of this necessary energy dissipation subsequent to impact loading is the creation of radiating cracks (RC). The frequency of RC in the hammerstone-broken EXP assemblage and the FLK-Zinj assemblage is significantly greater than in the AHD assemblage (Tables 5.14 and 5.15; Fig. 5.11). The AHD and FLK-NN2 RC frequencies are not significantly different. Principal Component Analysis shows that the RC vector plays a major role in differentiating the carnivore-accumulated AHD and FLK-NN2 assemblages from the hammerstone-broken EXP assemblage and FLK-Zinj (Fig. 5.12).

8) Although both the fractographic and zooarchaeological literature indicate that hackle marks (HK) are characteristic of impact fracture, this was not born out in this study. The frequencies of HK were not significantly different for any of the assemblages (Tables 5.14 and 5.15; Fig. 5.11). This may suggest that material properties of bone allow for the creation of a fracture feature that mimics the appearance of hackle marks, but for which the

fracture mechanics are different than the glass and ceramics most often used in fracture mechanics and fractographic studies.

9) A new fracture feature, lateral stress (LS) was observed in the experimental hammerstone-broken limb assemblage reported here, as well as previous impact experiments conducted by the author. This feature has the appearance of a small ridge, groove, or crack and is found on the fracture surface immediately adjacent to the loading point just below the cortical surface (Figs. 2.29 – 2.31, 2.19, and 2.21). This feature may be what has been referred to as a truncated cone (Subhash et al. 2008) that was beginning to form as it was overtaken or subsumed by another fracture front. As expected LS frequencies were significantly greater in the EXP and FLK-Zinj assemblages than in the AHD and FLK-NN2 assemblages (Tables 5.14 and 5.15; Fig. 5.11). Principal Component Analysis shows that the LS vector plays a major role in differentiating the carnivore-accumulated AHD and FLK-NN2 assemblages from the hammerstone-broken EXP assemblage and FLK-Zinj (Fig. 5.12).

10) Because the fractographic literature indicates that fracture features are better-expressed on materials broken by impact loading than static loading, it was expected that the overall frequency of fracture features should be greater in EXP and FLK-Zinj than that of the AHD and FLK-NN2 assemblages. Not surprisingly, since most of the fracture features examined were shown to be characteristic of hammerstone-impact, more fracture features were observed in the EXP and FLK-Zinj assemblages than in the AHD and FLK-NN2 assemblages (Table 5.14, Fig. 5.10).

11) Finally, it was expected that if certain fracture feature frequencies were found to be indicative of impact fracture differentiating the EXP and FLK-Zinj assemblages from the AHD and FLK-NN2 assemblages, then these features should tend to be directly associated with percussion marks (PM) not tooth marks (TM). Loading points displaying cones, incipient flakes, radiating cracks, and/or lateral stress features were in the EXP and FLK-Zinj assemblages were significantly more likely to be directly associated with PMs than

TMs (χ^2 , $p < 0.0001$ for both comparisons; Table 5.19). PMs directly co-occur with 62.2% (84/135) of LDPTs with CO, LS, RC, and/or IF features observed in the EXP assemblage and 29.9% (111/371) of the FLK-Zinj assemblage. What appear to be tooth marks are directly associated with 31 AHD specimens that display one or more of the target features (i.e., IF, RC, CO, and/or LS).

Additionally, 43% of the 56 of the EXP specimens with one of the target features, but which are not directly associated with a PM at the load point do display a PM elsewhere on the specimen. Thus, of the 160 EXP specimens with a load point that displays a target fracture feature, 81.3% (130) display a PM somewhere on the specimen. For FLK-Zinj, 29.5% of the specimens with a target feature not directly associated with a PM display a PM elsewhere on the specimen. Of the 246 specimens from FLK-Zinj with a load point displaying a target fracture feature, 74.8% (184) display a PM or conjoin with a specimen that does.

These data demonstrate that incipient flakes, radiating cracks, cones, and lateral stress are characteristic of hammerstone-impact fracture. The fractographic approach and quantification of certain fracture features has resulted in a method and features that may improve estimates on hominin involvement in fossil assemblages.

Insights into understanding fracture patterns and features at FLK-Zinj are also provided by the frequencies of diagnostic carnivore damage. Carnivore damages tabulated for the assemblages include tooth marks, tooth notches, and lever-up fragments. Over 70% of AHD, FLK-NN2, and EXP specimens display one or more tooth marks. Only 41% of the FLK-Zinj specimens display what appears to be a TM. However, TM frequencies yielded by more detailed and rigorous analyses are significantly lower. Dominguez-Rodrigo and Barba (2006, 2007b) who paid particular attention to mimics created by bioerosion give a FLK-Zinj TM frequency of 18%. Similarly, Parkinson (2013; Parkinson et al. 2015) observed TMs on only 24.5% of the FLK-Zinj limb specimens. There are a large number of indeterminate linear marks on

the FLK-Zinj limb bones and on some specimens the density of these marks is high. It seems likely then that the number of TMs given for this study here is too high and includes a large number of marks that at least two other analysts would categorize as either indeterminate marks or bioerosion.

It was argued that the more reasonable estimate of carnivore interaction with the assemblage was the frequency of TMs on fracture surfaces, the medullary wall, and cancellous bone and/or the number of specimens displaying evidence of carnivore-induced fracture. Accordingly, the estimate of the carnivore involvement in modification of the the FLK-Zinj assemblage likely ranges between 5.6%, the frequency of bones with evidence of carnivore breakage, and 25%, the frequency of specimens with tooth marks on the fracture, medullary, or cancellous surfaces. Of these The presence of TMs on fracture surfaces and medullary walls created and exposed by impact fracture on 40 specimens demonstrates that carnivores scavenged some of the hominin food refuse at FLK-Zinj (Table 5.18; Fig. 5.15).

Finally, it should be noted that the frequency of FLK-Zinj specimens that display a PM reported here (34%) is greater than that reported in previous studies (Table 1.1). This greater percussion mark frequency is attributable to the identification of previously overlooked LDPTs by via fracture feature analysis, the use of tungsten lamps, and the microscopic examination of all surfaces.

7.4 The Extent of early Homo Involvement with the FLK-Zinj Fossil Assemblage

This study has shown that cones, radiating cracks, incipient flakes, and lateral stress are significantly more frequent in assemblages created by hammerstone impact, are rarely observed in assemblages created by carnivores, and are overwhelmingly associated with percussion marks. It seems reasonable to conclude that these features are characteristic of hammerstone-impact fracture. Accordingly, FLK-Zinj specimens that display one or more of these features are interpreted to have been broken by hominins processing limb bones for marrow. Accordingly, it is estimated then that 56.8% (287) of the 505 FLK-Zinj limb

pieces were broken by hammerstone-wielding hominins – a 35% increase over that obtained by using percussion marks alone. This study has shown for the first time that Oldowan hominins were responsible for the bulk of FLK-Zinj limb bone breakage. Given that only 5.6% of the assemblage displays evidence of carnivore-induced breakage, it seems more than likely that considerably more than 56.8% of the limb assemblage was broken by hominins.

In summary this fractographic study of bone fracture of has demonstrated the following:

- 1) Observed carnivore bite-forces & hammerstone impact-force estimates can differ by orders of magnitude and have with limited potential overlap.
- 2) Fractographic concepts and an understanding specific material responses to static and impact loading extremes aid the study of bone fracture.
- 3) Fragmentation is a cumulative process subject to a variety of configurational factors that make it difficult to apply to the diagnosis of hammerstone- and carnivore-induced fracture.
- 4) Assemblages in which bones were broken by hammerstone-impact will display more load points than assemblages broken by carnivore chewing.
- 5) A fractographic principle that the greater the applied force, the greater the frequency and expression of fracture features is confirmed for bone fracture.
- 6) Bones broken by percussion display a greater frequency cones, radiating cracks, incipient flakes, and lateral stress features than do bones broken by the static loading of carnivore chewing may be used to define impact fracture.
- 7) Contrary to expectations, hackle marks & bulbar scars are not characteristic of impact.
- 8) FLK-NN2 fracture feature frequencies are quite similar to those of AHD supporting previous interpretations that it is a carnivore accumulation.
- 9) FLK-Zinj fracture feature frequencies are similar to those of EXP supporting previous interpretations that early *Homo* habitually processed bone for marrow.

10) Fractographic analyses increases the estimate of hammerstone-broken bones in FLK-Zinj to 54%, 27 - 40% over that obtained by using percussion marks alone demonstrating that early *Homo* was *the major breakage agent* at FLK-Zinj while carnivore breakage was minimal.

7.5. Socioecological Implications of Food Transport by Oldowan Hominins

Analysis of fracture features given here as well as previous studies of cut mark frequencies (e.g., Bunn and Kroll 1986; Oliver 1994; Dominguez-Rodrigo, Barba, and Egland 2007), recent detailed analysis of tooth mark locations (Parkinson 2013), and new studies of bovid age profiles (which suggest hominin ambush hunting) (Bunn and Pickering 2010; Bunn and Gurtov 2014) all indicate that early *Homo* habitually acquired carcass parts, and transported them to FLK-Zinj for processing and consumption. The transport of food is a novel behaviour among mammals in general and among primates in particular. The socioecological implications of food transport by Oldowan hominins were explored by examining the ecological and biological factors that seem to drive this behaviour in social carnivores.

In particular, many carnivores that transport food live in open habitats and are members of a highly competitive carnivore guild. Competition for food at kill or death sites is often keen and dangerous. Plio-Pleistocene hominins occupied or at least frequented similar open habitats also occupied by a number of predators. Thus, social carnivores and early *Homo* shared some similar ecological constraints including living in open habitats occupied by a number of dangerous predators and the likely presence of altricial (or certainly highly dependent) young. Further, the inability of early *Homo* to quickly process, masticate, and digest large quantities of animal tissue constitutes another biological constraint that would have promoted food transport away from competitive and dangerous death/kill sites. It is argued that food transport by early *Homo* represents the intersection of two anti-predator defensive strategies — the need to avoid dangerous competitive interactions with carnivores at kill sites, and the need to reduce risks for

altricial young and mothers. One likely result of this two-pronged anti-predator defensive strategy was the development of a dual foraging units. Group members not encumbered by altricial, or at least highly dependent, young could have foraged widely for both animal and plant foods while mothers, altricial young, and possibly helpers restricted their foraging activities to more restricted areas where risks presented by predators were reduced. Further, this model may form a basis to define proximate and measurable biological and ecological variables that promoted the evolution of sharing and cooperative behaviour in humans.

References Cited

- Abu Alhaija, E.S.J., Al Zo'ubi, I.A., Al Rousan, M.E., Hammad, M.M., 2010. Maximum occlusal bite forces in Jordanian individuals with different dentofacial vertical skeletal patterns. *Eur. J. Orthod.* 32, 71-77.
- Aiello L.C., 1997. Brains and guts in human evolution: the expensive tissue hypothesis. *Braz. J. Genet.* 20:141-48
- Aiello, L., Wells, J.C.K., 2002. Energetics and the evolution of the genus *Homo*. *A. Rev. Anthropol.* 31, 323-338.
- Aiello L.C., Wheeler P., 1995. The expensive tissue hypothesis: the brain and digestive system in human and primate evolution. *Curr. Anthropol.* 36, 199-221.
- Alcántara, V., Barba, R., Barral, J., Crespo, A., Eiriz, A., Falquina, A., Herrero, S., Ibarra, A., Megías, M., Pérez, M., Pérez, V., Rolland, J., Yravedra, J., Vidal, A., Domínguez-Rodrigo, M., 2006. Determinación de procesos de fractura sobre huesos frescos: un sistema de análisis de los ángulos de los planos de fracturación como discriminador de agentes bióticos. *Trabajos de Prehistoria* 63, 25–38.
- Altmann, J., 1980. Baboon mothers and infants. Harvard University Press, Cambridge.
- Andrew, W., Hickman, C.P., 1974. Histology of the vertebrates: a comparative text. The C.V. Mosby Company, St. Louis.
- Andrews, P., Evans, E. N., 1983. Small mammal bone accumulations produced by mammalian carnivores. *Paleobiology*, 3, 289-307.
- Anyonge, W. 1993. Body mass in large extant and extinct carnivores. *J. Zool.* 231, 339-350.
- Ashley, G.M., 2007. Orbital rhythms, monsoons, and playa lake response, Olduvai Basin, equatorial East Africa (ca. 1.85–1.74 Ma). *Geology* 35(12), 1091–1094.
- Ashley, G.M., Liutkus, C.M., 2002. Tracks, trails and trampling by large vertebrates in a rift valley paleo-wetland, lowermost Bed II, Olduvai Gorge, Tanzania. *Ichnos* 9, 23–32.
- Ashley, G.M., Tactikos, J.C., Owen, R.B., 2009. Hominin use of springs and wetlands: Paleoclimate and archaeological records from Olduvai Gorge (~1.79–1.74 Ma). *Palaeogeogr Palaeoclimatol Palaeoecol*, 272, 1-16.
- Ashley, G.M., Barboni, D., Dominguez-Rodrigo, M., Bunn, H.T., Mabulla, A.Z., Diez-Martin, F., Barba, R., Baquedano, E. 2010a. A spring and wooded habitat at FLK Zinj and their relevance to origins of human behavior. *Quat. Res.*, 74(3), 304-314.
- Ashley, G.M., Barboni, D., Dominguez-Rodrigo, M., Bunn, H.T., Mabulla, A. Z., Diez-Martin, F., Barba, R., Baquedano, E. 2010b. Paleoenvironmental and paleoecological reconstruction of a freshwater oasis in savannah grassland at FLK North, Olduvai Gorge, Tanzania. *Quat. Res.*, 74(3), 333-343.
- Atha J., Yeadon, M.R., Sandover J., 1985. The damaging punch. *Br. Med. J.* 291, 1756–1757.

- Ball, A. and McKenzie, H.W., 1994. On the low velocity impact behaviour of glass plates. *J.Physiq. III*, 4, 783-788.
- Balme, G.A., Batchelor, A., Woronin Britz, N., Seymour, G., Grover, M., Hes, L., McDonald, D.W., Hunter, L. T., 2013. Reproductive success of female leopards *Panthera pardus*: the importance of top-down processes. *Mammal Rev.* 43, 221-237.
- Beardsley, C.L., Bertsch, C.R., Marsh, J.L., Brown, T.D., 2002. Interfragmentary surface area as an index of comminution energy: proof of concept in a bone fracture surrogate. *J. Biomech.* 35, 331–338.
- Beardsley, C., Anderson, D.D., Marsh, J.L., Brown, T.D., 2005. Interfragmentary surface area as an index of comminution severity in cortical bone impact. *J. Orthop. Res.* 23, 686–690.
- Beardsley, C., Marsh, J.L., Brown, T.D., 2004. Quantifying Comminution as a Measurement of Severity of Articular Injury. *Clin. Orthop.* 423, 74–78.
- Becker, W.T., 2002. Fracture appearance and mechanisms of deformation and fracture. In: Becker, W.T., Shipley, R.J. (Eds.), *Failure analysis and prevention*, ASM Handbook, Vol. 11. ASM International, Materials Park, OH, pp. 559-586.
- Binder, W., 2004. Personal communication: table listing the age, sex, and 123 bite force measurements summarized but not provided in Binder and Van Valkenburgh (2000).
- Binder, W. and Van Valkenburgh, B., 2000. Development of bite strength and feeding behaviour in juvenile spotted hyenas (*Crocuta crocuta*). *J. Zool. Lond.* 252, 273-283.
- Binford, L.R., 1981. *Bones: Ancient Men and Modern Myths*. Academic Press, New York.
- Binford, L.R., 1986. Comment on Bunn, H.T., Kroll, E.M., 1986. Systematic butchery by Plio-Pleistocene hominids at Olduvai Gorge, Tanzania. *Curr. Anthropol.* 27, 431-452.
- Binford, L.R., 1988. Fact and fiction about the *Zinjanthropus* floor: data, arguments and interpretations. *Curr. Anthropol.* 29, 123-135.
- Binford, L.R., Mills, M.G.L., Stone, N.M., 1988. Hyena scavenging behavior and its implications for the interpretation of fauna assemblages from FLK 22 (the Zinj floor) at Olduvai Gorge. *J. Anthropol. Archaeol.* 7, 99-135.
- Blumenschine, R.J., 1987. Characteristics of an early hominid scavenging niche. *Curr. Anthropol.* 28, 383-407.
- Blumenschine, R.J., 1988. An experimental model of the timing of hominid and carnivore influence on archaeological bone assemblages. *J. Archaeol. Sci.* 15, 483-502.
- Blumenschine, R.J., 1995. Percussion marks, tooth marks, and experimental determinations of the timing of hominid and carnivore access to long bones at FLK-*Zinjanthropus*, Olduvai Gorge, Tanzania. *J. Hum. Evol.* 29, 21-51.
- Blumenschine, R.J., Selvaggio, M.M., 1988. Percussion marks on bone surfaces as a new diagnostic of hominid behaviour. *Nature* 333, 763-765.

Blumenschine, R.J., Cavallo, J.A., Capaldo, S.D., 1994. Competition for carcasses and early hominid behavioral ecology: a case study and conceptual framework. *J. Hum. Evol.* 27, 197-213.

Blumenschine, R.J., Peters, C.R., Masao, F.T., Clarke, R.J., Deino, A.L., Hay, R.L., Swisher, C.C., Stanistreet, I.G., Ashley, G.M., McHenry, L.J., Sikes, N.E., Van der Merwe, N.J., Tactikos, J.C., Cushing, A.E., Deocampo, D.M., Njau, J.K., Ebert, J.I., 2003. Late Pliocene Homo and Hominid Land Use from Western Olduvai Gorge, Tanzania. *Science* 299, 1217-1221.

Bogin, B., 2006. Modern human life history: the evolution of human childhood and fertility. In: Hawkes, K., Paine, R.R. (Eds.), *The evolution of human life history*. Santa Fe, NM: School of American Research, pp. 197–230.

Bonnichsen, R., 1979. Pleistocene bone technology in the Berengian Refugium. *Archaeological Survey of Canada Paper No. 89*. National Museum of Canada, Ottawa.

Bonnichsen, R., Will, R.T., 1980. Cultural modification of bone: the experimental approach in faunal analysis. In: Gilbert, B.M. (Ed.), *Mammalian osteology*. Modern Printing, Laramie, WY, pp. 7-30.

Bonnichsen, R., & Sorg, M. H. (Eds.), 1989. *Bone modification*. Center for the Study of the First Americans, Institute for Quaternary Studies, University of Maine.

Bourne, N.K., Rosenberg, Z., Mebar, Y., Obara, T., Field, J.E., 1994. A high speed photographic study of fracture wave propagation in glasses. *J. de Physique IV, Colloque C8*, 635-640.

Bouزيد, S., Nyoungue, A., Azari, Z., Bouaouadja, N., Pluvinage, G., 2001. Fracture criterion for glass under impact loading. *Int. J. Impact Engineering*. 25, 831-845.

Brain, C.K., 1981. *The Hunters or the Hunted? An introduction to African cave taphonomy*. University of Chicago Press, Chicago.

Brantingham P.J. 1998. Hominid-carnivore coevolution and invasion of the predatory guild. *J. Anthropol. Archaeol.* 17, 327–353.

Bunn, H.T., 1982. *Meat-eating and human evolution: studies on the diet and subsistence patterns of Plio-Pleistocene hominids in East Africa*. Ph.D. dissertation. University of California, Berkeley.

Bunn, H.T., 1983a. Evidence on the diet and subsistence patterns of Plio-Pleistocene hominids and Koobi Fora, Kenya and Olduvai Gorge, Tanzania. In: Clutton-Brock, J. and Grigson, C. (Eds.), *Animals and Archaeology*, vol. I, *Hunters and Their Prey*. BAR International, No. 163. Oxford, pp. 21-30.

Bunn, H.T., 1983b. Comparative analysis of modern bone assemblages from a San hunter-gatherer camp in the Kalahari Desert, Botswana, and from a spotted hyaena den near Nairobi, Kenya. In: Clutton-Brock, J., Grigson, C. (Eds.), *Animals and Archaeology: 1. Hunters and Their Prey*. BAR International, No. 163. Oxford, pp. 143e148.

- Bunn, H.T., 1986. Patterns of skeletal representation and hominid subsistence activities at Olduvai Gorge, Tanzania, and Koobi Fora, Kenya. *J. Hum. Evol.* 15(8), 673–690.
- Bunn, H.T., 1989. Diagnosing Plio-Pleistocene hominid activity with bone fracture evidence. In: Bonnicksen, R. and Sorg, M.H. (Eds.), *Bone Modification*. Center for the Study of the First Americans, Orono Maine, pp. 299-316.
- Bunn H.T., 1997. The bone assemblages from the excavated sites. In: Isaac G.L. (Ed.), *Koobi Fora Research Project Volume 5: Plio-Pleistocene Archaeology*. Clarendon Press, Oxford, pp. 402-458.
- Bunn H.T., 2001. Hunting, power scavenging, and butchering by Hadza foragers and by Plio-Pleistocene Homo. In: Stanford, C.B., Bunn, H.T., (Eds.), *Meat-eating and Human Evolution*. Oxford Univ. Press, Oxford, pp. 199-218.
- Bunn, H.T., Harris, J.W.K., Isaac, G., Kaufulu, Z., Kroll, E., Schick, K., Toth, N., Behrensmeyer, A.K., 1980. FxJj50: An early Pleistocene site in northern Kenya. *World Archaeol.* 12, 109-136.
- Bunn, H.T., Kroll, E.M., 1986. Systematic butchery by Plio-Pleistocene hominids at Olduvai Gorge, Tanzania. *Curr. Anthropol.* 27, 431-452.
- Bunn, H.T., Kroll, E.M. 1988. Reply to L.R. Binford's "Fact and fiction about the *Zinjanthropus* floor: data, arguments and interpretations. *Curr. Anthropol.* 29(1), 135-155.
- Bunn, H.T., Ezzo, J.A., 1993. Hunting and scavenging by Plio-Pleistocene hominids: nutritional constraints, archaeological patterns, and behavioral implications. *J. Archaeol. Sci.* 20, 365-398.
- Bunn, H.T., Pickering, T.R., 2010. Bovid mortality profiles in paleoecological context falsify hypotheses of endurance running–hunting and passive scavenging by early Pleistocene hominins. *Quatern. Res.* 74, 395-404.
- Bunn, H.T., Gurtov, A.N., 2014. Prey mortality profiles indicate that Early Pleistocene Homo at Olduvai was an ambush predator. *Quatern. Int.* 322, 44-53.
- Callister, W.D., Gethwisch, D.G. 2012. *Fundamentals of Materials Science and Engineering: An Integrated Approach*. John Wiley & Sons, New York.
- Capaldo, S.D., 1995. Inferring hominid and carnivore behavior from dual-patterned archaeofaunal assemblages. Ph.D. dissertation, Rutgers University.
- Capaldo, S.D., 1997. Experimental determination of carcass processing by Plio-Pleistocene hominids and carnivores at FLK 22 (*Zinjanthropus*), Olduvai Gorge, Tanzania. *J. Hum. Evol.* 33, 555-597.
- Capaldo, S.D., Blumenschine, R.J., 1994. A quantitative diagnosis of notches made by hammerstone percussion and carnivore gnawing in bovid long bones. *Am. Antiq.* 59, 724–748.
- Carbone, C., Du Toit, J.T., Gordon, I.J., 1997. Feeding success in African wild dogs: does kleptoparasitism by spotted hyenas influence hunting group size?. *Journal of animal Ecology*, 66, 318-326.

- Caro, T.M., 1994. Cheetahs of the Serengeti Plains: Group Living in an Asocial Species. University of Chicago Press, Chicago.
- Cerling, T.E., Mbuya, E., Kirera, F.M., Manthi, F.K., Grine, F.E., Leakey, M.G., Sponheimer, M., Uno, K.T., 2011. Diet of *Paranthropus boisei* in the early Pleistocene of East Africa. *Proc. Nat. Acad. Sci.* 108, 9337–9341.
- Cesari, P., Bertuccio, M., 2008. Coupling between punch efficacy and body stability for elite karate. *Journal of Science and Medicine in Sport*, 11, 353-356.
- Christiansen, P., 2007. Comparative bite forces and canine bending strength in feline and sabertooth felids: implications for predatory ecology. *Zool. J. Linn. Soc.* 151, 423-437.
- Christiansen, P., Adolfssen, J.S. 2005. Bite forces, canine strength and skull allometry in carnivores (Mammalia, Carnivora). *J. Zool.*, 266, 133-151.
- Christiansen, P., Adolfssen, J.S., 2007. Osteology and ecology of *Megantereon cultridens* SE311 (Mammalia; Felidae; Machairodontinae), a sabrecat from the Late Pliocene – Early Pleistocene of Seneze, France. *Zool. J. Linn. Soc.* 151, 833-884.
- Christiansen, P., Wroe, S., 2007. Bite forces and evolutionary adaptations to feeding ecology in carnivores. *Ecology*, 88, 347-358.
- Clutton-Brock, T.H., 1991. The evolution of parental care. Princeton University Press, Princeton, NJ.
- Coqueugniot, H., Hublin, J.J., Veillon, F., Houët, F., Jacob, T. 2004. Early brain growth in *Homo erectus* and implications for cognitive ability. *Nature*, 431, 299-302.
- Cotterell, B., Kamminga, J., 1987. The formation of flakes. *Am. Antiq.* 52(4), 675-708.
- Courchamp, F., Rasmussen, G. S., Macdonald, D. W., 2002. Small pack size imposes a trade-off between hunting and pup-guarding in the painted hunting dog *Lycaon pictus*. *Behavioral Ecology*, 13, 20-27.
- Courtney, A.C., Wachtel, E.F., Myers, E.R., 1995. Age-related reductions in the strength of the femur tested in a fall-loading configuration. *J. Bone Joint Surg.* 77, 387-395.
- Creel, S., Creel, N.M., 1998. Six ecological factors that may limit African wild dogs, *Lycaon pictus*. *Animal Conservation*, 1, 1-9.
- Currey, J.D., 2002. Bones: Structure and Mechanics. Princeton University Press, Princeton, NJ.
- Dapena J., Anderst, W., Toth, N. 2006. The biomechanics of the arm swing in Oldowan stone flaking. In: Toth N, Schick K, (Eds.), *The Oldowan: Case Studies into the Earliest Stone Age*. Stone Age Inst. Press, Gosport, IN. pp. 333–38.
- Dart, R.A., 1949a. The predatory implemental technique of *Australopithecus*. *Am. J. Phys. Anthropol.* 7, 1-38.
- Dart, R.A., 1949b. The bone-bludgeon hunting technique of *Australopithecus*. *S. Afr. J. Sci.* 2, 150-152.

- Dart, R. A. 1957. The osteodontokeratic culture of *Australopithecus prometheus*. Trans. Mus. Mem. no. 10.
- Davis, K.L., 1985. A taphonomic approach to experimental bone fracturing and application to several South African Pleistocene sites. Ph.D. dissertation, State University of New York, Binghamton.
- de Heinzelin, J., Clark, J.D., White, T., Hart, W., Renne, P., WoldeGabriel, G., Beyene, Y., Vrba, E., 1999. Environment and behavior of 2.5-million-year-old Bouri hominids. *Science* 284, 625-629.
- de la Torre, I., Mora, R., 2005. Unmodified lithic material at Olduvai Bed I: manuports or ecofacts? *J. Archeol. Sci.* 32, 273-285.
- de la Torre, I., Mora, R., Dominguez-Rodrigo, M., de Luque, L., Alcalá, L., 2003. The Oldowan industry of Peninj and its bearing on the reconstruction of the technological skills of Lower Pleistocene hominids. *J. Hum. Evol.* 44, 203-224.
- Dean, C., Leakey, M.G., Reid, D., Schrenk, F., Schwartz, G.T., Stringer, C., Walker, A. 2001. Growth processes in teeth distinguish modern humans from *Homo erectus* and earlier hominins. *Nature*, 628-631.
- Deocampo, D.M., 2002. Sedimentary structures generated by *Hippopotamus amphibius* in a lake-margin wetland, Ngorongoro Crater, Tanzania. *Palaios* 17, 212–217.
- Dennell, R.W., Coard, R., Turner, A. 2008. Predators and scavengers in Early Pleistocene southern Asis. *Quat. Intern.* 192, 78-88.
- Diez, J.C., Fernandez-Jalvo, Y, Rosell, J, and Caceres, I. 1999. Zooarchaeology and taphonomy of Aurora Stratum (Gran Dolina, Sierra de Atapuerca, Spain). *J. Hum. Evol.* 37, 623-652.
- Dominguez-Rodrigo, M., 1997a. Meat-eating by early humans at the FLK 22 *Zinjanthropus* site, Olduvai Gorge (Tanzania): an experimental approach using cut mark data. *J. Hum. Evol.* 33, 669-690.
- Dominguez-Rodrigo, M., 1997b. A reassessment of the study of cut mark patterns to infer hominid manipulation of fleshed carcasses at the FLK Zinj site, Olduvai Gorge, Tanzania. *Trabajos de Prehistoria* 54, 29-42.
- Dominguez-Rodrigo, M., 1999a. Flesh availability and bone damage in carcasses consumed by lions: paleoecological relevance in hominid foraging patterns. *Palaeogeogr. Palaeoclimat. Palaeoecol.* 149, 33-388.
- Dominguez-Rodrigo, M., 1999b. Meat-eating and carcass procurement by hominids at the FLK-Zinj 22 site, Olduvai Gorge (Tanzania): a new experimental approach to the old hunting-versus-scavenging debate. In: Ullrich, H. (Ed.), *Hominid Evolution: Lifestyles and Survival Strategies*. Edition Archaea, Schwelm, Germany, pp. 89-111.
- Dominguez-Rodrigo, M., 2002. Hunting and scavenging by early humans: the state of the debate. *J. World Prehist.* 16(1), 1-54.

- Dominguez-Rodrigo, M., Barba, R., 2006. New estimates of tooth mark and percussion mark frequencies at the FLK Zinj site: the carnivore-hominid-carnivore hypothesis falsified. *J. Hum. Evol.* 50, 170-194.
- Dominguez-Rodrigo, M., Barba, R., Egeland, C.P. (Eds.), 2007a. *Deconstructing Olduvai: A Taphonomic Study of Bed I Sites*. Springer, New York.
- Dominguez-Rodrigo, M., Barba, R., 2007b. New estimates of tooth mark and percussion mark frequencies at the FLK Zinj site: the carnivore-hominid-carnivore hypothesis falsified (I). In: Dominguez-Rodrigo, M., Barba, R., Egeland, C.P. (Eds.), *Deconstructing Olduvai: A Taphonomic Study of Bed I Sites*. Springer, New York, pp. 39-74.
- Dominguez-Rodrigo, M., Barba, R., 2007c. The behavioral meaning of cut marks at the FLK-Zinj level: the carnivore-hominid-carnivore hypothesis falsified (II). In: Dominguez-Rodrigo, M., Barba, R., Egeland, C.P. (Eds.), *Deconstructing Olduvai: A Taphonomic Study of Bed I Sites*. Springer, New York, pp. 75-100.
- Donadio, E., Buskirk, S.W., 2006. Diet, morphology, and interspecific killing in Carnivora. *The Am. Nat.* 167(4), 524-536.
- Egeland, C.P., 2007a. Zooarchaeological and taphonomic perspectives on hominid and carnivore interactions at Olduvai Gorge, Tanzania. Ph.D. Dissertation, Indiana University, Bloomington.
- Egeland, C.P., 2007b. Zooarchaeology and taphonomy of FLK-North North 2. In: Dominguez-Rodrigo, M., Barba, R., Egeland, C.P. (Eds.), *Deconstructing Olduvai: A Taphonomic Study of Bed I Sites*. Springer, New York, pp. 229-237.
- Egeland, C.P., 2014. Taphonomic estimates of competition and the role of carnivore avoidance in hominin site use within the Early Pleistocene Olduvai Basin. *Quatern. Int.* 322-323, 95-106.
- Egeland, C.P., Pickering, T.R., Domínguez-Rodrigo, M., Brain, C.K., 2004. Disentangling Early Stone Age palimpsests: determining the functional independence of hominid- and carnivore-derived portions of archaeofaunas. *J. Hum. Evol.* 47, 343-357.
- Eisenberg, J.F., 1981. *The Mammalian Radiations: An Analysis of Trends in Evolution, Adaptation and Behavior*. University of Chicago Press, Chicago.
- Erickson, G. M., Lappin, A. K., Parker, T., Vliet, K. A., 2003. The ontogeny of bite-force performance in American alligator (*Alligator mississippiensis*). *J. Zool. Soc. London* 260, 317-327.
- Esakul, K.A. (Ed.), 1993. *Handbook of Case Histories in Failure Analysis, Vol 2*. ASM International.
- Ewer, R.F., 1973. *The Carnivores*. Cornell University Press, Ithaca.
- Faith, J.T., 2007. Sources of variation in carnivore tooth-mark frequencies in a modern spotted hyena (*Crocuta crocuta*) den assemblage, Amboseli Park, Kenya. *J. Archaeol. Sci.* 34(10), 1601–1609.

- Faith, J.T., Domínguez-Rodrigo, M., Gordon, A.D., 2009. Long-distance carcass transport at Olduvai Gorge? A quantitative examination of Bed I skeletal element abundances. *J. Hum. Evol.* 56, 247-256.
- Fanshawe, J.H., Fitzgibbon, C.D., 1993. Factors influencing the hunting success of an African wild dog pack. *Anim. Behav.* 45, 479-490.
- Fernández-Jalvo, Y., Andrews, P., Pesquero, D., Smith, C., Marín-Monfort, D., Sánchez, B., Geigl, E. B., Alonso, A., 2010. Early bone diagenesis in temperate environments: Part I: Surface features and histology. *Palaeogeogr. Palaeoclimatol. Palaeoecol.* 288, 62-81.
- Ferraro, J.V., Plummer, T.W., Pobiner, B.L., Oliver, J.S., Bishop, L.C., Braun, D.R., Ditchfield, P.W., Seaman III, J.W., Binetti, K.M., Seaman Jr., J.W., Hertel, F., Potts, R., 2013. Earliest archaeological evidence for persistent hominin carnivory. *PLoS One* 8 (4) e62174.
- Foley, R.A., 1989. The evolution of hominid social behavior. In: Standen, V., Foley, R.A. (Eds.), *Comparative Socioecology: The Behavioral Ecology of Humans and of Other Animals*. Blackwell Scientific Publications, Oxford, pp. 473-494.
- Foley, R.A., 2002. The evolutionary consequences of increased carnivory in hominids. In: Stafford, C.B. and Bunn, H.T. (Eds.), *Meat-eating and human evolution*. Oxford University Press, New York, pp. 305-331.
- Frame, L.H., Malcolm, J. R., Frame, G.W. van Lawick, H., 1979. Social organization of African wild dogs (*Lycaon pictus*) on the Serengeti Plains, Tanzania, 1967-1978. *Zeitschrift fur Tierpsychologie* 50, 225-249.
- Fréchette, V.D., 1990. Failure analysis of brittle materials: advances in ceramics, vol. 28. American Ceramic Society, Westerville, Ohio.
- Galán, A.B., Rodríguez, M., de Juana, S., Domínguez-Rodrigo, M., 2009. A new experimental study on percussion marks and notches and their bearing on the interpretation of hammerstone-broken faunal assemblages. *J. Archaeol. Sci.* 36, 776-784.
- Gauld, S., Oliver, J.S., Kansa, S.W., Campbell, S., Carter, E. (*in prep.*). Ritual cannibalism and feasting at Domuztepe, Late Neolithic Mesopotamia.
- Gentry, A.W., Gentry, A., 1978. Fossil bovidae (Mammalia) from Olduvai Gorge, Tanzania. *Bull. Br. Mus. Nat. Hist.* 29, 289-446.
- Gifford, D., Crader, D.C., 1977. A computer coding system for archaeological faunal remains. *Am. Antiq.* 42, 225-238.
- Gittleman, J.L., 1989. Carnivore groups living: comparative trends. In: Gittleman, J.L. (Ed.), *Carnivore Behavior, Ecology and Evolution*. Cornell University Press, Ithaca, pp. 183-207.
- Graves, R.R., Lupo, A.C., McCarthy, R.C., Wescott, D.J., Cunningham, D.L. 2010. Just how strapping was KNM-WT 15000?. *J. Hum. Evol.*, 59, 542-554.
- Grayson, D.K., Meltzer, D.J. (2002). Clovis hunting and large mammal extinction: a critical review of the evidence. *J. World Prehist.* 16, 313-359.

- Griffith, A.A., 1921. The Phenomena of Rupture and Flow in Solids. *Philos. Trans. R. Soc. Lon.* A221, 163-198.
- Griffith, A.A., 1924. The Theory of Rupture. In: Bienzeno, C.B., Burgers, J.M. (Eds), *Proceedings of the First International Congress for Applied Mechanics Delft, Waltman, Holland*, pp. 55-63.
- Ham, A.W., 1969. *Histology*. J.B. Lippincott Co, Philadelphia.
- Hannus, L.A. 1989. Flaked Mammoth Bone from the Lange/Ferguson Site White River Badlands Area, South Dakota. In: Bonnichsen, R., Sorg, M.H. (Eds.), *Bone Modification*. Center for the Study of the First Americans, Orono, Maine, pp. 395-412.
- Hannus, L.A. 1990. The Case for Mammoth Bone-Butchering Tools. In: Agenbroad, L. D., Mead, J., and Nelson, L. (eds.), *Megafauna and Man: Discovery of America's Heartland*. Mammoth Site of Hot Springs, Hot Springs, South Dakota, pp. 86-99.
- Harmand, S., Lewis, J.E., Feibel, C.S., Lepre, C.J., Prat, S., Lenoble, A., Boes, X., Quinn, R.L., Brenet, M., Arroyo, A., Taylor, N., Clement, S., Daver, G., Brugal, J.-P., Leakey, L., Kent, D.V., Mortlock, R.A., Wright, J.D., Roche, H., 2015. 3.3-million-year-old stone tools from Lomekwi 3, West Turkana, Kenya. *Nature*, 521, 310-315.
- Hay, R.L., 1973. Lithofacies and environments of Bed I, Olduvai Gorge, Tanzania. *Quatern. Res.* 3, 541–560.
- Haynes, G., 1981. Bone modifications and skeletal disturbances by natural agencies Unpublished Ph.D. dissertation, Catholic University of America, Washington, D.C.
- Haynes, G., 1982. Utilization and skeletal disturbances of North American prey carcasses. *Arctic* 35, 266-281.
- Haynes, G., 1983a. Frequencies of spiral and green-bone fractures on ungulate limb bones in modern surface assemblages. *Am. Antiq.* 48,102-114.
- Hemmer, H., 2000. Out of Asia: a paleoecological scenario of man and his carnivorous competitors in the European Lower Pleistocene. *ERUAL* 92, 99-106.
- Hertz, H.H., 1881. On the contact of elastic solids. *Journal of Reine Angew. Math.* 92, 156-171; translated and reprinted (1896) in English in 'Herts's miscellaneous papers', MacMillan, London.
- Hill, A., 1981. A modern hyaena den in Amboseli National Park, Kenya. *Proc. of the PACPQS: Nairobi*, 137-138.
- Hill, A., 1983. Hyaenas and early hominids. In: Clutton-Brock, J., Grigson, C. (Eds.), *Animals and Archaeology: 1. Hunters and Their Prey*. BAR International Series, 163, Oxford, pp. 87-92.
- Hill, A., 1984. Hyaenas and hominids: taphonomy and hypothesis testing. In: Foley, R. (Ed.), *Hominid Evolution and Community Ecology*. Academic Press, New York, pp. 111-128.

- Hill, A., 1989. Bone modification by modern spotted hyaenas. In: Bonnicksen, R., Sorg, S.H. (Eds.), *Bone Modification*. Center for the Study of the First Americans, Orono, Maine, pp. 169-178.
- Holen, S.R., 2007. The age and taphonomy of mammoths at Lovewell Reservoir, Jewell County, Kansas, USA. *Quat. Int.* 169-170, 51-63.
- Holekamp, K.E., Smale, L., 1990. Provisioning and food sharing by lactating spotted hyenas, *Crocuta crocuta* (Mammalia: Hyaenidae). *Ethology*, 86, 191-202.
- Hoo, R.P., 2011. Multi-scale mechanics of bone. Ph.D. Dissertation, University of New South Wales.
- Hu, Y., Hu, S., Wang, W., Wu, X., Marshall, F. B., Chen, X., Wang, C., 2014. Earliest evidence for commensal processes of cat domestication. *Proc. Natl. Acad. Sci.* 111, 116-120.
- Hull, D. 1999. *Fractography*. Cambridge University Press, Cambridge.
- Isaac, G.Ll., 1978a. Food sharing and human evolution: archaeological evidence from the Plio-Pleistocene of East Africa. *J. Anthropol. Res.* 34, 311-325.
- Isaac, G.Ll., 1978b. The food-sharing behavior of protohuman hominids. *Sci. Am.* 238, 90-108.
- Isaac, G.Ll., 1984. The archaeology of human origins: Studies of the Lower Pleistocene in east Africa, 1971-1981. In: Wendorf, F., Close, A. (Eds.), *Advances in World Archaeology 3*. Academic Press, New York, pp. 1-87.
- Jaeger, J.J., 1976. Les rongeurs (Mammalia, Rodentia) du Pleistocene inferieur d'Olduvai Bed I (Tanzanie), 1ere partie: Les Murides. In: Savage, R. J. G., Coryndon, S. C. (Eds.) *Fossil Vertebrates of Africa, Vol. 4*. Academic Press, London, pp. 57-120.
- Johnson, E., 1985. Current developments in bone technology. In: Schiffer, M. (Ed.), *Advances in Archaeological Method and Theory, vol. 5*. Academic Press, New York, pp. 157-235.
- Kaiser, T.M., 2000. Proposed fossil insect modifications to fossil mammalian bone from Plio-Pleistocene Hominid-bearing deposits of Laetoli (Northern Tanzania). *Annals of the Entomological Society of America* 93, 693-700.
- Kappler, J., 1984. Plio-Pleistocene environments of Bed I and lower Bed II, Olduvai Gorge, Tanzania. *Palaeogeogr. Palaeoclimatol. Palaeoecol.* 48, 171-196.
- Katz, L.J., Yoon, H.S., Lipson, S., Maharidge, R., Meunier, A., Christel, P., 1984. The effects of remodeling on the elastic properties of bone. *Calcif. Tissue Int.* 36, S31-S36.
- Kelly, M.J., Durant, S.M., 2000. Viability of the Serengeti cheetah population. *Conserv. Biol.* 14, 786-797.
- Kim, J.-H., Kim, J.-W., Myoung, S.-W., Pines, M., Zhang, Y., 2008. Damage maps for layered ceramics under simulated mastication. *J. Dent. Res.* 87, 671-675.

- Kimbel, W.H., Walter, R.C., Johanson, D.C., Reed, K.E., Aronson, J.L., Assefa, Z., et al., 1996. Late Pliocene *Homo* and Oldowan Tools from the Hadar Formation (Kada Hadar Member), Ethiopia. *J. Hum. Evol.* 31, 549-561.
- Kingdon, J., 1977. East African mammals: an atlas of evolution in Africa. Volume IIIA, Carnivores. University of Chicago Press, Chicago.
- Kleinman, D.G., Eisenberg, J. F., 1973. Comparisons of canid and felid social systems from an evolutionary perspective. *Anim. Behav.* 21, 637-659.
- Koester, K.J., Ager, J.W., III, Ritchie, R.O., 2008. The true toughness of human cortical bone measured with realistically short cracks. *Nature Materials* 7, 672 – 677.
- Kress, T.A., Porta, D.J., 2001. Characterization of leg injuries from motor vehicle impacts. Proceedings of the 17th International Technical Conference on the Enhanced Safety of Vehicles. ESV Paper 443, 1-14.
- Krishnan, R.V., Radhakrishnan, S., Raghuram, A.C., Ramachandran, V., 1993. Aircraft Accident Caused by Explosive Sabotage. In: Esakul, K.A. (Ed.), Handbook of Case Histories in Failure Analysis, 1992, Vol 2. ASM International.
- Kruuk, H., 1972. The spotted hyena: a study of predation and social behavior. University of Chicago Press, Chicago.
- Lamprecht, J., 1978. The relationship between food competition and foraging group size in some larger carnivores. *Z. Tierpsychol.* 46:337-343.
- Lamprecht, J., 1981. The function of social hunting in larger terrestrial carnivores. *Mammol. Rev.* 11, 169-179.
- Laurenson, M.K., 1994. High juvenile mortality in cheetahs (*Acinonyx jubatus*) and its consequences for maternal care. *J. Zool.* 234, 387–408.
- Lawn, B.R., 1998. Indentation of ceramics with spheres: a century after Hertz. *J. Am. Ceramics Soc.* 81, 1977-1994.
- Lawn, B.R., Marshall, D.B., 1979. Mechanisms of microcontact fracture in brittle solids. In: Hayden, B. (Ed.), Lithic use-wear analysis. Academic Press, New York, pp. 63-82.
- Lawrence, L.A., Ott, E.A., Miller, G.J., Poulos, P.W., Piotrowski, G., Asquith, R.L., 1994. The mechanical properties of equine third metacarpals as affected by age. *Journal of Animal Science* 72, 2617-2623.
- Leakey, M.D. 1971. Olduvai Gorge, Vol. 3: Excavations in Bed I and II, 1960-1963. Cambridge University Press, Cambridge.
- Leakey, M.G., Spoor, F., Brown, F.H., Gathogo, P.N., Kiarie, C., Leakey, L.N., McDougall, I. 2001. New hominin genus from eastern Africa shows diverse middle Pliocene lineages. *Nature* 410, 433–440.
- Legendre, S., Roth, C., 1988. Correlation of carnassial tooth size and body weight in recent carnivores (Mammalia). *Hist. Biol.* 1, 85-98.

- Leonard, W., Robertson, M. L., 1997. Comparative primate energetics and hominid evolution. *Am. J. Phys. Anthropol.* 102: 265-281.
- Lewis, M.E., 1997. Carnivoran paleoguilds of Africa: implications for hominid food procurement strategies. *J. Hum. Evol.* 32, 257-288.
- Lindner, D.L., Marretta, S.M., Pijanowski, G.J., Johnson, A.L., Smith, C.W., 1995. Measurement of bite force in dogs: a pilot study. *J. Vet. Dent.* 12(2), 49-52.
- Li, S., Abdel-Wahab, A., Silberschmidt, V.V., 2012. Analysis of fracture processes in cortical bone tissue. *Eng. Fract. Mech.* 110, 448-458.
- Lovejoy, C.O., 1981. The origin of man. *Science* 211, 341-350.
- Lyman, R.L., 1994. Vertebrate taphonomy. Cambridge University Press, Cambridge.
- Marder, M., 1996. Energetic developments in fracture. *Nature* 381, 275-276.
- Marder, M., Fineberg, J., 1996. How things break. *Physics Today* 49, 24-30.
- Martens, M., van Audekercke, R., de Meester, P., Mulier, J.C., 1986. Mechanical behaviour of femoral bones in bending loading. *J. Biomech.* 19(6), 443-454.
- Martin, L.D., 1989. Fossil history of the terrestrial carnivora. In: Gittleman, J.L. (Ed.), *Carnivore behavior, ecology and evolution*. Cornell University Press, Ithaca, pp. 536-568.
- Martin R.D., 1996. Scaling of the mammalian brain: the maternal energy hypothesis. *New Physiol. Sci.* 11, 149-56.
- McGrew W., 1992. Chimpanzee material culture. Cambridge University Press, Cambridge.
- McHenry, H., Coffing, K., 2000. Australopithecus to Homo: transformations in body and mind. *A. Rev. Anthro.* 29,125-146.
- McHenry, L.J., 2005. Phenocryst composition as a tool for correlating fresh and altered tephra, Bed I, Olduvai Gorge, Tanzania. *Stratigraphy*, 2, 101–115.
- McHenry, L.J., Stollhofen, H., Stanistreet, I.G., 2013. Use of single-grain geochemistry of cryptic tuffs and volcanoclastic sandstones improves the tephrostratigraphic framework of Olduvai Gorge, Tanzania. *Quat. Res.*, 80, 235-249.
- Mech, L.D., 1970. *The Wolf : The Ecology and Behavior of an Endangered Species*. University of Minnesota Press, Minneapolis.
- Medvedovski, E., 2010. Ballistic performance of armour ceramics: influence of design and structure. Part 2, *Ceram. Int.*, 36, (7), 2117-2127.
- Myers, T.P., Voorhies, M.R., Corner, R.G., 1980. Spiral fractures and bone pseudotools at paleontological sites. *Am. Ant.* 45, 483-490.
- Mills, M. G. L. 1982. Factors affecting group size and territory size of the brown hyaena, *Hyena brunnea*, in the southern Kalahari. *J. Zool.* 198, 39–51.

- Mills, M.G.L., 1989. The comparative behavioral ecology of hyenas: the importance of diet and food dispersion. In: Gittleman, J.L. (Ed.), *Carnivore Behavior, Ecology, and Evolution*, Cornell University Press, Ithaca, pp. 125-142.
- Moehlman, P.D., 1987. Social organization in jackals: the complex social system of jackals allows the successful rearing of very dependent young. *Am. Sci.* 366-375.
- Moehlman, P.D., 1989. Intraspecific variations in canid social systems. In: Gittleman, J.L. (Ed.), *Carnivore Behavior, Ecology, and Evolution*, Cornell University Press, Ithaca, pp. 143-163.
- Monahan, C. M., 1996. New zooarchaeological data from Bed II, Olduvai Gorge, Tanzania: Implications for hominid behavior in the Early Pleistocene. *J. Hum. Evol.* 31, 93-128.
- Mora, R., de la Torre, I., 2005. Percussion tools in Olduvai Beds I and II (Tanzania): Implications for early human activities. *J. Anthropol. Archaeol.* 24: 179-192.
- Morlan, R. E., 1980. Taphonomy and archaeology in the upper Pleistocene of the Northern Yukon Territory: A Glimpse of the peopling of the New World. *Archaeological Survey of Canada Paper No. 94*. National Museum of Canada, Ottawa.
- Morlo, M., Gunnell, G.F., Nagel, D., 2010. Ecomorphological analysis of carnivore guilds in the Eocene through Miocene of Laurasia. In: Goswami, A., Friscia, A. (Eds.), *Carnivoran Evolution: New Views on Phylogeny, Form, and Function*, Cambridge University Press, Cambridge, pp. 269-310.
- Nakayama, M., 1966. *Dynamic karate*. Kodansha International, Tokyo.
- Nalla, R.K., Kinney, J.H., Ritchie, R.O., 2003. Mechanistic fracture criteria for the failure of human cortical bone. *Nat. Mater.* 2, 402-413.
- Neto, O.P., Pacheco, M.T.T., Bolander, R., Bir, C., 2009. Force, reaction time, and precision of kung fu strikes 1, 2. *Perceptual and motor skills*, 109, 295-303.
- Odell, G.H., 2004. *Lithic analysis*. Kluwer Academic/Plenum, New York.
- Oliver, J.S., 1986. The taphonomy and paleoecology of Shield Trap Cave (24CB91), Carbon County, Montana. Unpublished Ms. thesis, Institute for Quaternary Studies, University of Maine at Orono, Orono Maine.
- Oliver, J.S., 1989. Analogues and site context: Bone damages from Shield Trap Cave (24CB91), Carbon County, Montana, U.S.A. In: Bonnicksen, R., Sorg, M.H., (Eds.) *Bone Modification*. Center for the Study of the First Americans, Orono, Maine, pp. 73-98.
- Oliver, J.S., 1994. Estimates of hominid and carnivore involvement in the FLK-*Zinjanthropus* fossil assemblage: Some socioecological implications. In: Oliver, J.S., Sikes, N., Stewart, K. (Eds.), *Early hominid behavioral ecology: New looks at old questions*. Special Publication of the *J. Hum. Evol.* 27, 47-75.

- Oliver, J.S., 1993. Carcass processing by the Hadza: bone breakage from butchery to consumption. In: Hudson, J., (Ed.) From bones to behavior: ethnoarchaeological and experimental contributions to the interpretation of faunal remains. Center for Archaeological Investigations, Occasional Paper No. 21. Southern Illinois University at Carbondale, pp. 200-227.
- Owens, D.D., Owens, M.J., 1979. Communal denning and clan associations in brown hyenas (*Hyaena brunnea*, Thunberg) of the central Kalahari Desert. *African Journal of Ecology*, 17, 35-44.
- Palmqvist, P., Martínez-Navarro, B., Pérez-Claros, J.A., Torregrosa, V., Figueirido, B., Jiménez-Arenas, J.M., Espigares, M.P., Ros-Montoya, S., De Renzi, M.I., 2011. The giant hyena *Pachycrocuta brevirostris*: modelling the bone-cracking behavior of an extinct carnivore. *Quat. Int.* 243, 61–79.
- Palomares, F., Caro, T.M., 1999. Interspecific killing among mammalian carnivores. *The American Naturalist*, 153, 492-508.
- Pante, M.C., Blumenschine, R.J., Capaldo, S.D., & Scott, R.S., 2012. Validation of bone surface modification models for inferring fossil hominin and carnivore feeding interactions, with reapplication to FLK 22, Olduvai Gorge, Tanzania. *J. Hum. Evol.* 63, 395-407.
- Pante, M.C., Scott, R.S., Blumenschine, R.J., Capaldo, S.D., 2015. Revalidation of bone surface modification models for inferring fossil hominin and carnivore feeding interactions. *Quat. Int.* 355, 164-168.
- Parkinson, J.A., 2013. A GIS image analysis approach to documenting Oldowan hominin carcass acquisition: Evidence from Kanjera South, FLK Zinj, and neotaphonomic models of carnivore bone destruction. Ph.D. Dissertation, City University of New York.
- Parkinson, J.A., Plummer, T., Hartstone-Rose, A., 2015. Characterizing felid tooth marking and gross bone damage patterns using GIS image analysis: An experimental feeding study with large felids. *J. Hum. Evol.* 80, 114-134.
- Pickering, T.R., Dominguez-Rodrigo, M., Egland, C.P., Brain, C.K., 2005. The contribution of limb bone fracture patterns to reconstructing early hominid behavior at Swartkrans Cave (South Africa): Archaeological applications of a new analytical method. *Int. J. Osteoarchaeol.* 15, 247-260.
- Pickering, T.R., Egland, C.P., 2006. Experimental patterns of hammerstone percussion damage on bones: implications for inferences of carcass processing by humans. *J. Arch. Sci.* 33, 459-469.
- Piekarski, K., 1970. Fracture of bone. *J. Appl Phys.* 41, 215-223.
- Palmqvist, P., Martínez-Navarro, B., Pérez-Claros, J.A., Torregrosa, V., Figueirido, B., Jiménez-Arenas, J.M., Patrocínio Espigares, M., Ros-Montoya, S., De Renzi, M., 2011. The giant hyena *Pachycrocuta brevirostris*: modelling the bone-cracking behavior of an extinct carnivore. *Quat. Int.* 19(1), 61-79.

- Pereira, L.M., Owen-Smith, N., Moleón, M., 2013. Facultative predations and scavenging by mammalian carnivores: seasonal, regional, and intra-guild comparisons. *Mammal Rev.* 44, 44-55.
- Pierce, J.D., Reinbold, K.A., Lyngard, B.C., Goldman, R.J., Pastore, C.M., 2006. Direct measurement of punch force during six professional boxing matches. *J. Quantitative Analysis in Sports*, 47, 118-164.
- Pieter, F., Pieter, W., 1995. Speed and force in select taekwondo techniques. *Biology of Sport*. 12, 257-266.
- Plummer, T., 2004. Flaked stones and old bones: Biological and cultural evolution at the dawn of technology. *Yearb. Phys. Anthropol.*, 47, 118-164.
- Plummer, T., Bishop, L., 1994. Hominid paleoecology at Olduvai Gorge, Tanzania as indicated by antelope remains. In: Oliver, J.S., Sikes, N., Stewart, K. (Eds.), *Early hominid behavioral ecology: new looks at old questions*. Special Publication of the J. Hum. Evol. 27, 47-75.
- Pobiner, B.L., Rogers, M.J., Monahan, C.M., Harris, J.W.K., 2008. New evidence for hominin carcass processing strategies at 1.5 Ma, Koobi Fora, Kenya. *J. Hum. Evol.* 55, 103-130.
- Pobiner, B.L., 2015. New actualistic data on the ecology and energetics of hominin scavenging opportunities. *J. Hum. Evol.* 80, 1-16.
- Pokines, J.T., Kerbis Peterhans, J., 2007. Spotted hyena (*Crocuta crocuta*) den use and taphonomy in the Masai Mara National Reserve, Kenya. *J. Archeol. Sci.* 34, 1914-1931.
- Polis, G.A., Myers, C.A., Holt, R.D., 1989. The ecology and evolution of intraguild predation: potential competitors that eat each other. *Annu. Rev. Ecol. Syst.* 20,297–330.
- Potts, R. 1988. *Early hominid activities at Olduvai*. Aldine, New York.
- Potts, R., Shipman, P., 1981. Cutmarks made by stone tools from Olduvai Gorge, Tanzania. *Nature* 291, 577-588.
- Pruim, G.J., de Jongh, ten Bosch, J.J., 1980. Forces acting on the mandible during bilateral static bite at different bite force levels. *J. Biomech.* 13, 755-763.
- Quinn, G.D., 2007. *Fractography of glass and ceramics*. National Institute of Standards and Technology Special Publication 960-17, Washington, DC.
- Rable, W., Haid, C., Martin, K., 1996. Biomechanical properties of the human tibia: fracture behavior and morphology. *Forensic Sci. Int.* 83, 39-49.
- Radchenko, A.V., Kobenko, S.V., 2000. Effect of oriented elastic and strength characteristics on the impact fracture of anisotropic materials. *Doklady Physics* 45, 397-400.
- Radsheer, M.C., van Eijden, T.M.G.J., van Ginkel, F.C., Prah Andersen, B., 1999. Contribution of jaw muscle size and craniofacial morphology to human bite force magnitude. *J. Dent. Res.* 78, 31-42.

- Ramrakhiani, M., Pal, D., Murthy, D. 1980. Effects of dynamic impacts on human bone. *J. Bioscience* 2: 139-144.
- Rasa, A., 1984. *Mongoose watch: A family observed*. John Murray Ltd., London.
- Rho, J.Y., Kuhn-Spearing, L., Zioupos, P., 1998. Mechanical properties and the hierarchical structure of bone. *Medical engineering & physics* 20, 92-102.
- Rood, J.P., 1986. Ecology and social evolution in the mongooses. In: Rubenstein, D.I., Wrangham, R.W. (Eds.), *Ecological aspects of social evolution*. Princeton University Press, Princeton, NJ, pp. 131-152.
- Roylance, D., 2001. *Introduction to fracture mechanics*. National Bureau of Standards, Special Pub. 647-1, 1-17.
- Sambrook, P., 2001. Bone structure and function in normal and disease state. In: Sambrook P., Schrieber L., Taylor T., Ellis A. (Eds.), *The musculoskeletal system*. Churchill Livingstone, Edinburgh, Scotland, pp 67-84.
- Schaller, G.B., 1968. Hunting behaviour of the cheetah in the Serengeti National Park, Tanzania. *E. Afr. Wildl. J.* 6, 95-100.
- Schaller, G.B., 1972. *The Serengeti lion: a study of predator-prey relations*. University of Chicago Press, Chicago.
- Schaller, G.B., Lowther, G.R., 1969. The relevance of carnivore behavior to the study of early hominids. *S.J. Anthropol.* 25, 307-341.
- Schick, K., Toth, N., Gehling, T., Pickering, T.R. 2007. Taphonomic analysis of an excavated striped hyena den from the eastern desert of Jordan. In: Pickering, T., Schick, K., Toth, N. (Eds.), *Breathing Life into Fossils: Taphonomic Studies in Honor of CK (Bob) Brain*. Stone Age Institute Press, Bloomington, Indiana, 75-106.
- Selvaggio, M., 1994. Evidence from carnivore tooth marks and stone-tool-butchery marks for scavenging by hominids at FLK Zinjanthropus Olduvai Gorge, Tanzania. Unpublished Ph.D. dissertation, Rutgers University.
- Selvaggio, M., 1998. Evidence for a three-stage sequence of hominid and carnivore involvement with long bones at FLK *Zinjanthropus*, Olduvai Gorge, Tanzania. *J. Archeol. Sci.* 285,191-202.
- Semaw, S., Renne, P., Harris, J.W., Feibel, C.S., Bernor, R.L., Fesseha, N., Mowbray, K. 1997. 2.5-million-year-old stone tools from Gona, Ethiopia. *Nature* 385, 333-336.
- Semaw S., Rogers M.J., Quade J., Renne P., Butler R., Dominguez-Rodrigo M., Stout D., Hart W., Pickering T., Simpson S., 2003. 2.6-Million-year-old stone tools and associated bones from OGS-6 and OGS-7, Gona, Afar, Ethiopia. *J. Hum. Evol.* 45,169–177.
- Semken, H.A.,1980. Holocene climatic reconstructions derived from the three micromammal bearing cultural horizons of the Cherokee Sewer Site, northwestern Iowa. In: Anderson, D.C., Semkin, H.A. (Eds.), *The Cherokee Excavations: Holocene Ecology and Human Adaptations in Northwestern Iowa*. Academic Press, New York, pp. 67-99.

- Sharon, E., Gross, S., Fineberg, J., 1995. Local crack branching as a mechanism for instability in dynamic fracture. *Physical Review Letters* **74**, 5096-5099
- Shipman, P., 1981. Applications of scanning electron microscopy to taphonomic problems. In: Griffin, J.B., Rothschild, N. (Eds.), *The Research Potential of Anthropological Museum Collections*, Annals of the New York Academy of Sciences, NY, pp. 357-385.
- Shipman, P., 1986. Scavenging or hunting by early hominids? *Am. Anthropol.* **88**, 27-43.
- Sikes, N., 1994. Early hominid habitat preferences in East Africa: paleosol carbon isotope evidence. In: Oliver, J.S., Sikes, N., Stewart, K. (Eds.), *Early hominid behavioral ecology: New looks at old questions*. Special Publication of the *J. Hum. Evol.* **27**, 25-45.
- Sikes, N., Ambrose, S., 1993. Modeling hominid home range size using dental anatomy to estimate trophic level. Paper presented at the 2nd Annual Paleoanthropology Society Meeting, Toronto.
- Simpson, G.G. 1970. Uniformitarianism. An inquiry into principle, theory, and method in geohistory, and biohistory. In: Hecht, M.K., Steere, W.C. (Eds.), *Essays in evolution and genetics in honor of Theodosius Dobzhansky*, Appleton-Century-Crofts, New York, pp. 43-96.
- Smith P.K., Hamill, J., 1986. The effect of punching glove type and skill level on momentum transfer. *Journal of Human Movement Studies* **12**:153–61.
- Sponheimer, M., Passey, B.H., De Ruiter, D.J., Guatelli-Steinberg, D., Cerling, T.E., Lee-Thorp, J.A. 2006. Isotopic evidence for dietary variability in the early hominin *Paranthropus robustus*. *Science*, **314**, 980-982
- Stanford, D., Bonnicksen, R., Morlan, R.E. 1981, The Ginsberg experiment: modern and prehistoric evidence of bone-flaking technology. *Science*, **212**, 438-440.
- Stanley, S.M., 1992. An ecological theory for the origin of *Homo*. *Paleobiology* **18**, 237-257.
- Stevenson, M.E., Jones, S.E., Bradt, R.C., 2001. Fracture patterns of a composite safety glass panel during high velocity projectile impacts. In: Varner, J.R., Quinn, G.D. (Eds.), *Fractography of glasses and ceramics, IV*. Am. Ceram. Soc., Westerville, OH, pp. 473-488.
- Steyn, V., Funston, P.J., 2009. Land-use and socio-spatial organization of female leopards in a semi-arid wooded savanna, Botswana. *South African Journal of Wildlife Research*, **39**, 126-132.
- Strømsøe, K., Høiseth, A., Alho, A., Kok, W.L., 1995. Bending strength of the femur in relation to non-invasive bone mineral assessment *J. Biomech.* **28**(7), 857-861.
- Subhash, G., Maiti, S., Geubelle, P.H., Ghoshz, D., 2008. Recent advances in dynamic indentation fracture, impact damage and fragmentation of ceramics. *Journal of the American Ceramic Society* **91**, 2777–2791.
- Susman, R.L., 1991. Who made the Oldowan tools? Fossil evidence for tool behavior in Plio-Pleistocene hominids. *J. Anthropol. Res.* **47**, 129-151.

- Tappen, N.C., 1969. The relationship of weathering cracks to split-line orientation in bone. *Am. J. Phys. Anthropol.* 31, 191-198.
- Thomason, J.J., 1991. Cranial strength in relation to estimated biting forces in some mammals. *Canadian Journal of Zoology* 69, 2326-2333.
- Thompson, J.L., Nelson, A.J. 2011. Middle childhood and modern human origins. *Human Nature*, 22, 249-280.
- Treves, A., Palmqvist, P., 2007. Reconstructing hominin interactions with mammalian carnivores (6.0–1.8 Ma). In: Gursky, S.L., Nekaris, K.A.I. (Eds.), *Primate anti-predator strategies*. Springer US, pp. 355-381.
- Tsirk, A., 1996. Hackles revisited. In: Varner, J.R., Fréchette, V.D., Quinn, G.D. (Eds.), *Fractography of Glasses and Ceramics III*. The American Ceramic Society, Westerville, Ohio, pp. 447-472.
- Tsirk, A., 2010. Fracture markings from flake splitting. *J. Archaeol. Sci.*, 37, 2061-2065.
- Turner, A., 1990. The evolutions of the guild of larger terrestrial carnivores during the Plio-Pleistocene in Africa. *Geobios* 23, 349-368.
- Van Eijden, T.M.G.J., 1991. Three-dimensional analyses of human bite-force magnitude and moment. *Archs. Oral Biol.* 36 (7), 535-539.
- van Lawick, H., van Lawick, J., 1971. *Innocent killers*. Houghton Mifflin, Boston.
- Van Valkenburgh, B., 1985. Locomotor diversity between past and present guilds of large predatory mammals. *Paleobiology*. 11, 406–428.
- Van Valkenburgh, B., 1988. Trophic diversity in past and present guilds of large predatory mammals. *Paleobiology*. 14, 155–173.
- Van Valkenburgh, B., 1989. Carnivore dental adaptations and diet: a study of trophic diversity within guilds. In: Gittleman, J.L. (Ed.), *Carnivore Behavior, Ecology, and Evolution*. Vol 1. Cornell University Press, Ithaca, pp. 410–436.
- Van Valkenburgh, B., 1991. Iterative evolution of hypercarnivory in canids (Mammalia: Carnivora): evolutionary interactions among sympatric predators. *Paleobiology*. 17, 340–362.
- Varner, J.R., 2002. Fracture modes and appearances in ceramics. In: Becker, W.T., Shipley, R.J. (Eds.), *Failure analysis and prevention*, ASM Handbook, Vol. 11. ASM International, Materials Park, OH, pp. 663-670.
- Villa P., Mahieu, E., 1991. Breakage patterns of human long bones. *J. Hum. Evol.* 21, 27-48.
- Villmoare, B., Kimbel, W.H., Seyoum, C., Campisano, C.J., DiMaggio, E.N., Rowan, J., Braun, D.R., Arrowsmith, J.R., Reed, K.E., 2015. Early *Homo* at 2.8 Ma from Ledi-Geraru, Afar, Ethiopia. *Science* 347, 1352-1355.

- Voigt, M., 1989. A telescoping effect of the human hand and forearm during high energy impacts. *J.Biomech.*, 22, 1095.
- Vos, J. A., Binkhorst, R.A., 1966. Velocity and force of some Karate arm-movements. *Nature* 211, 89-90.
- Walilko, T. J., Viano, D.C., Bir, C.A., 2005. Biomechanics of the head for Olympic boxer punches to the face. *Br. J. Sports. Med.* 39, 710–719.
- Walker, J.D., 1975. Karate strikes. *Am. J. Physics* 43, 845–849.
- Wall-Scheffler, C.M., Meyers, M.J., 2013. Reproductive costs for everyone: How femal loads impact human mobility. *J. Hum. Evol.* 64, 448-456.
- Wang, X., Mabrey, J.D., Mauli Agrawal, C., 1998. An interspecies comparison of bone fracture properties. *Bio-Medical Materials and Engineering* 8, 1-9.
- Watson, J.C., Payne, R.C., Chamberlain, A.T, Jones, R.K., and Sellers, W.I. 2008. The energetic costs of load-carrying and the evolution of bipedalism. *J. Hum. Evol.* 54, 675-683.
- Waugh, L.M., 1937. Influence of diet on the jaws and face of the American Eskimo. *J. Am. Dent. Assoc.* 24, 1640-1647.
- Weatherholt, A.M., Fuchs, R.K., Warden, S.J., 2012. Specialized connective tissue: bone, the structural framework of the upper extremity. *J. Hand Ther.* 25(2), 123-132.
- Wegst, U.G.K., Schecter, M., Donius, A.E., Hunger, P.M., 2010. Biomaterials by freeze casting. *Philos. Trans. R. Soc. Lond. A* 368, 2099-2121.
- Werdelin, L., Lewis, M.E., 2001. A revision of the genus *Dinofelis* (Mammalia, Felidae). *Zoological Journal of the Linnean Society*, 132, 147-258.
- White, T.D., 1992. Prehistoric cannibalism at Mancos 5MTUMR-2346. Princeton University Press, Princeton.
- Woodward, R.L., Baxter, B.J., Pattie, S.D., McCarthy, P., 1991. Impact fragmentation of brittle materials. *J. de Physique IV, Colloque C3*, 259-264.
- Wroe, S., McHenry, C., Thomason, J., 2005. Bite club: Comparative bite force in big biting mammals and the prediction of predatory bhaviour in fossil taxa. *Proc. R. Soc. B* 272, 619-625.
- Wroe, S., Ferrara, T.L., McHenry, C.R., Curnoe, D., Chamoli, U., 2010. The craniomandibular mechanics of being human. *Proc. R. Soc. B* 277, 3579-3586.
- Yoffe, E.H., 1951. The moving Criffith crack. *Phil. Mag.* 42, 739-750.
- Zapffe, C.A., Clogg, M. Jr., 1944. Fractography: a new tool for metallurgical research. *Am. Soc. of Metals*, 34, 71-107.

Zioupos, P., Kaffy, C., Currey, J.D., 2006. Tissue heterogeneity, composite architecture and fractal dimension effects in the fracture of ageing human bone. *Int. J. Fract.* 139, 407-424.